Insertional Mutagenesis to Identify Novel Determinants of Pathogenicity in *Magnaporthe oryzae*

Submitted by Muhammad Sougatul Islam

to the University of Exeter as a thesis for the degree of
Doctor of Philosophy in Biological Sciences
November 2012

I certify that all material in this thesis which is not my own work has been identified and that no material has been previously submitted and approved for the award of a degree by this or any other University.

Muhammad Sougatul Islam

Abstract

Rice blast disease is caused by the filamentous fungus *Magnaporthe oryzae* and is the most destructive disease of cultivated rice. It was the first plant pathogenic fungus to have its genome sequence published which opened up the opportunities to discern the principal genetic components that confer pathogenicity on the fungus. The availability of the genome sequence has also presented fresh challenges in terms of converting sequence data into meaningful biological information. Functional genomics studies involve the generation of genome-wide mutant collections and comprehensive screens with potential to identify novel pathogenicity determinants. In this study I utilized *Agrobacterium tumefaciens* mediated random insertional mutagenesis to study the infection mechanism of *M. oryzae*. A collection 10,200 *M. oryzae* T-DNA insertion mutants were generated as part of this study and pathogenicity was assayed by high-throughput disease screening. From the primary qualitative screening I obtained 200 mutants that were reduced or lacking in pathogenicity. Quantitative re-screening allowed selection of 71 T-DNA mutants, including 9 non-pathogenic and 63 reduced virulence mutants exhibiting at least a 50% reduction in disease symptoms. Finally, we selected 8 non-pathogenic mutants for detailed phenotypic and gene functional analysis. A novel approach was used to retrieve T-DNA tagged genes from mutants of interest. Next generation DNA sequencing (NGS) was used to retrieve T-DNA flanking sequences in a high-throughput manner. The efficiency of NGS to facilitate the high-throughput large scale insertional mutagenesis was therefore demonstrated. Out of 8 selected mutants, I identified three novel genes that putatively encode a transcription factor, a PH domain containing signalling protein and a MAP kinase. I also provided evidence that, MGG_05343 is a functional C6 zinc finger transcription factor involved in conidiogenesis. The PH domain containing protein MGG_12956 is involved in vegetative growth,

condiogenesis and virulence. The novel kinase MGG_15325 is a *S. cerevisiae IME2* homolog that belongs to the Ime2 class of non-classical MAP kinase subfamily. Intriguingly, *M. oryzae IME2* seems to have an essential role in growth in planta because the mutant was able to penetrate and colonize plant tissue but failed to cause necrotic rice blast lesions. Identification of these novel genes will allow us greater insight into the processes required for condiogenesis, vegetative and invasive growth and a more integrated understanding of the post-penetration phases of plant tissue colonization. Interestingly, I identified two mutants tagged with T-DNA insertion in the autophagy genes *ATG2* and *ATG3*, reaffirming the importance of infection-associated autophagy in plant infection by *M. oryzae* and we characterized the *ATG3* gene. In addition, I generated a resource of 63 unidentified T-DNA mutants which can potentially lead to identification of more novel determinants of pathogenicity in rice blast disease.

Table of Contents

2 General Material & Methods

List of Figures

List of Tables

Acknowledgements

I would like to express my deep feeling of gratitude to "The Halpin PhD Programme for Rice Blast Research" for providing the generous funding which enabled me to carry out this research in a world leading laboratory. I would like to convey my thanks to Dr Leslie and Claire Halpin for their periodic presence and encouragement throughout the time of my PhD study. I am thankful to my supervisor Prof. Nick Talbot for providing me the opportunity to be part of his laboratory and letting me grow as an independent researcher by his insight, guidance and enthusiasm. I appreciate the academic and support staff in the College of Life and Environmental Sciences for their help whenever necessary. I would like to thank Dr. Darren Soanes for his work and analysis to facilitate the next generation sequencing part of my study. I must recognize the effort of Nick Tongue and Barbara Saddler for their everyday support, patience and maintenance which were very significant for our day-to-day research work. Many thanks to all the member of the Halpin research laboratory, in particular Michael Kershaw and Tina Penn for all of their support and suggestions during last four years in the laboratory. I cherish good memories with Muhammad Badaruddin for all our pleasant times in the lab and two other very friendly and brilliant Halpin scholars Yasin Dagdas and Yogesh Gupta. I acknowledge the continuous support and encouragement from all of my family members back in Bangladesh. My sincere and deepest gratitude goes to my parents for their contribution and enthusiasm for coming up to this doctoral studies and I dedicate this thesis to them. Very special thanks go to my wife Munia Amin for her support, care and patience alongside her own PhD studies. Last but not the least, my son Amr bin Muhammad whose smile was an integral part of my life in the final year of my PhD.

Abbreviations

aa	Amino acid
AB	*Agrobacterium* broth
AMP	Adenosine monophosphate
ATP	Adenosine-5'- triphosphate
AS	Acetosyringone
ATMT	*Agrobacterium tumefaciens* mediated transformation
BSA	Bovine serum albumin
bp	Basepair
cAMP	Cyclic 3', 5' adenosine monophosphate
cDNA	Complementary DNA
cm	Centimetre
CFEM	Cysteine-rich EGF-like
CM	Complete medium
CTAB	Cetyltrimethylamonium bromide
dATP	2'-deoxyadenosine triphosphate
DBD	DNA binding domain
DIC	Differential interference microscopy
DMSO	Dimethyl sulfoxide
DNA	Deoxyribonucleic acid
DTT	Dithiothreitol
EDTA	Ethylenediaminetetracetic acid
°C	Degree Celcius
ddH2O	Double distilled water/ deionised water
DNA	Deoxuribonucleic acid
FAO	Food and agriculture organization
g	Grams
g	Relative centrifugal force
g L^{-1}	Grams per litre
GDP	Guanosine diphosphate
GEF	Guanine nucleotide exchange factor
GTP	Guanosine-5'-triphosphate
GFP	Green fluorescent protein
GPCR	G-protein couped receptor
HCl	Hydrogen chloride
h	Hour
HT	High-throughput
iPCR	Inverse PCR
IH	Invasive hyphae
IBMX	3-lsobutyl-1-Methylxanthine
kb	Kilobase
LB	Left border
µg	Microgram
µL	Microlitre
µm	Micrometre
mg	Milligram

min	Minute(s)
mL	Millilitre
mm	Millimetre
mM	Millimolar
MPa	Megapascal
M	Molar
MAPK	Mitogen-activated protein kinase
MAPKK	Mitogen-activated protein kinase kinase
MAPKKK	Mitogen-activated protein kinase kinase kinase
MM	Minimal medium
NADPH	Nicotinamide adenine dinucleotide phosphate
ng	Nanogram
NGS	Next generation sequencing
nt	Nucleotide(s)
OM	Osmotic medium
ORF	Open reading frame
PCR	Polymerase chain reaction
PDA	Potato dextrose agar
PEG	Polyethylene glycol
PH	Pleckstrin homology
PKA	Protein kinase A
PP	Penetration peg
%	Percentage
RB	Right border
RFLP	Restriction fragment length polymorphism
REMI	Restriction enzyme mediated integration
RGS	Regulator of G-protein signalling
RNA	Ribonucleic acid
RNase	Ribonuclease
rpm	Revolutions per minute
SAGE	Serial analysis of gene expression
SAM	Sterile α-motif
SDS	Sodium dodecyl sulphate
STM	Spore tip mucilage
TAIL-PCR	Thermal asymmetric interlaced PCR
T-DNA	Transfer DNA
Tris	Tris(hydroxymethyl)methylamine
TAE	Tris-acetate EDTA buffer
TBE	Tris-borate EDTA buffer
TE	Tris-EDTA
UTR	Untranslated region
UV	Ultraviolet
vir	Virulence
v/v	Volume to volume
w/v	Weight per volume
X-gal	5-bromo-4-chloro-3-indolyl-β-D-galactosidase

Chapter 1

Introduction

1.1 Food Security

1.1.1 The challenge of food security

Food security is defined as being achieved when people have physical, social and economic access to sufficient, safe and nutritious food in order to meet their dietary needs for an active and healthy life (FAO, 2009). In contrast, food insecurity exists when people do not have access to adequate amount of foods and this ultimately leads to undernourishment and hunger (FAO, 2009). Food security is an important global issue because the world's population is set to reach 9.1 billion by 2050 and majority of population growth will occur in developing countries (FAO, 2009; Ash *et al*., 2010). Ensuring a food supply for such a huge population will be challenging. Annual cereal production will need to rise from current 2.1 billion tonnes to about 3 billion per annum (FAO, 2009). Globally, 870 million people are currently undernourished (in terms of dietary energy supply) which represents 12.5 percent of the global population, or one in eight people. About 98% of them (850 million) live in developing countries, where the extent of undernourishment is now estimated at 14.9 percent of the global population (FAO, 2012). Although, the production of all major food crops and livestock has shown a steady upward trend in the last 50 years (Godfray *et al*., 2010), but we still have to achieve a 50 to 100% increase in current food production by 2050 in order to secure the global food supply (Baulcombe, 2010). Another important fact is that the global growth in the yields of major cereal crops has dropped from 3.2 % per year in 1960 to just 1.5 % in 2000. A continuous linear increase in the current rate of yield increase will not be even able to meet the demand of food (FAO, 2009). This observation poses a fresh challenge for

science and technology to reverse the scenario. Moreover, the recent increases in food prices in global markets and the subsequent increases in the number of hungry and malnourished people, has warned policy makers about the fragility of the global food system (FAO, 2009). Policy makers and think tanks are therefore seeking pragmatic strategies to meet the requirements of a growing population, while a decrease in land and water, increased costs of fuel, energy and fertilizers, changes in climate conditions and crop losses due to biotic infection and natural disaster, are some of the major issues that have added challenges to food security (Tilman *et al*., 2001, Baulcombe, 2010). Therefore, reforms in policy and investment are necessary to ensure food security, including human resource development for agricultural research, water resource management and farm- and community-based agricultural and natural resource management (Rosegrant and Cline, 2003). Extensive research is also important in order to utilize the available resources to maximize the output and remove the current obstacles to sustainable food production (Fedoroff *et al*., 2010). To achieve this goal, research stakeholders and investors must promote scientific development of this area with an emphasis in the developing world, where advanced technology-driven initiatives can provide real change (Baulcombe, 2010).

1.1.2 The impact of phytopathogens on global food security

Plant diseases have posed a significant constraint on global food production since ancient times. For this reason they are regarded as major threats to global food security which has been established by their resulting yield losses of food crops (Normile, 2010; Pennisi, 2010). It has been estimated that at least 10% of the world's total crops are lost to plant diseases annually, which exacerbates food shortages. This significantly contributes to malnourishment of 870 million people worldwide (Strange & Scott, 2005). In developed countries, plant diseases take their toll on consumers by increasing the food price because of the cost of

control measures, the development of disease resistant crops and storage and distribution costs (Talbot & Foster, 2001). The United States is the largest agricultural economy on earth and is provided with the best technology and disease management, yet it is estimated that $9.1 billion losses occur to crops due to phytopathogens each year (Agrios, 1997). In contrast, the developing world is much more vulnerable to plant diseases because the majority of poor and malnourished people live in these regions of the world (FAO, 2012). Fourteen crops provide the bulk of food for human consumption including rice, wheat, maize, barley and potatoes as staple crops and numerous other crops supply important nutritional requirements although they are grown less intensely. All of these crops are susceptible to a variety of pathogens both in the field and post-harvest (Strange and Scott, 2005). The major pathogens that pose significant threats to food security are viruses, bacteria, oomycetes, nematodes, parasitic plants, and most notably, fungi. (Strange and Scott, 2005; Agrios, 2005; Pennisi, 2010). In the past, phytopathogens have shown significant impacts on human civilization. Historic out-breaks of potato late blight caused by *Phytophthora infestans* in the 1840s caused severe famines in Northern Europe. The devastation in Ireland led to the great Irish potato famine. Around a million people died of starvation and more than a million people emigrated to North America (Carlile *et al*., 2001; Strange, 2003). Later in history another great disaster named "Great Bengal Famine" of 1943 occurred in which an estimated 2 million people died. The fungus *Cochliobolus miyabeanus* caused destruction of the rice crop and the dependence on a single crop was the underlying reason for the severe famine that resulted (Padmanabhan, 1973). In the late nineteenth century, coffee rust destroyed all commercial coffee plantations in South East Asia. The disease, caused by *Hemilleia vastatrix*, was first seen in Sri Lanka in 1869 and within the next 10 years it ruined the local coffee industry. Subsequently, the disease disseminated to all coffee-growing regions of the world, except Hawaii. (Agrios, 2005). Disease epidemics continued to cause problems and

one of them was southern corn leaf blight disease struck maize grown in the US in 1970-1971 destroying more than 15% of the US maize crop and resulting in the loss of $5 million worth of maize. Although, no people died because of the availability of alternative food sources but the impact was severe on the agricultural economy (Strange & Scott, 2005). This epidemic was caused by *Cochliobolus heterostrophus* which is able to produce host-selective, low molecular weight toxins as virulence factors (Turgeon & Baker, 2007).

In the recent past, emerging fungal pathogens have posed an additional threat to food security. Among them is *Puccinia graminis,* which causes black stem rust on wheat around the world (Stokstad, 2009). In the 1950s, epidemics had destroyed wheat fields in North America and caused 40% losses to estimated yield. Norman Borlaug bred new varieties of resistant wheat and by 1980 the wheat yield was boosted up after introgression of resistance genes in new varieties. However, in 1999 a hypervirulent new strain of *P. graminis* emerged in Uganda, named Ug99 (Stokstad, 2009). Since then, the Ug99 strain has appeared in North-East Africa, Yemen and Iran and threatens wheat production throughout the Middle East, the West and South Asia. If the strain appears in South Asia, it could cause serious famines because poor farmers cannot afford fungicides to control the disease (Stokstad, 2007; Pennisi, 2010). *Puccinia graminis Ug99* causes the plant to fall over (lodging) and can result in entire yield loss. It is estimated that if the disease reaches the Indian Punjab region, losses could reach $3 billion per annum. In the US, the annual loss could exceed more than $10 billion (Pennisi, 2010).

1.2 The importance of fungal pathogens in plant diseases

1.2.1 Understanding fungal diseases and pathogenicity

The economic impact of fungal diseases has driven the necessity for scientific research on plant pathogenic fungi. This has significantly contributed to the development of an understanding of disease mechanisms, host resistance and subsequent disease control strategies. Nevertheless, development of novel disease control measures, such as the use of fungicides and breeding new varieties for disease resistance, are not sufficient to save 5-10% crops losses to fungal pathogens each year in the developed world (Bowyer, 1999). The advent of molecular genetics enabled scientists to carry out functional analysis of fungal pathogens since the first DNA-mediated transformation of a fungal pathogen (Oliver *at el.*, 1987; Parsons *at el.*, 1987). Remarkable progress has been made over the last twenty five years in identifying genes from fungal pathogens and understanding their role in disease process. For example, development of various DNA-mediated transformation methods increased the number of different fungi that were subjected to gene manipulation (Strange & Scott, 2005). Furthermore, random mutagenesis and targeted gene deletion analysis revolutionized gene functional analysis in fungal phytopathogens.

The pathogenicity of a fungus is a complex phenotype which involves a number of factors throughout different stages of fungal development. Important developmental stages are the initial attachment of spore to the plant surface, spore germination, elaboration of specialized infection structure, cuticle penetration, invasion of host tissue, suppression of host plant defences, tissue colonization, acquisition of nutrients from the host and dissemination of infective propagules (Schafer, 1993; Talbot, 1995). Advances in comparative and functional genomics have provided the opportunity to improve our understanding of host-pathogen

interactions very rapidly. In recent years, the genome sequences of several phytopathogenic fungi have been sequenced, published and are now publicly available (Loftus *et al*., 2005; Kamper *et al*., 2006; Ma *et al*., 2009, 2010; Goodwin *et al*., 2011). In recent years, the development of high-throughput sequencing technologies has facilitated genomics and transcriptomics studies on a large scale. The emerging discipline of functional genomics utilizes these tools in parallel with conventional molecular genetics and showed promise in providing better understanding of fungal pathogenicity. Comparative genomics has also provided the opportunity to identify genes involved in pathogenicity of poorly understood and less studied pathogens (Xu *et al*., 2006; Hedeler *et al*., 2007; Soanes *et al*., 2008). A lot of effort has been extended to explore the underlying mechanisms of pathogenesis and the biology of phytopathogens which should pave the way to find durable strategies for disease control. Nevertheless, there is still much to do in order to fight plant diseases and achieve sustainable food security.

1.2.2 Major groups of fungal phytopathogens

Fungi are the most destructive phytopathogens and are considered the major causes of crop loss (Agrios, 2005). In the last decade in the USA, 12 fungal species were listed as the most threatening of 19 phytopathogens (Madden & Wheelis, 2003). Factors that have enabled fungal species to cause catastrophic plant diseases include their ability to produce enormous inoculum by prolific sporulation to facilitate spread of infections. Usually, the infection cycle is completed within a few days which giving rises to infectious propagules at regular intervals for further infection. Spores propagate and result in a high density inoculum that can be dispersed in the field by rain or dew-drop splash. Furthermore, fungi produce a diverse array of phytotoxic compounds or release a battery of enzymes that can cause destruction of plant tissue. Fungi can sequester essential nutrients away from the economically valuable plant

structures by production or induction of growth regulators (e.g. cytokinins) that leads to yield loss as consequences (Strange & Scott, 2005; Toth & Birch, 2005). More than 100,000 species of fungi have been identified, mostly saprotrophs, that derive nutrients from degradation of dead organic matter. Among them, over 10,000 species have been identified that are plant pathogenic compared to only around 50 species that cause diseases in human (Pennisi, 2001; Agrios, 2005).

Basidiomycetes include fungi that produce mushrooms and are typically saprotrophic that live on dead or decaying substrates. Sexual spores are known as basidiospores and are formed on a club shaped structures called basidia. Two common groups of basidiomycete fungi are phytopathogenic. One group includes the rust fungi, which include the biotrophic stem rust fungus *Puccinia graminis*. It causes disease on a broad range of cereals and grasses (Agrios, 1997; Carlile *et al.*, 2001). The other group is the smut fungi and amongst the most common smut is the corn smut fungus, *Ustilago maydis*. This is a heterothallic basidiomycete, with a dimorphic life cycle which consists of a saprotrophic asexual phase and a parasitic sexual phase. Smut is a foliar disease where characteristic galls form on leaves, stem, tassels and ears of maize (Agrios, 1997; Banuett, 1992).

A number of phytopathogens also belong to the oomycetes (phylum Oomycota) which are not true fungi but are classified in the kingdom Chromista (Agrios, 1997). They are non-photosynthetic osmotrophs. A number of significant differences exist between fungi and Oomycetes. Oomycetes are diploid for most of their life cycle whereas the majority of true fungi are haploid. Moreover, Oomycete cell wall materials are predominantly composed of cellulose and β-glucans while fungal cell walls are mainly composed of chitin and glucans (Werener *et al.*, 2002). The most destructive representative of this group is the necrotrophic

pathogen *Phytophthora infestans*, the causative agent of potato late blight disease. A number of *Phytophthora* species are able to destroy a range of economically important crops (Carlile *et al.*, 2001).

Many important phytopathogens are ascomycete fungi. They are commonly known as filamentous fungi. Filamentous fungi represent a diverse group of eukaryotes characterized by their simple filamentous and branched growth pattern and their ability to produce asexual spores (Agrios, 2005). During the sexual life cycle meiosis occurs within the ascus to generate haploid ascospores (Agrios, 1997), but ascomycete plant pathogens are predominantly clonal in the field. Conidiospores are produced in bulk and disseminated rapidly to spread infections (Carlile *et al.*, 2001). *Magnaporthe oryzae* is a highly destructive ascomycete fungus of cereal crops and the cause of rice blast disease.

1.3 Rice blast disease

1.3.1 The significance of rice blast disease

Magnaporthe oryzae (previously known as *Magnaporthe grisea*) pathotype *oryza* is a heterothallic ascomycete fungus that causes the most destructive foliar disease of rice, known as rice blast (Couch & Kohn, 2002). The *Magnaporthe grisea* species complex consists of many phylogenetic species (Couch & Kohn, 2002) that can cause disease on over 50 grass and sedge species (Ou *et al.*, 1987). Rice blast disease is considered as the most serious threat to cultivated rice in the world with epidemics particularly common in South America and South East Asia (Zeigler *et al*., 1994; Baker *et al*., 1997; Talbot, 2003). Each year the disease causes enormous rice yield losses in more than 85 countries, which could provide sufficient rice to feed over 60 million people (Zeigler *et al*., 1994). An estimated 10-30% of the global rice production is lost annually due rice blast disease. For instance, in 1995 a serious outbreak

of rice blast occurred in Bhutan that devastated more than 700 hectares of cultivated land and resulted in the loss of 1090 tonnes of rice (Talbot, 2003; Thinlay *et al.*, 2000). In the last decade, rice blast epidemics have occurred particularly in China where 5.7 million hectares of rice was destroyed between 2001 and 2005 (Wilson & Talbot, 2009). Rice blast disease is characterized by the appearance of ellipsoid, necrotic lesions which lead to general leaf senescence and desiccation (Baker *et al*., 1997) and is responsible for the loss of approximately 150 million tonnes of rice worldwide annually (International Rice Research Institute, 2003). *M. oryzae* also infects wheat (*Triticum aestivum*) (Silva *et al.*, 2009) and in Brazil it is considered as one of the major emerging crop diseases (Urashima *et al.*, 2004). Serious outbreaks of wheat blast challenge the production of wheat in the northern Parana state of Brazil and the situation was mode more serious due to unavailability of efficient fungicides and disease-resistant wheat cultivars (Igarashi *et al*., 1986, Urashima & Kato, 1993). In addition to rice and wheat, *M. oryzae* is also able to infect many agriculturally important crops including barley (*Hordeum vulgare*), maize (*Zea mays*), oats (*Avena sativa*), rye (*Secale cereale*), perennial ryegrass (*Lolium perenne*), millet (*Eleusine coracana*) and several weeds and ornamental grasses (Igarashi *et al*., 1986; Dean *et al*., 2005; Skamnoti & Gurr, 2009).

The fungus causes blast symptoms on all aerial parts of rice plants including neck, panicle, collar and node blast. Leaf blast and panicle blast are two most prevalent forms of the disease (Ou, 1985). Leaf blast occurs during the seedling stage and resultant infections causes yield losses by reducing green leaf area (Roumen, 1992). The disease can even kill rice seedlings completely and severely affects plant growth and development. The most destructive phase of the disease however, is neck blast, which is characterized by infection at the base of the panicle (Talbot, 1995; Hamer & Talbot, 1998). *M. oryzae* colonizes the panicle neck and

disrupts the supply of photosynthate to the developing grain which results in light grain or empty panicles (Bonman *et al*., 1989). In fact, neck blast is much more destructive than leaf blast in field conditions because of its impact on yield (Zhuang *et al*., 2002).

1.3.2 Measures to control rice blast disease

Traditional ways of controlling plant diseases includes exclusion, elimination or reduction of pathogen inoculum and disease development. Exclusion of pathogens by quarantining infected plants is traditionally used as a first line of defence. To eliminate or reduce pathogens good cultural practices such as intercropping, crop rotation, multi-cropping and post-harvest protections can be applied. As a last line of defence in field conditions when plants are attacked by pathogens, pesticides are used (Strange & Scott, 2005). For controlling rice blast disease in conventional ways, similar strategies have been applied. Less expensive and low impact rice blast preventive measures include burning of crop residues, such as diseased straw and stubble, planting of disease-free seed, avoiding excess nitrogen-based fertilizer application, water-seeding and growth under conditions of continuous flooding (Skaminioti & Gurr, 2009).

Rice blast disease has predominantly been controlled by conventional plant breeding and fungicide application. The most cost-effective and preferred means of combating rice blast disease is by development of high-yielding rice cultivars carrying single dominant disease resistance (R) genes. These single gene resistances are usually however overcome in 2-4 years (Babujee and Gnanamanickam, 2000; Bonman *et al.*, 1992). The strategy of pyramiding resistance genes has also been applied in order to prevent breakdown of resistance, by introgression of several R genes with different resistance spectra into a single rice cultivar (Bonman *et al.*, 1992; Hittalmani, *et al.*, 2000). Conceptually, this is based on the lineage-

specific exclusion strategy formulated to reduce selection pressure on a single blast isolate (Zeigler et al., 1995). This strategy has been applied in rice blast-prevalent regions of Southern India and Thailand (Babujee and Gnanamanickam, 2000). Another widely exploited approach is the introgression of broad-spectrum R genes which are able to provide resistance against different strains of *M. oryzae*. It has been proven to provide cost-effective durable resistance (Bonman *et al.*, 1992; Dai *et al.*, 2007). Among other methods, cultivar mixtures have been used to constrain the emergence of aggressive field strains of *M. oryzae* (Zhu *et al.*, 2000). In low risk areas, partial resistance has also been tested. An ideal breeding programme for blast resistance combining cultivar-specific resistance genes and minor resistance genes has, however yet to be developed but offers the best promise of long term durable rice blast resistance (Bonman *et al.*, 1992; Ballini *et al.*, 2008).

Biological control of rice blast has been studied using avirulent isolates of *M. oryzae* (Ashizawa *et al.*, 2005). The rice phylloplane fungal isolate MKP5111B for example suppresses *M. oryzae* infection which suggests that disease resistance response can be induced (Ohtaka e*t al.*, 2008) A number of recent studies have also reported the use of antagonistic bacteria such as *Pseudomonas fluorescens, Bacillus polymyxa* (Karthikeyan & Gnanamanickam, 2008), *Bacillus licheniformis* (Tendulkar *et al.*, 2007) and *Streptomyces* sp. PM5 (Prabavathy *et al.*, 2006) to control *M. oryzae.* Although biological control is desirable because of its low cost, its effectiveness is yet to be proven in field experiments.

Rice blast disease has also been controlled by an array of fungicides. The global market for anti-blast chemicals with their proposed modes of action is shown in Table 1.1 (Skamnioti & Gurr, 2009). Fungicide management of *M. oryzae* infection has had only limited success due to emergence and persistence fungicide-resistant strains. The only exception is MBI-R

(melanin biosynthesis inhibitor) fungicides and no blast resistant strains have evolved during the last 30 years of use (Kurahashi, 2001). Despite several attempts, the development of genetically modified (GM) blast resistant rice varieties has not been successful when single R genes have been deployed due to high genetic variability of the fungus in the field, their ability to form new pathotypes rapidly (Latterell & Rossi, 1986) and potential environmental and health effects (Skaminioti & Gurr, 2009). Now, the challenge is to develop an understanding of the host-pathogen interaction in the rice blast pathosystem and translate this knowledge into practice to develop durable rice blast disease control.

Table 1.1: Global market for leading rice blast fungicides (data taken from Skamnioti & Gurr, 2009).

Country	Global Fungicide Market (%)	Commonly used Fungicide, Trade Name and Manufacturer	Mode of Action
Japan	46	Probenazole in Oryzemate™, Meiji Seika	Activation of plant defence response
South Korea	14	Tricyclazole in Segard™, Dow Agrosciences	Melanin biosynthesis inhibitor-R (polyhydroxyl-napthalene reductase)
China	9	Azoxytrobin in Quadris™, Syngenta	QoI complex 3 inhibitor (mitochondrial respiration inhibitor)
India	6	Isoprothiolane in Fuji-one™, Nihon Nohyaku	Phospholipid biosynthesis (methyltransferase) and/or choline biosynthesis inhibitor
USA	4	Propiconazole in Tilt™, Syngenta	Sterol biosynthesis (14-demethylase) inhibitor

1.3.3 *M. oryzae* as a model phytopathogen to study plant-fungal interaction

Emergence of *M. oryzae* as a model organism to study host-pathogen interactions has been mainly driven by its economic significance (Skamnoti & Gurr, 2009; Wilson & Talbot, 2009). In addition, a number of advantages of studying *M. oryzae* have also significantly contributed, including the culturability of the fungus away from its host plant in standard growth medium, an effective DNA-mediated transformation system, the ease of random insertional mutagenesis on the haploid asexual infectious phase and the possession of a sexual stage to allow classical genetics. Acting in concert, those factors developed *M. oryzae* as a tractable model pathogen for molecular genetics. Inevitably, the *M. oryzae*-rice has therefore emerged as a model for understanding plant-pathogen interaction (Valent & Chumley, 1991; Valent *et al*., 1991; Talbot, 1995; Talbot, 2003). Generation of temperature-sensitive alleles, targeted insertion of reporter genes and creation of point mutations by gene replacement have also enabled reverse genetics to be applied more efficiently in *M. oryzae* (Wilson & Talbot, 2009). High-throughput methods for RNA interference-mediated gene silencing has been successfully applied (Quoc *et al.*, 2008). Furthermore, *M. oryzae* can be easily studied by live-cell imaging using a wide range of reporters (Czymmek *et al.*, 2002) as well as immunolocalization, ultrastructural analysis and biochemical analysis of the fungus (Czymmek *et al.*, 2002; Thornton and Talbot, 2006). Genome sequence of *M. oryzae* has provided the opportunity to attribute the biological role of genes that confer pathogenicity as well as identification of novel genes (Dean *et al.*, 2005). In the last decade, many other phytopathogenic fungal genome sequences have been released (Galagan *et al.*, 2005; Soanes *et al.*, 2007; Soanes *et al.*, 2008) and this has opened the door for comparative genomic study to accelerate the exploration of pathogenicity in rice blast disease. It has the potential to develop our understanding of the evolution of fungal virulence and to identify gene families responsible for pathogenicity (Soanes *et al.*, 2002, Veneault-Fourrey & Talbot, 2005). More

recently, the development of high-throughput next generation DNA sequencing techniques has facilitated transcriptomic analysis by RNAseq and HT-SuperSAGE (Soanes *et al.*, 2012). The unprecedented speed and productivity of sequencing technologies offers genome-scale studies to be carried out in order to understand pathogenicity at a systems level (Nagarajan & Pop, 2010). The evolution of modern molecular genetic techniques has also allowed scientists to carry out gene functional analysis of *M. oryzae* and many genes essential for causing rice blast diseases have been identified in this way (Wilson & Talbot, 2009). Despite these technical advances and their applications, the molecular genetic basis of the rice blast disease is yet to be fully understood.

1.3.4 Life cycle of *Magnaporthe oryzae*

The asexual life cycle commonly propagates *M. oryzae* in the field (Zeigler *et al*., 1994). Initiation of foliar infection involves the transfer of three-celled spores or conidia, formed under humid conditions from the characteristic, large ellipsoid lesions that occurs on the surface of diseased rice leaves (Ou, 1985) (Figure 1.1). Dispersal of spores occurs *via* wind dispersal and/or dew drops during periods of high humidity (>93%) (Talbot, 1995; Balhadere & Talbot, 2000). Subsequently, spores adhere to the waxy, hydrophobic leaf cuticle (Uchiyama & Okuyama, 1990) using an adhesive mucilage called spore tip mucilage (STM), released from the apex of the spore (Figure 1.1) (Hamer *et al.*, 1988). STM provides tight attachment to the non-stick hydrophobic leaf surface. The presence of free water causes germination of the spore very rapidly within 2 hours of its landing on a leaf. A polarized germ tube emerges, typically from the apical cell of the conidium at its tapering end (Bourett & Howard, 1990). The germ tube is sensitive to the leaf surface and involved in perception of the topography and rigidity of the surface that is then favourable for appressorium formation (Bourett & Howard, 1990). After growing to a length of around 15-30 μm, the germ tube tip

swells and its growth changes direction. After 4 hours, the germ tube stops growing at its tip and becomes flattened against the surface of the leaf in a process called 'hooking' (Talbot, 2003). "Hooking" is the point when the leaf surface is perceived by the germinated spore and appressorium formation is initiated on a conducive surface (Bourett & Howard, 1990). Development of the appressorium begins with swelling of the germ tube tip (Bourett & Howard, 1990). Appressorium formation requires the absence of exogenous nutrients and presence of a hard, hydrophobic surface (Dean, 1997). On the leaf surface, appressorium formation is also switched on upon sensing cutin monomers by the fungus. Therefore, appressorium development can be induced on normally non-inductive surfaces in the presence of soluble cutin (*cis*-9, 10-epoxy-18-hydroxyoctadecanoic acid) or lipid (1, 16-hexadecanediol) monomers (Talbot, 1993; Ebbole, 1997). These early environmental cues lead to activation of multiple signalling cascades instrumental in appressorium development.

Within the germ tube, a single mitotic division takes place. A nucleus from the conidium migrates to the germ tube and divides into two daughter nuclei by a single mitosis that occurs 4 to 6 hours after surface attachment (Veneault-Fourrey *et al*., 2006). One of the daughter nuclei moves back to the conidium, while the second moves to the developing appressorium. After 15 hours, the three nuclei that are present in the conidium are broken down by autophagy and the only nucleus remains in the mature appressorium. As the appressorium develops, a specialized septum is formed which separates the conidium and germ tube. The conidium eventually dies and the remaining single intact appressorium provided with all the nutrients of the conidium to prepare for plant infection (Veneault-Fourrey *et al*., 2006).

Biogenesis of a combination of an inner melanin layer and outer chitin layer causes a thickening of the highly differentiated cell wall of the appressorium. The melanin layer is synthesized between the cell wall and cell membrane. This layer acts as a barrier to the efflux

of solutes from the appressorium which is therefore, essential for turgor generation (Bourett & Howard, 1990). Carbohydrates and lipids stored in the conidium are mobilized to the developing appressorium and their subsequent degradation results in a large increase in solute concentration (Thines *et al.,* 2000). The mature appressorium generates enormous turgor pressure (8 MPa) which is up to fifty times that of a car tyre, by accumulating high concentration of glycerol (3.22 M) followed by an influx of water (Howard *et al*., 1991; de Jong *et al.,* 1997). The penetration peg is produced as a narrow hypha from the appressorial pore at the point of contact between the appressorium and the leaf cuticle, where the outer fibrous layer of the chitin cell wall is initially absent (Bourett & Howard, 1990). The appressorium converts turgor into physical force through the emerging penetration peg which mechanically breaches the leaf cuticle to invade the leaf epidermis (Howard *et al*., 1991). Mechanical rupture of the cuticle was observed in a similar fungus *Colletotrichum graminicola* (Bechinger *et al.,* 1999) in which melanin also provides an impermeable layer in the appressorium. Further evidence for the role of melanin came from the study of three melanin deficient mutants in *M. oryzae, albino, buf* and *rosy*. Being deficient in melanin synthesis, these mutants are unable accumulate glycerol and fail to develop the necessary high turgor pressure required for plant infection (Chumley & Valent, 1990; Howard *et al*., 1991; de Jong *et al*., 1997).

Following cuticle rupture, the penetration peg swells into a primary infection hypha in epidermal cells and subsequently differentiates into bulbous, branched invasive hyphae that colonize adjacent tissue (Heath *et al.,* 1990; Talbot, 1995; Kankanala *et al*., 2007). Within three days of the initiation of infection, up to 10% of the biomass of infected rice leaf is fungal material (Talbot *et al.,* 1993). Chlorosis occurs in localised areas of diseased leaves and a toxic compound named tenuazonic acid is found in diseased rice tissue (Lebrun *et al.,*

1990, Valent & Chumley, 1991). After 4 days of infection, elliptical necrotic disease lesions appear on the leaf surface, coalescing and leading to severe disease symptoms. Conidia are produced in copious amount from disease lesions, spread under highly humid conditions by wind or dew-drop splash and re-initiate the disease cycle in a new host (Talbot, 2003).

1.4 The role of cell signalling in infection related development of *M. oryzae*

Fungal phytopathogens undergo a series of morphological and physiological programmes to cause diseases. These developmental transitions encompass cell signalling to regulate fungal growth and development on the plant surface and during colonization of different plant tissues (Dean, 1997). Signal perception from the external environment and translation into gene expression are essential components for infection by plant pathogenic fungi. For instance, *M. oryzae* has the largest number of putative receptor proteins among sequenced fungi and therefore, it has a potentially greater flexibility to respond to extracellular signals (Dean *et al*., 1997). Signals from the plant-pathogen interface induce rapid responses through cellular signalling pathways. For example, the commitment to develop infection structures, such as the appressorium relies on perceiving such environmental signals and subsequent signalling events leading to the new gene expression (Dean *et al*., 1997; Lee *et al*., 2003). There are two signal transduction pathways that have been demonstrated to play important roles in appressorium formation in *Magnaporthe oryzae* (Figure 1.4). These are the cyclic AMP signalling and Pmk1 MAP kinase signalling pathways (Adachi & Hamer, 1998; Xu, 2000; Li *et al.*, 2012).

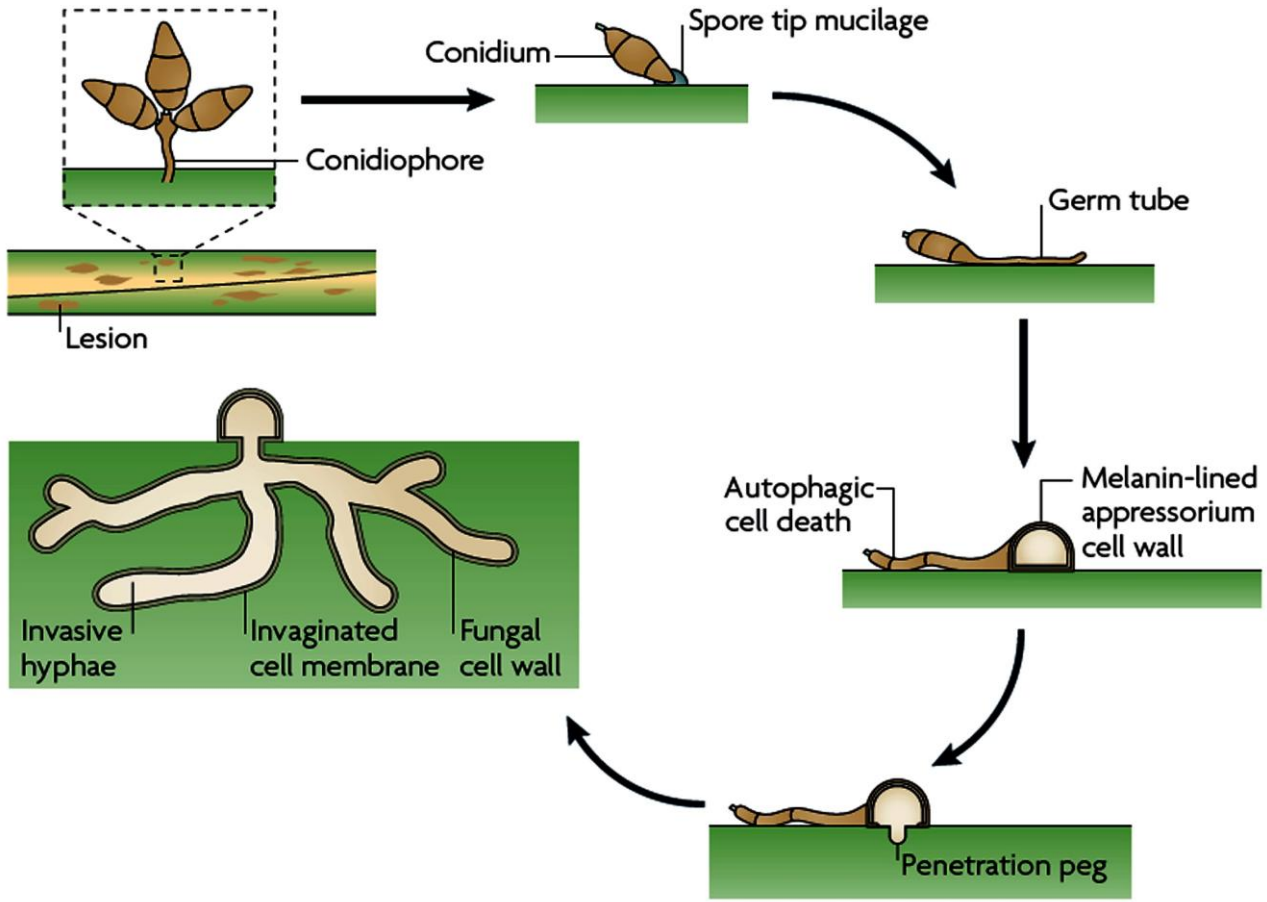

Figure 1.1: Asexual life cycle of rice blast fungus *Magnaporthe oryzae*. *M. oryzae* is an ascomycete fungus which causes rice blast disease. The fungus infects rice in its asexual life cycle. The infection cycle starts when a three-celled asexual spore called the conidiospore lands on the rice leaf surface. Upon attachment to the hydrophobic leaf surface, conidial germination gives rise to a polarized germ tube from one of the apical cells. The germ tube flattens and its tip swells, which leads to development of a dome-shaped appressorium. The appressorium matures and simultaneously conidial cell death occurs by an autophagic process. The appressorium cell wall thickens by deposition of melanin that allows accumulation of glycerol resulting from degradation of carbohydrates and lipids. High concentrations of glycerol generate substantial turgor that is translated into mechanical force to rupture the rice leaf cuticle with a narrow penetration peg. After gaining entry to the host, the fungus starts growing invasively by forming bulbous and branched hyphae. Tissue colonization occurs by cell-to-cell movement of hyphae through plasmodesmata. During this phase, the fungus suppresses host plant defences by deploying effectors and then switches into a necrotrophic phase of growth to derive nutrients from the host. Ellipsoid necrotic disease lesions appear on the leaf surface between 72 and 96 after initial infection. Profuse sporulation occurs in lesions and conidiospores are spread under humid conditions by wind or dew-drop splash to initiate the infection cycle again on a new host. (Diagram taken from Wilson & Talbot, 2009).

1.4.1 Cyclic AMP (cAMP) signalling

Cyclic AMP or cAMP (Cyclic adenosine 5'-monophosphate) is a well characterized secondary messenger in both prokaryotes and eukaryotes. It is also well known for its essential role in growth and morphogenesis in fungi (Kronstad, 1997; Adachi & Hamer, 1998). The cAMP signalling pathway is generally characterized by the presence of a transmembrane cell surface receptor that senses extracellular signals and transduces this signal via a heterotrimeric G-protein complex (Lee *et al*., 2003). It is believed that during the early germ tube elongation phase of blast infection, the cAMP response pathway is triggered. Adenylate cyclase synthesizes cAMP from ATP under starvation conditions (Talbot, 2003). Adenylate cyclase, a product of the *MAC1* gene, is a membrane-bound enzyme and upon receiving a signal through transmembrane receptors it generates cAMP (Choi & Dean, 1997). Targeted deletion of *MAC1* gene results in mutant (Δ*mac1*) which is non-pathogenic because the Δ*mac1* is unable to synthesize cAMP and impaired in differentiation into appressoria (Choi & Dean, 1997). Addition of exogenous cAMP allows appressorium development and restores pathogenicity of the mutant. This line of evidence confirms that the catalytic activity of the *MAC1* gene is necessary for appressorium development and pathogenesis (Choi & Dean, 1997; Kronstad, 1997; Adachi & Hamer, 1998; Lee & Dean, 1993). Further evidence came from an extragenic suppressor mutant of Mac1. Δ*mac-1 sum 1-99* which restores wild type appressorium formation of *Δmac1* mutants because of a single base changes in the cAMP-binding domain of the regulating sub-unit of Protein kinase A (PKA). The mutant *Δmac-1 sum 1-99* does not require cAMP to bind to the regulatory unit of PKA and therefore complements for absence of *MAC1*. Suppression of the Δ*mac1* phenotype was however only partial because of the impaired disease symptoms of Δ*mac-1 sum 1-99* (Adachi & Hamer, 1998).

PKA is a tetrameric holoenzyme consisting of two catalytic and two regulatory subunits (Kronstad, 1997). The regulatory sub-unit of PKA has binding pockets for cAMP and upon cAMP binding the sub-unit is inactivated and released. Subsequently, the detached catalytic subunit is activated and phosphorylates target proteins (Kronstad, 1997). The role of PKA has been investigated in *M. oryzae* by carrying out targeted gene deletion of the *CPKA* gene, which encodes a catalytic subunit of PKA. Δ*cpka* mutants are non-pathogenic because of delayed development of variable sized non-functional appressoria (Mitchell & Dean, 1995; Xu *et al*., 1997). It has also been suggested that the Δ*cpka* mutants have defects associated with either turgor generation or penetration peg emergence because the mutants retain the ability to colonize plant tissues when infected through wounds (Kronstad, 1997; Adachi & Hamer, 1998; Knogge *et al*., 1999; Balhadère & Talbot, 2000). Δ*cpka* mutants could be stimulated to form appressoria by addition of cAMP, indicating that additional PKA enzymes may exist in *M. oryzae*. Later on, the genome sequence of *M. oryzae* revealed a second PKA-encoding gene and gene functional analysis will develop our knowledge to understand the early phase of plant infection mediated by the cAMP signalling pathway (Dean *et al*., 2005).

Additionally, two proteins are believed to be crucial player in surface recognition during appressorium development. One of these is a class I hydrophobin Mpg1 which encodes a hydrophobin that is highly expressed during germ tube elongation (Talbot *et al.*, 1993, 1996; Kershaw & Talbot, 1998). Hydrophobins are secreted proteins that spontaneously aggregate to form a hydrophobic layer at the cell periphery (Wessels, 1994). Mpg1 provide a means of attachment of the fungus to the leaf surface increases the wettability of the leaf surface and facilitates the action of hydrophilic STM secreted at the germ tube-rice leaf interface (Talbot *et al.*, 1996). An Δ*mpg1* mutant is reduced in pathogenicity due to reduced appressoria formation. Application of exogenous cAMP induces *Δmpg1* mutants to form appressoria and

restores pathogenicity. This observation indicates that attachment of the germ tube to the leaf surface is a pre-requisite for triggering the signalling cascades that leads to appressorium morphogenesis (Talbot *et al*., 1993).

PTH11 encodes a membrane-localized protein which acts as a receptor for inductive surface cues, such as surface hardness and hydrophobicity. The localisation of Pth11 to cell membrane suggested its potential involvement in surface recognition (DeZwaan *et al.*, 1999). Intriguingly, Δ*pth11* mutants are severely impaired in appressorium formation on hydrophobic surfaces but this can be suppressed by the addition of exogenous cAMP and diacylglycerol (DAG). This strongly suggests that Pth11 feeds in activates downstream intracellular signalling events leading to appressorium differentiation (DeZwaan *et al.*, 1999).

1.4.2 G protein signalling

A well studied class of signalling components are heterotrimeric guanine nucleotide-binding proteins (G-proteins). They are responsible for transmitting signals from activated cell surface receptors to intracellular effectors to regulate a variety of cellular functions in eukaryotic cells (Lee *et al*., 2003). *M. oryzae* has the largest repertoire of predicted G protein-coupled receptors (GPCRs) (Dean *et al.*, 2005). Genome sequencing of *M. oryzae* revealed a large set of 61 unidentified GPCRs and 12 of them belong to a subfamily that contains a conserved fungal-specific extracellular membrane-spanning domain (the CFEM domain) at the amino terminus (Dean *et al.*, 2005; Kulkarni *et al.*, 2005). Pth11 belongs to this novel class of filamentous ascomycete-specific G-protein coupled receptor protein family. It has seven transmembrane regions and a cysteine-rich EGF-like (CFEM domain) amino-terminal domain which is extracellular (Kulkarni *et al.*, 2005). All of the CFEM GPCRs are expressed during infection-related development and two of them are specifically expressed during

appressorium formation (Dean *et al.*, 2005). This suggests that such a large set of GPCRs may enable *M. oryzae* to sense many diverse environmental signals throughout the different stages of the disease process.

G-proteins consist of three subunits, α, β and γ and are present in conjunction with seven-transmembrane G protein-coupled receptors at the cell membrane. Upon detection of surface cues, they transduce information to the cAMP response and other signalling pathways (Bölker, 1998). Binding of a ligand to the receptor activates G-proteins and subsequently converts G-α subunit-bound GDP to GTP which leads to the dissociation of the G-α subunit from G-βγ (Simon *et al*., 1991; Bölker, 1998). Activated G-α-GTP is diffusible in the cytoplasm and can transmit a signal via activation of effectors, such as adenylate cyclase which yields the secondary messenger cAMP (Lee *et al*., 2003). In *M. oryzae*, three G-α subunit genes *MAGA, MAGB* and *MAGC* have been characterized (Liu & Dean, 1997) along with one G-β subunit gene *MGB1* (Nishimura *et al*., 2003) and one G-γ subunit encoding gene (MGG_10193, Dean *et al*., 2005). Targeted gene deletion revealed that *MAGA* has no role in vegetative growth, conidiation or appressorium morphogenesis but is responsible for the production of mature asci (Liu & Dean, 1997). Deletion of *MAGC* reduces conidiation and production of mature asci, but it has no role in vegetative growth or appressorium development. Among these three proteins, targeted deletion of the gene encoding *MAGB*, an inhibitory group I protein (G-αi), is found to have the most severe effect on *M. oryzae*. The Δ*magB* mutant showed significantly reduced vegetative growth, conidiation, appressorium formation and also failed to produce perithecia (Liu & Dean, 1997). Restoration of pathogenicity on exogenous application of cAMP suggested that *MAGB* is an upstream activator for generating cAMP signal which is involved in appressorium development (Deising *et al*., 2000; Lengeler *et al*., 2000; Lui & Dean, 1997; Tucker & Talbot, 2001;

Talbot, 2003). Site-directed mutagenesis of *MAGB* in *M. oryzae*, suggested that the G-βγ subunit may be a repressor of adenylate cyclase under certain conditions. Investigation of the deletion mutant of Gα subunit encoding gene provided the evidence that in its absence the isolated G-βγ subunit prevents appressorium formation by constitutive repression of adenylate cyclase (Fang & Dean, 2000; Talbot, 2003)

G-protein cascades are negatively regulated by regulators of G-protein signalling (RGS) proteins, which function as GTPase-activating proteins (GAPs). The guanine nucleotide state of Gα determines the duration of G-protein signalling (Dohlman & Thorner, 2001). Rgs proteins function primarily as GTPase-accelerating proteins and increase the hydrolysis rate of GTP bound to G-α subunits, thus allowing reassociation of GDP-Gα with G-βγ leading to attenuation of signalling (Siderovski & Willard, 2005). *RGS1* is a negative regulator of G-protein signalling that affects conidiation and pathogenesis and enables eukaryotic cells to perceive and respond to external stimuli (Siderovski *et al*., 1996; Koelle, 1997; Dohlman & Thorner, 1997, 2001; Liu *et al*., 2007). The Δ*rgs1* mutant of *M. oryzae* was able to develop appressoria even on non-inductive (hydrophilic) surfaces as well as hydrophobic surfaces, implicating Rgs1 as a crucial negative regulator of appressorium formation that couples surface dependency with infection-related morphogenesis. On the other hand, Δ*rgs1* mutant was unable to form appressoria on a soft surface, even in the presence of exogenous cAMP which indicates that a thigmotrophic cue is also necessary for initiating appressorium formation (Liu *et al*., 2007). Rgs1 physically interacts with an activated form of MagA during appressorium initiation (Liu *et al*., 2007). Interestingly, like Δ*rgs1, MAGA* Rgs-insensitive mutants accumulated excessive cAMP and developed appressoria on non-inductive surfaces. This observation suggests that Rgs1 regulates the nucleotide state of MagA during appressorium development which in turn controls GTP-MagA-dependent

adenylate cyclase activation and a consequent increase in intracellular cAMP levels (Liu *et al*., 2007). Rgs1 was also found physically to interact with MagB and negatively regulate the G-α subunit MagB during asexual development (Liu *et al*., 2007). Furthermore, the same study observed direct interactions between activated MagC and Rgs1 and suggested a role of MagC in maintaining mycelial hydrophobicity during vegetative growth (Liu *et al*., 2007). In this study, Rgs1 was assigned a negative regulatory for all Gα subunits to control important development events during asexual and pathogenic development in *M. oryzae* (Liu *et al*., 2007).

In a previous study, the *MGB1* gene, which encodes the G-β subunit of G-proteins in *M. oryzae* was characterized (Nishimura *et al*., 2003). The Δ*magb1* mutant is severely defective in conidiogenesis and appressorium development (Nishimura *et al*., 2003). As intracellular cAMP levels of Δ*mgb1* mutants were reduced, therefore exogenous application of cAMP was carried out which partially restored conidiation and appressorium formation, but infection-incompetent appressoria were still unable to penetrate the host surface. Transformants carrying multiple copies of *MGB1* make appressoria even on hydrophilic surfaces, indicating that elevated levels of functional *MGB1* over-activates G-β signalling, which lead to perturbation in surface sensing mechanism of *M. oryzae* for appressorium formation (Nishimura *et al*., 2003). The results suggested that *MGB1* is also involved in cAMP signalling for regulating conidiation, surface recognition and appressorium formation. Furthermore, *Mgb1* was found to interact physically with Mst50 which is a scaffold protein in the Pmk1 MAPK pathway (Nishimura *et al*., 2003) which implicates that upstream activation of the Pmk1 MAPK is mediated by heterotrimeric G-protein signalling in response to physical cues, such as hydrophobicity and surface hardness (Wilson & Talbot, 2009). However, cross-talk between the Pmk1 MAPK pathway and the cAMP response pathway via

G protein signalling was observed in a previous study which showed that Δ*pmk1* mutants respond to cAMP (Xu & Hamer, 1996).

Very recently, an insertional mutagenesis screen identified a gene called *RIC8* which was suggested to be involved in multiple steps during infection-related morphogenesis (Li *et al*., 2010). The Δ*ric8* mutants were defective in asexual reproduction, appressorium formation and fertility in *M. oryzae* (Li *et al*., 2010). The mutant was non-pathogenic to rice and barley and even failed to infect abraded leaf surfaces indicating that Ric8 protein is essential for pathogenicity and not only for appressorium formation (Li *et al*., 2010). Deletion of *RIC8* leads to lower expression of genes-encoding Gα subunits (*MAGA*, *MAGB* & *MAGC*) and the G-γ subunit (*MGG1*), but does not affect the expression of *MGB1*. Yeast-2-hybrid analysis confirmed that Ric8 physically interacts with the Gα subunit protein MagB, excluding other G-proteins which act upstream of the cAMP response pathway necessary for appressorium morphogenesis (Li *et al*., 2010). Therefore, it is believed that Ric8 may act as a novel regulator of G-protein signalling and is essential for infection-related morphogenesis of *M. oryzae* (Li *et al*., 2010).

1.4.3 Pmk1 MAPK signalling pathway

Mitogen–activated protein kinases (MAPKs) are serine/threonine kinases responsible for transducing signals from the cell surface to the nucleus via transcription factors in order to bring about gene expression (Banuett, 1998; Lev *et al*., 1999). MAPK cascades are highly conserved in eukaryotes. They have been characterized in a diverse range of organisms, ranging from yeast to mammals (Herskowitz, 1995, Waskiewicz & Cooper, 1995). MAPK cascades regulate a variety of developmental processes in eukaryotes (Xu, 2000). MAPKs are regulated by a MAPK kinase or MEK (for MAPK/ERK kinase), which in turn is activated by

third kinases termed MAPKKK (MEKK). These proteins form a single protein complex via a scaffold protein (Ste5) in the well-characterized pheromone signalling pathway in yeast (Zhao *et al*., 2007). To date, three MAPK genes have been identified and characterized in *M. oryzae* that are instrumental in appressorium morphogenesis, invasive growth and cellular stress in *M. oryzae* (Dean, 1997; Hamer & Talbot, 1998; Xu, 2000; Zhao *et al*., 2007). *PMK1* regulates appressorium morphogenesis and pathogenicity, *MPS1* is involved in penetration and sporulation and *OSM1* is involved in osmoregulation. The homologous MAPKs in *Saccharomyces cerevisiae* are *FUS3/KSS1, SLT2* and *HOG1*, respectively (Dixon *et al*., 1999; Xu & Hamer, 1996; Xu *et al*., 1998). *PMK1* was the first MAP kinase gene identified in *M. oryzae* and is responsible for appressorium formation (Xu & Hamer, 1996). Targeted deletion of *PMK1* generated mutants able to produce normal mycelium and conidia, but unable to form appressoria and consequently non-pathogenic. Conidial attachment to hydrophobic surfaces and germination of the mutant *Δpmk1* is as efficient as the isogenic wild-type strain, but it fails to produce appressoria (Xu & Hamer, 1996). The *Δpmk1* mutant also fails to grow invasively in rice plants after inoculation through wound sites. Furthermore, *Δpmk1* is responsive to exogenous cAMP which results in hooking and swelling of the germ tube tip, but still fails to differentiate appressoria. These observations suggest that *PMK1* acts downstream of the cAMP response signal pathway and is necessary for appressorium morphogenesis (Xu & Hamer, 1996).

In *M. oryzae*, several upstream components of the *PMK1* pathway have been identified and investigated in detail (Zhao *et al*., 2007, Wilson & Talbot, 2009). These include the *MST7* MAPK kinase (MEK) and *MST11* MEK kinase, which are functional homologues of the *S. cerevisiae STE7* MAPK/ERK kinase (MEK) and *STE11* MEK kinase, respectively and the scaffold protein encoding gene *MST50*, which is a homologue of *STE50* in yeast (Zhao *et al*.,

2005; Park *et al*., 2006; Zhao & Xu, 2007; Zhao *et al*., 2007). Similar to Δ*pmk1*, mutants Δ*mst7*, Δ*mst11* and Δ*mst50* deletion mutants are impaired in appressoirum morphogenesis and are consequently non-pathogenic. A dominant active allele of *MST7* (*MST7*$^{S212D\ T216E}$) was expressed in Δ*mst7*, Δ*mst11* and Δ*mst50* mutants and resulted in appressorium formation but no lesion formation was observed. This in turn indicates that Mst11 and Mst50 are positioned upstream of the Mst7 kinase in the MAPK cascade (Park *et al*., 2006; Zhao *et al*., 2007). From yeast two-hybrid analysis no direct interaction was observed between Pmk1 and either Mst11 or Mst7 and only a weak interaction was detected between Mst11 and Mst7. Mst11 contains an N-terminal sterile α-motif (SAM) domain that is known to interact with SAM domain containing proteins. Mst50 also has a SAM domain and directly interacts with Mst11 and Mst7 but not with Pmk1. Removal of SAM domain resulted in the inability of Mst50 to interact with Mst11. These results indicate that, Mst50 may interact with the upstream components of the signalling cascade, and function as an adapter protein for the Mst11-Mst7-Pmk1 cascade and may also stabilize the Mst7-Mst11 interactions (Zhao *et al*., 2007). Bimolecular fluorescence complementation and co-immunoprecipitation provided evidence of a direct interaction between Mst7 and Pmk1 mediated by the putative MAPK docking site in Mst7 and that may occur specifically during appressorium formation (Zhao & Xu, 2007). The absence of a clear *STE5* homologue in the *M. oryzae* genome suggests that Mst50 may also serve a scaffolding function. Moreover, Δ*mst50* mutants are defective in appressorium formation and are also non-pathogenic which supports its role as a scaffold protein (Zhao & Xu, 2007).

It is believed that the final target of Pmk1 may be a transcription factor similar to Ste12 because in yeast *FUS3* and *KSS1* regulate the transcription factor encoded by *STE12*. A homologue of *STE12* has been identified in *M. oryzae*, and named *MST12* (Park *et al*., 2002).

Functional characterization of Δ*mst12* mutants revealed that the mutant is able to differentiate into melanized appressoria but non-pathogenic to susceptible rice and barley lines. Infection through wounded sites showed that Δ*mst12* mutants were defective in invasive growth and does not produce spreading lesions. Appressoria formed by the Δ*mst12* mutant exert normal turgor pressure but fail to develop a penetration peg either on cellophane membranes or plant epidermal cells (Park *et al*., 2004). The mutant Δ*mst12* also appeared to be defective in microtubule organization and lacks vertical microtubules necessary for penetration peg emergence (Park *et al*., 2004). Taken together, these results suggest that *PMK1* independently regulates appressorium formation and invasive hyphae growth through regulating a diverse set of target proteins. The Mst12 transcription factor is one of the downstream targets of Pmk1 for invasive growth *in planta*, but remaining of the transcription factor(s) downstream of Pmk1 are yet to be identified and this will be crucial for understanding the process of appressorium morphogenesis (Park *et al*., 2002, 2004; see Wilson & Talbot, 2009).

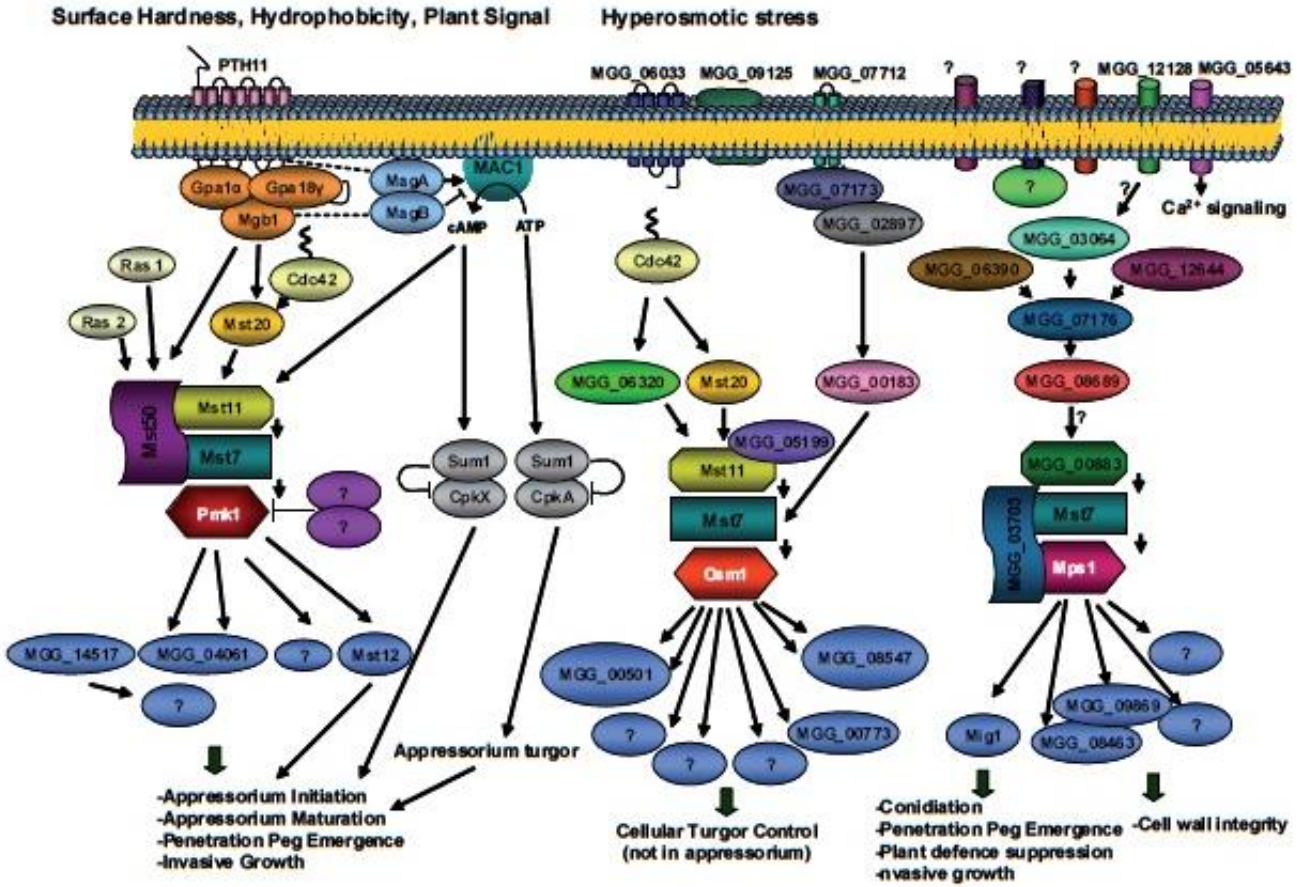

Figure 1.2: MAPK signalling pathways and the cyclic AMP signalling pathway is necessary for infection-related development in rice blast fungus *Magnaporthe oryzae.* In *M. oryzae* three MAP kinase pathways are known to be involved in the regulation of appressorium development, penetration peg formation, invasive growth and accumulation of the compatible solute arabitol in mycelia. *PMK1*, *OSM1* and *MPS1* are the functional homologues of the *FUS3/KSS*, *HOG1* and *MPS1 S. cerevisiae.* Among those pathways Only PMK1 and MPS1 pathways are essential for infection related development in *M.oryzae*. The Mst50 scaffold protein tethers the Pmk1 MAPK module to produce a phospho-relay, leading to movement of the phosphorylated Pmk1 MAPK to the nucleus, where transcription factors such as Mst12 are activated. The Pmk1 MAPK pathway regulates appressorium formation and later stages of invasive growth through the Mst12 transcriptional factor. Osm1 regulates the accumulation of the compatible solute arabitol in mycelia but not the accumulation of glycerol for generation of turgor in appressoria. Mps1 is necessary for penetration peg formation and plant tissue colonization. The Mps1 pathway may be activated through calcium signalling or protein kinase C. The transcription factor Mig1 is activated by Mps1 and is necessary for invasive growth and plant defence suppression. Activation of the Mps1 pathway may occur through calcium channel proteins (Cch1, *MGG_ 05643* or Mid1, *MGG_12128*) or protein kinase C (*MGG_08689*). The Swi4 and Swi6 homologues, *MGG_08463* and *MGG_09869* respectively may be involved in the cell wall integrity response via Mps1 Kinase pathway. Activation of the Pmk1 pathway involves Ras proteins, Cdc42, and the Gβ-subunit protein Mgb1. Crosstalk with the cAMP pathway may occur through the Gα-subunit protein MagB. The cAMP response pathway is regulated by the G proteins MagA and MagB, which potentially interact with the Pth11, the membrane bound G protein coupled receptor. Adenylate cyclase Mac1 causes the accumulation of cAMP, which binds to the regulatory protein kinase A subunit Sum1, allowing detachment of the catalytic subunit CpkA. Proteins annotated with gene numbers are *S. cerevisiae* homologues, although their functions in *M. oryzae* are not characterized. A protein annotated with a question mark has no homologue in *M. oryzae*. (Adapted from Lengeler *et al*., 2000; Xu *et al*., 1998; Xu &Hamer, 1996; Park *et al*., 2006; Rispail *et al*., 2009 and Wilson & Talbot, 2009. Provided courtesy of Romain Huguet).

1.4.4 Mps1 and Osm1 MAPK signalling pathways

A second MAPK, *MPSI* was identified in *M. oryzae* and is involved in infection related development. *MPSI* is a homologue of the *S. cerevisiae* MAP kinase-encoding *SLT2* that is involved in cell wall remodelling in response to heat and osmotic stress (Xu *et al*., 1998). This MAPK cascade is composed of the MAPKKK, Bck1; two redundant MAPKK, Mkk1 and Mkk2 and the MAPK, Slt2. The MAPKKs and MAPK in this pathway are bound by a scaffold protein Spa2 (van Drogen & Peter, 2002). Functional characterization showed that Δ*mps1* mutants can form appressoria but fail to develop a penetration peg, suggesting that penetration requires remodelling of the appressorium wall through an Mps1-dependent signalling pathway (Xu *et al*., 1998). The Δ*slt2* mutant in yeast shows hypersensitivity to cell wall degrading enzymes. The Δ*mps1* mutant showed a similar phenotype and additionally was defective in conidiogenesis (Xu *et al*., 1998). Nevertheless, Δ*mps1* mutant are able to trigger early plant defence responses and rearrange the actin cytoskeleton at the site of the penetration peg (Xu *et al*., 1998). An investigation of the Mck1 (MAPKKK) showed a similar mutant phenotype and Δ*mck1* mutants produce a significantly reduced number of conidia and form aberrant appressoria (Jeon *et al*., 2008). Moreover, Δ*mck1* mutants are hypersensitive to cell wall-degrading enzymes, undergo autolysis and are non-pathogenic (Jeon *et al*., 2008). From cytorrhysis assays, Δ*mck1* mutants were found to be impaired in turgor generation. More importantly, the mutant was unable to infect wounded leaves, indicating that this gene is necessary for *in planta* colonization (Jeon *et al*., 2008). A downstream target of the *MPS1* MAPK, the *MIG1* gene, encodes a MADS-box transcription factor homologous to *S. cerevisiae RML1*. The MADS-box domain is necessary for the function of Mig1, but dispensable for its nuclear localization (Mehrabi *et al*., 2008). Similar to Δ*mps1* mutants, Δ*mig1* mutants form normal melanised appressoria but are unable to infect susceptible rice and barley varieties (Mehrabi *et al*., 2008). The appressorium formed

by a Δ*mig1* mutant can develop penetration pegs and differentiate into primary invasive hyphae but cannot undergo differentiation to secondary infectious hyphae *in planta*. Yeast-2-hybrid analysis showed that Mig1 interacts with Mps1 protein and it is believed to function downstream of the Mps1 MAPK pathway (Mehrabi *et al*., 2008).

The third MAPK characterized in *M. oryzae* is *OSM1,* responsible for regulation of hyperosmotic stress. *OSM1* is a functional homologue of *HOG1* in yeast (Brewster *et al*., 1993; Dixon *et al*., 1999). In the budding yeast *S. cerevisiae,* the high osmolarity glycerol MAP kinase (Hog1) cascade controls glycerol synthesis in response to hyperosmotic stress (Brewster *et al*., 1993). The mutant Δ*osm1* showed sensitivity to osmotic stress and morphological defects when grown under hyperosmotic conditions. A acute osmotic stress did not affect glycerol accumulation and turgor generation in appressoria of Δ*osm1* mutants but they showed a dramatic reduction in the ability to synthesize arabitol in the mycelium. Additionally, Δ*osm1* mutants were fully pathogenic. This suggests that glycerol accumulation in appressorium turgor generation is independent of the *OSM1* MAPK cascade and distinct pathways are responsible for appressorial turgor generation and cellular turgor during hyperosmotic conditions in *M. oryzae* (Dixon *et al*., 1999).

1.5 Study of fungal pathogenicity

1.5.1 Functional genomic tools for studying fungal pathogenicity

Pathogenicity is difficult to define because of the complexity of the phenotype and involvement of a wide variety of factors at different stages of fungal development. Important developmental stages include attachment to the plant surface, spore germination, cuticle penetration, plant infection, colonization of tissue, evasion of host defences, manipulating of host metabolism, production of toxins to kill the infected host and dissemination of disease to new hosts (Dobinson and Hamer, 1992; Schafer, 1994; Talbot, 1995). Stated simply, the pathogenicity of an organism is defined as its ability to cause disease. Diverse signalling pathways, alterations in morphology and metabolism, production of effector proteins are all involved in pathogenicity. Although, saprophytic and nonpathogenic fungi have many components in common with pathogenic organisms, such as cell wall degrading enzymes, there must be discernible factors that enable pathogenic fungus to colonize living plant tissue and cause disease. Therefore, it is important to define those determinants that enable phytopathogen to cause disease in order to understand pathogenicity (Talbot, 1995). The term virulence can refer to genes that encode proteins involved in pathogenicity of an organism, those are required for full symptom development. Virulence genes may be specific for one or a few related host plants (Agrios, 1997). In order to understand pathogenicity, the development of innovative and efficient tools to investigate the biology of pathogens has always been challenging in plant pathology.

Molecular genetics approaches have led to development of new methods to identify genes involved in pathogenicity. In classical genetics, mutants were traditionally isolated by chemical or ultraviolet light mutagenesis followed by investigation for phenotypes of interest and subsequent identification of pathogenicity loci by complementation (Brown and Holden, 1998).

These techniques results in the loss or alteration of gene function by causing base pair deletions or substitutions. Genetic analysis of these mutants is labour intensive and time consuming because it needs isolation of the mutated gene by genetic complementation using a genomic DNA library generated from a wild-type strain (Brown and Holden, 1998). These disadvantages led to the advent of insertional mutagenesis by chromosomal integration of transforming DNA. The objectives of insertional mutagenesis are disruption of the genome of an organism efficiently and randomly so that genes are tagged by the transforming DNA which can then be retrieved (Mullins & Kang, 2001). Insertional mutagenesis involves delivery of fungal transformation vectors to tag genes upon their incorporation in the genome and identification of the mutated locus from the mutant of interest by conventional cloning. The presence of a suitable selectable marker links the insertion and observed phenotype and also makes the recovery of tagged DNA easier (Brown and Holden, 1998). Furthermore, fungal transformation has proven to be a suitable method for generating large mutant collection (Sweigard et al., 1998; Balhadère et al., 1999; Michielse et al., 2005; Betts et al., 2007; Meng et al., 2007). Insertional mutageneses has therefore, become an efficient tool for forward genetic study of fungal pathogenesis (Hamer *et al*., 2001; Clergeot *et al*., 2001).

.

The first *M. oryzae* strain transformed was a nonpathogenic laboratory strain using a procedure developed for *Aspergillus nidulans* (Parsons et al., 1987; Dobinson & Hamer, 1992). *M. oryzae* can be now easily transformed and transformation frequencies range between 20-50 transformants ug^{-1} of DNA (Leung et al., 1990; Valent and Chumley, 1991). The relative ease of transformation and advantage of using a number of selectable markers such as hygromycin, bialophos, sulfonylurea, phleomycin and carboxin (Weld et al., 2006), has facilitated the application of reverse genetic approaches in *M. oryzae*. Gene replacement strategies have, for example allowed the identification of many

pathogenicity genes. This has often, however involved identification of conserved genes based on homologous sequences from other organisms (Mitchell & Dean, 1995; Choi & Dean, 1997; Xu *et al*., 1997; Adachi & Hamer; 1998; Dixon *et al*., 1999; Foster *et al*., 2003; Veneault-Fourrey *et al*., 2006; Kershaw & Talbot, 2009). Another approach undertaken is differential cDNA screening which is based on identification of changes in gene expression during host infection screens (Talbot *et al*., 1993; McCafferty & Talbot, 1998). Two other similar approaches later developed that enabled genome wide differential expression analysis. Microarray and the SAGE (serial analysis of gene expression) technique involved analysis of expression changes between population in a given condition and identification of potential factors from differential display (Lorenz, 2002; Soanes *et al.*, 2012). Among other strategies, deductive approaches have also been applied to determine pathogenicity genes and their function. A landmark example of this approach was the functional characterization of components of melanin biosynthetic pathway in *M. oryzae* (Howard and Ferrari, 1989; Chumley and Valent, 1990). Furthermore, yeast two-hybrid analysis has been used to study protein-protein interactions and identification of potential interactors of implicated in pathogenicity (Fields & Song, 1989; Zhao *et al*., 2007).

1.5.2 Insertional mutagenesis as a tool for identifying pathogenicity genes

Utilization of the power of insertional mutagenesis for investigating the genetics of fungal pathogenicity requires an efficient method for generating transformants that contain random single copy insertions of transforming DNA. Several methods have been developed to achieve this goal (Brown and Holden, 1998). Fungi have been transformed with heterologous plasmid DNA carrying a selectable marker. This method has been successfully applied for identification of virulence genes from plant pathogens, such as *Ustilago maydis* (Giasson *et al.,* 1995) and *Colletotrichum lindemuthianum* (Dufresne *et al.,* 1998). Although plasmid

transformation results in single copy insertion, transformation efficiency is normally very low (Daboussi *et al.*, 1989; Hogan *et al.*, 1997; Dufresne *et al.*, 1998). The most important disadvantage of this technique however is that, in many fungi multiple plasmid DNA insertion occurs at high frequencies, either at different genomic sites or in tandem at one genomic site (Fincham, 1989; Wang *et al.*, 1988; Worsham *et al.*, 1990, Varma *et al.*, 1992)

An alternative method developed for random gene disruption in fungi is transposon mutagenesis (Kempken and Kuck, 1996; Brown and Holden, 1998; Villalba et al., 2001). Transposons are mobile genetic elements (transposable DNA), able to integrate, exit and reintegrate themselves throughout the genome (Mullins & Kang, 2001). Therefore, these self-mobile DNA segments once inserted in the genome can move from place to place. Their ability to transposes can be utilized as a mean of disrupting unknown regions throughout the genome. Transposons are suitable for generating random mutations to interrupt unknown gene function (Mullins and Kang, 2001). A Tc1-mariner transposable element named *impala* was for example, identified and characterized from *F. oxysporum* and used as a mutagenic system in different unrelated fungal species (Hua-Van *et al.*, 1998). Later, this *impala* transposon was introduced into *M. oryzae* to generate mutations. It transposed successfully and led to identification of mutants defective in mycelial growth and virulence (Villalba et al., 2001). The transposon shows considerable promise for random insertional mutagenesis of fungal phytopathogens. Transposons can for instance be engineered for heterologous host. The main advantage of transposon mutagenesis is that no transformation is required therefore and efficiency is not a limiting factor. Moreover, this strategy is particularly suitable for fungal species recalcitrant to transformation. Transposition is also relatively free from genomic lesions and rearrangements; therefore it has the potential to be applied high throughput mutagenesis technique in some fungal pathogens. However,

the major disadvantage of fungal transposon mutagenesis is its bias towards transposition into non coding regions (Firon *et al.*,2003; Ladendorf *et al.,* 2003).

The efficiency of insertional mutagenesis by plasmid transformation was significantly increased by restriction enzyme mediated integration or REMI. This technique is a further development of plasmid transformation, is based on the finding that addition of restriction enzymes during transformation is able to increase the efficiency of transformation. Therefore, REMI essentially dealt with the efficiency problem of plasmid transformation (Mullins & Kang, 2001) and was used to increase the frequency of insertional mutagenesis single-copy integrations in fungi (Kahmann and Basse, 1999). The strategy of REMI encompasses transformation of protoplasts or spores with a linearized plasmid and the restriction endonuclease (RE) used to linearize the vector (Riggle & Kumamoto, 1998). The presence of same RE in the transformation mix that is used to linearize the plasmid generates potential integration sites (cohesive ends) by inducing double stranded DNA breaks in the genome (Riggle & Kumamoto, 1998). These exposed sites are compatible with cleaved ends of transforming vector which results in a higher rate of transformation (Mullins & Kang, 2001). In *Colletotrichum graminicola*, REMI resulted in a 27-fold increase in the frequency of transformation compared to the linearized plasmid (Thon *et al.*, 2000). REMI was therefore applied to a number of phytopathogens for gene functional analysis (Maier & Schafer, 1999; Kahmann and Basse, 1999; Balhadere *et al.,* 1999).

The technique was used in *M. oryzae* and improved the transformation efficiency approximately ten-fold (Shi and Leung, 1995; Sweigard *et al.*, 1995). REMI allowed the cloning of several pathogenicity genes such as the AAL-toxin-synthesizing gene of *Alternaria alternata* (Akamatsu *et al.*, 1997) and the polyketide PM toxin of *Mycosphaerella*

zeae-maydis (Yun *et al.*, 1998). In *M. oryzae*, 27 pathogenicity mutants were identified from a collection of 5,538 REMI-generated strains and led to identification of 8 new pathogenicity loci. *PTH11*, the GPCR essential for appressorium morphogenesis was identified from this study. (Sweigard *et al.*, 1998). Another collection of REMI mutants allowed identification of 5 more pathogenicity mutants in *M. oryzae* (Balhadère *et al.*, 1999). Other important phytopathogenic fungus in which the REMI mutagenesis have been applied include the cucurbit pathogen *Colletotrichum magna* (Redman *et al.*, 1999), maize pathogen *Ustilago maydis* (Bolker *et al.*, 1995), maize and cereal pathogen *Gibberella fujikuroi* (Linnemannstöns *et al.*, 1999), maize pathogen *C.graminicola* (Epstein *et al.*, 1998; Thon *et al.*, 2000), the melon pathogen *Fusarium oxysporum* (Sanchez *et al.*, 1998) and maize pathogen *Cochliobolus heterostrophus* (Lu *et al.*, 1994).

Despite its success, REMI has some inherent limitations that challenge its success as a random insertional mutagenesis method. Estimation of the proportion of mutable genes on the basis of genome size, G+C contents and mean gene size showed that saturation mutagenesis by REMI using a 6 bp recognition RE could result insertion in half of the total number of genes in *A. nidulans* being targeted (Brown & Holden, 1998). RE directed plasmid insertions at the 3' ends of genes or in introns may however not affect gene function (Brown & Holden, 1998). Tandem insertions in a proportion of transformants were also observed that may arise from concatamers of linearized plasmid before integration or repeated homologous recombination. Dephosphorylation of the linearized plasmid to prevent concatamers formation was not even able to decrease the frequency of tandem insertion in some fungi (Shi *et al.*, 1995; Granado *et al.*, 1997; Itoh & Scott, 1997). The randomness of the REMI method is also not beyond doubt and it was hypothesized that physical packing of the genome could be responsible for non-random integrations. The most highly transcribed areas of the genome

were also proposed to be more likely to be digested by RE (a relaxed state due to transcriptional activity) than transcriptionally inactive areas because their chromatin structure is more relaxed to permit gene expression (Maier & Schafer, 1999). Therefore REMI DNA integration is not entirely random and favours highly transcribed parts of the genome (Lu et al., 1994; Sweigard et al., 1998). RE -generated double stranded DNA breaks are repaired either through vector integration or host DNA repair system. Aberrant DNA repair during REMI also results in a variety of insertion events including single insertion with deletion of flanking RE sites, large genome deletions or inversions and even ectopic integration in the absence of an appropriate RE site (Brown *et al.*, 1998; Balhadere *et al.*, 1999; Redman *et al.*, 1999; Thon *et al.*, 2000; Chung, 2003; Rogers *et al.*, 2004; Weld *et al.*, 2006). Sweigard *et al.* (1998) for example found only two thirds of the REMI pathogenicity mutants in *M. oryzae* were tagged. Similar results were reported for *Cochliobolus heterostrophus* (Lu et al., 1994), but in the case of *Ustilago maydis*, up to 50% of mutants were found to be untagged by DNA insertion (Kahmann and Basse, 1999). All of these studies proposed inaccurate DNA repair as the possible reason. The likelihood of a high proportion of untagged mutations therefore outweighs the advantages of REMI because of the difficulty in identification of mutated genes by recovery of the insert flanking sequences in such cases (Bolker et al., 1995). Furthermore, multiple insertions make the recovery of flanks time consuming and cumbersome (Mullins & Kang, 2001). In the last decade, *Agrobacterium tumefaciens* mediated transformation (ATMT) has emerged as a significant and convenient mutagenesis strategy because it overcomes the disadvantages posed by REMI. Due to its manifold advantages to tag genes involved in pathogenicity, ATMT has already been used in a number of phytopathogenic filamentous fungi. I have recorded some of the virulence genes identified by different insertional mutagenesis method from important fungal phytopathogens in Table 1.2.

Table 1.2: Examples of virulence genes of phytopathogenic fungi identified by insertional mutagenesis. In this table, a summary of virulence genes, identified in major phytopathogens using insertional mutagenesis strategy is presented.

Gene Identified	Organism	Method	Reference
PTH1, PTH2, PTH3, PTH4,PTH8, PTH9, PTH10, PTH11	*M. oryzae*	REMI	Sweigard *et al.*, 1998 (a, b)
CON1, CON4, CON5, CON6, CON7	*M. oryzae*	REMI	Shi *et al.*, 1998
ACR1	*M. oryzae*	REMI	Lau & Hamer, 1998
CLK1	*C. lindemuthianum*	Plasmid Insertion	Dufresne *et al.*, 1998
PDE1, PDE2, IGD1, MET1, GDE1	*M. oryzae*	REMI	Balhadere *et al.*, 1999
SPO11	*C. cinereus*	REMI	Cummings *et al.*, 1999
AKT1, AKT2	*A. alternata*	REMI	Tanaka *et al.*, 1999
CLTA1	*C. lindemuthianum*	Plasmid Insertion	Dufresne *et al.*, 2000
ACR1	*M. oryzae*	Transposon	Nishimura *et al.*, 2000
PLS1	*M. oryzae*	Plasmid Insertion	Clergeot *et al.*, 2001

ORP1	*M. oryzae*	Transposon	Villalba *et al.*, 2001
ARG1	*F. oxysporum*	REMI	Namiki *et al.*, 2001
CBL1, MSY1	*F. graminearum*	REMI	Seong *et al.*, 2005
MGG1	*M. oryzae*	ATMT	Liang *et al.*, 2006
APH1	*C. lagenarium*	Plasmid Insertion	Takano *et al.*, 2006
MGA1	*M. oryzae*	ATMT	Gupta & Chatto, 2007
ARG2, ADE5	*F. graminearum*	REMI	Kim *et al.*, 2007
ABC4	*M. oryzae*	ATMT	Gupta & Chatto, 2008
MCK1	*M. oryzae*	ATMT	Jeon *at al.*, 2008
ATG26	*C. orbiculare*	REMI	Asakura *et al.*, 2009
FTL1	*F. graminearum*	REMI	Ding *et al.*, 2009

Importin-β2, β-1,3(4)-glucanase Ornithine decarboxylase ATP-binding endoribonuclease Carbamoyl-phosphate synthetase N-acetylglutamate kinase N-acetylglutamyl-phosphate reductase	*C. higginsianum*	ATMT	Huser *et al.*, 2009
DES1	*M. oryzae*	ATMT	Chi *et al.*, 2009
FOXG_00016 (Hypothetical protein)	*F. oxysporum*	ATMT	Lopez-Berges *et al.*, 2009
EPI	*L. maculans*	ATMT	Remy *et al.*, 2009
COS1	*M. oryzae*	ATMT	Zhou *et al.*, 2009
GARP1	*V. dahliae*	ATMT	Gao *et al.*, 2010
PRE6	*U. maydis*	ATMT	Ji *et al.*, 2010
LDB1	*M. oryzae*	ATMT	Li *et al.*, 2010
RIC8	*M. oryzae*	ATMT	Li *et al.*, 2010
COM1	*M. oryzae*	ATMT	Yang *et al.*, 2010
EG1, HMGS, MFS1, GPI, GPIM3	*V. dahliae*	ATMT	Maruthachalam *et al.*, 2010
ZIF1	*F. graminearum*	ATMT	Wang *et al.*, 2011

SOM1, CDTF1	*M. oryzae*	ATMT	Yan *et al.*, 2011
CDC15	*M. oryzae*	ATMT	Goh *et al.*, 2011
PP2A, SPT3	*B. cinerea*	ATMT	Giesbert *et al.*, 2011
FRP1	*F. oxysporum*	ATMT	Duyvesteijn *et al.*, 2005
CHSV	*F. oxysporum*	Plasmid Insertion	Madrid *et al.*, 2003
SGE1, PAC2	*F. oxysporum*	ATMT	Michielse *et al.*, 2009
FOW2	*F. oxysporum*	REMI	Imazaki *et al.*, 2007
FSR1	*F. verticillioides*	REMI	Shim *et al.*, 2006
SAP1	*F. oxysporum*	REMI	Yoshida *et al.*, 2008
KLAP1	*C. acutatum*	REMI	Chen *et al.*, 2005
PEX6	*C. lagenarium*	REMI	Kimura *et al.*, 2001
MYP1	*U. maydis*	Plasmid Insertion	Giasson and Kronstad (1995)

TAUD, CLD, ABC2, IFR Pyruvate kinase Dynamin A Mitotic-specific cyclin B Hypothetical protein (MGG_09285.5) Hypothetical protein (MGG_02425.5) 14-3-3 protein (MGG_01588.5)	*M. oryzae*	ATMT	Betts *et al.*, 2007
RYP1, MFS, SWR1, DFG5 *SEC62, CSNB, MCH2, ATG22* *VPS17, NCA2, CHSVI, STUA* etc. (Total 111 Loci)	*F. oxysporum*	ATMT	Michielse *et al.*, 2009

1.6 *Agrobacterium tumefaciens* mediated insertional mutagenesis

1.6.1 Mechanism of *Agrobacterium tumefaciens* mediated plant infection

Agrobacterium tumefaciens is a gram negative bacterium which was identified in 1907 as the causative agent of crown gall disease (Smith and Townsend, 1907). Wounded plant cells secretee exudate includes amino acids, sugar and organic acids that attract *A. tumefaciens* to wound site and process of gall formation initiates (Winans, 1992). At the beginning *A. tumefaciens* attaches to the plant surface by acetylated polysaccharides and at a later phase by means of cellulose fibrils (Gelvin, 2000). Subsequent activation of genes leads to T-DNA transfer from the Ti plasmid (tumour inducing) and development of characteristic tumour or gall formation. Factors that are necessary for switching on the process of T-DNA transfer include acidic pH, the presence of phenolic compounds such as acetosyringone, and monosaccharides. Activation of a two-component regulatory system consists of VirA /VirG genes in the Ti plasmid are instrumental for the overall process (Figure 1.3) (Stachel *et al.,* 1986; Bolton *et al.,* 1986; Melchers *et al.,* 1989; Albright *et al.,* 1989; Winans, 1992; Winans, 1992; Lee *et al.,* 1999; Li *et al.,* 2002).

The transmembrane receptor kinase VirA is autophosphorylated upon sensing the exudate and, consequently, the cytoplasmic VirG protein is phosphorylated (Jin et al., 1990). The transcriptional activator VirG then binds to DNA and promotes expression of a set of *vir* gene operons located on the Ti plasmid. Expression of the *vir* genes induces translocation of a segment of DNA (T-DNA) from the Ti plasmid of bacterium into the plant nucleus and the T-DNA becomes integrated in plant chromosomal DNA (Winans, 1992). The *virC* and *virD* gene products are required to produce a single stranded T-DNA copy which is transferred to host cells (Michielse *et al.,* 2005). The proteins VirD1 and VirD2 perform recognition and nicking of single stranded T-DNA (Winans, 1992; Michielse *et al.,*

2005). Previously, it was postulated that DNA synthesis starts at the free 3'-OH of the right border nick and terminates at the left border repeat. This results in strand displacement and release of a single stranded T-DNA. The formation of the T-strand is stimulated by a 25-bp overdrive sequence located near the right border repeat (van Haaren *et al.*, 1987; Veluthambi *et al.*, 1988). VirC1 stimulates T-strand copying by binding to this overdrive sequence (Toro *et al*,. 1988).

The T-DNA region is flanked by ~25 bp sequence that is a cis-acting signal for the T-DNA delivery process. Once copying is completed, the protein VirD2 remains covalently attached to 5' end of T-DNA and VirE2 proteins coat the DNA fragment. Evidence suggests that VirD2 is the navigator that possesses a nuclear localization signal and therefore leads the T-DNA towards the host cell nucleus (Gelvin, 2000; Michielse *et al.*, 2005). The T-DNA is transferred from *Agrobacterium* to the plant cell by a type IV secretion system. The secretion apparatus is formed by multiple proteins encoded by the virB operon (*virB*1-11) and VirD4 protein which form a transport pore and a structure called a T-pilus. The T-pilus is composed of T-pilin, a processed form of VirB2. (Kado, 1994; Baron and Zambryski, 1996; Christie, 1997; Lai and Kado, 1998). The coupling protein VirD4 actually mediates the interaction between the T-DNA fragment and the virB protein complex in the T-pilus. The type IV secretion system also secretes virulence proteins VirE2, VirE3, and VirF in to the plant cell along with the T-DNA/VirD2 complex (Regensburg-Tuink and Hooykaas 1993; Schrammeijer *et al.*, 2003; Vergunst *et al.*, 2000, 2003).

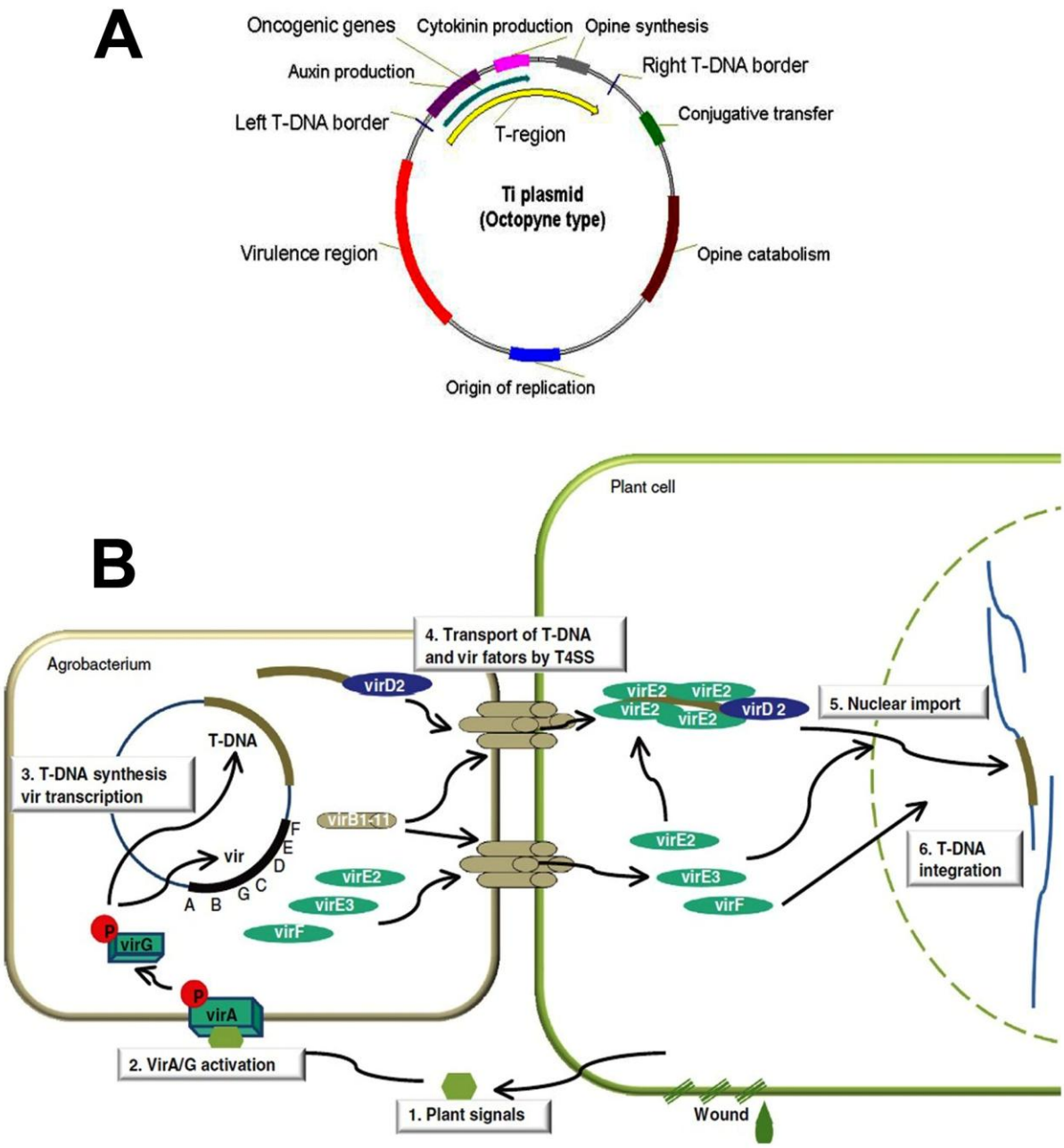

Figure 1.3: An overview of the mechanism of *Agrobacterium* T-DNA transfer and integration into host chromosome. A. Architecture of the Ti plasmid. Virulence genes are encoded by *vir* operon which is involved T-DNA transfer process. Genes carried within the T-DNA ar e expressed in host cells, and produce growth regulators auxin and cytokinin and opines for their own survival. **B. 1.** Plant signals induce VirA activation which in turn activates VirG. **2.** VirG protein activates expression of *vir* gene in *Agrobacterium*. **3.** VirC and VirD protein copy the T-DNA for transfer. VirB1-11 proteins construct a transfer channel called T-pilus through which T-DNA is transported to the host cell. VirD2 navigates the T-DNA to its destination and VirE2 protein coats it to protect from host nucleases. **4.** T-DNA is transported through a bacterial type IV secretion system (T4SS) and Vir proteins are transferred into the plant cell to assemble a T-DNA/Vir protein complex. **5.** The T-DNA complex is imported through the nuclear pore in an unfolded state into the host cell nucleus **6.** VirF protein plays a role in T-DNA integration into the host chromosomes which occurs by illegitimate recombination. (Image A obtained from www.arabidopsis.info and Image B from Pitzschke and Hirt, 2010).

VirE2 is single stranded DNA binding protein and is believed to protect T-DNA from nucleases by coating it and keeping it in an unfolded state to facilitate transfer through nuclear pore (Citovsky *et al.,* 1989). The underlying mechanism of T-DNA integration in the host genome has not yet explored in detail. It is thought that proteins encoded by *vir* genes contribute to T-DNA integration in the plant genome but host proteins play dominant roles in this process (Hooykaas and Beijersbergen, 1994; Bundock *et al.,* 1995; Gelvin, 2000; Zhu *et al.,* 2000; van Attikum *et al.,* 2001; Tzfira and Citovsky 2002;). *A. tumefaciens* infection is manifested by formation of galls or tumors. Tumorigenesis is induced by the plant hormones auxin and cytokinin which are synthesized in excessive amounts by the genes within the T-DNA. The T-DNA also contains genes responsible for producing opines which supply nutrients for the *Agrobacterium* in the plant (Ream, 1989).

1.6.2 Development of *Agrobacterium tumefaciens* as an insertional mutagenesis tool for studying fungal pathogenicity

Agrobacterium tumefaciens -mediated transformation (ATMT) AMT can be used to transform different types of tissues and in most cases does not require preparation of protoplasts that can be time-consuming (Meyer *et al.,* 2003; Michielse *et al.,* 2005). AMT is a simple method that produces significantly greater frequencies of transformation (Meyer *et al.,* 2003; Michielse *et al.,* 2005) than other approaches. Even, fungal species recalcitrant to standard transformation techniques have been successfully transformed via AMT (Weld *et al.,* 2006). A detailed description of this approach will be provided in the following section.

Initial studies on *Agrobacterium* T-DNA transfer process to plant cells demonstrated the prospect of this natural genetic engineer to plant transformation. Three salient features made

it an attractive choice for practical use. Firstly, the tumors form which upon transformation of plant cells resulted from T-DNA transfer and integration and expression of genes carried within T-DNA. Secondly, the genes carried within the T-DNA are transcribed only in plant cells and are not necessary for the transfer process. Thirdly, and most importantly, engineered DNA placed between the T-DNA borders are transferred to plant cells, irrespective of their origin. This was the main advantage that has brought out the unprecedented opportunities in plant biotechnology. There are two major regions in the 200 kb Ti plasmid. Proteins encoded by the *vir* (virulence) region are involved in the formation, transport and integration of the T-DNA in host genome. Therefore this region is indispensible for T-DNA transformation process. But the T-DNA region carrying genes encoding enzymes that produce plant growth regulators can be deleted without affecting the T-DNA transfer and used to introduce alternative genes into plants. (Zhu *et al.*, 2000; Zupan *et al*., 2000)

Replacement of the T-DNA with constructs containing selective markers and gene constructs has revolutionized plant molecular biology. These suitable features allowed the development of first vector and bacterial strain systems for plant transformation (for review Hooykaas and Schilperoort, 1992; Deblaere *et al.*, 1985; Hamilton, 1997; Torisky *et al.*, 1997). Since then, *A. tumefaciens* has become a dominant workhorse of plant molecular biology. *Agrobacterium* naturally infects only dicotyledonous plants and therefore monocotyledonous plants which include many economically important plants such as cereal crops could not be manipulated for a long time. *Agrobacterium* mediated gene transfer into monocotyledonous plants became possible after substantial effort when efficient methods were developed for rice (Hiei *et al.*, 1994; Cheng *et al.*, 1998), banana (May *et al.*, 1995), corn (Ishida *et al.*, 1996), wheat (Cheng *et al.*, 1997) and sugarcane (Enríquez-Obregón 1997, 1998). Later, *Agrobacterium* mediated transformation has played a key role in the

development transgenic varieties of agronomically important crops such as corn, canola, soybeans, potatoes, tomatoes and cotton (Gelvin, 2003) and rice (Supartana *et al.,* 2005; Hiei *et al*., 2006; Hiei and Komari, 2006; Kant *et al*., 2007; Zhang *et al*., 2007). *Agrobacterium tumefaciens* mediated transformation (ATMT) has also been used as a tool for gene functional analysis of model plants by generating large collection of loss-of-function mutations derived from random T-DNA insertion (Koncz *et al.,* 1989; Ream, 1989; Koncz *et al.,* 1992; Jeon *et al.*,2000). For instance, a collection of >225,000 T-DNA insertional strains were generated in *Arabidopsis thaliana* with the aim of saturating the genome and disrupting all the predicted genes. A total of 88,000 T-DNA insertions were mapped and approximately three quarters of the predicted genes were mutated using this method (Alonso *et al*., 2003). Thus, the feasibility of T-DNA mediated insertional mutagenesis for large scale functional genomic studies became apparent.

The breakthrough was first applied to mycology when the yeast *S. cerevisiae* was first transformed using *A. tumefaciens* (Bundock *et al.*, 1995). Afterwards, the method was successfully applied to several filamentous fungi such as *Aspergillus awamorii*, *Aspergillus niger*, *Fusarium venenatum*, *Trichoderma reesei*, *Colletotrichum gloeosporioides* and *Neurospora crassa* (de Groot *et al.,* 1998). De Groot *et al.* (1998) eventually established its promise in functional genomics research of filamentous fungi. Subsequently, a number of fungi including Zygomycetes (e.g *Rhizopus oryzae*) (Michielse *et al.,* 2004), Basidiomycetes (*Cryptococcus neoformans*) (Idnurm *et al.,* 2004) and several additional Ascomycete fungi were transformed by T-DNA insertion (Michielse *et al.*, 2005). Eventually, recalcitrant Oomycetes (e.g. *Phytophthora infestans*) (Vijn and Govers, 2003) were also transformed using this method (Michielse *et al.,* 2005). Interestingly, ATMT transformed some fungal species which were recalcitrant to other more conventional fungal transformation methods

such as *Agaricus bisporus*, *Calonectria morganii*, *Fusarium circinatum*, and *Helminthosporium turcicum* (Amey *et al.*, 2002; de Groot *et al.*, 1998; Fitzgerald *et al.*, 2003; Meyer *et al.*, 2003). The ability of *A. tumefaciens* to transfer its DNA into diverse groups of fungi indicated its potential for fungal biotechnology.

1.6.3 Advantages of ATMT for large scale insertional mutagenesis study

ATMT of plants and later in fungi utilizes the binary vector system. In this binary system, the T-DNA and the *vir* region are placed on two separate plasmids. This facilitates genetic manipulation within the T-DNA (Hoekema *et al.*, 1983; Michielse *et al.*, 2005). One of the most important advantages of using ATMT is the choice of starting material for the transformation. A range of fungal materials can be used for transformation such as conidia, vegetative hyphae, fruiting bodies and even blocks of mushroom mycelial tissue (de Groot *et al.*, 1998; Chen *et al.*, 2000). Therefore, it eliminates the necessity for time consuming protoplast preparation, which can be very variable depending on the quality of cell wall digesting enzyme preparations and fungal hyphae (Michielse *et al.*, 2005). ATMT generally results in a high percentage of transformants containing single copy T-DNA insertions (Abuodeh *et al.*, 2000; Amey *et al.*, 2002; Bundock *et al.*, 2002; Campoy *et al.*, 2003; Combier *et al.*, 2003; Covert *et al.*, 2001; de Groot *et al.*, 1998; Fitzgerald *et al.*, 2003; Hanif *et al.*, 2002; Leclerque *et al.*, 2003; Malonek and Meinhardt 2001;Michielse *et al.*, 2004; Mullins *et al.*, 2001; Rho *et al.*, 2001; Sullivan *et al.*, 2002; Tanguay and Breuil, 2003; Zwiers and De Waard 2001; Michielse *et al.*, 2005; Betts *et al.*, 2007; Michielse *et al.*, 2009). A large scale study of a collection of >55,000 transformant of ATMT transformant in *M. oryzae* showed that more than 80% were single copy T-DNA insertions (Betts *et al.*, 2007). T-DNA borders are relatively well preserved during integration into the yeast or fungal genome compared to plants. Often, T-DNA ends are found

where the Ti plasmid DNA was nicked by VirD2. This phenomenon is very significant for recovery of tagged genes (Bundock and Hooykaas, 1996).

It is also believed that the T-DNA integrates randomly in a recipient fungal genome (Abuodehet *et al.*, 2000; Bundock *et al.*, 2002; Combier *et al.*, 2003; de Groot *et al.*, 1998; Degefu and Hanif 2003; Leclerque *et al.*, 2003; Michielse *et al.*, 2004; Mullins *et al.*, 2001; Rho *et al.*, 2001; Betts *et al.*, 2007). Bundock *et al.* (2002), for example reported non-sequence specific, and random T-DNA integration patterns based on mapping a large collection of *S. cerevisiae* transformants. The integration pattern of the analyzed transformants showed 24% in upstream promoter regions, 26% in ORFs, 6% in downstream elements and 41% in intergenic regions, respectively (Bundock *et al.*, 2002). Furthermore, the frequency of ATMT transformation is higher than other methods used in filamentous fungi. Up to 800 transformants μg^{-1} of DNA can be generated compared to <40 transformants μg^{-1} of DNA in a conventional fungal-transformation experiment (de Groot *et al.*, 1998). Betts *et al.* reported similar observations when ATMT was compared with standard protoplast transformation in *M. oryzae*. By optimizing parameters such as the ratio *Agrobacterium* strain and *M. oryzae* cells and co-cultivation time, they reported that transformation can occur up to 0.3% of conidia (Betts et al., 2007). These features of ATMT have established the method as an efficient mean of generating large mutant collection of phytopathogenic fungi by insertional mutagenesis.

1.6.4 Factors affecting the efficiency of ATMT

There are several factors that must be taken into consideration and optimized for success of the deployment ATMT as an insertional mutagenesis method. These factors include the qualities of starting fungal material, the *Agrobacterium* strain, binary vector and

transformation conditions. Although a range of fungal materials can be transformed, the efficiency is not the same for different tissues or cells of an individual fungus. For example, in the case of the basidiomycete fungus *Agaricus bisporus* the transformation efficiency depends on the choice of the starting material and higher efficiencies have been observed with vegetative and fruiting body mycelia (Chen *et al.*, 2000; Mikosch *et al.*,2001) compared to germinated conidia (de Groot *et al.*, 1998; Mikosch *et al.*,2001). In some fungi, protoplasts can be used for ATMT. For instance, ATMT of *Rhizopus oryzae* and *Mucor circinelloides* were only possible with protoplasts as the recipient material and not with spores or germinated spores (Michielse *et al.*, 2005). Often, older cultures are less efficiently transformed as observed in *Blastomyces dermatitidis*. Therefore, the age of starting material also influences the efficiency of ATMT (Sullivan *et al.*, 2002).

Agrobacterium strains such as LBA4404, EHA105, and LBA1100 have been used in fungi (Michielse *et al.*, 2005). The use of supervirulent *Agrobacterium* strain A281 or its derivative AGL1 has been shown to achieve higher transformation efficiencies in *S. cerevisiae, Monascus purpureus, Phytophthora infestans* and *Cryphonectria parasitica* compared to strain LBA1100 (Piers *et al.*, 1996; Campoy *et al.*, 2003; Vijn and Govers, 2003; Park and Kim, 2004). The use of plasmids containing a constitutive mutation in the virG gene (GN54D) resulted in an increase in *Phytophthora infestans* transformation frequencies (Vijn and Govers, 2003). On the other hand, several studies reported that transformation efficiencies vary between different isolates of the same fungal species (Covert *et al.*, 2001; Fitzgerald *et al.*, 2003; Sullivan *et al.* 2002). For construction of the largest ever ATMT collection of *M. oryzae*, Betts *et al.* (2007) used two *Agrobacteirum* strains, AGL1 (containing the pCAMBIA1300 based binary vector pBHt1 or pBHt2) and EHA105 (containing the binary vector pAD1624) were used. Vector pAD1624 contains a constitutive virG gene (virGN54D)

which enables transformation without induction of acetosyringone (AS) for expression of *vir* genes (Betts *et al.*, 2007).

Another important consideration is the induction of *vir* genes in *Agrobacterium* strain during co-cultivation of transformation. For some strains, induction is necessary for T-DNA transfer. Induction may be carried out with exogenous AS before and during co-cultivation. It is critical to have acetosyringone present during the co-cultivation period because inappropriate induction of *vir* genes may lead to low transformation frequencies due to decreased T-DNA transfer (Michielse *et al.*, 2005). For some fungi, such as *Beauveria bassiana*, *Fusarium oxysporum* and *Magnaporthe oryzae*, addition of AS in the pre-culture of *Agrobacterium* is an absolute requirement for transformation and its absence led to reduced transformation frequency and a delay in the appearance of transformants (Leclerque *et al.*, 2003; Mullins *et al.*, 2001; Rho *et al.*, 2001). The concentration of AS is also subject to optimization because Leclerque et al. (2003) observed that applying up to 500 µM of AS during co-cultivation and also in pre-culture increased the transformation efficiency. Conversely, a plasmid containing a constitutively active virG gene can be advantageous to use because it avoids the application of AS (Abuodeh *et al.*, 2000).

One of the most crucial steps of ATMT is the co-cultivation period. The co-cultivation time and the temperature at which the host cell-*Agrobacterium* mixture is incubated are often the determining conditions of efficiency of an ATMT method (Mullins *et al.*,, 2001; Rho *et al.*, 2001; Combier *et al.*,, 2003; Meyers *et al.*,, 2003; Rolland *et al.*, 2003; Gardiner and Howlett, 2004; Michielse *et al.*, 2004). The optimal co-cultivation temperature range for fungal transformation is between 22ºC and 25ºC, although transformation occurs up to 37ºC (Mullins *et al.*, 2001; Rho *et al.*, 2001; Combier *et al.*, 2003; Meyers *et al.*, 2003; Rolland

et al., 2003; Gardiner and Howlett, 2004; Michielse *et al.*, 2004). When, the effect of co-cultivation time and temperature is combined, transformation frequency increases with an increase of temperature up to 28ºC during a short co-cultivation period of 24 hours. However, in the case of prolonged co-cultivation (48 hours) the increment in temperature does not have any effect but instead may lead background to fungal growth (Michielse *et al.*, 2004b). The pH of media during co-cultivation may also play a role in transformation efficiency. The optimal pH was found between 5.0 and 5.3 for ATMT of *Colletotrichum trifolii* and *Colletotrichum lagenarium* (Takahara *et al.*, 2004; Tsuji *et al.*, 2003). Furthermore, transformation efficiency is also affected by the ratio of fungal recipient cells and *A. tumefaciens* cells during co-cultivation. In most cases a higher ratio of *Agrobacterium* to fungal cells results in an increase in transformation efficiency. However, this ratio is dependent on the *Agrobacterium* strain and fungal strain used and must be optimized to achieve maximum number of transformants. Otherwise, the presence of excessive *Agrobacteirum* cells can lead to a decrease in transformation frequency (Meyer *et al.*, 2003; Michielse *et al.*, 2005). Similarly, high number of fungal recipient cells might make it more difficult to isolate individual primary transformants (Covert *et al.*, 2001). In addition, the inclusion of too many *Agrobacterium* cells may lead to excessive growth during co-cultivation that in turn causes difficulties in eliminating the bacteria form the transformants (Meyer *et al.*, 2003; Michielse *et al.*, 2005).

1.6.5 Application of ATMT for identifying novel virulence determinants in filamentous fungi

Application of ATMT as a forward genetic tool has enabled isolation of mutants with desired phenotypes and subsequent elucidation of gene function in a number of plant pathogenic fungi. Michielse *et al.* (1998) reported that at least 64 fungal species have been transformed

using ATMT by 2005 since its introduction in 1995 (Bundock *et al.*, 1995; Michielse *et al.*, 2005). This figure underlines the utility of ATMT that has led to its wide application in studying fungal pathogenicity. Some of the genes identified by ATMT from important phytopathogens are listed in Table 1.3. Pathogenicity genes have also been identified from *M. oryzae* by using *Agrobacterium* mediated insertional mutagenesis. In 2007, Jeon *and* co-workers presented a high-throughput functional genomics study of the rice blast fungus *M. oryzae* by using ATMT. The T-DNA insertions in this collection of 21,070 mutants showed coverage of 61% of the *M. oryzae* genome and enabled identification of more than 200 novel gene loci that are necessary to cause rice blast disease although very few have since been characterized (Jeon *et al.*, 2007). Another study by Betts *et al.* (2007) generated >56,000 *M. oryzae* transformants by insertional mutagenesis and >39,000 was generated by ATMT. They presented the most comprehensive ATMT mediated insertional mutagenesis and also identified more than 200 novel mutants (Betts *et al.*, 2007). Another, milestone in ATMT mediated insertional mutagenesis was achieved in the filamentous phytopathogen *Fusarium oxysporum*. Micheles *et al.* (2009) constructed an ATMT library of 10,290 *F. oxysporum* transformants and identified 111 novel pathogenicity loci through comprehensive phenotypic screening (Micheles *et al.*, 2009). Their studies showed the efficiency of this platform to identify novel determinants of pathogenicity and were the principal reason for adopting the technique in this study to investigate pathogenicity of the rice blast pathogen *M. oryzae.*

1.7 Introduction to the Current Study

During the past two decades, infection related morphogenesis has been studied extensively in the fungus *M. oryzae* and many genes required for pathogenicity have been identified. Nevertheless, our knowledge of the molecular basis of pathogenicity in rice blast disease is still limited because of the complex nature of the process. Therefore, we need to expand our current knowledge of rice blast disease through identifying novel genes and then functionally characterizing them in detail to unveil the underlying mechanism of the disease process. To answer some of the key questions in the frontiers of rice blast disease research we need to identify novel determinants of pathogenicity (Wilson & Talbot, 2009). In this study, I have applied an insertional mutagenesis based forward genetic approach to identify completely novel genes in *M. oryzae*.

In this study, I generated a library of 10,200 *M. oryzae* transformants by ATMT. I then screened this library of T-DNA insertion mutants for either loss or reduction in pathogenicity using a high-throughput qualitative pathogenicity assay. Mutants selected from primary screening were then screened through a rigorous quantitative pathogenicity assay. Following several rounds of screening I finally identified *M. oryzae* 71 mutants including 9 non-pathogenic and 62 reduced virulence mutants. I selected 8 non-pathogenic mutants for detailed phenotypic and molecular genetic characterization. In order to retrieve the T-DNA tagged genes of selected mutants, I applied next generation sequencing (NGS) for the first time in an insertional mutagenesis study of phytopathogenic fungi. Out of 8 non-pathogenic mutants, three novel genes were identified which include genes that putatively encode an unusual MAP kinase, a transcription factor and a signalling protein. The characterization of these genes is reported. In addition, two autophagic genes, *ATG2* and *ATG3* were tagged by

T-DNA insertions which have previously been shown to be essential for infection related autophagy and pathogencity. I also report characterization of *ATG3* gene.

Chapter 2

General materials and methods

2.1 Growth and maintenance of fungus stocks

The *Magnaporthe oryzae* isolates used and generated in this study are stored in the laboratory of Professor N. J. Talbot (School of Biosciences, University of Exeter). To enable long-term storage, *M. oryzae* was grown through filter paper disks (3 mm, Whatman International), which were desiccated and stored at -20°C. The fungus was routinely incubated in a controlled temperature room at 24°C with a 12-h light/12-h dark cycle. The fungus was routinely grown in complete medium (CM) (glucose, 10 g L^{-1}, peptone, 2 g L^{-1}, yeast extract, 1 g L^{-1} (BD Biosciences), casamino acids 1 g L^{-1}, trace elements (zinc sulphate heptahydrate, 22 mg L^{-1}, boric acid 11 mgL^{-1}, manganese(II) chloride tetrahydrate 5 mg L^{-1}, iron(II) sulphate heptahydrate 5 mg L^{-1}, cobalt(II) chloride hexahydrate, 1.7 mg L^{-1}, copper(II) sulphate pentahydrate 1.6 mg L^{-1}, sodium molybdate dehydrate 1.5 mg L^{-1}, ethylenediaminetetraacetic acid [EDTA] 50 mg L^{-1}), vitamin supplement [biotin, 100 µg L^{-1}, pyridoxine, 100 µg L^{-1}, thiamine, 100 µg L^{-1}, riboflavin, 100 µg L^{-1}, p-aminobenzoic acid 100 µg L^{-1}, nicotinic acid 100 µg L^{-1}], nitrate salts [sodium nitrate 6 g L^{-1}, potassium chloride 0.5 g L^{-1}, magnesium sulfate heptahydrate, 0.5 g L^{-1}, potassium dihydrogen phosphate 1.5 g L^{-1}], pH to 6.5, agar, 15 g L^{-1}) as described by Talbot *et al.* (1993). All chemicals were obtained from Sigma (Sigma-Aldrich Company Ltd., Gillingham, UK) unless otherwise stated.

2.2 Pathogenicity and infection-related development assays

2.2.1 Assays for conidial germination and appressorium formation rates

Conidial germination and the development of appressoria were monitored over time on borosilicate glass coverslips (Fisher Scientific UK Ltd.), using a method adapted from Hamer *et al.*, 1988. A conidial suspension of $5x10^4$ conidia mL^{-1} was prepared in double-distilled water and a 50 µL aliquot was placed onto the surface of the coverslips. Following incubation in a moist chamber at 24°C for 24 h, 300 conidia were counted in order to record the percentage of germinated spores as well as the percentage of spores that had developed an appressorium. Developing conidia were observed under an Olympus IX-81 inverted epifluorescence microscope fitted with an HQ^2 camera.

2.2.2 Plant infection assays

In order to assay the pathogenicity of *M. oryzae*, host (rice) infections were carried out using a dwarf Indica rice (*Oryza sativa*) cultivar CO-39, which is susceptible to rice blast disease (Valent *et al.*, 1991). Pathogenicity assays on barley were carried out using a highly susceptible cultivar, Golden Promise (Lau and Hamer, 1996). Conidia from twelve-day-old plate cultures of *M. oryzae* grown on CM agar were harvested in 3 mL of sterile deionized water. The resulting suspension was filtered through sterile Miracloth (Calbiochem) and subjected to centrifugation at 10,000 x *g* (IEC, micromax) for 5 min at room temperature. The conidial pellet was resuspended in 0.2% gelatin (BDH) to a final concentration of 5×10^4 conidia mL^{-1}. The suspension was spray-inoculated onto 14-day old (2-3 leaf stage) rice and 10-day old barley plants grown in 9 cm diameter pots (8 plants per pot) using an artist's airbrush (Badger Airbrush, Franklin Park, Illinois, USA). After spray-inoculation, plants were incubated in polythene bags for 48 h and then grown for a further 3-4 days in a controlled environment chamber (REFTECH, Holland) at 24°C with a 12 h light – 12 h dark

cycle and 90% relative humidity (Valent & Chumley, 1991). During the incubation time plants were watered daily and adequately. Characteristic rice blast disease lesion formation was monitored from 3 days post-inoculation and lesion density was recorded 5-6 days after inoculation.

2.2.2 Penetration assay on onion epidermis

Appressorium-mediated penetration of onion epidermal strips was assessed using a procedure based on that of Chida and Sisler (1987). White onions were freshly cut into 3-cm^2 pieces; the epidermal layer peeled away and soaked in chloroform for 15 min. They were then transferred in water and washed for 30 min. After washing, epidermal layers were transferred onto microscopic slides with the hydrophobic side up and dried on a paper towel. Once dried, slides were placed in a moistened chamber. Conidial suspensions at a concentration of 5 x 10^4 conidia mL^{-1} were prepared in 0.2% gelatin (BDH) and a 50 µL aliquot was inoculated onto the adaxial surface of epidermal layers and incubated at 24ºC. Penetration frequency was scored at 24-30 h after inoculation by using an Olympus IX-81 inverted epifluorescence microscope fitted with an HQ^2 camera.

2.2.3 Penetration assay on rice leaf sheath

Appressorium-mediated penetration of the rice leaf epidermis was assayed using a procedure based on that of Kankanala *et al.*, (2007). Approximately 5 cm long leaf sheath segments were collected from 3-week old rice seedlings and trimmed with a razor blade to expose the epidermis. A conidial suspension at a concentration of 1x10^5 conidia mL^{-1} was prepared in 0.25% gelatin (BDH) and the inoculum injected into the hollow space enclosed by the sides of the leaf sheath. The inoculated sheaths were then incubated in a moist container (containing wet filter paper) at 24°C for 24-48 h and in a horizontal position to let the

suspension settle on the mid-vein region. When ready for microscopy, the sheaths were trimmed to remove the sides to expose the epidermal layer and lower mid-vein cells were removed very carefully to produce sections two to three cell layers thick. This epidermal layer was then mounted on a glass slide and the tissue invasion was observed using an Olympus IX-81 inverted epifluorescence microscope fitted with HQ^2 camera.

2.2.4 Incipient Cytorrhysis assay for measurement of appressorial turgor

Incipient Cytorrhysis of appressoria was assessed following methods described by Howard *et al.* (1991) and de Jong *et al.* (1997). The method allows an estimation of appressorial turgor by determination of the concentration of extracellular solute required to cause collapse of an appressorium, which is dependent on the concentration of solutes within the appressoria. In order to assess the percentage of collapse of appressoria, a range of aqueous glycerol concentrations from 0.5 M to 4.0 M were used. A conidial suspension in ddH_2O at a concentration of $5x10^4$ conidia mL^{-1} was placed as drops of 50 µL volume on plastic coverslips and incubated in a moist container at 24°C for 24 h to allow appressoria formation. Water was then carefully removed using a pipette and replaced with an equal volume of glycerol at the indicated concentration. The number of appressoria that had collapsed after 15 minutes of exposure to the glycerol solution was determined microscopically using a Nikon Optiphot-2 microscope with Hoffman modulation contrast illumination. For each concentration of glycerol used, three replicates of 100 conidia were examined.

2.3 Nucleic acid analysis

2.3.1 Extraction of *M. oryzae* DNA

2.3.1.1 Extraction of fungal genomic DNA

For large scale extraction of genomic DNA, liquid medium was used to grow *M. oryzae*. Liquid cultures of *M. oryzae* were generated by blending a 2 cm^2 plug of mycelium into 150 mL of liquid complete medium CM in a commercial blender (Waring, Christison Scientific). The cultures were incubated at 24°C for 48 h in an orbital incubator (New Brunswick Scientific) until a mat of white fungal mycelium had formed beneath the surface of the medium. The mycelium was harvested by filtration through sterile Miracloth (Calbiochem) and blotted dry with paper towels (Kimberley Clark Corporation) in a class II microbiological cabinet. The mycelium was then placed in a clean and chilled mortar and ground to a fine powder with liquid nitrogen. The powder was then placed in 1.5 mL microfuge tubes (eppendorf) containing 500 µL of 2 x CTAB buffer (0.055 M CTAB [Hexadecyltrimethylammonium bromide, H5882, Sigma], 0.1 M Tris [Tris-Hydroxymethylaminomethane, Trisma Sigma], 0.0078 M EDTA [Ethylenediaminetetraacetic acid, 0.7 M NaCl).Samples were incubated at 65°C for 30 min with occasional shaking. An equal volume of chloroform: pentanol (24:1 v/v) was added and the tubes were shaken vigorously for 30 min at room temperature. Following centrifugation at 17,000 x *g* for 10 min using a microfuge (IEC, micromax) the supernatant was transferred to a new tube. The chloroform: pentanol (24:1 v/v) extraction was repeated again and the aqueous phase transferred to a fresh tube and an equal volume of isopropanol added to precipitate the nucleic acids. The tubes were incubated on ice for 5 min and the DNA precipitate was recovered by centrifugation in a microfuge at 17,000 x *g* for 10 min at 4°C. The supernatant was discarded and the pellet was dried on paper towels by placing the tubes on inverted position for 10 min. The nucleic acid pellet was re-suspended in 500 µL of TE buffer (10

mM Tris, 1 mM EDTA, [pH 8.0]) and then re-precipitated during a 20 min incubation at -20°C using 0.1 vol of 3 M sodium acetate (pH 5.2) and two vol of ethanol 100% (v/v). The purified nucleic acid was recovered by centrifugation for 20 min at 17,000 x *g* and washed with 500 µL of 70% (v/v) ethanol. The nucleic acid pellet was dried for 10 min in a vacuum rotary desiccator and re-suspended in 25-100 µL TE (pH 8.0) containing RNase A (10 µg mL^{-1}). Nucleic acids were quantified using a Nano Drop spectrophotometer (Thermo Scientific). To assess the quality of extracted genomic DNA, 2 µL of each samples were checked by 0.8% (w/v) agarose gel electrophoresis using 1x TAE buffer. Genomic DNA samples were routinely stored at 4°C.

2.3.1.2 Small scale extraction of fungal genomic DNA

In order to screen T-DNA insertion mutants of *M. oryzae* for copy number of insertion, complemented mutants and fungal transformants for homologous recombination events, a small scale DNA extraction protocol was followed. Cultures of *M. oryzae* were grown by placing a small plug of mycelium onto CM agar overlaid with a cellophane disc (Lakeland). The cultures were incubated at 24°C until a small mat of fungal mycelium had grown over the surface of the cellophane disc (8-12 days). The cellophane disc was then peeled from the agar plate along with the fungal mycelium, placed into a mortar and ground with a pestle to a fine powder in liquid nitrogen. The powder was placed in a 1.5 mL microfuge tube containing 500 µL of 2 x CTAB buffer and incubated at 65°C for 30 min with occasional shaking. An equal volume of chloroform: pentanol (24:1 v/v) was added and the tubes shaken vigorously for 30 min at room temperature. Centrifugation was carried out at 17,000 x g for 10 min using a microfuge (IEC, Micromax) and the supernatant transferred to new tubes. The chloroform: pentanol (24:1 v/v) extraction was repeated and aqueous phase transferred to a fresh tube and an equal volume of isopropanol added to precipitate the

nucleic acids. The tubes were incubated on ice for 5 min and the DNA precipitate was recovered by centrifugation in a microfuge at 17,000 x *g* for 10 min at 4°C. The nucleic acid pellet was re-suspended in 500 µL of TE buffer (10 mM Tris, 1 mM EDTA, [pH 8.0]) and then re-precipitated during a 20 min incubation at -20°C using 0.1 vol of 3 M sodium acetate (pH 5.2) and two vol of ethanol 100% (v/v). The purified nucleic acid was recovered by centrifugation for 20 min at 17,000 x *g* and washed with 200 µL of ethanol, 70% (v/v). The pellet was dried for 5 min in a vacuum rotary desiccator and resuspended in 50 µL of TE (pH 8.0) containing RNase A (10 µg mL^{-1}). Nucleic acids were quantified using a NanoDrop spectrophotometer (Thermo Scientific). To assess the quality of extracted genomic DNA, 2 µL of each samples were checked by 0.8% (w/v) agarose gel electrophoresis using 1 x TAE buffer, to assess the quality of extracted DNA. Genomic DNA samples were routinely stored at 4°C.

2.3.2 DNA manipulations

2.3.2.1 Digestion of genomic or plasmid DNA with restriction enzymes

Restriction endonucleases were routinely obtained from Promega UK Ltd. (Southampton, UK) or New England Biolabs (Hitchin, UK). DNA digestion was carried out using buffer solutions provided by the manufacturer. For plasmid and genomic DNA digestion, 0.2-1 µg DNA and 5-10 units of enzyme were incubated in a total volume of 30 µL at the optimum temperature for 2-4 h. For Southern blot analysis, 10 µg DNA and 20 units of enzyme in a total volume of 50 µL were incubated at the optimum temperature overnight. As an aid to DNA digestion, bovine serum albumin (BSA) at a concentration of 0.1 mg mL^{-1} was used.

2.3.2.2 DNA gel electrophoresis

Digested DNA was fractionated by gel electrophoresis in agarose gel matrices, 0.8% (w/v) using a 1 x TBE buffer (TBE 90 mM, EDTA 2 mM) and ethidium bromide (final concentration 0.5 µg mL^{-1}) was added in the agarose gel to help visualization. To determine the size of DNA fragments, 1 kb plus size marker (Invitrogen) was used during gel electrophoresis. Fractionated DNA fragments were visualized using a UV transilluminator (UVP, inc.) and with a gel documentation system (Image Master VDS) with a Fujifilm Thermal Imaging system, FTI-500 (Phamacia Biotech).

2.3.2.3 Amplification of DNA by Polymerase Chain Reaction (PCR)

DNA fragments were routinely amplified by polymerase chain reaction (PCR). PCR reactions contained: 50-100 ng template DNA, forward and reverse primers, 800 ng of each, magnesium chloride, 2.5 mM, 10x reaction buffer (potassium chloride, 0.5 M, Tris-HCl, 0.1 mM (pH 9 at 25 ºC) and Triton X-100, 1%), deoxynucleotide triphosphates (Amersham Biosciences) 0.2 mM of each, DNA polymerase 1.5 units and water (Sigma) to a total volume of 25 µL. GoTaq® Flexi DNA polymerase (Promega) was the DNA polymerase used for routine amplification. To amplify longer targets or when high fidelity amplification was required, Herculase® DNA polymerase was used. Routinely, PCR amplification reactions were performed in an Applied Biosystems GeneAmp®PCR system 2400 cycler. An initial denaturation step was carried out at 94ºC for 5 min, followed by PCR cycling parameters of: 94ºC for 30 s, 55-62ºC for 30 s and 72ºC for 1 min/kb target length for 30-35 cycles, followed by a final extension at 72ºC for 10 min. Amplified PCR products were gel-purified prior to ligation or other applications.

2.3.2.4 Gel purification of DNA fragments

DNA fragments were purified from agarose gels using a commercial kit (Wizard® SV Gel and PCR Clean-Up System) according to the manufacturer's instructions (Promega). Fragments were excised from the gel using a razor blade and placed in a pre-weighed 1.5 mL microfuge tube. The gel fragment was weighed and an equal volume of Membrane Binding solution (4.5 M guanidine isothiocyanate, 0.5 M potassium acetate, pH 5.0) was added. Samples were incubated at 65 °C and mixed by vortexing every 2-3 min until the gel slice had dissolved. Once dissolved, the solution was placed in a Wizard® SV Minicolumn held in a 2 mL collection tube and subjected to centrifugation for 1 min at 17,000 x *g* in a microfuge (IEC, Micromax). Then the flow-through was discarded and the column was placed back in the collection tube. To wash the membrane-bound DNA, 700 µL of Membrane Wash Solution (potassium acetate, 10 mM (pH 5.0), ethanol 80%, EDTA 16.7 µM (pH 8.0)) was added in the column and centrifugation carried out for 1 min at 17,000 x g. The flow-through was discarded and the wash repeated with 500 µL of Membrane Wash Solution for 5 min at 17,000 x *g*. The flow-through was discarded and the column processed by centrifugation for an additional min at 17,000 x *g*. The Wizard® SV Minicolumn was placed in a clean 1.5 mL microfuge tube and 30 µL of sterile nuclease-free water was added in the column. Following incubation at room temperature for 1 min, the DNA was eluted by centrifugation for 1 min at 17,000 x *g*. The gel purified DNA was routinely stored at -20 °C.

2.3.2.5 DNA sequence analysis

All DNA sequence analyses were carried out at Eurofins MWG Operon (Anzinger Str. 7a, 85560 Ebersberg, Germany).

2.3.2.6 Southern blot analysis

Blotting of agarose DNA gels was performed according to Southern (1975). Each gel was submerged in 0.25 M HCl for 15 min to de-purinate the fractionated DNA and then denatured by immersing in denaturing solution (NaOH 0.4 M, NaCl 0.6 M) for 30 min. The gel was then neutralized by neutralization buffer (NaCl 1.5 M, Tris-HCl 0.5 M, [pH 7.5]) for 30 min before capillary blotting onto Hybond-N (Amersham Biosciences). Gel blots were performed by placing the inverted gel onto a sheet of filter paper wick, which was supported on a perspex sheet with each end of the wick submerged in 20xSSPE solution (NaCl 3.6 M, NaH_2PO_4 200 mM, EDTA 22 mM). Hybond-N membrane was then placed onto the gel and overlaid with five layers of wet Whatman 3 mm paper and five layers of dry Whatman 3 mm paper onto which a 10 cm high pile of paper towels (Kimberley Clark Corporation) was placed. Exposed areas of perspex sheet were covered by cellophane to minimize the loss of SSPE by evaporation. At the end, a 500 g weight was placed on the stack and the blot was left to stand at room temperature overnight. The Hybond-N membrane was removed by dismantling the blot and air dried for an hour. The transferred DNA was UV cross-linked to the membrane using a BLX crosslinker (Bio-link®).

2.3.2.7 Radiolabelled DNA probe construction

DNA hybridisation probes were labelled by the random primer method (Feinberg & Vogelstein, 1983) using a Ready-To-Go kit (Amersham Biosciences) according to the manufacturer's instructions. A 50 ng aliquot of DNA was made to a final volume of 47 µL in nuclease free water. The sample was boiled for 5 min to denature the DNA and then rapidly chilled on ice for 2 min. The tube was briefly subjected to centrifugation and the contents were added to a Ready-To-Go reaction mix bead, containing buffer, dATP, dGTP, dTTP, FLPCpure™ Klenow Fragment (7-12 units) and random oligodeoxyribonucleotides,

primarily 9-mers. The reagents were mixed by gently pipetting and 2 µL of [α-^{32}P] dCTP (3,000 Ci/mmol) added. The labelling reaction was then incubated at 37 °C for 10 min before being stopped by addition of 100 µl of labelling stop dye (SDS 0.1%, EDTA 60 mM, bromophenol blue 0.5%, blue dextran 1.5%). Un-incorporated isotope was removed by passing the labelling reaction through a Biogel P60 (Bio-Rad) column, and collecting the dextran blue-labelled fraction. The probe was denatured by heating at 100°C for 5 min and quenched on ice for 2 min, before adding to the hybridisation mixture.

2.3.2.8 Hybridization conditions

DNA gel blot hybridisations were performed using standard procedures (Sambrook *et al.*, 1989). Blots were incubated in hybridisation bottles (Hybaid Ltd.) in a hybridisation oven (Hybaid) for 4 h at 65°C in 30 ml of pre-hybridisation solution (6 x SSPE diluted from a 20 x stock [NaCl 3M, $NaH_2PO_4.H_2O$ 0.2 M, EDTA 25 mM, adjusted to pH 7.4 with NaOH 10 M], 50 x Denhardt's solution [diluted from a 50 x stock prepared with 5 g Ficoll {type 400, Pharmacia}, 5 g polyvinylpyrrolidone in 500 mL double distilled water], SDS 0.5%)) with 200 µL denatured Herring sperm DNA (1% [w/v] in NaCl 0.1 M) (Sigma). A denatured radiolabelled probe was then added to the mixture and incubated overnight at 65 ˚C. Following hybridisation for 16-18 h, the blot was washed at high stringency. The pre-hybridisation solution was removed along with any unbound probe and 30 ml of 2 x SSPE wash solution (SDS 0.1%, sodium pyrophosphate [PPi] 0.1%, 2 x SSPE [diluted from the 20 x SSPE stock] [pH 7.4]) was added. The mixture was then incubated for 30 min at 65°C. Then the wash solution was removed and replaced with 30 ml of 0.2 x SSPE wash solution (SDS 0.1%, sodium pyrophosphate [PPi] 0.1%, 0.2 x SSPE [pH 7.4]) and the blot was incubated for 30 min at 65°C. After discarding the washed solution the membrane was air dried 3for 1h. Autoradiography was carried out by exposing membranes to X-ray film (Fuji

medical X-ray film, Fuji Photo Film (U.K.) Ltd.) at -80°C in the presence of an intensifying screen (Amersham). X-ray films were developed using Kodak chemicals in an OPTIMAX X-Ray Film Processor (Protec).

2.4 DNA cloning procedures

2.4.1 Bacterial DNA mini preparations (Alkaline Lysis Plasmid Miniprep)

Small-scale preparations of plasmid DNA from bacterial colonies were made by modifying a larger scale method based on Sambrook *et al.* (1989). Single bacterial colonies were picked and used to inoculate 4 mL Luria-Bertani broth (LB) (tryptone 10 g L^{-1}, yeast extract 5 g L^{-1}, sodium chloride 10 g L^{-1}, [pH 7.5]) containing the appropriate antibiotic in a universal bottle. Cultures were grown overnight at 37 °C, with vigorous aeration (225 rpm) in an Innova 4000 rotary incubator (New Brunswick Scientific). For long-term storage of bacterial cells a fraction of the initial 4 mL culture was retained to make a glycerol stock. For this, an 800 µL aliquot of bacterial solution was added to 1.5 mL microfuge tubes containing 200 µL of sterile glycerol (100%). The suspension was vortexed rapidly and stored at -80 °C. The remaining culture was transferred to fresh 1.5 mL microfuge tubes and harvested by centrifugation at 5,000 x *g* (IEC, Micromax) for 5 min. The supernatant was removed by aspiration and the bacterial pellet re-suspended in 200 µL of ice-cold cell re-suspension solution (glucose 50 mM, Tris-HCl 25 mM [pH 8.0], EDTA 10 mM [pH 8.0]) by vigorous vortexing using a Whirlimixer (Fisher Scientific). Then 400 µL of freshly prepared lysis solution (NaOH 0.2 M [freshly diluted from a 10 M stock], SDS 1%) was added to the resuspended cell and mixed by rapid inversion, ensuring that the entire surface of the tube came into contact with the solution. The tube was placed on ice for 5 min and then 300 µL of ice-cold neutralisation solution (potassium acetate 3 M, glacial acetic acid 11.5% [v/v]) was

added and the contents mixed by vortexing gently in an inverted position for 10 s. The tube was stored on ice for 3-5 min, and processed by centrifugation at 12,000 x *g* for 5 min in a microfuge. The supernatant was transferred to a fresh tube and the double-stranded DNA was precipitated using an equal volume of isopropanol (propan-2-ol) at room temperature. The mixture was vortexed and allowed to stand for 2 min at room temperature. Precipitated DNA was recovered by centrifugation at 17,000 x *g* for 10 min at 4ºC and the resulting supernatant decanted. The precipitated nucleic acids were washed with 1 mL 70% (v/v) of ethanol at 4 ºC and centrifugation carried out at 17,000 x *g* for 5 min in a microfuge. The supernatant was discarded and the pellet dried for 5 min in a vacuum rotary dessicator (microfuge rotary concentrator 5301, in dessicator mode). The pellet was re-suspended in 50 µL TE (Tris-HCL 10 mM [pH 7.5], EDTA 1 mM [pH 8.0]) containing DNase-free pancreatic RNase (20 µg mL^{-1}) and incubated at 37°C for 30 min. The DNA preparations were stored at -20ºC.

2.4.2 High quality plasmid DNA preparations

High quality plasmid DNA for sequencing or fungal transformation was prepared using a commercially available kit (Promega PureYield™ Plasmid Midiprep System, Cat. No. A2492) following manufacturer's instructions. Single bacterial colonies were picked and used to inoculate 50-100 mL Luria-Bertani broth (LB) (tryptone 10 g L^{-1}, yeast extract 5 g L^{-1}, sodium chloride 10 g L^{-1}, [pH 7.5]) containing the appropriate antibiotic in a duran bottle (Scott). Cultures were grown overnight (16 h) at 37 °C, with vigorous aeration (225 rpm) in an Innova 4000 rotary incubator (New Brunswick Scientific). Cultures of Bacterial cells were recovered by centrifugation in a 50 mL tube (Falcon 2059, BD Biosciences) at 10,000 x *g*, re-suspended in 3 mL of cell resuspension solution (Tris-HCL 50 mM [pH 7.5], EDTA 10 mM, RNase A 100 µg mL^{-1}). Then 3 mL of cell lysis solution (NaOH 0.2 M, SDS 1%) was added and the contents mixed by gently inverting the tubes 3-5 times. The tube was incubated for 3

min at room temperature and 5 mL of neutralization Solution (4.09 M guanidine hydrochloride [pH 4.2]), 759 mM potassium acetate, 2.12 M glacial acetic acid) was added to the lysed cells and mix by gently inverting the tube 5–10 times. The lysate was transferred into an oakridge tube and subjected to centrifugation at 15,000 × g for 15 minutes at room temperature using a swinging bucket rotor (JS13.1 swinging bucket rotor in a Beckman J2-MC high-speed centrifuge). A column stack was assembled by nesting a PureYield™ Clearing Column (blue) on the top of a PureYield™ Binding Column (white). The assembled column stack was placed onto the vacuum manifold. Then the cleared lysate was carefully decanted into the PureYield™ clearing column. Once the column was ready, the vacuum was applied until all the lysate had passed through both columns. The vacuum was released and PureYield™ clearing column removed, leaving the PureYield™ binding column on the vacuum manifold. Then 5.0ml of Endotoxin removal wash (guanidinium chloride 50-75%, propan-2-ol 55 mL added in 15 mL of concentrate) was added to the column and the vacuum was applied to pull the solution through the column. After that 20mL of Column wash solution (ethanol 60%, KOH 60mM, Tris-HCl 8.3mM and EDTA 0.04mM.) was added into the column and the vacuum applied to draw the solution through. The membrane was allowed to dry completely by applying a vacuum for 30 seconds to 1 minute. The PureYield™ binding column was removed from the vacuum manifold and placed into a sterile 50mL tube (Falcon™). Then 600 µL of nuclease free water was added to the DNA binding membrane in the column and subjected to centrifuge 2,000 × g for 5 minutes. Finally, the filtrate was collected from the 50mL tube and transferred to a sterile 1.5mL microfuge tube. The DNA preparations were stored at -20ºC.

2.4.3 DNA ligation and selection of recombinant clones

For routine cloning of amplicons, the pGEM-T vector (Promega) was used. The pGEM-T vector allows T**:**A cloning of PCR fragments generated by certain thermostable DNA polymerases (*Taq* polymerase) and facilitates the selection of recombinant clones using α-complementation of lacZ (Sambrook et al., 1989). DNA fragments amplified by polymerase not compatible with T**:**A cloning were heated at 70ºC for 30 min in the presence of 0.2 mM dATPs, 5 units of *Taq* polymerase, 10x *Taq* polymerase buffer and 2.5 mM $MgCl_2$ in a total volume of 10 µL before cloning in order to add a Poly $(A)^+$ tail to facilitate cloning into pGEM-T. DNA fragments amplified by the polymerase chain reaction (PCR) were gel-purified and then ligation reactions were carried out in a total volume of 10 µL, using 10 x reaction buffer (Tris-HC, 300 mM [pH 7.8 at 25°C], $MgCl_2$ 100 mM, dithiothreitol [DTT] 100 mM and ATP 10 mM) (Promega), T4 DNA ligase 3 units (Promega), and vector and insert DNA at a 1:3 molar ratio. Ligation reactions were incubated for 3 h at room temperature. Ligations into the pGEM-T vector were incubated overnight at 4ºC.

To clone restriction enzyme digested DNA in other vectors; treatment with calf intestinal alkaline phosphatase (CIAP) (NEB) was carried out to prevent re-circularization of digested DNA. In a restriction digest of 30 µL, 3.5 µL of NEB buffer 3 (NaCl 100 mM, Tris-HCl 50 mM, $MgCl_2$ 10 mM, DTT [dithiothreitol] 1 mM , 1 µL of CIAP and 0.5 µL of nuclease free water H_2O was added to make a total volume of 35 µL. The mixture was then incubated at 37°C for 1 h. Finally, the digested DNA was gel purified and ligation reaction prepared. Routinely, vector and insert were added to the ligation mixture at 1:3 molar ratio and the reactions carried out in a total volume of 10 µL using 3 units of T4 DNA ligase (Promega) and 10 x T4 DNA ligase buffer (Promega). Ligation reaction was incubated overnight at 4ºC.

For the efficient cloning of weakly amplified PCR products or for DNA fragments > 5 kb, the StrataClone™ PCR Cloning Kit (Agilent Technologies) were used according to the manufacturer's instructions. StrataClone PCR cloning technology exploits the combined activities of topoisomerase I from *Vaccinia* virus and Cre recombinase from bacteriophage P1. This vector allows lac*Z*' α-complementation cassette for blue-white screening of recombinant clones. For StrataClone cloning reactions, 50 ng of insert DNA was added to 3 µL StrataClone™ cloning buffer and 1 µL StrataClone™ vector mix in a total volume of 6 µL. Reactions were incubated for 5 min at room temperature and then placed on ice.

2.4.4 Preparation of competent cells

Stocks of laboratory-prepared transformation-competent cells were generated using a protocol adapted from Sambrook *et al*. (1989). Single bacterial colonies were obtained by streaking bacterial cells across a plate of LB (tryptone 10 g L-1, yeast extract 5 g L-1, sodium chloride 10 g L-1, agar 18 g L-1, (pH 7.5),) and incubating at 37°C for 16 h. A single colony was used to generate an overnight culture in 10 mL LB broth (37°C, 200 rpm). A 2.5 mL aliquot of this culture was inoculated into 250 mL of SOC (tryptone 20 g L^{-1}, yeast extract 5 g L^{-1}, sodium chloride 8.6 mM, magnesium sulphate 10 mM, magnesium chloride 10 mM) and this was allowed to grow until an OD_{600}=0.6 had been reached (Sambrook *et al.*, 1989). The culture was then transferred to a 50 mL Oakridge tube and incubated on ice for 10 min. Cells were recovered by centrifugation at 2,510 x g (Beckman J2-MC, JS13.1 rotor) for 10 min at 4°C. To each tube, 15 mL filter-sterilised FSB (potassium acetate 10 mM [pH 7.5], manganese(II) chloride 45 mM, calcium chloride 10 mM, potassium chloride 100 mM, hexamine-cobalt chloride 3 mM, glycerol 10% [pH 6.4]) was added and the cells were re-suspended by gentle pipetting. Samples were incubated on ice for 10 min and the centrifugation step repeated once. The cells were then re-suspended in 4 mL FSB and

dimethyl sulfoxide was added to a final concentration of 3.4% (v/v). The resulting mixture was incubated on ice for 15 min and a further volume of dimethyl sulfoxide was added, such that the final concentration reached 6.5% DMSO (v/v). The cells were then dispensed into 100 µL aliquots in pre-chilled microfuge tubes. Samples were immediately frozen by immersion in liquid nitrogen and stored at -80 °C.

2.4.5 Transformation of bacterial hosts

Transformation was routinely carried out using *Escherichia coli* strain XL-1 Blue (Stratagene). XL1–Blue has a genotype supE44 hsdR17 recA1 endA1 gyrA46 thi relA1 lac-[F′ pro AB+ lacIq lacZΔM15 Tn10 (tet r)]. A 100 µl aliquot of competent cells was decanted into pre-chilled 15 ml tubes (Falcon 2059, BD Biosciences). The tubes were incubated on ice for 10 min before 50 ng DNA was added and the mixture incubated on ice for a further 30 min. Cells were heat-shocked at 42 °C for 45 s and then transferred to ice for 2 min. At this point, 800 µl of SOC (tryptone 20 g L-1, yeast extract 5 g L-1, NaCl 0.5 g L-1, glucose 20 mM, $MgSO_4$ 10 mM, $MgCl_2$ 10 mM) preheated to 42ºC, was added to each tube and the recovering cells were incubated at 37°C for 1 h with gentle shaking (125 rpm). Aliquots were plated on LB agar with the appropriate antibiotic. Where α-complementation selection was available (Sambrook *et al.*, 1989) the agar contained isopropyl-thiogalactoside (IPTG, 0.8 mg mL^{-1} per plate) (Calbiochem [VWR International Ltd.]) and 5-bromo-4-chloro-3-indolyl-β-D-galactopyranoside (X-gal 0.8 mg mL^{-1} per plate) (Calbiochem [VWR International Ltd.]). Plates were inverted and incubated at 37 °C overnight.

Bacterial transformation of StrataClone ligation reactions was carried out using SoloPack competent cells. StrataClone SoloPack competent cells are optimized for high efficiency transformation and recovery of high-quality recombinant DNA. The cells are endonucleases

(*end*A) and recombination (*rec*A) deficient and are restriction deficient. The cells lack the tonA receptor, conferring resistance to T1, T5, and φ80 bacteriophage infection and lack the F´ episome. StrataClone SoloPack competent cells are resistant to streptomycin. An aliquot of 2 µL of the ligation reaction was added to 50 µL of competent cells and incubated on ice for 20 min. Cells were heat-shocked at 42°C for 45 s and then transferred to ice for 2 min. At this point, 250 µL of LB (tryptone 10 g L^{-1}, yeast extract 5 g L^{-1}, NaCl 10 g L^{-1}, [pH 7.5]) was added to the cells which were then incubated at 37 °C for 1 h with gentle shaking (125 rpm). Aliquots were placed on LB agar with the appropriate antibiotic and X-gal (0.8 mg mL^{-1} per plate) (Calbiochem [VWR International Ltd.]) for blue-white screening, plates were inverted and incubated at 37 °C overnight.

2.4.6 Recombination-mediated PCR-directed cloning in yeast

The yeast uracil auxotrophic *ura3* (-) strain used for transformation was grown in 3 mL YPD medium (Yeast extract 10 g L^{-1}, peptone 20 g L^{-1}, D-Glucose 20 g L^{-1}) at 30^{o}C for overnight with 225 rpm. Prior to transformation 2 mL of overnight culture was inoculated in to 50 mL YPD medium and grown at 30^{o}C for 4-5 h with 225 rpm. The cells were precipitated by centrifugation at 1500 x *g* for 5 min at room temperature. After discarding the supernatant, the cell pellet was thoroughly resuspended in 10 mL dist water and the cells were precipitated by centrifugation at 1500 x *g* for 5 min at room temperature. After washing, the supernatant was removed and cell pellet resuspended in 300 µL of distilled water. In a fresh eppendorf tube 50 µL denatured herring sperm DNA (1% [w/v] in 0.1 M NaCl), an equal amount of linearized vector and insert (~ 500 ng), 50 µL yeast cells, 32 µL 1 M lithium acetate (in H_2O) and 240 µL 50% PEG 4000 (w/v in H_2O) were added per transformation. The ingredients were mixed by pipetting up and down and the tubes were incubated at 30°C for 30 min. After that, tubes were incubated at 45°C for 15 min. Tubes were removed from heat shock

immediately after 15 min and cells precipitated by centrifugation at 1500 x *g* for 2 min at room temperature. The supernatant was removed completely with pipette and the cells resuspended in 200 µL H_2O. From the resuspended cells, 20 µL was transferred into fresh eppendorf tube and 180 µL of water added. Both the aliquots of cells (diluted and concentrated) were spread on yeast synthetic dropout media (Glucose 20 g L^{-1}, yeast nitrogen base w/o amino acids 1.7 g L^{-1}, ammonium sulphate 5 g L, casein hydrolysate 5 g L^{-1}, adenine 20 mg L^{-1}, tryptophan 20 mg L^{-1} and agar 20 mg L^{-1}) plates. Plates were incubated at 30^{o}C for until transformants appeared (~2-3 days).

2.4.7 Extraction of yeast plasmid DNA from yeast cells

Selected yeast colonies were transferred from plate into 50 mL yeast synthetic drop-out medium (YDM) and the cultures grown for 36 h at 30^{o}C with continuous shaking at 125 rpm. The cells were precipitated by centrifugation for 5 min at 1500 x *g*. The pellet was resuspended in 500 µL sterile distilled water. Cells were precipitated again by centrifugation for 5 sec at 17,000 x *g*, supernatant discarded and resuspended in residual water by vortexing. To this, 200 µL of yeast lysis buffer, 200 µL of phenol: chloroform: iso-amylalcohol (25:24:1) and 0.3 g of acid-washed glass beads (425-600 µm) were added. The tubes were vortexed vigorously at 2000 rpm for 30 min and 200 µL TE (pH 8.0) added. The tubes were subjected to centrifugation for 5 min at 17,000 x *g* and the aqueous phase transferred to a new tube. A 50 µL aliquot of 3 M sodium acetate (pH 5.5) and 1 mL of absolute ethanol were added and the tubes incubated for 30 min at -20^{o}C. Following centrifugation 17,000 x *g* for 20 minutes, the supernatant was discarded. The pellet was resuspended in 400 µL of TE and treated with 4 µL RNase A (10 mg mL^{-1}) at 37^{o}C until the pellet was dissolved. A 10 µL aliquot of 4 M ammonium acetate and 1 mL of absolute ethanol were added to the mixture. The mixture was processed by centrifugation at 17,000 x *g* for 2 minutes and supernatant was

discarded. The pellet was washed with 500 µL of 70 % ethanol. The remaining pellet was air-dried and resuspended in 20 µL of distilled water. In order to recover more DNA for fungal transformation, 10 µL of the extracted plasmid was transformed into *E. coli*.

2.5 DNA-mediated transformation of *M. oryzae*

A 2.5 cm^2 section of *M. oryzae* mycelium was removed from a CM plate culture, blended in 150 ml complete medium and incubated at 24°C with shaking at 125 rpm in an orbital incubator for 48 h. The mycelium was harvested by filtration through sterile Miracloth (Calbiochem) and washed in sterile distilled water. The mycelium was transferred to a Falcon tube (Becton Dickinson) with 40 mL OM buffer ($MgSO_4$ 1.2 M, $Na_2HPO_4$10 mM (pH 5.8), Glucanex 5% [Novo Industries, Copenhagen]) and shaken gently at 75 rpm for 3 h at 30 °C in an orbital incubator. The resulting protoplasts were transferred to sterile polycarbonate Oakridge tubes (Nalgene) and overlaid with an equal volume of cold ST buffer (sucrose 0.6 M, Tris-HCl 0.1 M [pH 7]). Protoplasts were recovered by centrifugation at 5000 x *g*, for 15 min at 4 °C in a swinging bucket rotor (Beckman JS-13.1) in a Beckman J2.MC centrifuge. The protoplasts were recovered at the OM/ST interface and transferred to a sterile Oakridge tube, which was filled with cold STC buffer (sucrose 1.2 M, Tris-HCl 10 mM (pH7.5), $CaCl_2$ 10 mM). Protoplasts were precipitated at 3,000 x *g* for 10 min at 4 °C, (Beckman JS-13.1 rotor), washed twice more with 10 ml STC, with complete re-suspension each time. After re-suspending in 1 mL of STC, the concentration of protoplasts was determined by counting using a haemocytometer (Corning).

DNA-mediated transformation of *M. oryzae* was carried out in 1.5 ml microfuge tubes by combining an aliquot of purified protoplasts (10^7 mL^{-1}) with DNA (4-8 µg) in a total volume of 150 µL. The mixture was incubated at room temperature for 25 min and then 1 ml of PTC

(PEG 4000, 60%, Tris-HCl 10 mM [pH 7.5], $CaCl_2$ 10 mM) was added in 2-3 aliquots and mixed by gentle inversion. The mixture was incubated at room temperature for 20 min then added to 150 mL molten (46°C) 1.5% agar/OCM (CM osmotically stabilised with 0.8 M sucrose), mixed gently and poured into 5 sterile petri dishes (~30 mL $plate^{-1}$), as described by Talbot *et al.* (1993).

For selection of transformants on hygromycin B (Calbiochem), plate cultures were incubated in the dark for at least 16 h at 24 °C and then overlaid with approximately 15 mL of CM/1.5% agar containing 200 µg mL^{-1} (freshly diluted from a stock of 50 mg mL^{-1}) hygromycin B. For selection of bialophos or Basta (glufosinate ammonium) resistant transformants, BDCM/1.5% agar (yeast nitrogen base without amino acids and $((NH_4)_2SO_4$, 1.7 g L^{-1} [Difco], NH_4NO_3 2 g L^{-1}, asparagine 1 g L^{-1}, glucose 10 g L^{-1}, sucrose 0.8 M [pH 6]) was used instead of OCM. In the overlay, CM was replaced with BDCM/1% agar (without sucrose) and glufosinate ammonium at a concentration of 30 µg mL-1 was added in it. For selection of Chlorimuron ethyl (sulfonylurea) resistant transformants, BDCM/1.5% agar was used instead of OCM and overlaid with of BDCM/1% agar (without sucrose) containing 150 µg mL^{-1} Chlorimuron ethyl (freshly diluted from a stock solution of 100 mg mL^{-1} in DMF). When overlaid with BDCM/1% agar, approximately 15 mL was used for each plate. Transformants were selected after growing for 12 days at 24°C (Sweigard *et al.*, 1997) and transferred to selection plated for further processing.

Chapter 3

Construction and screening of an ATMT Library of *Magnaporthe oryzae*

3.1 Introduction

In this chapter I report the construction of a large mutant collection of *Magnaporthe oryzae* by insertional mutagenesis. We have exploited the ability of *Agrobacterium tumefaciens* to insert its T-DNA into the genome of the fungus in a random fashion (de Groot *et al.*, 1998). In order to identify potential novel determinants of pathogenicity, a collection of 10,000 random insertion mutant lines of *M. oryzae* was generated using the wild-type strain Guy11. We also developed a high-throughput screening regime to determine whether mutants were impaired in their ability to cause disease in rice plants. The entire mutant library was screened using this high-throughput procedure and we identified a collection of mutants that were either reduced in virulence or non-pathogenic.

A number of molecular techniques have been developed to study pathogenicity in fungal pathogens. A forward genetics approach for defining genes those are essential or important for disease starts by identifying mutants defective in pathogenicity. Insertional mutagenesis offers a mechanism not only for identifying mutants of interest but also for cloning the corresponding genes (Sweigard *et. al.*, 1998; Balhadére *et. al.*, 1999; Betts *et al.* 2007; Jeon *et al.* 2007;). This process has been shown to have potential for discovering novel genes that encode determinants of pathogenicity. Insertional mutagenesis approaches have been successfully used in *M. oryzae* in order to identify novel pathogenicity genes (Balhadére

et al., 1999; Sweigard *et al.*, 1998). In these studies, a limited number of insertion strains were generated using less efficient REMI (restriction enzyme mediated insertion) and screened for defects in pathogenicity. Balhadére *et al.* (1999) screened 1,150 REMI mutants of *M.oryzae* and tagged five loci involved in pathogenicity (*PDE1, PDE2, IGD1, MET1,* and *GDE1).* Earlier, Sweigard *et al.* (1998) reported screening of 5,538 REMI mutants of *M.oryzae* and identified eight loci involved in pathogenicity (*PTH1, PTH2, PTH3, PTH4, PTH8, PTH9, PTH10 & PTH11).*

In order to generate a large mutant collection and subsequent comprehensive pathogenicity studies, recently *Agrobacterium tumefaciens* mediated transformation (ATMT) has been applied as an efficient tool for carrying out random mutagenesis in a variety of phytopathogenic fungi for the purpose of determining gene function (de Groot *et al.*, 1998; Covert *et al.*, 2001, Mullins and Kang, 2001; Mullins *et al.*, 2001, Gelvin 2003). *A. tumefaciens* is a Gram-negative plant pathogenic bacterium which can transfer a segment of DNA, known as T-DNA into a number of plant species where T-DNA becomes integrated into the plant genome. This property has been used to generate large libraries of T-DNA insertion mutants in *Arabidopsis thaliana* and rice (*Oryza sativa*). Similarly, both Bundock *et al.* (1996) and Piers *et al.* (1996) demonstrated that *Agrobacterium* is also able to deliver its T-DNA into chromosomes of the budding yeast, *S. cerevisiae* (Bundock *et al.*, 1996; Piers *et al*. 1996). Later, *A. tumefaciens* mediated transformation was reported for several species of filamentous fungi (Chen *et al.*, 2000; Michielse *et al.*, 2005) including some species that were recalcitrant to transformation by other methods (Chen *et al.*, 2000; Covert *et al.*, 2001; Degefu and Hanif, 2003; Malonek and Meinhardt, 2001). The advantages of ATMT include relatively high transformation efficiencies, the ability to transform spores and mycelium directly without preparing protoplasts, low insert copy number, random distribution of the

inserted DNA throughout the genome, relative ease of recovering DNA sequence flanking insertion sites due to the presence of a T-DNA tag and comparatively limited arrangements of genomic insertion sites (Mullins and Kang, 2001; Mullins *et al.* 2001; Khang *et al.* 2005; Malz *et al.* 2005; Michielse *et al.* 2005a; Michielse *et al.* 2005b; Sugui *et al.* 2005; Weld *et al.* 2006; Betts *et al.* 2007). Transformation of different types of fungal tissue such as hyphae, spores, protoplasts and blocks of mushroom mycelia is also possible (de Groot *et al.* 1998; Mullins *et al.* 2001). During the past decade at least 64 fungal species have been successfully transformed by ATMT (Michielse *et al.* 2005), which has led to the identification of many functional genes, significantly those involved in fungal pathogenicity (Rogers *et al.*, 2004; Indrum *et al.*, 2004; Walton *et al.*, 2005; Di Pietro *et al.* 2003; Betts *et al.* 2007; Li *et al.* 2009). Therefore, ATMT is regarded as the most efficient method for transformation and gene disruption studies (Mullins *et al.* 2001; Betts *et al.* 2007). In the last decade, *Agrobacterium tumefaciens*-mediated transformation (ATMT) has been developed as a large-scale gene tagging method in *M. oryzae* (Betts *et al.* 2007; Choi *et al.* 2007; Gupta and Chattoo 2007; Jeon *et al.* 2007; Meng *et al.* 2007; Li *et al.* 2009).

To identify novel determinants of pathogenicity we chose to saturate the *M. oryzae* genome by random insertion of *Agrobacterium* T-DNA. Using this approach, we reasoned that any genes of interest should be recoverable because they are tagged. Our aim was to identify unknown genes that are necessary for infection-related morphogenesis and pathogenicity of *M. oryzae*. A mutant library containing more than 10,000 hygromycin-resistant transformants of *M. oryzae* has been generated using ATMT. From this library of mutants, a representative number were tested for copy number and random insertion. We also developed a very high-throughput system for screening the mutants by modifying the standard pathogenicity assay. This high-throughput procedure facilitated screening of a large number of mutants routinely.

In this chapter, I demonstrate that ATMT is an efficient system for high-throughput insertional mutagenesis. I also present the development of a highly efficient pipeline for downstream analysis of *M. oryzae* mutants.

3.2 Materials and Methods

3.2.1 Generation of T-DNA tagged mutant library of *M. oryzae*

3.2.1.1 *Agrobacterium* strains and binary vectors

The wild type *Magnaporthe oryzae* strain Guy-11 is stored at the laboratory of N. J. Talbot (Geoffrey Pope building, University of Exeter, UK) and was used to construct the library of T-DNA mutants. In this study, *Agrobacterium tumefaciens* ALG-1 strain (Lazo *et al.,* 1991) containing plasmid pCAMBGFP was used for T-DNA library construction. ALG-1 strain was stored at -80°C in 20% glycerol stocks in the laboratory of N. J. Talbot (Geoffrey Pope building, University of Exeter, UK) by addition of sterile glycerol to liquid cultures (Sambrook and Russell, 2001). The plasmid pCAMBGFP is a binary vector based on pCAMBIA1300 (Figure 3.1A) (CAMBIA, Canberra, Australia) (Sesma & Osbourn, 2004). This vector contains hygromycin resistance gene cassette (Carroll *et al*., 1994) and the sGFP gene (encoding a GFP variant that contains a serine to threonine substitution at amino acid 65) from pCT74 (Lorang *et al.,* 2001) (Figure 3.1C). A 2.9 kb *Xho*I-*Eco*RI double digested restriction fragment containing a modified hygromycin resistance gene under the control of the *Aspergillus nidulans TRPC* promoter together with the *sGFP* gene under the control of the *Pyrenophora tritici-repentis TOXA* gene promoter was isolated from the vector pCT74 (Lorang *et al.,* 2001) (Figure 3.1B). This restriction fragment was ligated into *Xho*I/*Eco*RI digested pCAMBIA1300 to replace the pCAMBIA1300 cassette containing the hygromycin gene under the control of the *Cauliflower mosaic virus* 35S (CaMV35S) promoter. The resulting vector pCAMBGFPwas introduced into *Agrobacterium tumefaciens* strain AGL-1 and transformed into *M. oryzae* to for the construction of insertional mutant library (Rho *et al.,* 2001)

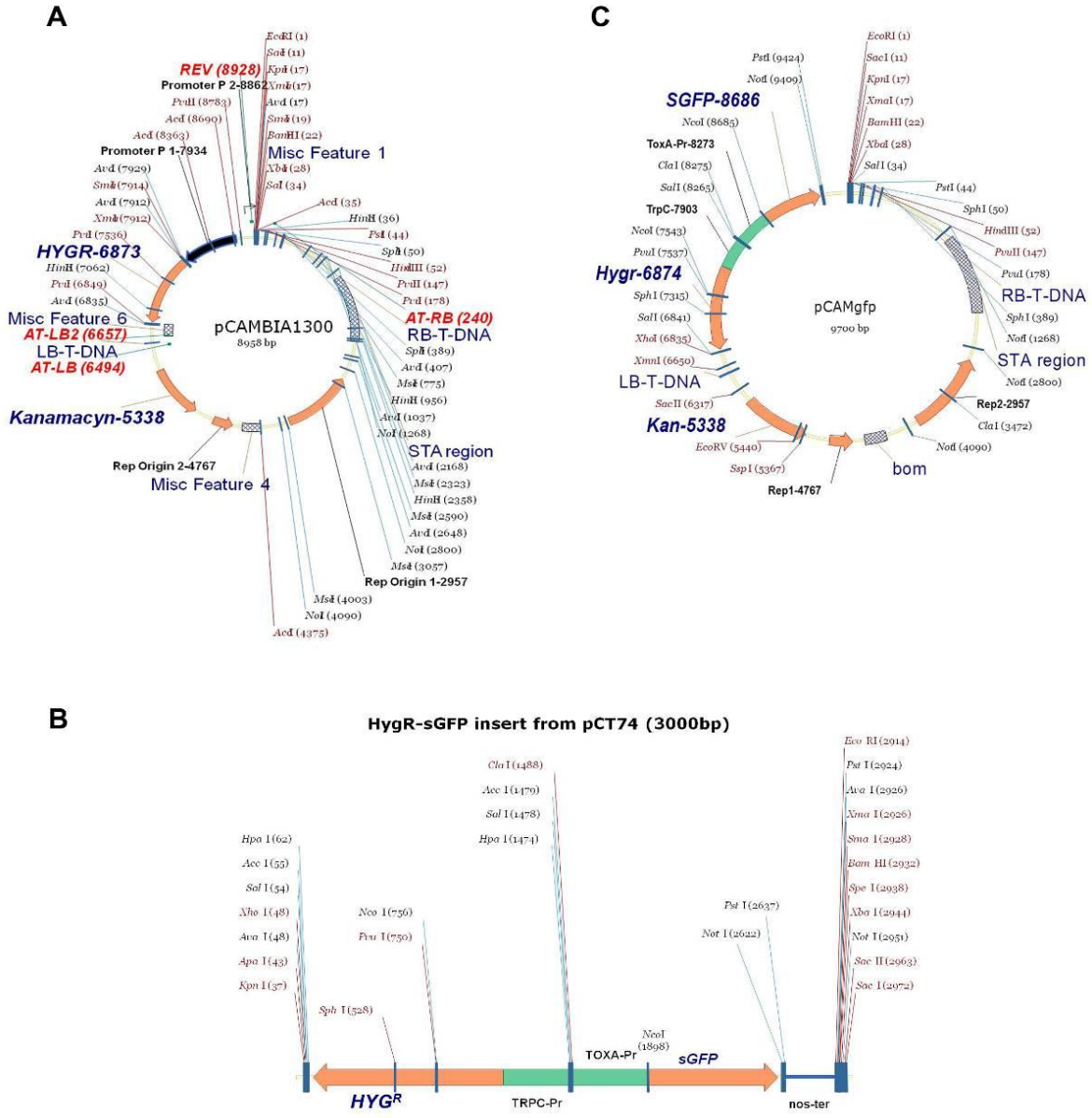

Figure 3.1: Structure of the vector pCAMBGFP used to generate ATMT library of *M. oryzae*. A. Structure of the vector pCAMB1300. **B.** A 2.9 kb *Xho*I-*Eco*RI restriction fragment was isolated from pCT74 which contains a modified hygromycin resistance gene under the control of the *TRPC* promoter and *sGFP* gene under the control of the *TOXA* gene promoter. This restriction fragment was ligated into *Xho*I/*Eco*RI-digested pCAMBIA1300 to replace the hygromycin cassette gene under the control of the *Cauliflower mosaic virus* 35S (CaMV35S) promoter. C. Modified vector pCAMBGFP was introduced into *Agrobacterium tumefaciens* strain AGL-1 and transformed into *M. oryzae* (Images obtained and modified from Sesma & Osburn, 2004).

3.2.2.2 *Agrobacterium tumefaciens*-mediated transformation (ATMT) of *M. oryzae*

For each round of transformation, *A. tumefaciens* strains were streaked from glycerol stocks, onto solid AB plates (Agrobacteirum Broth, 18 mM K_2HPO_4,10 mM NaH_2PO_4, 0.2% glucose, 0.6 mM $CaCl_2$, carbenicillin 60 µg/mL, 1.4% agar) (Chilton *et al.*, 1974) containing 50 µg mL^{-1} of kanamycin (diluted from 50 mg mL^{-1} stock) and incubated at 28°C overnight. Vector pCAMBGFP contains the kanamycin resistance gene and the addition of kanamycin was necessary to suppress undesired growth of other bacterial species and strains. A single colony was used to start each liquid culture and transferred into 2 mL of minimal medium (Mullins *et. al.*, 2001; Betts *et. al.*, 2007) containing 50 µg mL^{-1} of kanamycin (diluted from a 50 mg mL^{-1} stock) solution and incubated for 48 h at 28°C with 250 rpm shaking. The cells were diluted to an A_{600} of 0.15 in 5 mL of induction medium (Mullins *et al.*, 2001; Betts *et al.*, 2007) containing 200 µM acetosyringone (Aldrich Chemical, Milwaukee, WI) and 50 µg mL^{-1} of kanamycin and grown at 28°C for 6 h to reach an A_{600} of 0.25. (Mullins *et al.*, 2001; Betts *et al.*, 2007). While bacterial cells were becoming ready for transformation, spores were harvested from 10 day-old *M. oryzae* plates with sterile distilled water (ddH_2O) and filtered through sterile Miracloth (Calbiochem, La Jolla, CA). Conidia were then washed by centrifugation for 5 min at 2,000 x *g*, resuspeneded in sterile distilled water (ddH_2O), counted using a haemocytometer and diluted to a concentration of 1 x 10^6 conidia mL^{-1}. A 100 µL aliquot of AGL-1 culture was then mixed with 100 µL of conidial suspension (1 x 10^6 conidia mL^{-1}) (in this mixture, the fungal cell/bacterial cell ratio was 1:250) (Betts *et al.*, 2007). The mixed aliquot (200 µL) were spread, using 3mm sterile glass beads on autoclaved cellulose nitrate (CN) membranes (Whatman 47mm , 0.45pm pore size, WON type, Cat. No. 7141114) which had been placed on AIM (AB medium [18 mM K_2HPO_4,10 mM NaH_2PO_4, 0.2% glucose, 0.6 mM $CaCl_2$, carbenicillin 60 µg/mL] supplemented with 25 mM 2-(N-morpholino)-ethanesulfonic acid,

pH 5.8) agar plates. The cells were co-cultivated for 48 hours at 28°C prior to selection (Betts *et. al.,* 2007). After this period (using aseptic techniques), CN membranes were cut into several small pieces to enhance growth of individual mutants in the media and transferred into PDA plates containing 250 µg mL^{-1} hygromycin B (to select transformed conidia), 400 µg mL^{-1} cefotaxime, 100 µg mL^{-1} carbenicillin and 60 µg mL^{-1} streptomycin to counter select the bacteria cells on the plates. PDA plates were then incubated at 24°C for 5-6 days. Then colonies were transferred onto CM (containing 20% sucrose) containing 300 µg mL^{-1} hygromycin B (Betts *et. al.*, 2007). CM plates were made in square Petri dishes divided in 25 grids and a piece of sterile 3 mm cellulose paper was placed on each grid. Finally, once the mutants had grown enough (~7 days) to colonise the grid, the filters were transferred into 48 well plates (greiner bio-one) and desiccated for 2 weeks in desiccation chambers containing silica beads. The 48 well plates containing filters of single *M. oryzae* mutants were safely stored in sealed box containing desiccant (silica beads) at -20°C.

3.2.3 Determination of the T-DNA insertion copy number of ATMT library by Southern blot hybridization

In order to determine the number of T-DNA copies inserted in the genome of each mutant, screening was carried out by Southern blot hybridization analysis. A representative number (336) of mutants from the whole library of 10,200 mutants were randomly selected and screened by Southern blot analysis. Mutants were grown on CM agar plates by placing a small piece of filters from the original stock. Once they were grown, a small plug of mycelium was transferred onto CM plates overlaid with a cellophane disc (Lakeland) and grown for 10 days. DNA was extracted routinely by mini CTAB extraction procedure (Section 2.3.1.2). For DNA digestion, both *Xho*I and *Hin*dIII restriction enzymes were used.

A 2.9 kb *Xho*I-*Eco*RI double digested restriction fragment of pCAMBGFP was used as a probe for copy number detection.

3.2.4 High-throughput pathogenicity screening of T-DNA mutants

A high throughput pathogenicity assay was developed for primary screening of the *M. oryzae* insertion lines. Our aim was to establish a procedure by which we could screen a large number of mutants at the same time and on a routine basis. Therefore, we modified the standard procedure for assaying pathogenicity. To produce fungal inoculum, filters of mutants was grown on CM medium in. In order to maintain high-throughput, mutants were grown in multiwell (6-well) plates. A dwarf Indica rice (*Oryza sativa*) *cv.* CO-39, which is very susceptible to rice blast (Valent *et al*., 1991) was used for infection assays. In order to maintain the highthroughput screening of a large number of mutants, rice plants were grown in 5 cm plastic pots on large a scale (3 plants in each pot) and two-week old rice seedlings were used for pathogenicity assays. Spores were harvested from 10-day old cultures by adding 1 mL of 0.2% gelatin solution to each well followed by gentle scraping with a sterile glass rod. A50 µL aliquot of conidial suspension was added to 1 mL of 0.2% gelatin solution to spray it on to each pot of rice plants. Rice plants were sprayed with an artist's airbrush with inert nitrogen gas as a propellant. Spray-inoculated plants were kept in the growth room with controlled temperature and humidity (24°C and 96% humidity) with a 12 h light – 12 h dark cycle. Plants were incubated in polythene bags for 48 hours after spraying and then incubated for a further 72 hours opened with occasional water spray. Diseased leaf samples were collected 5 days after inoculation and the lesion desity counted. Mutants were sprayed in batches of 48 and wild type Guy11 and Δ*pmk1* strains were included in the each batch as positive and negative controls, respectively. The high-throughput pathogenicity assay for primary screening is shown and explained in Figure 3.8.

3.3 Results

3.3.1 Generation of T-DNA tagged mutant library of *M. oryzae*

We have generated a library of 10,200 *M. oryzae* mutants with *Agrobacterium* T-DNA insertions in their genome, with an aim to screen them for defects in pathogenicity. Transformations were carried out in collaboration with Dr. Zaira Caracuel-Rios. We exploited the high-efficiency of ATMT to construct this collection of insertional mutants. For the initial two rounds of transformation only 50 mutants were recovered each time in order to optimize the procedure. Once the procedure started working it was scaled up and in later rounds of transformation 500-600 transformants were routinely generated in each transformation. Maximum number of transformants produced in a single round was 876 and all of the 10,200 transformants were generated in 20 rounds of transformations. Therefore, the average number of transformants generated per round was 510. T-DNA mutants were stored as a single culture after production. Filters stocks of mutants were preserved in 48 well plates, kept in boxes containing desiccant and stored at -20°C. Mutants were numbered numerically and each mutant was designated by adding a prefix "M" before any particular mutant number (here "M" stands for "Mutant"). Such as, mutant number 1880 was designated as M1880 in all the experiments and analysis carried out it in this study.

In order to assess the integration of T-DNA in mutants, we randomly selected 10 mutants and observed the expression of *sGFP* during appressorium development. The T-DNA used contains the *sGFP* gene under control of the *Pyrenophora tritici-repentis TOXA* gene promoter (Lorang *et al.*, 2001). Therefore mutants should constitutively express *sGFP* over the time course of appressorium development. Harvested conidia from each mutant were inoculated onto borosilicate coverslips and incubated at 24ºC. Examination by epifluorescence microscopy was carried out at 0, 2, 4, 6 and 24 hours following incubation.

GFP fluorescence was consistently detected during conidial germination and in developing and matured appressorium for all the mutants and it was localized in the cytoplasm (For typical example see Figure 3.2). This observation provided the first evidence each mutant contains integrated T-DNA in their genome and thus the GFP was expressed constitutively from the integrated T-DNA construct.

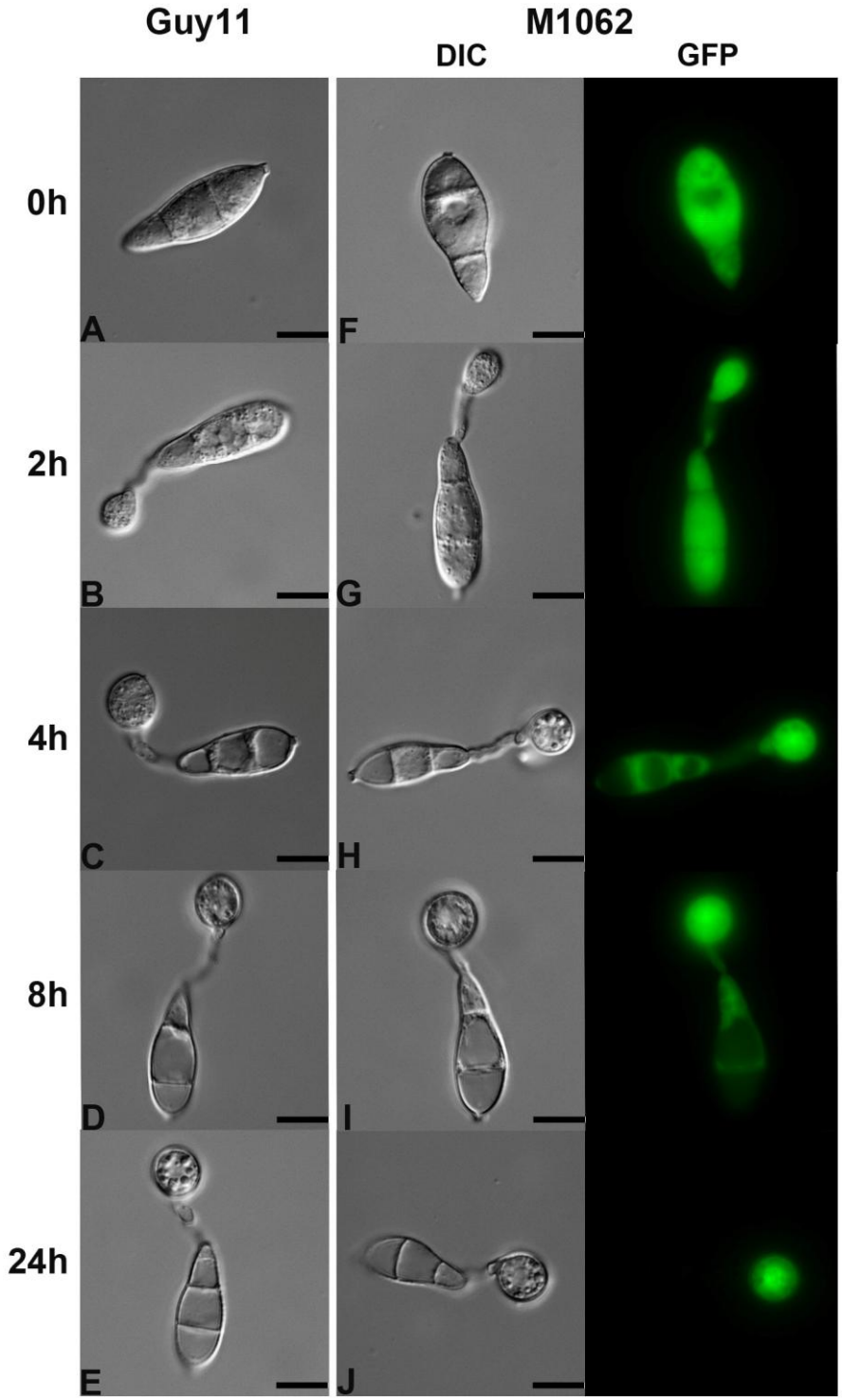

Figure 3.2: Expression and localization of GFP in a T-DNA mutant during appressorium development. Conidia from a randomly selected mutant M1062 was inoculated onto glass coverslips along with wild type Guy11 as a control. Expression of GFP and its localization was observed over a period of 24 h using an Olympus IX-81 inverted epifluorescence microscope fitted with a HQ^2 camera. Representative DIC (differential interference contrast) and fluorescence images are shown at each time point. Scale Bar = 10 µm.

3.3.2 T-DNA copy number analysis of the ATMT library of mutants

We analyzed the ATMT library by Southern hybridization to determine the copy number and distribution of T-DNA inserts in the genome. For this purpose, genomic DNA was extracted from 336 randomly selected mutants and analyzed by Southern hybridization. For DNA digestion we used both *Hin*dIII and *Xho*I enzymes and both have a single restriction site in the T-DNA. There is a *Hin*dIII site (Figure 3.3) upstream of the right border (RB) and an *Xho*I site (Figure 3.3) downstream of the left border (LB) in the T-DNA. Therefore, using both enzymes we were able to identify the actual copy number of T-DNA inserted in the genome and validate the analysis independently. The strategy for T-DNA copy number analysis is schematically explained in Figure 3.3. For each restriction site, an equal number of 168 mutants were analyzed for copy number. For each Southern blot Guy11 genomic DNA was included as a negative control in the first lane. In this analysis, all strains were found to be transformants. A 2.9 kb *Xho*I/*Eco*RI double digested pCMABGFP fragment was used as a probe in our analysis. The probe contains the hygromycin resistance gene cassette and s*GFP* fragment located within the T-DNA borders (Figure 3.1).

The results of Southern hybridization analysis are shown in Figures 3.4-3.7. The pattern of hybridization exhibited predominantly single fragments for both *Hin*dIII and *Xho*I digests. In the case of *Hin*dIII-digested DNA the percentage of single fragments was 84% and for *Xho*I, it was 84.5%. This suggests that in more than 80% of instances a single copy T-DNA was integrated in the genome. Among the remainder, 12% of the mutant contained double and 3% contained three or more T-DNA insertions. This distribution of hybridizing fragments on the blot shows that the T-DNA insertion is predominantly a random process. The result of the Southern hybridization analysis of our *M. oryzae* ATMT library is summarized in Table 3.1.

Table 3.1: Summary of the T-DNA copy number analysis of *M. oryzae* ATMT library.

T-DNA Copy	Number of Mutants	Percentage Copy Number (%)
1	283	84.2
2	43	12.8
3 or more	10	3
Total	336	100

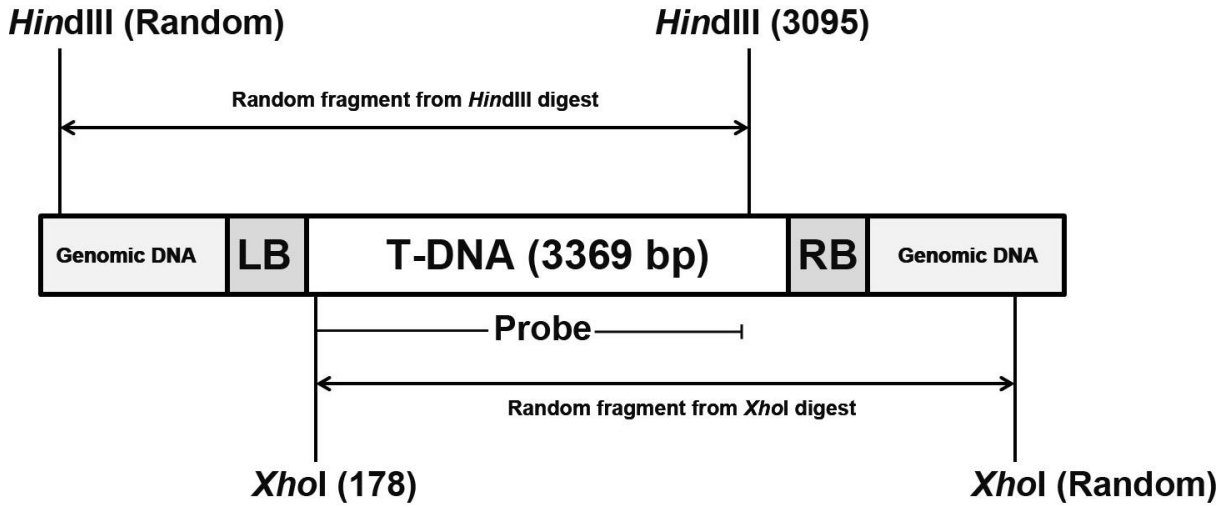

Figure 3.3: Schematic representation of the strategy to determine T-DNA copy number of ATMT mutants. Size of the T-DNA that was transferred to mutants is 3369 bp. *Hin*dIII and *Xho*I have a restriction sites at the 3095 position and 178 position of the T-DNA respectively. Upon digesting DNA randomly in the genomic DNA, both enzyme produce random sizes of DNA fragment that contains most of the T-DNA. An *Xho*I/*Eco*RI digested 2.9 Kb T-DNA fragment (from pCAMBGFP plasmid) was used as a probe which is able to hybridize with T-DNA in both enzyme digested fragments.

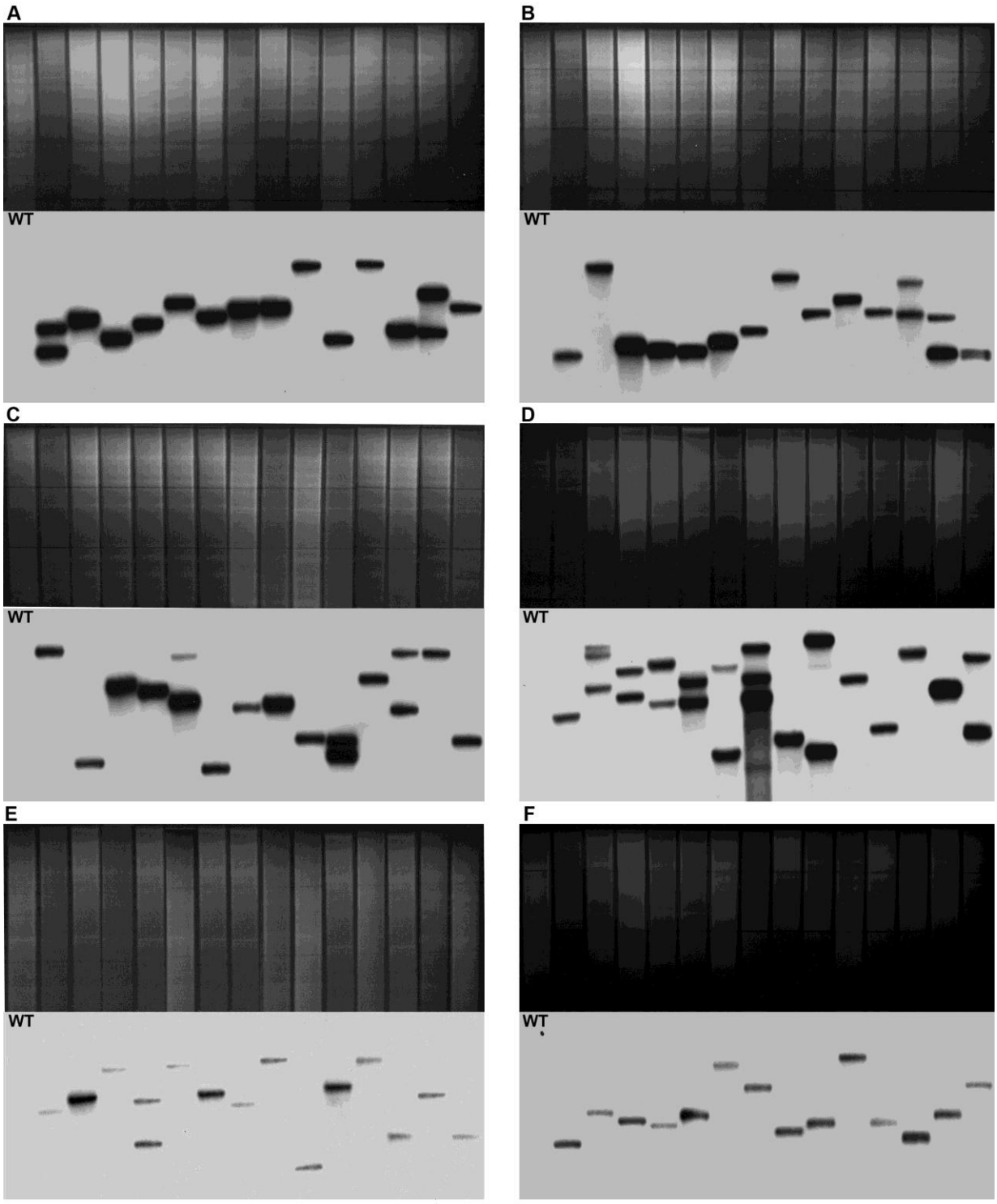

Figure 3.4: Determination of the T-DNA insertion copy number by Southern hybridization.

A-F. DNA gel blot analysis of randomly selected mutants from ATMT library. DNA was digested with *Hin*dIII, fractionated by gel electrophoresis, blotted and probed with a 2.9 kb *Xho*I/*Eco*RI double digested pCAMBGFP fragment. Each blot shows T-DNA copy number of 14 randomly selected mutant samples and wild type Guy11 was included as negative control in the first lane (shown as WT).

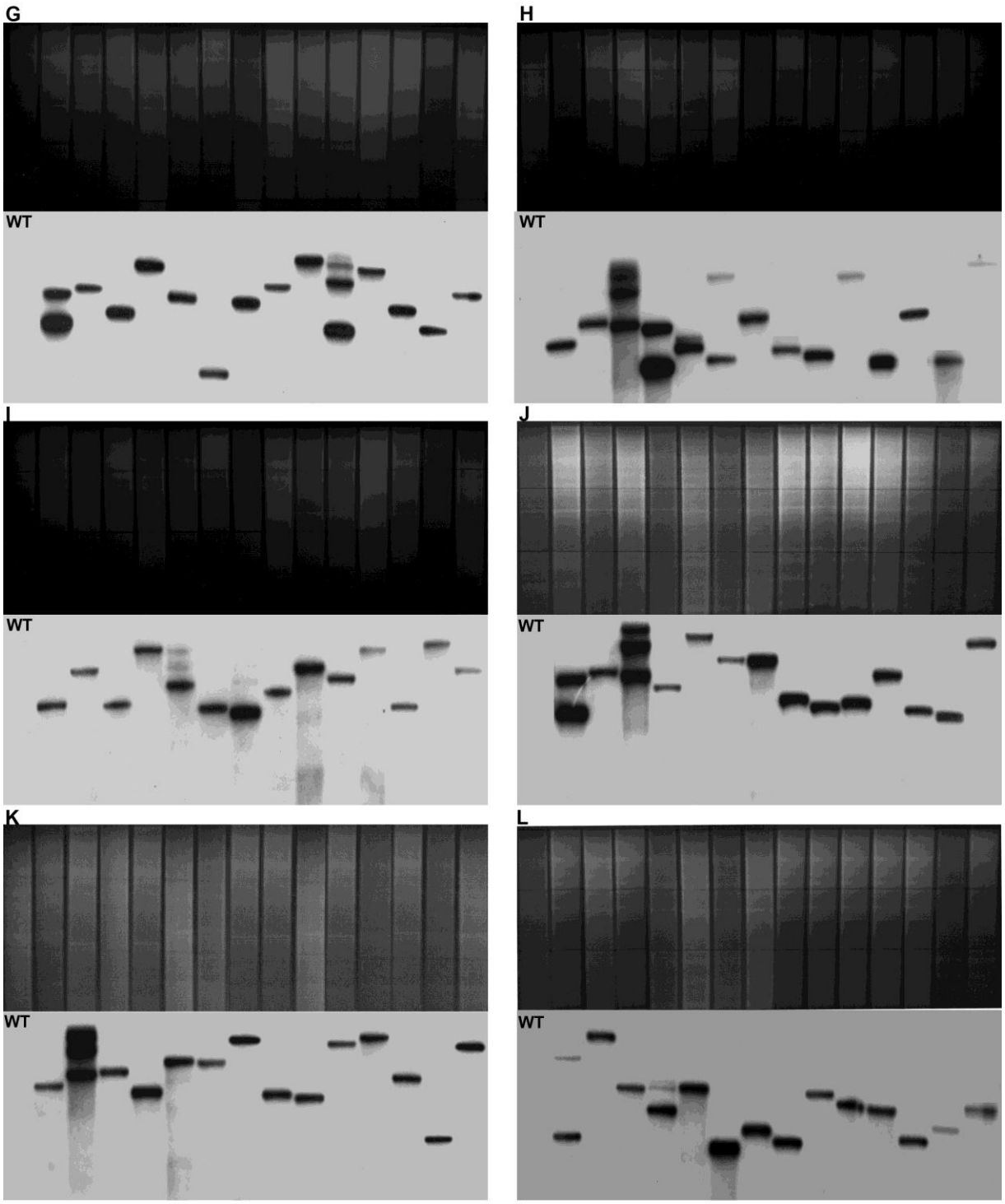

Figure 3.5: Determination of the T-DNA insertion copy number by Southern hybridization.

G-L. DNA gel blot analysis of randomly selected mutants from ATMT library. DNA was digested with *Hin*dIII, fractionated by gel electrophoresis, blotted and probed with a 2.9 kb *Xho*I/*Eco*RI double digested pCAMBGFP fragment. Each blot shows T-DNA copy number of 14 randomly selected mutant samples and wild type Guy11 was included as negative control in the first lane (shown as WT).

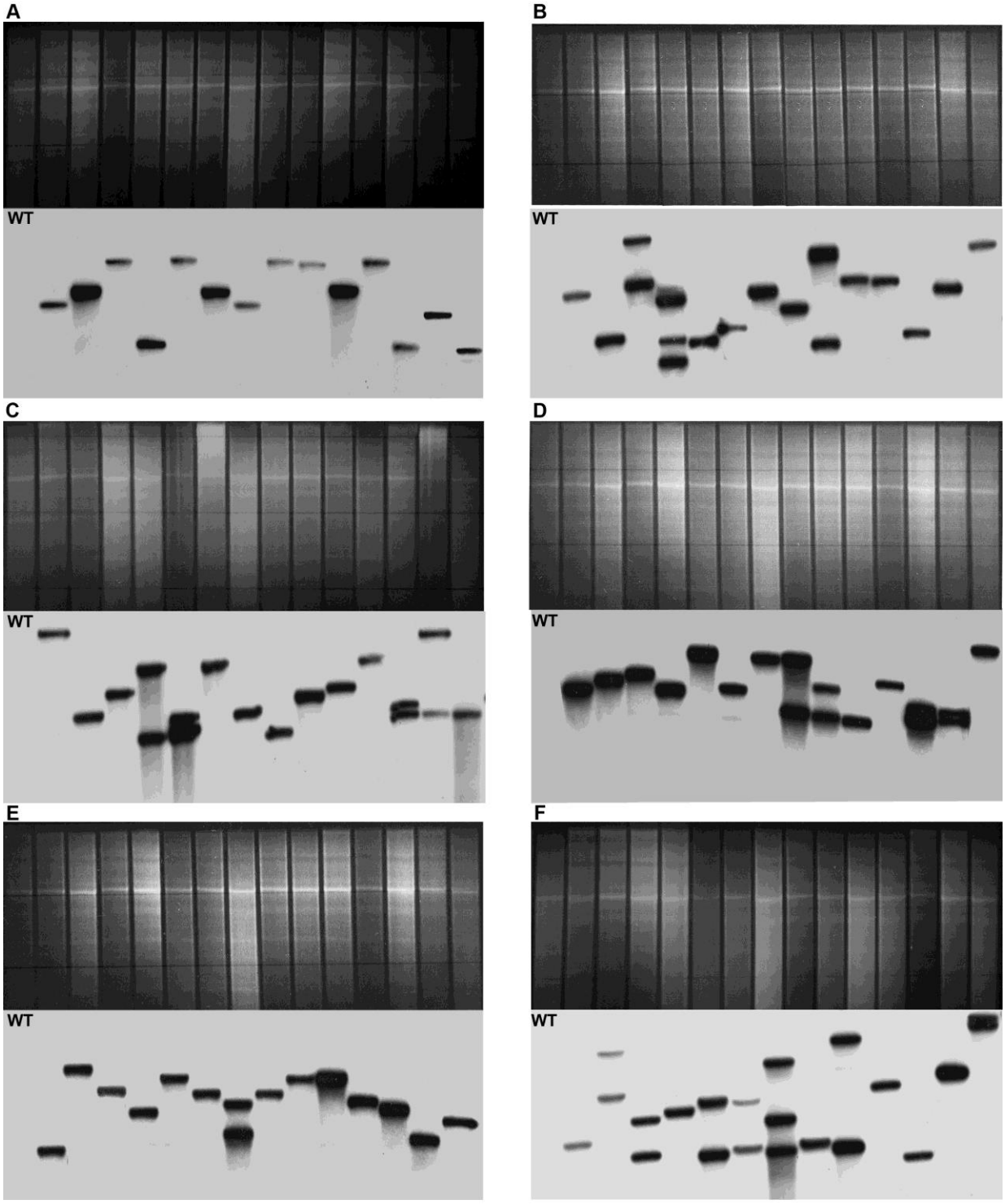

Figure 3.6: Determination of the T-DNA insertion copy number by Southern hybridization.

A-F. DNA gel blot analysis of randomly selected mutants from ATMT library. DNA was digested with *Xho*I, fractionated by gel electrophoresis, blotted and probed with a 2.9 Kb *Xho*I/*Eco*RI double digested pCAMBGFP fragment. Each blot shows T-DNA copy number of 14 randomly selected mutant samples and wild type Guy11 was included as negative control in the first lane (shown as WT).

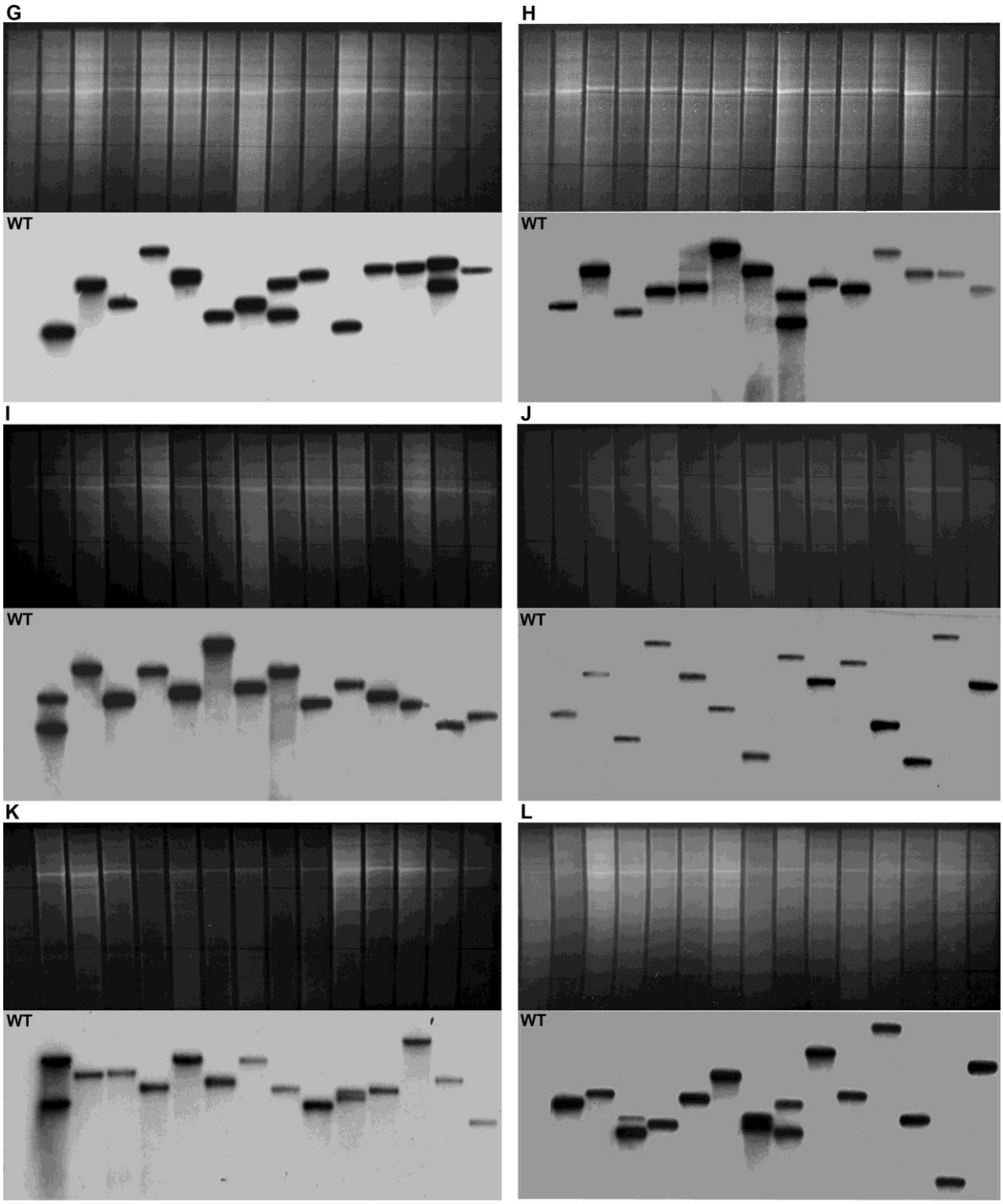

Figure 3.7: Determination of the T-DNA insertion copy number by Southern hybridization.

G-L. DNA gel blot analysis of randomly selected mutants from ATMT library. DNA was digested with *Xho*I, fractionated by gel electrophoresis, blotted and probed with a 2.9 Kb *Xho*I/*Eco*RI double digested pCAMBGFP fragment. Each blot shows T-DNA copy number of 14 randomly selected mutant samples and wild type Guy11 was included as negative control in the first lane (shown as WT).

3.3.3 High-throughput pathogenicity screening of insertion lines

Primary pathogenicity screening of the ATMT library was carried out using the high throughput procedure described in the section 3.2.4 and the procedure is shown and explained in Figure 3.8. Rice blast disease symptoms were assayed 5 days after inoculation. The aim of initial screening was to identify potential non-pathogenic mutants and also the mutants reduced in pathogenicity. Reduction in pathogenicity was considered both in terms of lesion number and size. Therefore, we formalized a qualitative assay of the rice blast disease. The procedure facilitated selection of *M. oryzae* mutants according to a scoring scheme which was generated on the basis of appearance of the lesions which is shown in the Figure 3.9. In this qualitative pathogenicity assay procedure wild-type *M. oryzae* strain Guy11 was used as a positive control and the non-pathogenic mutant *Δpmk1* (Xu and Hamer, 1996) was used as a negative control. A seedling infected with the non-pathogenic mutant *Δpmk1* was scored as 0 and Guy11 was scored as a maximum of 3. Reduced virulence of transformants was scored as either 1 or 2, which represents substantial reduction in pathogenicity or a moderate (≤50 %) reduction, respectively. Transformants scored 0, 1 and 2 were then selected for re-screening by the standard procedure (Talbot *et al.*, 1993). From the primary screening of 10,200 T-DNA insertional mutants from the ATMT library, we selected 200 mutants with standardized inoculum of uniform spore suspension. In this selected pool of mutants, 18 were non-pathogenic and the remainder showed significant reduction in disease lesion number and size compared to wild type Guy11. Additionally, more than 300 mutants were found to be reduced in pathogenicity, but not significantly different from the wild-type ($p<0.05$) and therefore they were not selected for rescreening. The rest of the mutant library manifested typical rice blast disease lesions similar to the wild type strain Guy11.

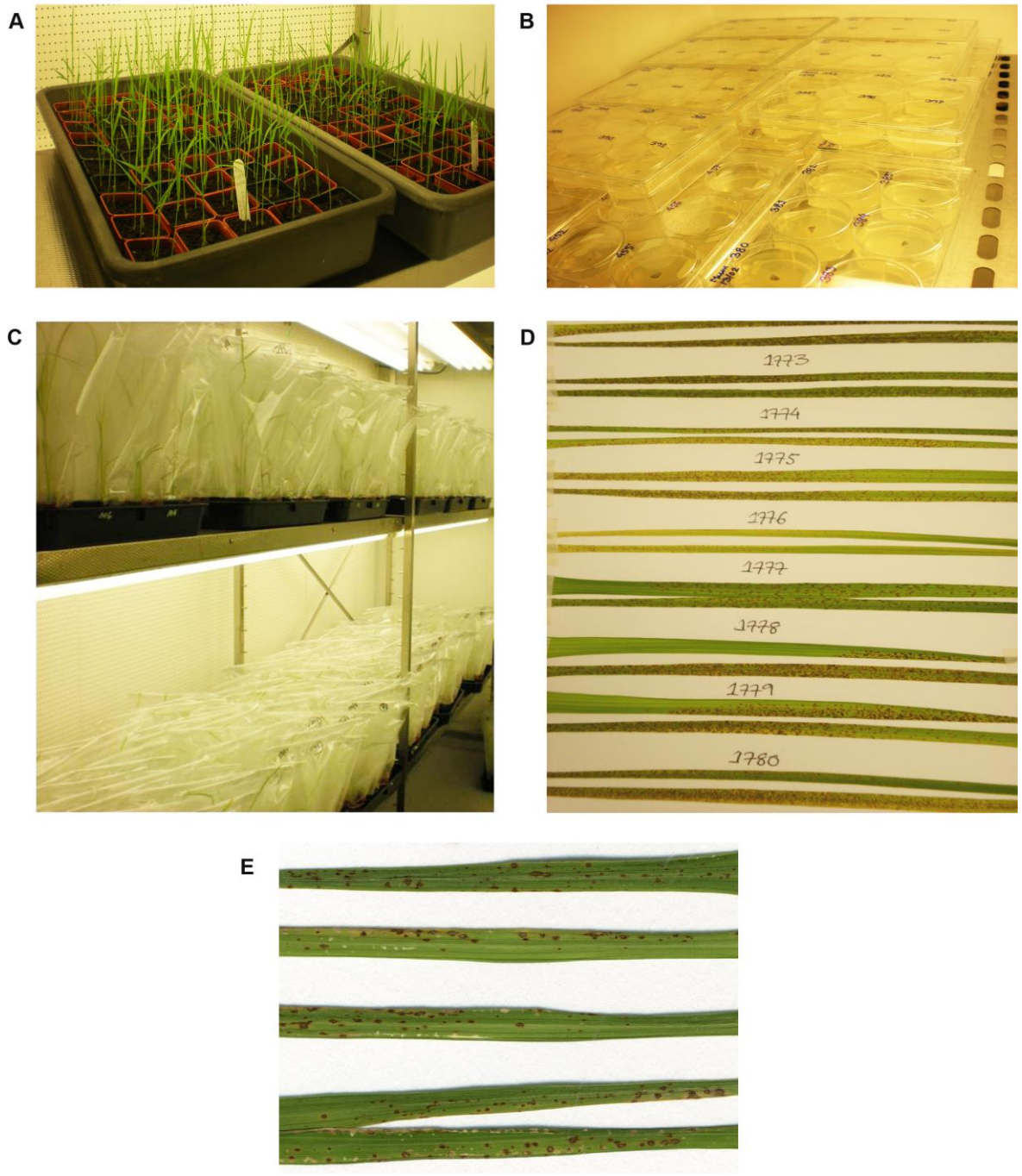

Figure 3.8: High-throughput pathogenicity screening of the ATMT library of *M. oryzae.* **A.** Rice *cv.* CO-39 was grown in 5 cm pots on a large scale (3 plants in each pot). **B.** Mutants were grown in 6-well plates instead of 9 cm round petri plates. **C.** Two-week old rice seedlings were spray-inoculated, covered by polythene bags and kept in the growth room with controlled temperature and humidity (24°C and 96% humidity). Plants were kept in bags for 48 hours after inoculation and incubated for a further 72 hours (opened) in the growth room. **D.** Diseased leaf samples were collected 5 days after inoculation and stored by attaching them to 3 mm paper sheets. **E.** The wild-type Guy11 strain was inoculated routinely as a positive control for pathogenicity assays.

Figure 3.9: Scoring system for the selection of *M. oryzae* T-DNA mutants showing reduced virulence in primary screening. The ability to cause rice blast disease by of *M. oryzae* T-DNA tagged mutants was assayed qualitatively during primary screening. Mutants were scored on a 0 to 3 scale based on the appearance of disease lesions as follows: **0**, no lesions (equivalent to the non-pathogenic phenotype of *Δpmk1*); **1,** severe reduction of pathogenicity in terms of lesion number and/or size; **2**, moderate reduction (≤50%) in capability of causing disease in terms of lesion number or size and; **3**, equivalent to the necrotic lesions produced by wild type Guy11. From the pathogenicity assay, mutants scoring 0, 1 or 2 were selected for rescreening by the standard procedure.

3.4 Discussion

In this chapter, I have reported the construction of a comprehensive insertion library of *Magnaporthe oryzae* strain Guy11 and subsequent high-throughput screening of this library to identify mutants impaired in pathogenicity. The mutant library of 10,200 mutants was successfully generated using ATMT as an insertional mutagenesis tool. I have also described the development of a highly efficient screening and analysis pipeline used to identify mutants of interest (Figure 3.10).

The main goal of this project was to saturate the *M. oryzae* genome with T-DNA insertions to disrupt genes involved in rice blast disease. For this purpose, my first objective was to develop a large mutant collection by exploiting the most efficient method of insertional strain generation, thus decreasing the amount of effort needed to generate each strain. Two other important aspects were taken into consideration. Firstly, we aimed to generate, predominantly single copy insertions per strain, thereby simplifying the identification of disrupted genes and, secondly, to generate random insertions into the genome. ATMT was our tool of choice because it possesses all the advantages required for a comprehensive forward genetics study (Betts *et al.*, 2007).

We used a modified vector pCAMBGFP because of its *sGFP* reporter gene within the T-DNA border. Inclusion of *sGFP* has several advantages. Constitutive GFP fluorescence proves the integrity of the T-DNA and facilitates following the growth of mutants in plants during leaf sheath assay (Kankanala *et. al.,* 2007). For Agrobacterium-mediated transformation using AGL-1, we used an optimized protocol according to Betts *et al.* (2007). In the co-cultivation step of the transformation, a high ratio (1:250) of the fungal

cell/bacterial cell was maintained to increase efficiency of transformation. Although the 1:100 ratio of fungal cell/bacterial cell can be used with some other *Agrobacterium* strains such EHA105, it has been established from previous studies that for AGL-1, a ratio of 1:250 is optimum (Betts *et al.,* 2007). It is conceivable that an increased number of bacterial cells per conidium might increase the likelihood that a conidium would be contacted and transformed by *A. tumefaciens* and in this way a high number of transformants could be generated in each round of transformation. We also observed that the co-cultivation time set for 48 h was a critical parameter. From previous studies it has been shown that the efficiency of ATMT increases with a co-cultivation time up to 48 h (Abuodeh *et al.,* 2000; Mullins *et al.,* 2001; Rho *et al.*, 2001; Betts *et al.,* 2007), without increasing the copy number of T-DNA insertions (Betts. *et al.,* 2007). Using appropriate concentration of antibiotics (cefotaxime, carbenicillin and streptomycin while growing the transformants from CN membrane on PDA plates), effectively counter selected bacterial growth and no significant bacterial growth was found in the later stages of processing transformants. Mutants were then transferred from PDA plates to CM plates for final selection in the presence of 300 µg mL^{-1} hygromycin B, and 20 % sucrose was used as an osmotic stabilizer. The presence of sucrose in CM at this stage efficiently reduced background growth as reported previously (Betts *et. al.,* 2007) and a negligible percentage of false mutants were found during subsequent processing. It is also evident from the presence of hybridization signals for all of the randomly selected mutants in the T-DNA copy number analysis (Figures 3.4-3.7), that efficient transformation occurred.

The success of a forward genetics approach through insertional mutant screening depends on the high percentage of single insertion mutants, which enables easy and unambiguous retrieval of tagged genes. In contrast, multiple or tandem insertions make the rescue and characterization

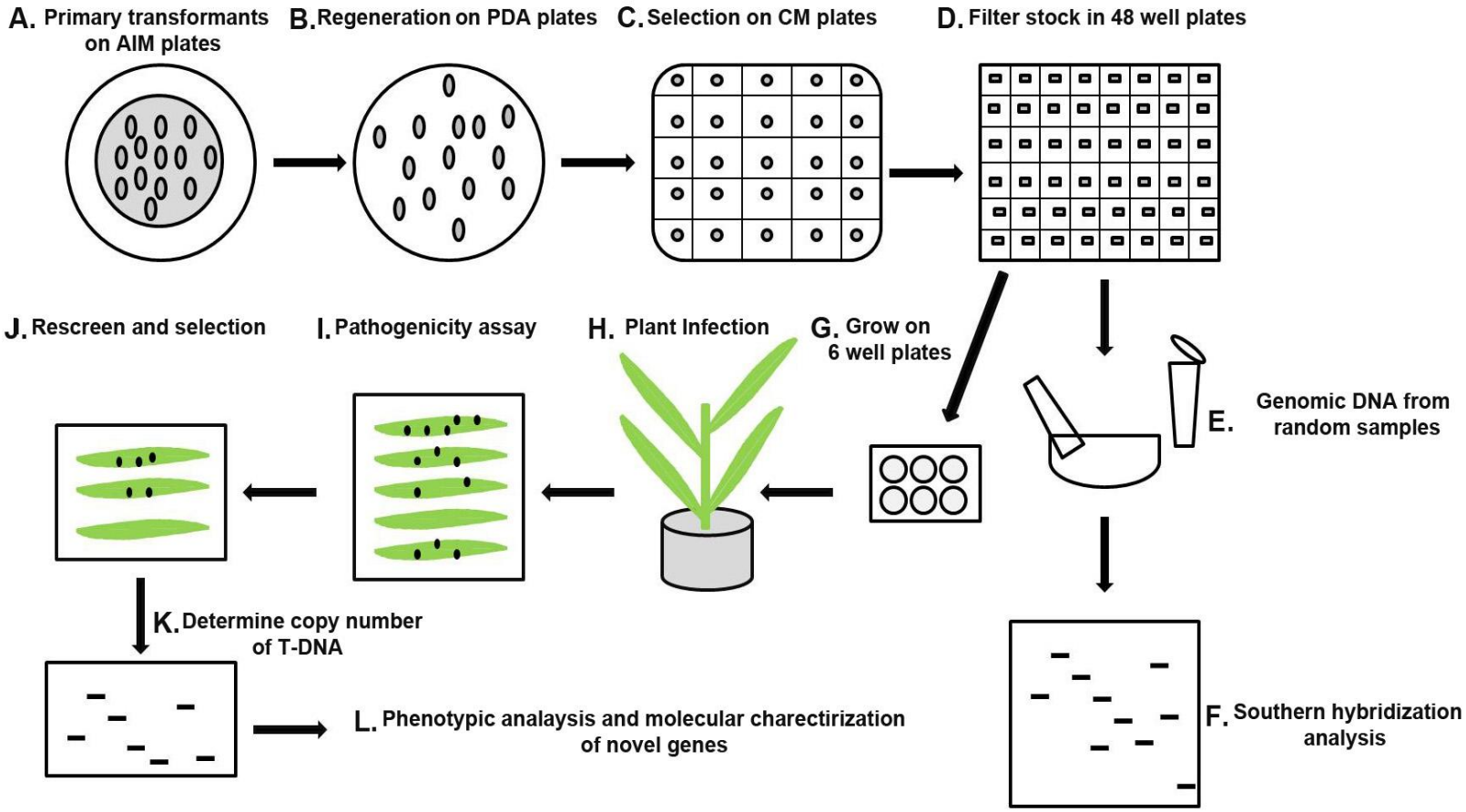

Figure 3.10: Construction, processing and high-throughput screening *M. oryzae* of ATMT library. A. *Agrobacterium tumefaciens* mediated transformation on CN membrane placed on AIM plates. **B.** Primary selection on PDA plates for Hyg^R *M. oryzae* and counter selection against *A. tumefaciens.* **C.** Final selection on CM plates for Hyg^R and generation of filter stocks. **D.** Filter stored in 48-well plates. **E.** Mutants were randomly selected from the library and genomic DNA extracted. **F.** Southern hybridization analysis was carried out to determine T-DNA insertion pattern and copy number. **G.** Mutants were grown in 6-well plates in large scale for pathogenicity screening. **H.** High-throughput plant infection assays were carried out systematically to identify mutants defective in pathogenicity. **I.** Primary pathogenicity screening identified mutants either reduced or lacking in pathogenicity. **J.** Selected mutants from primary screening were rescreened by standard procedure in order to determine the consistency of phenotype and finally selected for further analysis. **K.** T-DNA copy number of the selected mutants was determined. **L.** Phenotypic and molecular characterizations were carried out to determine the gene disrupted by T-DNA insertion and identification of novel genes.

more cumbersome (Betts *et al.,* 2007a). Therefore, it was necessary to carry out a detailed Southern hybridization analysis of the insertion patterns in transformed lines generated by ATMT. We used two distinct restriction enzymes for genomic DNA digestion in our study, so that the results could be compared and independently verified. We used *Hin*dIII and *Xho*I enzymes which have restriction sites near the right and left border of T-DNA, respectively. This approach facilitated the use of a 2.9 Kb *Xho*I/*Eco*RI double digested pCAMBGFP fragment as probe which also contains most of the T-DNA. As a result, in our analysis hybridization was efficient and unambiguous. *M. oryzae* transformants were selected randomly from the library and I have presented 12 blots for each enzyme used. The varied pattern of hybridization clearly shows that T-DNA integration was random. In case of *Hin*dIII and *Xho*I genomic DNA digests, 141 and 142 mutants out of 168 were single copy insertion transformants, respectively. This clearly shows the uniformity of results for both enzymes used. By percentage, 84% of the isolates in our ATMT library possessed a single T-DNA copy integrated in their genome. The remaining mutants were predominantly double copy insertion strains (~13%). In order to elucidate the randomness of T-DNA integration a representative sample from the comstructed library can be investigated to reveal the integration sites and subsequently analyzed to verify the random nature of T-DNA insertion. It may also potentially reaveal tandem insertion which could not be resolved by southern hybridization analysis.

The main goal in constructing the ATMT library was to identify pathogenicity mutants that have not previously been found. Therefore, screening of mutants in a technically feasible and reliable method was critical for the success of the project. In order to screen the library in a time efficient and routine manner we developed a high-throughput screening pipeline by modifying the standard protocol. Compared to previous studies, where a pathogenicity assay

was carried out rice seedlings grown in test tubes (Betts *et al.*, 2007) or by cut leaf assays (Balhadere *et al.*, 1999), we carried out pathogenicity assay on whole plants grown in soil. This assay therefore more accurately mimics the way rice blast disease spreads in the field (Valent & Chumley, 1991), therefore it is arguably more realistic to carry out infections to occur in this way. Additionally, identification of reduced mutants by leaf drop assays on cut leaves can potentially generate biased results because of the qualitative nature of the screening procedure. Therefore, the whole plant infection assay produces a more reliable pathogenicity phenotype. Spray inoculation in whole plant infection assay allowed us to compare the lesion density quantitatively and thus identification of reduced mutants is easier.

In order to screen a large number of transformants, we initially carried out inoculations without counting spore numbers and it was to ensure the high throughput of the assay. This clearly has a distinct disadvantage because of potential variation in the ability of mutants to sporulate. We decided, however, to set up a rapid infection screen and then to select out sporulation defective mutants at a later stage by inoculation with uniform spore suspension. We did not inoculate with a homogenous spore suspension (after appropriate counting) during the primary plant infection assay. Therefore, we used 50 µL of harvested suspension from each plate to maintain some degree of homogeneity throughout the screening. Using 6-well plates enhanced the preparation and handling of spore suspensions. Rice plants were grown in smaller pots (5 cm) to maximize the use of growth chamber space. Infected leaves were collected in 3mm paper sheets and compared with wild type Guy11 control both in terms of lesion number and size. By applying this high-throughput pathogenicity screening and score based assay platform, 200 reduced virulence mutants were identified. Out of those 200 mutants, 18 mutants were non-pathogenic and unable to cause disease. The remainder showed a significant reduction (≤50%) in pathogenicity. A number of other mutants were

found to be reduced but rejected because the reduction was not very severe. However, from the primary pathogenicity screening of 10,200 ATMT mutant of *M. oryzae*, 200 mutants were selected for rescreening by standard procedure. This selected cohort actually represents 1.96 % recovery of *M. oryzae* insertion mutants. If T-DNA insertion is a random process, then it suggests that a maximum of ~2 % of the total number of *M. oryzae* genes potentially associated with pathogenicity has been tagged in these mutants selected from primary pathogenicity screening.

Chapter 4

Selection of Mutants for Phenotypic and Molecular Genetic Analysis

4.1 Introduction

In this chapter I report the screening of the cohort of 200 T-DNA insertion mutants that were identified from primary pathogenicity screening. We followed the standard plant infection procedure for re-screening of mutants (Talbot *et.al.*, 1993). The main goal of re-screening was to select mutants on the basis of the consistency of their pathogenicity phenotype. Using the primary screening platform, we maintained the high-throughput that was initially developed but this did not take account of differences in the efficiency of sporulation among mutants. We therefore carried out a secondary screen in which uniform conidial suspensions were applied to rice seedlings. Thus, the primary screening was qualitative, but here we set out to select mutants for future analyses by quantitative screening. Therefore, we carried out a comprehensive screening by maintaining the homogeneity of spore suspension. From the first round of screens we selected a large collection of mutants showing either a reduction or complete loss of pathogenicity. We then carried out a further three rounds of pathogenicity assays to confirm the consistency and reproducibility of the phenotypes observed.

We then carried out detailed phenotypic characterization of the selected mutants. They were systematically investigated for vegetative growth and morphology, conidiation, germination, appressorium development, appressorium turgor generation and appressorium-mediated penetration of onion epidermis and rice leaf sheath layers. Based on this phenotypic characterization, we selected the best candidates for molecular genetic characterization and

the number of T-DNA copies per genome was also determined. In order to identify T-DNA tagged genes, we applied just conventional approaches such as, thermal asymmetric interlaced –PCR (TAIL-PCR) (Liu and Whittier, 1995; Mullins *et al.*, 2000; Betts *et al.*, 2007; Li *et al.*, 2010a, b; Goh *et al.*, 2011) and inverse PCR (iPCR) (Ochman *et al.*, 1988; Meng *et al.*, 2007; Betts *et al.*, 2007). We were able to rescue T-DNA flanks from two mutants by these two methods. TAIL-PCR and iPCR results were verified by showing restriction fragment length polymorphism (RFLP) between wild-type and corresponding mutant and also by complementing the mutant with putative tagged gene. We established the pipeline for identifying novel genes unambiguously so that the genes interrupted by T-DNA could be assigned a role in pathogenicity. We initially set out to use TAIL-PCR and iPCR. However, subsequently we also applied next generation DNA sequencing (NGS).

4.2 Material & methods

4.2.1 Selection of T-DNA tagged mutants for characterization

For screening selected mutants we followed the standard protocol described in section 2.2.2. After primary re-screening, all the selected mutants were screened three times following the same standard procedure. Pathogenicity data were stored in a Microsoft Excel® spreadsheet. Lesion density measurements were recorded from a 5-cm section of the most infected leaves. All statistical analysis was performed in Microsoft Excel® by automated macro-calculation. Statistical comparisons of experimental data were performed by conducting Student's t-test in Microsoft Excel® with a probability limit of $p<0.05$ or $p<0.01$ considered as significant. Bar charts showing quantitative analysis of rice infection assay with error bars indicating standard error were generated.

4.2.2 Phenotypic characterization of selected mutants

M. oryzae T-DNA mutants selected for phenotypic characterization were investigated for vegetative growth and morphology on CM, conidiation, germination and appressorium development, penetration in onion epidermis and rice leaf sheath and incipient cytorrhysis. All these experiments were carried following the procedure described in section 2.2.

4.2.3 Rescue of T-DNA flanks by PCR based methods

4.2.3.1 Thermal asymmetric interlaced (TAIL) polymerase chain reaction (PCR)

To rescue T-DNA flanks by a high-efficiency, thermal asymmetric interlaced (TAIL) polymerase chain reaction (PCR) strategy, the standard protocol described by Liu and Whittier (1995) was followed. Based on this strategy, a commercial TAIL-PCR kit was used in our study to identify T-DNA flanking genomic DNA of selected mutants. The Universal Vectorette™ System (Sigma Aldrich) is a high-efficiency PCR-based method for DNA walking and mapping that uses a form of unidirectional PCR for amplifying and sequencing unknown genomic or large construct DNAs. In this system, a Vectorette unit is employed, which consists of a double stranded linker with an internal mismatched region and a sticky end. The Universal Vectorette™ System offers the flexibility to generate Vectorette libraries from purified genomic DNA by *Bam*HI, *Cla*I, *Eco*RI, *Hin*dIII or blunt restriction enzyme digests. The system involves three steps. First, genomic DNA containing the target sequence is digested with any of the restriction enzymes and corresponding Vectorette units ligated. Second, PCR is performed on the Vectorette library using a primer complementary to the mismatched region of the Vectorette unit (Vectorette primer) and a primer specific to the known DNA sequence. PCR products are typically obtained from a single PCR run; however, nested PCR can be performed from nested primers are included to increase specificity when amplifying more complex templates. Third, the PCR products generated by the Vectorette

system can be used directly for cycle sequencing or cloned into commercially available vectors for further characterization.

We started TAIL-PCR by first digesting 1 µg of genomic DNA in a total reaction volume of 50 µL [2 µL DNA (500 ng/ µL), 5 µL of 10X buffer, 1 µL of enzyme (10U/µL) and 42 µL of sterile H_2O] using the recommended restriction enzyme (NEB) and the digestion reactions were incubated at 37ºC overnight. The enzyme was heat inactivated at 65ºC for 20 min. Vectorette ligation reaction was prepared by adding 5 µL Vectorette units (600 nM), 1 µL DNA ligase, 1 µL ATP (100 mM), 1 µL DTT (100 nM) into 50 µL of digested genomic DNA. Ligation reactions were performed for 4 h in a thermal cycler following the conditions; 16ºC for 60 min, 37ºC for 30 min, 16ºC for 60 min, 37ºC for 30 min, 16ºC for 60 min. T4 ligase enzyme was heat inactivated at 65ºC for 20 min. The Vectorette library was prepared and 4 µL of the library was checked by 1% agarose gel electrophoresis. The library was then divided into 2 equal halves (27 µL in each). One of them was diluted to 100 µL with nuclease free water. Both the diluted and undiluted Vectorette library was used in the TAIL-PCR. The PCR reaction was prepared by mixing 5 µL 10X AccuTaq buffer, 1 µL dNTPs (10 mM), 0.5 µL Vectorette primary primer (10 nM), 2.5 µL specific primer (20 nM), 2.5 µL AccuTaq DNA polymerase 2 µL of Vectorette library and 36.5 µL nuclease free water. For each round of PCR, two other reactions were set with the same composition except one of them had only Vectorette primary primer and the other with a specific primer. Those two PCR reactions were included as a control experiment to assess the non-specific amplification. PCR conditions were; 94°C, 2 sec; 72°C, 9 min; followed by 32 cycles of 94°C, 2 sec; 68°C, 9 sec; and a final extension step at 68°C for 10 min. TAIL-PCR products were gel purified by the Wizard® SV Gel and PCR Clean Up System (Promega)and re-dissolved in 10-20 µl of nuclease free water. PCR products were measured and 25-50 ng was used for nested

PCR. Nested PCR was performed using Go-Taq™ Green PCR mastermix (Promega). The nested PCR reaction was prepared by mixing 25 µL Go-Taq™ Green PCR mastermix, 1 µL nested Vectorette primer (10 nM), 1 µL nested specific primer (20 nM), 1 µL primary Vectorette PCR product and 9.5 µL nuclease free water. PCR products were gel purified by the Wizard® SV Gel and PCR Clean Up System (Promega) and re-dissolved in 10-20 µl of nuclease free water. PCR products were cloned into StrataClone vector (Agilent Technologies) and transformed into competent cells following the manufacture's protocols. Plasmid DNA was extracted from clones by the alkaline lysis method. Positive clones were identified and confirmed by restriction digestion of plasmids. Approximately 500 ng of plasmid DNA were used as a template for sequencing to identify the *M. oryzae* DNA flanks adjacent to the T-DNA insert. To perform the sequencing reaction, both the Vectorette sequencing primer and nested specific primers were used. All the inserts were sequenced by Eurofins MWG Operon (Germany). Obtained sequences were identified by doing BLAST searches against *M. oryzae* genome sequence.

4.2.3.2 Inverse PCR (iPCR)

Inverse PCR (iPCR) was performed following standard methods (Ochman *et al.*, 1988) and those described in Meng *et al.* (2007) and Betts *et al.* (2007). Approximately 500 ng of genomic DNA was digested for 4 h in a total reaction volume of 50 µL using the restriction enzyme *Nco*I (Promega) following manufacturers standard protocols. The enzyme was heat inactivated at 65^0C for 20 min. The ligation reaction was prepared in a total volume of 100 µL by adding 10 µL of 10X T4 DNA ligase buffer, 35 µL of sterile H_2O and 5 µL of T4 DNA ligase (NEB) in 50 µL of digest. Ligation reactions were incubated at 15ºC for 18 h. Ligated DNA was precipitated by adding $1/10^{th}$ vol of 3 M NaOAC and 2.5 vol. Of 95% ethanol and recovered by centrifugation at 17,000 x g for 10 min at 4°C. The pellets were washed with

70% ethanol, dried and resuspended in 40 µL of nuclease free water. A 10 µL exonuclease reaction was prepared by adding 5 µL 5X Lambda exonuclease buffer, 4 µL water and 1 µL Lambda exonuclease (NEB). The exonuclease preparation was added in 40 µL re-suspended ligation reaction and the exonuclease digestion was carried out at 37ºC for 4 h. The exonuclease was heat inactivated at 65ºC for 20 min.

After this step, ligated DNA was finally recovered by ethanol precipitation, dried and dissolved in 20 µL of nuclease free water. An aliquot of 1 or 2 µL of the re-suspended ligation mix was used for each iPCR reaction. To perform the PCR, 2 µL of ligation product was added to 48 µL of PCR mix containing: 5 µL 10X reaction buffer, 2 µL of each primer (20 pmol each), 1 µL dNTPs (25 mM) and 1µL (5U/µL) of Herculase polymerase (Agilent Technologies). PCR conditions were; 94°C for 2 min, followed by 35 cycles of 94°C, 30 sec; 60°C, 30 sec; 72°C, 3 min and a final extension step is 72°C for 10 min. PCR products were gel purified by the Wizard® SV Gel and PCR Clean Up System (Promega) and re-dissolved in 10-20 µl of nuclease free water. PCR products were cloned into StrataClone plasmid (Agilent Technologies) and transformed into competent cells following the manufacturer's protocols. Positive clones were identified by colony PCR and plasmid DNA was extracted from positive clones by alkaline lysis. Insert sizes were confirmed by restriction digestion of plasmids. Approximately 500 ng of plasmid DNA were used as template for sequencing to identify the *M. oryzae* DNA flanks adjacent to the T-DNA insert. To perform the sequencing reaction, the same oligonucleotide primers used for the iPCR reaction. All the inserts were sequenced by Eurofins MWG Operon (Germany). Retreived sequences were identified by doing BLAST searches against *M. oryzae* genome sequence.

Table 4.1: Primers used for TAIL-PCR and iPCR

Name	Sequence (5'→3')
RBp1	CGCCTTGCAGCACATCCCCCTTTC
RBp2	TCAGATTGTCGTTTCCCGCCTTCA
RBp3	CCTGAGCAAAGACCCCAACGAG
RBp4	ACTCACGGCATGGACGAGCTGT
RBp5	GCCCGGCTGCAGATCGTTCAAA
LBp1	GTTCCCGGTCGGCATCTACTCTAT
LBp2	CTACACAGCCATCGGTCCAGACGG
LBp3	TGCTGGGGCGTCGGTTTCCACTAT
LBp4	TCTGCGGGCGATTTGTGTACGC
RB_NcoI_R1	GTCCTCGATGTTGTGGCGGATCTT
RB_NcoI_R2	TGCCCTTCAGCTCGATGCGGTT
RB_NcoI_R3	TCCACTTCAAGCTCCCGCTGTG
RB_NcoI_R4	TGCAGGTCCTCGCGTGGTAGAA
LB_NcoI_R1	GAGGCGATGTTCGGGGATTCCCAA
LB_NcoI_R2	GGCTCCAACAATGTCCTGACGG
LB_NcoI_R3	TAGTCGAGTAGCTCTCGGACGC

4.3 Results

4.3.1 Selection of T-DNA tagged Mutants for Characterization

We selected 200 T-DNA tagged mutants from the initial qualitative screening which showed reduced virulence on rice cultivar CO-39 and all of them were re-screened by the standard procedure described in section 2.2.2. We selected mutants for phenotypic and molecular characterization by a quantitative pathogenicity assay. All the primary selected mutants were re-screened once and only those mutants that showed a ≤50% reduction in disease symptoms were selected for further screening. Mutants selected from the first round of re-screening were further screened three times to test their ability to produce uniform reductions in disease symptoms. From this rigorous screening regime, we identified 9 non-pathogenic mutants. Six of those non-pathogenic mutants were screened by standard procedures because they formed conidia. The results are shown in Figure 4.1. We collected at least 100 leaves for each mutant, to confirm the uniformity of disease symptoms observed. The pathogenicity mutants were also assayed for disease-causing ability on barley by using barley cultivar Golden Promise. All of the mutants were non-pathogenic on barley, as shown in Figure 4.2. Out of 9 non-pathogenic mutants, 3 of them were impaired in conidiation. To test their ability to form conidia, we harvested 100 plates for each mutant and screened to confirm their ability to conidiate. We also assayed their pathogenicity also by using a cut-leaf assay by applying a 50 µL suspension of mycelium on leaves. None of those mutants were able to produce rice blast disease lesions (Figure 4.3). To test the ability of mutants to grow inside plant tissue, we inoculated all non-conidiating mutants on abraded or wounded rice leaves. Rice leaves were abraded using sand paper to gently remove the cuticle and a suspension of mycelium was applied to the wounds. All three mutants produced a characteristic necrotic lesion that was also observed following inoculation with the wild-type Guy11 (Figure 4.4). Although M2048

showed reduced necrosis compared to Guy11. We concluded that the non-conidiating mutants are defective in conidiation but able to grow invasively and cause rice blast disease.

From the first round of re-screening we found 75 transformants which observed 50% reduction in pathogenicity. By further screening we confirmed 62 transformants which generated consistently uniform results that were statistically significant. Quantitative analysis of lesion number is shown in Figure 4.5-.4.10. In order to count lesion numbers, at least 50 leaves were collected for each mutant showing reduction in disease symptoms. Therefore, statistical analysis was carried out on large sample set. Among the reduced mutants, 27 of them were reduced by 75%. The remaining mutants were 50-75% reduced in pathogenicity. It is important to notice that we found a diverse array of reduced pathogenic mutants where some of them are reduced in lesion size, some are in number and some of them also produced larger lesions when compared to Guy11.

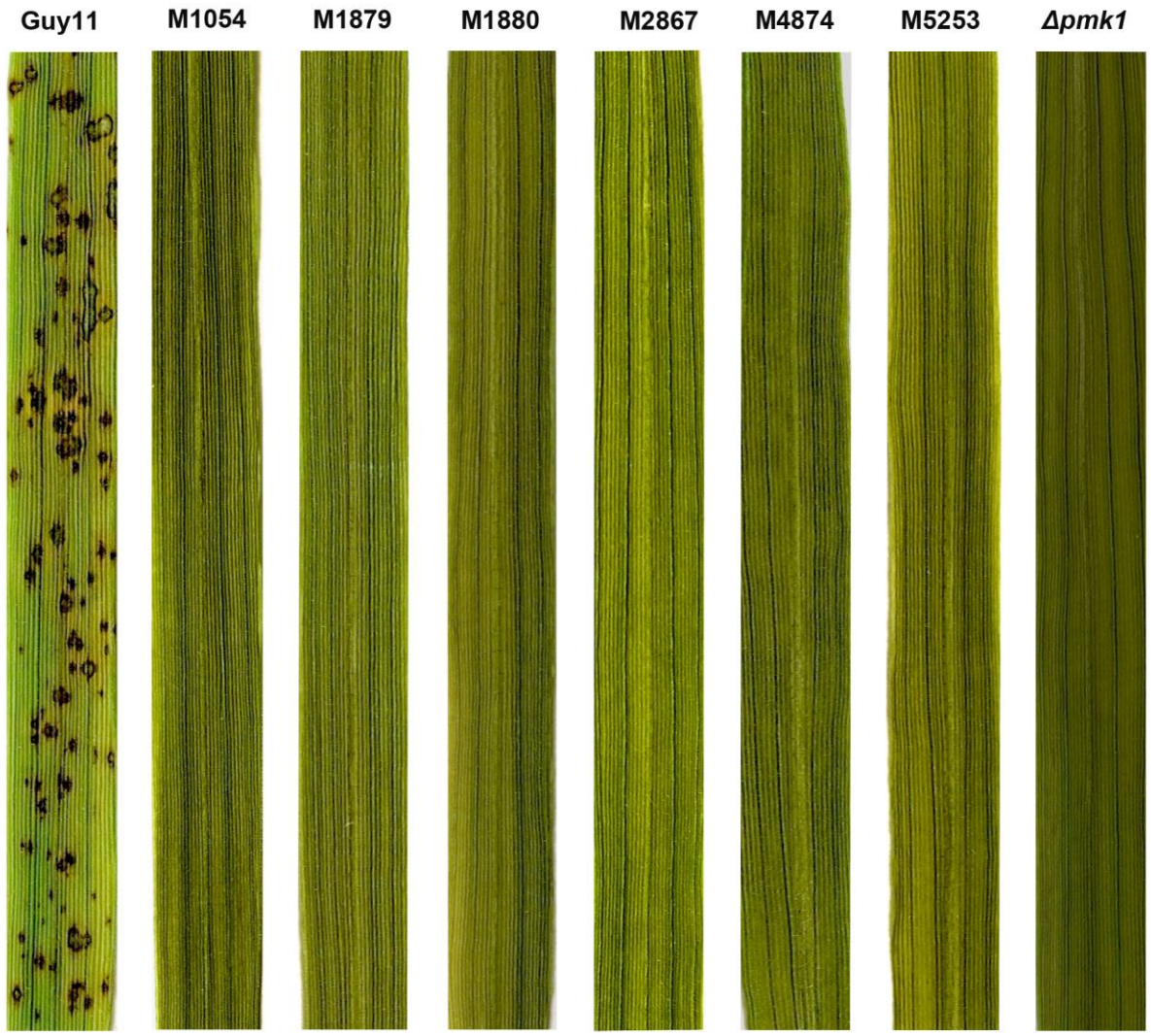

Figure 4.1: Selection of non-pathogenic mutants from pathogenicity assay. Two-week old seedlings of rice *cv.* CO-39 were spray inoculated with a conidial suspension at 5 x 10^{-4} conidia mL^{-1} and incubated at 24^{o}C, with high light and 96% humidity for five days. Plants were kept in polythene bags for 48 hours after inoculation and incubated for a further 72 hours opened in the growth room. For each mutant at least 100 individual leaf samples were collected and screened for lesions. Leaves shown here represent 9 mutants that were found completely non-pathogenic and unable to produce typical rice blast disease lesions. Four rounds of pathogenicity assays were carried out for these 6 mutants and uniform results obtained in each round.

Figure 4.2: Pathogenicity assay of selected non-pathogenic mutants on barley *cv.* Golden Promise. 10-day old seedlings barley *cv.* Golden Promise were spray inoculated with a conidial suspension at 5 x 10^{-4} conidia mL^{-1} and incubated at 24^{o}C, with high light and 96% humidity for five days. Plants were kept in polythene bags for 48 hours after inoculation and incubated for a further 72 hours opened in the growth room. For each mutant at least 50 individual leaf samples were collected and screened for lesions. Leaves show that in the same way as for rice those 9 non-pathogenic mutants were unable to produce typical rice blast disease lesions on barley. Wild-type Guy11 causes disease lesions on barley that are different from rice. Four rounds of pathogenicity assays were carried out for those 6 mutants and uniform results obtained in each round.

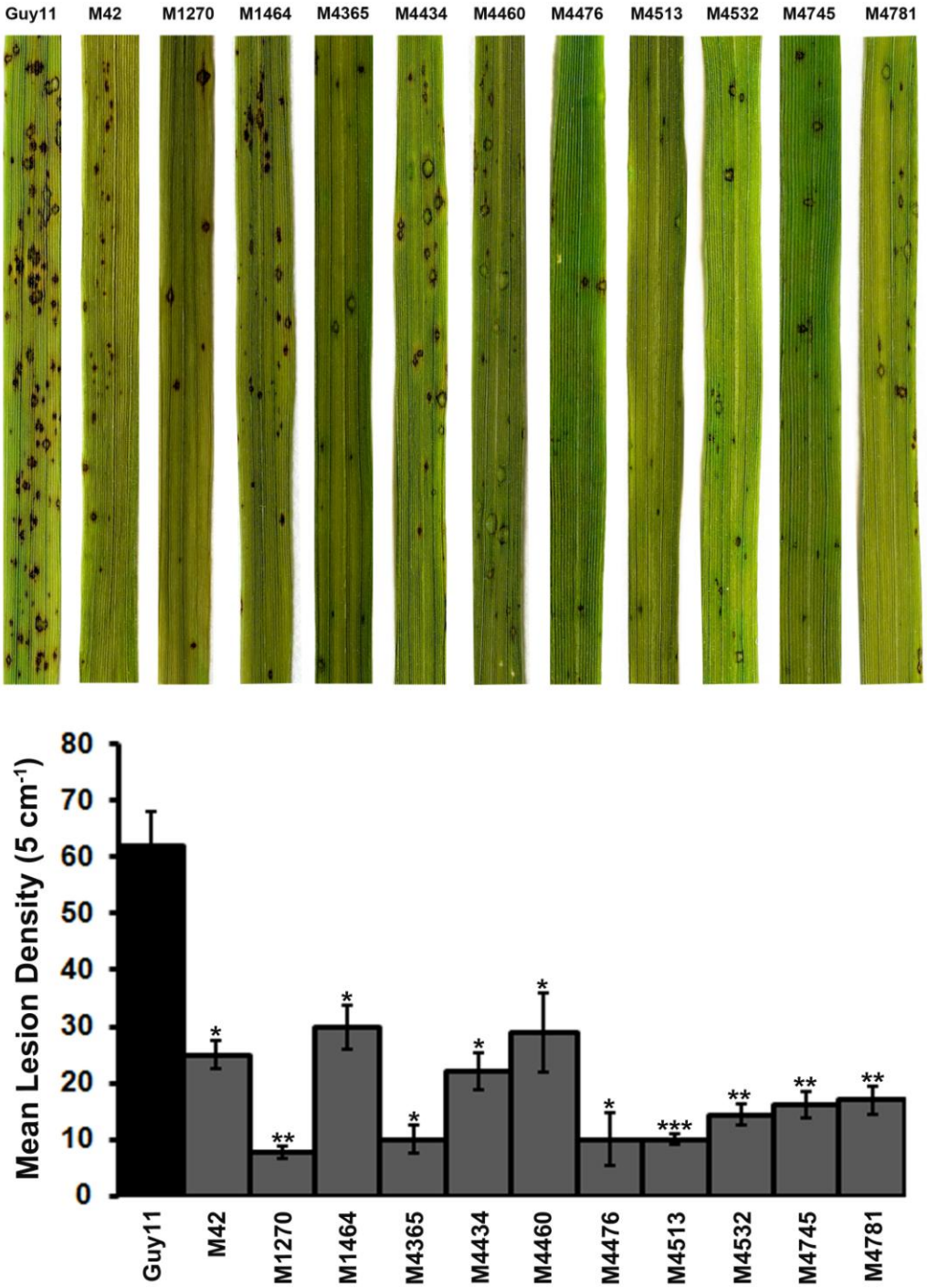

Figure 4.3: Selection of reduced mutants from pathogenicity assay. Two-week old seedlings of rice *cv.* CO-39 were spray inoculated with a conidial suspension at 5 x 10^{-4} conidia mL^{-1} and incubated at 24^{o}C, with high light and 96% humidity for five days. Plants were kept in polythene bags for 48 hours after inoculation and incubated for a further 72 hours opened in the growth room. Leaves shown here represent typical symptoms produced by each respective mutant. For each mutant at least 50 infected leaf samples were collected. Lesions were scored from a 5 cm length of most infected leaves. The graph shows mean lesion counts for each mutant. Pathogenicity assays were repeated three times and mean lesion counts were significantly different from that of wild-type Guy11 at $p<0.05$ (*****) or $p<0.01$ (******) or $p<0.001$ (*******) [Student's t-test].

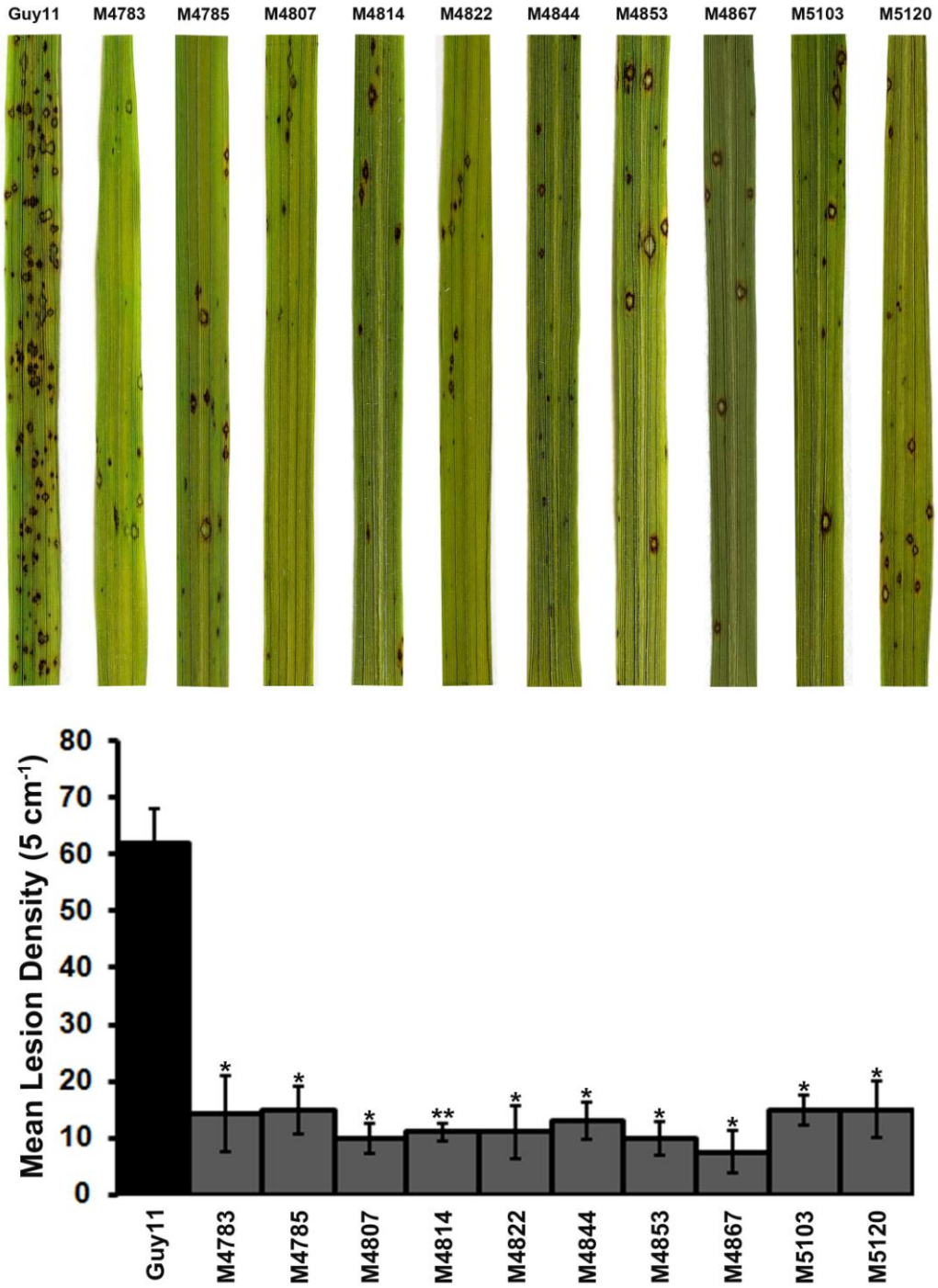

Figure 4.4: Selection of reduced virulence mutants from pathogenicity assay. Two-week old seedlings of rice *cv.* CO-39 were spray inoculated with a conidial suspension at 5 x 10^{-4} conidia mL^{-1} and incubated at 24^{o}C, with high light and 96% humidity for five days. Plants were kept in polythene bags for 48 hours after inoculation and incubated for a further 72 hours opened in the growth room. Leaves shown here represent typical symptoms produced by each respective mutant. For each mutant at least 50 infected leaf samples were collected. Lesions were scored from a 5 cm length of most infected leaves. The graph shows mean lesion counts for each mutant. Pathogenicity assays were repeated three times and mean lesion counts were significantly different from that of wild-type Guy11 at $p<0.05$ (*****) or $p<0.01$ (******) (Student's t-test].

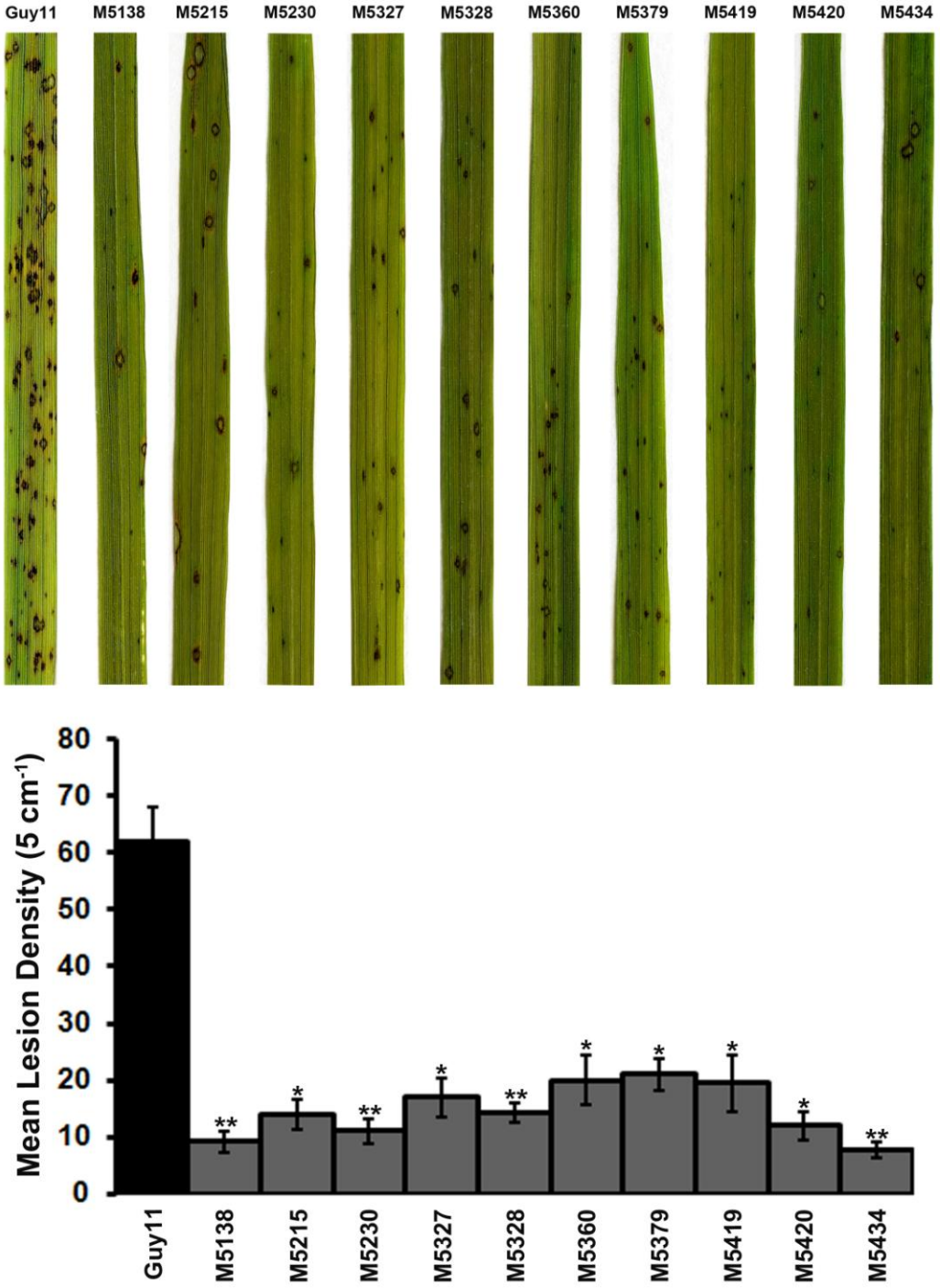

Figure 4.5: Selection of reduced virulence mutants from pathogenicity assay. Two-week old seedlings of rice *cv.* CO-39 were spray inoculated with a conidial suspension at 5 x 10^{-4} conidia mL^{-1} and incubated at 24^{o}C, with high light and 96% humidity for five days. Plants were kept in polythene bags for 48 hours after inoculation and incubated for a further 72 hours opened in the growth room. Leaves shown here represent typical symptoms produced by each respective mutant. For each mutant at least 50 infected leaf samples were collected. Lesions were scored from a 5 cm length of most infected leaves. The graph shows mean lesion counts for each mutant. Pathogenicity assays were repeated three times and mean lesion counts were significantly different from that of wild-type Guy11 at $p<0.05$ (*****) or $p<0.01$ (******) [Student's t-test].

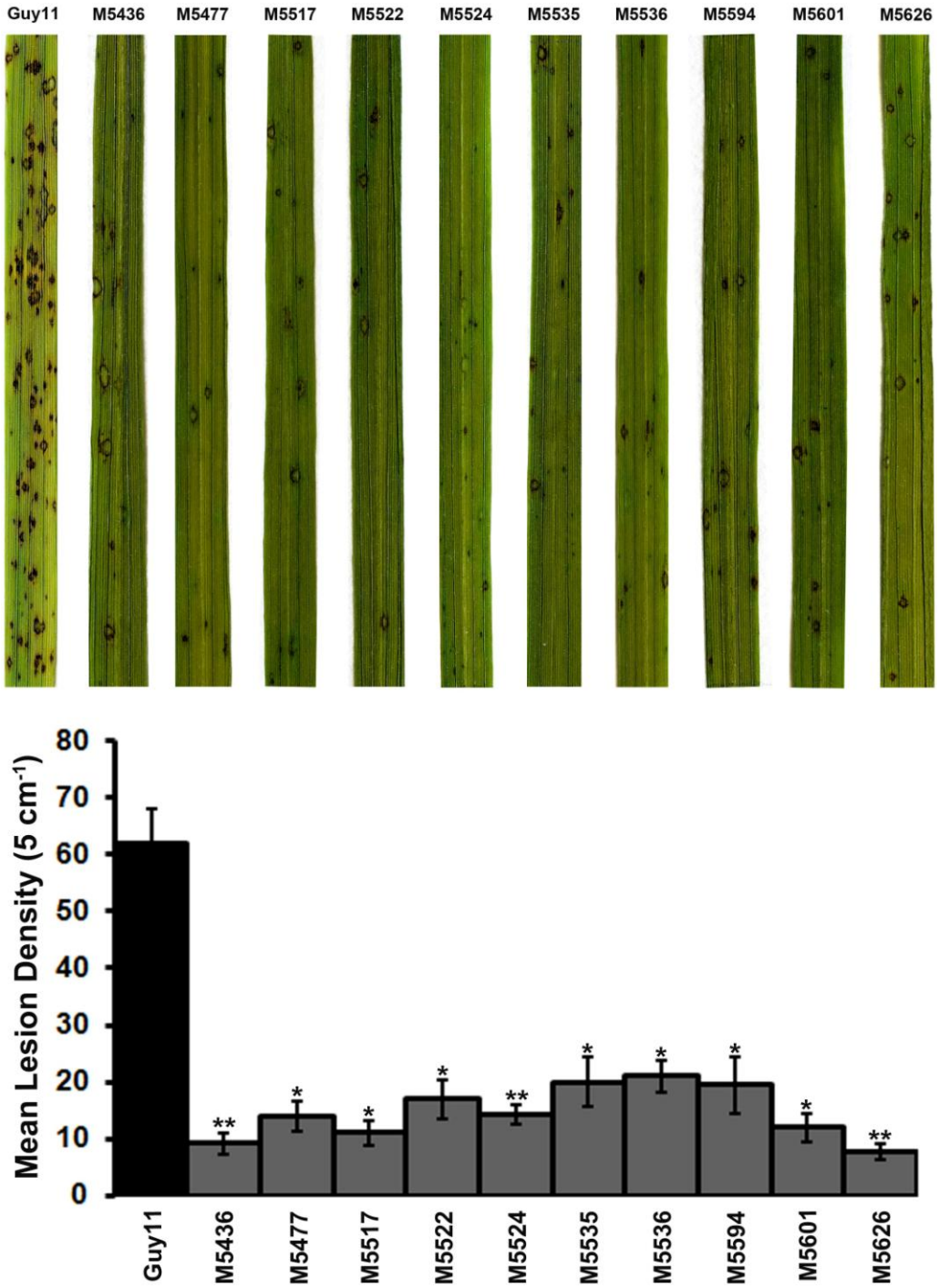

Figure 4.6: Selection of reduced virulence mutants from pathogenicity assay. Two-week old seedlings of rice *cv.* CO-39 were spray inoculated with a conidial suspension at 5 x 10^{-4} conidia mL^{-1} and incubated at 24^{o}C, with high light and 96% humidity for five days. Plants were kept in polythene bags for 48 hours after inoculation and incubated for a further 72 hours opened in the growth room. Leaves shown here represent typical symptoms produced by each respective mutant. For each mutant at least 50 infected leaf samples were collected. Lesions were scored from a 5 cm length of most infected leaves. The graph shows mean lesion counts for each mutant. Pathogenicity assays were repeated three times and mean lesion counts were significantly different from that of wild-type Guy11 at $p<0.05$ (*****) or $p<0.01$ (******) [Student's t-test].

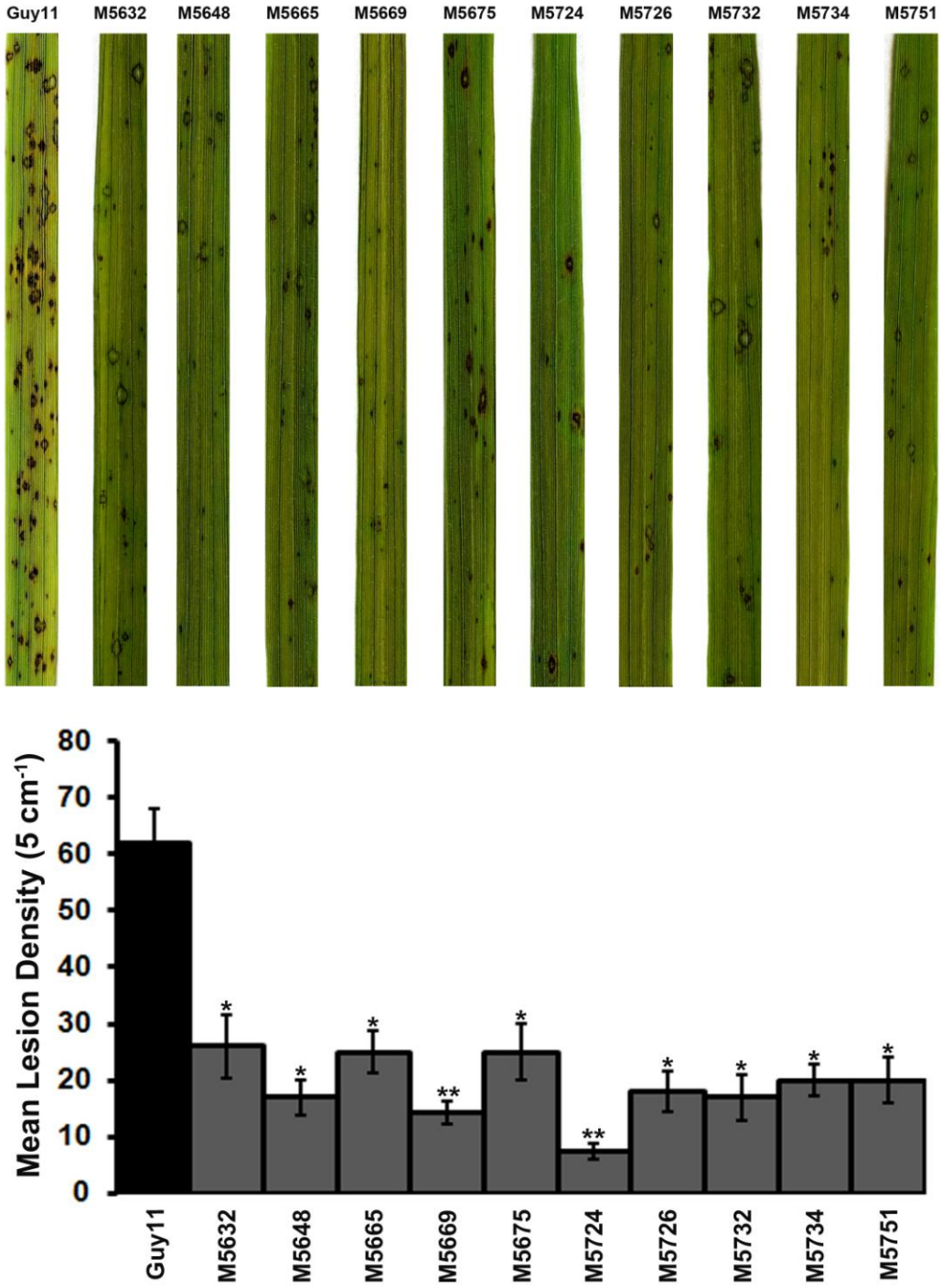

Figure 4.7: Selection of reduced virulence mutants from pathogenicity assay. Two-week old seedlings of rice *cv.* CO-39 were spray inoculated with a conidial suspension at 5 x 10^{-4} conidia mL^{-1} and incubated at 24^{o}C, with high light and 96% humidity for five days. Plants were kept in polythene bags for 48 hours after inoculation and incubated for a further 72 hours opened in the growth room. Leaves shown here represent typical symptoms produced by each respective mutant. For each mutant at least 50 infected leaf samples were collected. Lesions were scored from a 5 cm length of most infected leaves. The graph shows mean lesion counts for each mutant. Pathogenicity assays were repeated three times and mean lesion counts were significantly different from that of wild-type $p<0.05$ (*****) or $p<0.01$ (******) [Student's t-test].

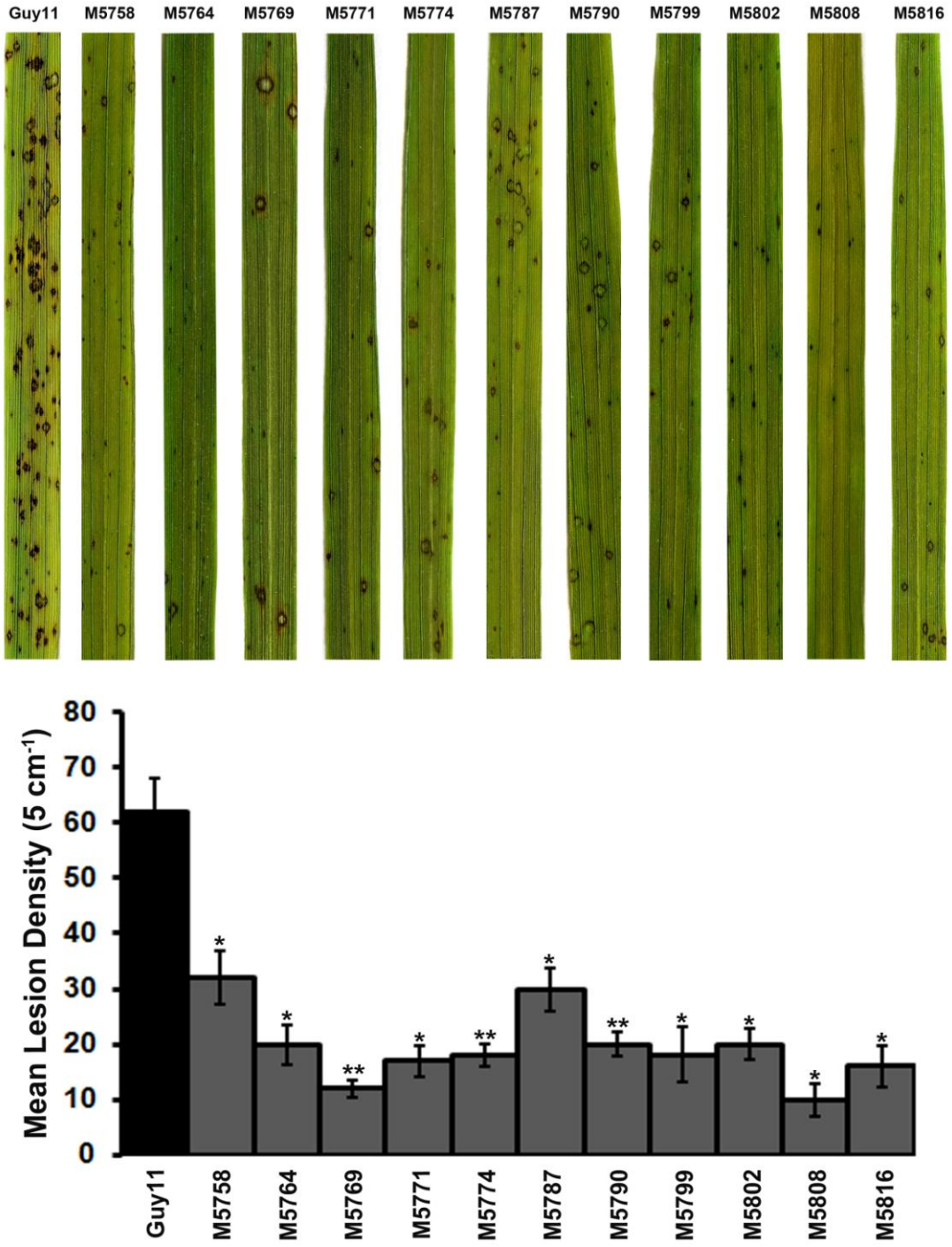

Figure 4.8: Selection of reduced virulence mutants from pathogenicity assay. Two-week old seedlings of rice *cv.* CO-39 were spray inoculated with a conidial suspension at 5 x 10^{-4} conidia mL^{-1} and incubated at 24^{o}C, with high light and 96% humidity for five days. Plants were kept in polythene bags for 48 hours after inoculation and incubated for a further 72 hours opened in the growth room. Leaves shown here represent typical symptoms produced by each respective mutant. For each mutant at least 50 infected leaf samples were collected. Lesions were scored from a 5 cm length of most infected leaves. The graph shows mean lesion counts for each mutant. Pathogenicity assays were repeated three times and mean lesion counts were significantly different from that of wild-type Guy11 $p<0.05$ (*****) or $p<0.01$ (******) [Student's t-test].

Figure 4.9: Pathogenicity assays for non-conidiating mutants of *M. oryzae*. Pathogenicity of three non-conidiating mutants was assayed by a cut-leaf assay. A 5 cm^2 plug of mycelium from the growing margins of a colony was cut taken and blended in water before applying to the rice leaves with a pipette. A 50 µL aliquot of suspended mycelium was used for each infection. Cut leaves from two-week old seedlings of rice *cv.* CO-39 were inoculated with harvested mycelium. Leaves were laid flat on agar surface in square petri dishes and incubated at 24^{o}C, with high light and 96% humidity for five days. The wild-type Guy11 shows typical large necrotic lesions. In comparison, the non-conidiating mutants only grew epiphytically and failed to cause characteristic necrotic rice blast disease lesions.

Figure 4.10: Pathogenicity assays for non-conidiating mutants on abraded leaves. Non-conidiating mutants were assayed for pathogenicity on abraded or wounded leaves by leaf drop assay. Cut leaves from two-week old seedlings of rice *cv.* CO-39 were abraded gently using a piece of sand paper. Leaves were then inoculated with a 50 µL suspension of harvested mycelium in droplets. Leaves were laid flat on agar surface in square petri dishes and incubated at 24^{o}C, with high light and 96% humidity for five days. The wild-type strain Guy11 shows typical large necrotic lesions. The non-conidiating mutants also infected wounded leaves and two of them (M48 and M2942) produced characteristic rice blast disease lesion as same as Guy11. But, mutant M2048 was reduced in virulence which was shown by smaller necrotic lesions compared to Guy11.

4.3.2 Phenotypic Characterization of the selected mutants

We selected 9 non-pathogenic and 62 reduced virulence T-DNA mutants from a rigorous re-screening regime. We initially selected 8 non-pathogenic mutants to characterize phenotypically (Figure 4.11). To characterize those mutants we observed their vegetative growth, assayed conidial germination and the frequency of appressorium development as well as the ability to penetrate onion and rice epidermis layers. The mutants charecterized phenotypically were M48, M1054, M1879, M1880, M2048, M2867, M2942 & M4874 respectively.

4.3.2.1 Vegetative growth and colony morphology of the selected mutants

Selected non-pathogenic and reduced-pathogenicity T-DNA mutants were grown on complete medium in 9 cm plates and images of the culture plate were recorded after 12 days of growth at 24°C as shown in Figure 4.11-16. We measured the diameter of each fungal colony after 12 days and compared it with wild-type Guy11. Among the non-pathogenic mutants, M1879, M2048 (defective in conidiation) and M5253 showed reduced vegetative growth (Figure 4.17A). Eight mutants showing reduced virulence that grew less well were M4513, M4844, M5764, M5790, M5799 and M5802 (Figure 4.17B & C). Some of the mutants such as M4807, M4814, M4822, M5120, M5360, M5379 and M5808 grew slightly larger colonies compared to Guy11, although not significant (statistics not shown). It is noteworthy that a number of the selected T-DNA mutants showed distinct morphological phenotypes compared to Guy11 (Figure 4.12-16).

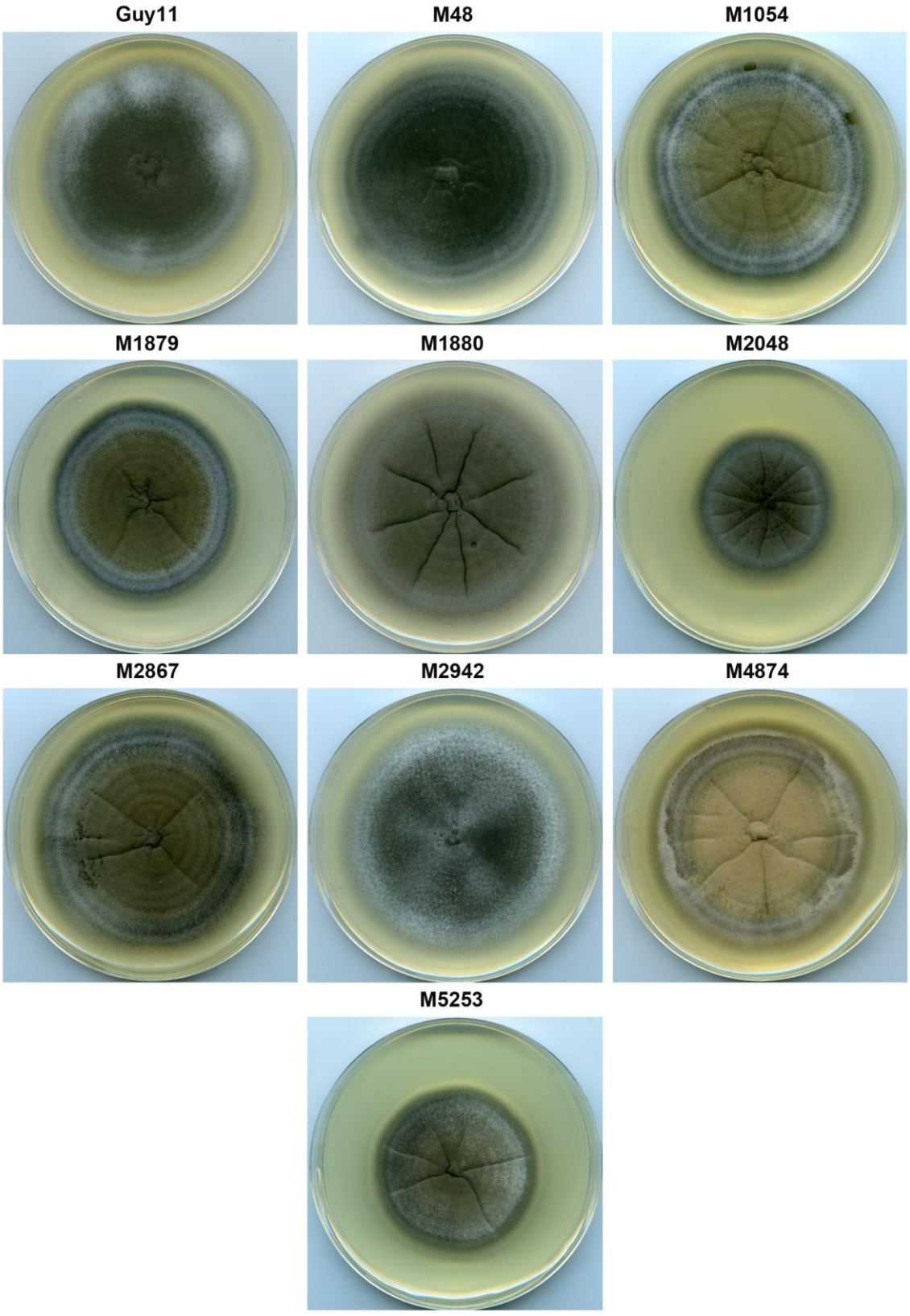

Figure 4.11: Growth and morphology of non-pathogenic T-DNA mutants of *M. oryzae* grown on CM. Selected non-pathogenic T-DNA mutants were grown on complete medium in 9 cm plates and images of the plates were recorded after 12 days of growth at 24°C. Mutants M1879, M2048 and M5253 were reduced in vegetative growth compared to Guy11.

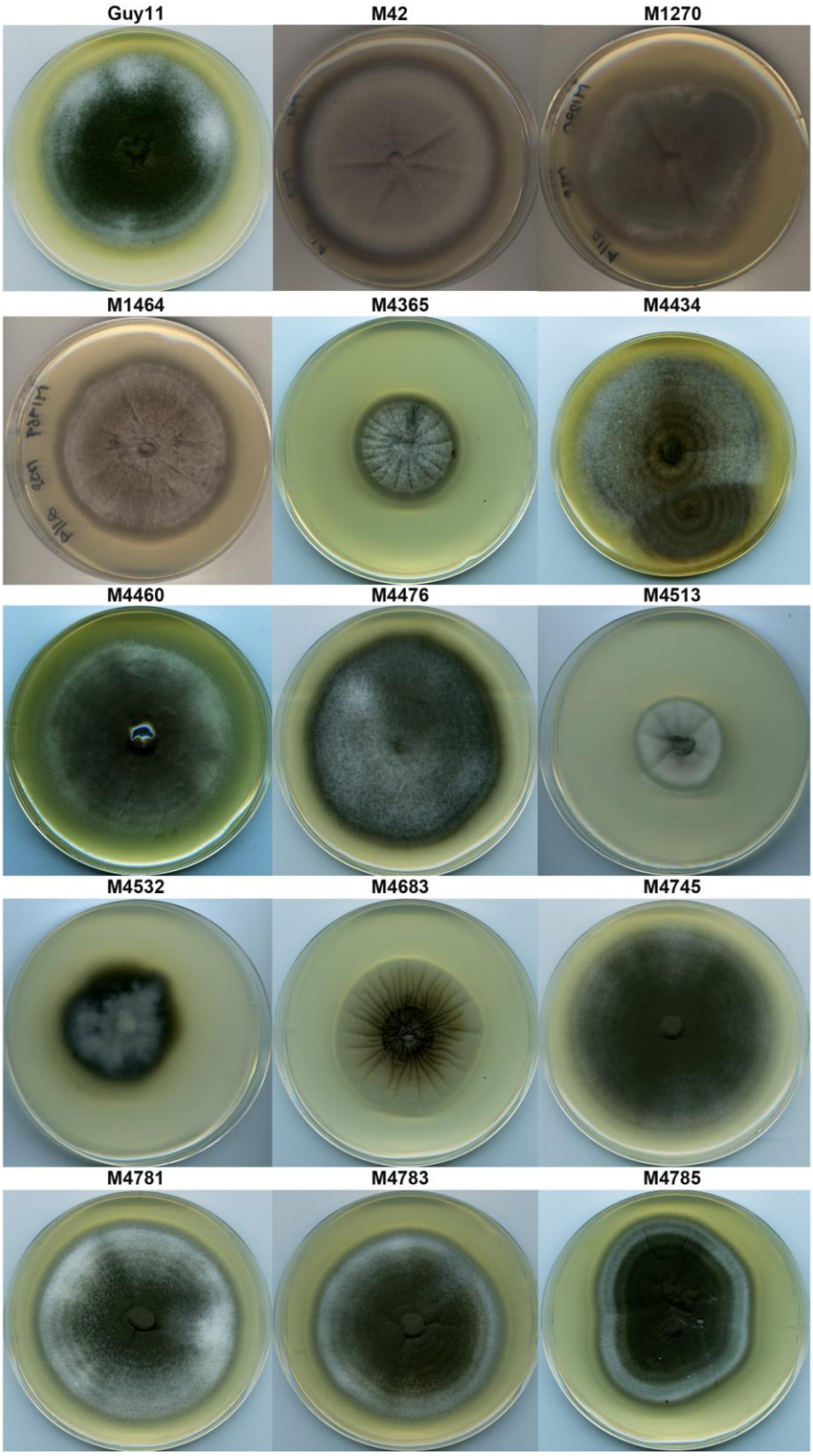

Figure 4.12: Growth and morphology of reduced virulence T-DNA mutants of *M. oryzae* grown on CM. Selected non-pathogenic T-DNA mutants were grown on complete medium in 9 cm plates and images of the plates were recorded after growing for 12 days at 24°C. Some mutants showed weak vegetative growth phenotype (e.g. M4365, M4513 and M4532) compared to Guy11.

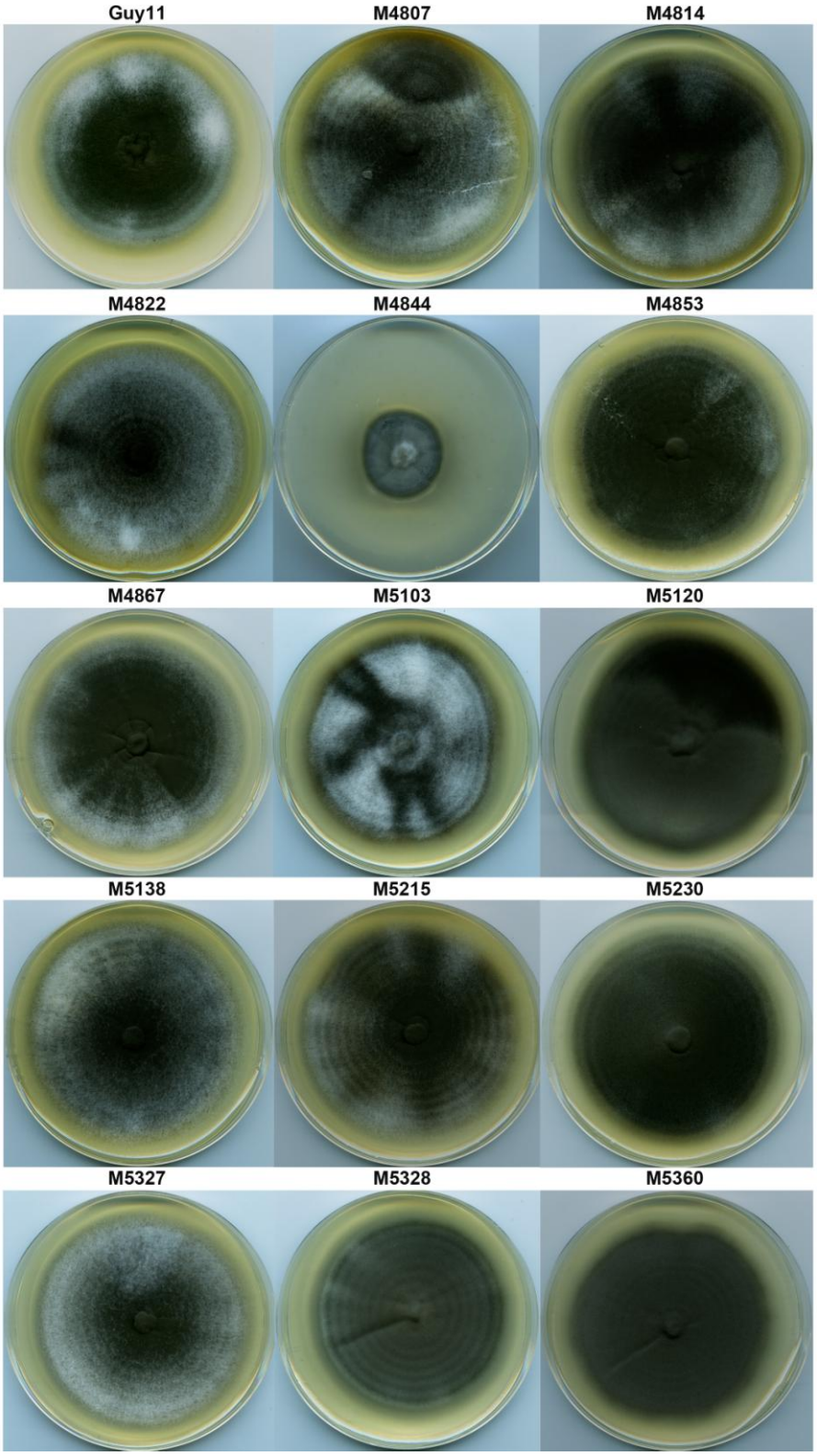

Figure 4.13: Growth and morphology of selected reduced virulence T-DNA mutants of *M. oryzae* grown on CM. Selected reduced virulence T-DNA mutants were grown on complete medium in 9 cm plates and images of the plates were recorded after 12 days of growth at 24°C. Mutant M4844 showed remarkably reduced growth and some of them had grown larger (e.g. M4807, M4814, M4822, M5120, M5360) compared to Guy11.

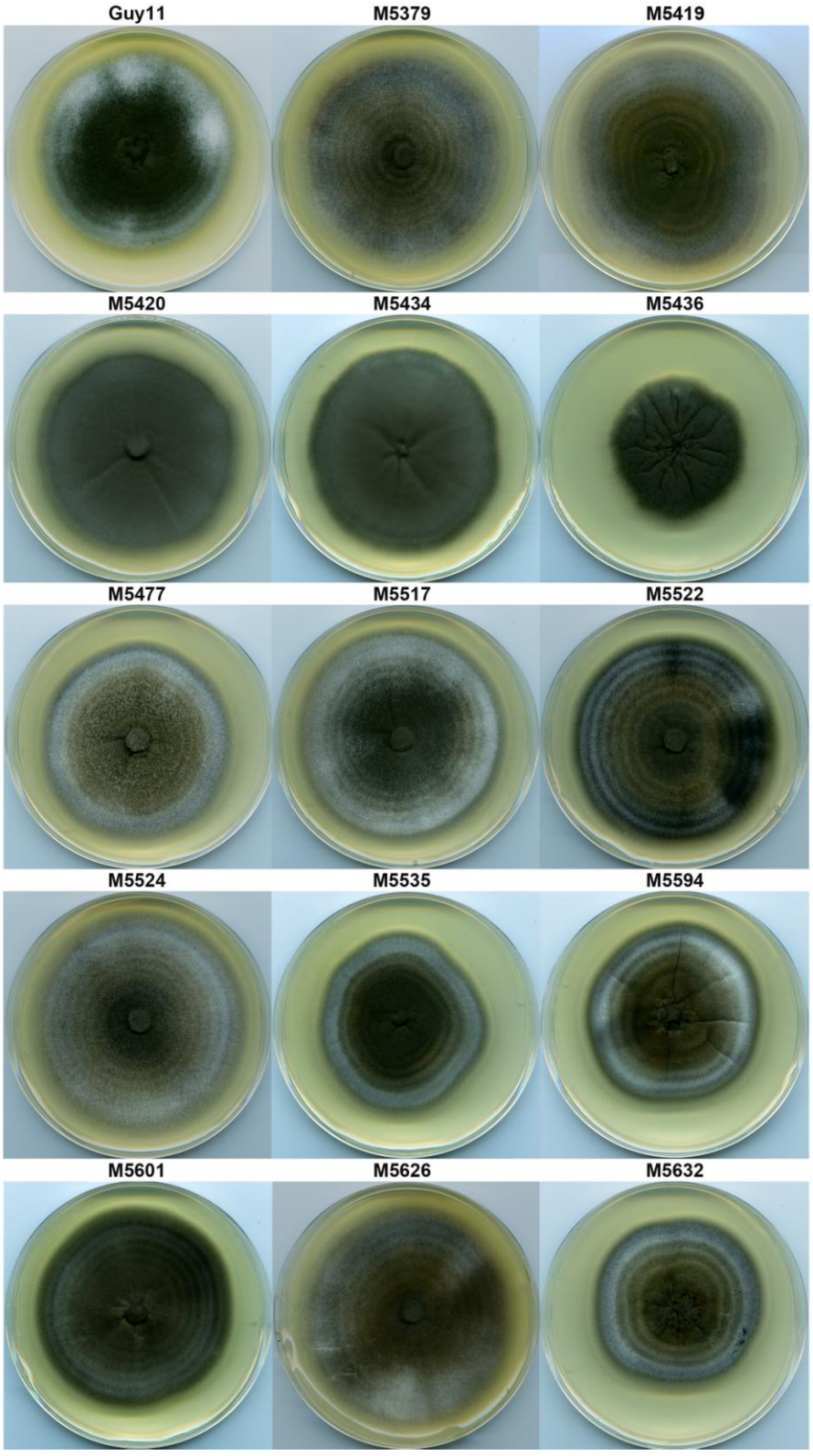

Figure 4.14: Growth and morphology of selected reduced virulence T-DNA mutants of *M. oryzae* grown on CM. Selected reduced virulence T-DNA mutants were grown on complete medium in 9 cm plates and images of the plates were recorded after growing for 12 days at 24°C. Mutants M5436, M5535, M5594 and M5632 showed reduced growth and some others grew larger (M5379 and M5419) compared to wild-type strain Guy11.

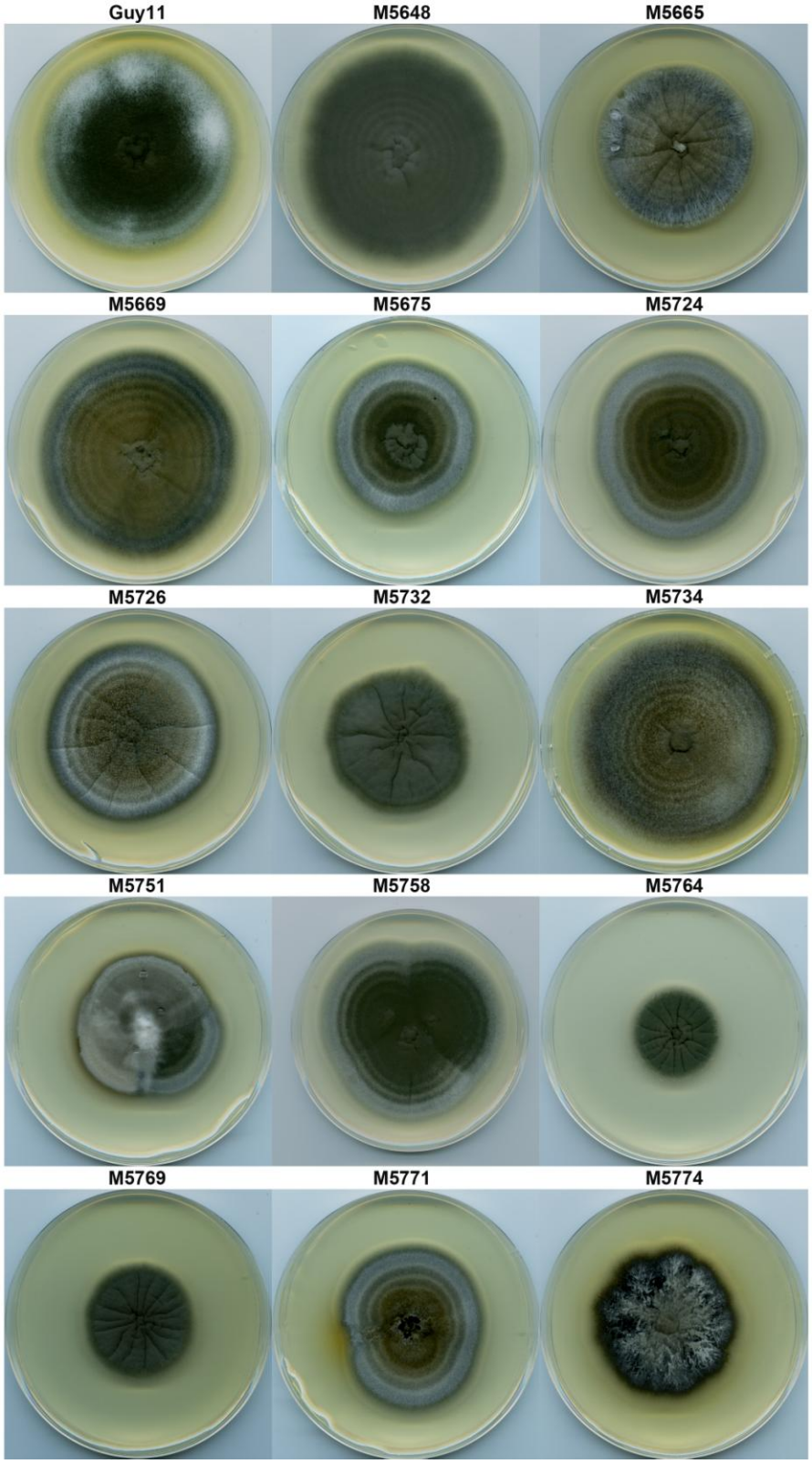

Figure 4.15: Growth and morphology of selected reduced virulence T-DNA mutants of *M. oryzae* grown on CM. Selected reduced virulence T-DNA mutants were grown on complete medium in 9 cm plates and images of the plates were recorded after 12 days of growth at 24°C. Some of the mutants were weak in vegetative growth (e.g. M5675, M5732, M5764, M5769) compared to wild-type strain Guy11.

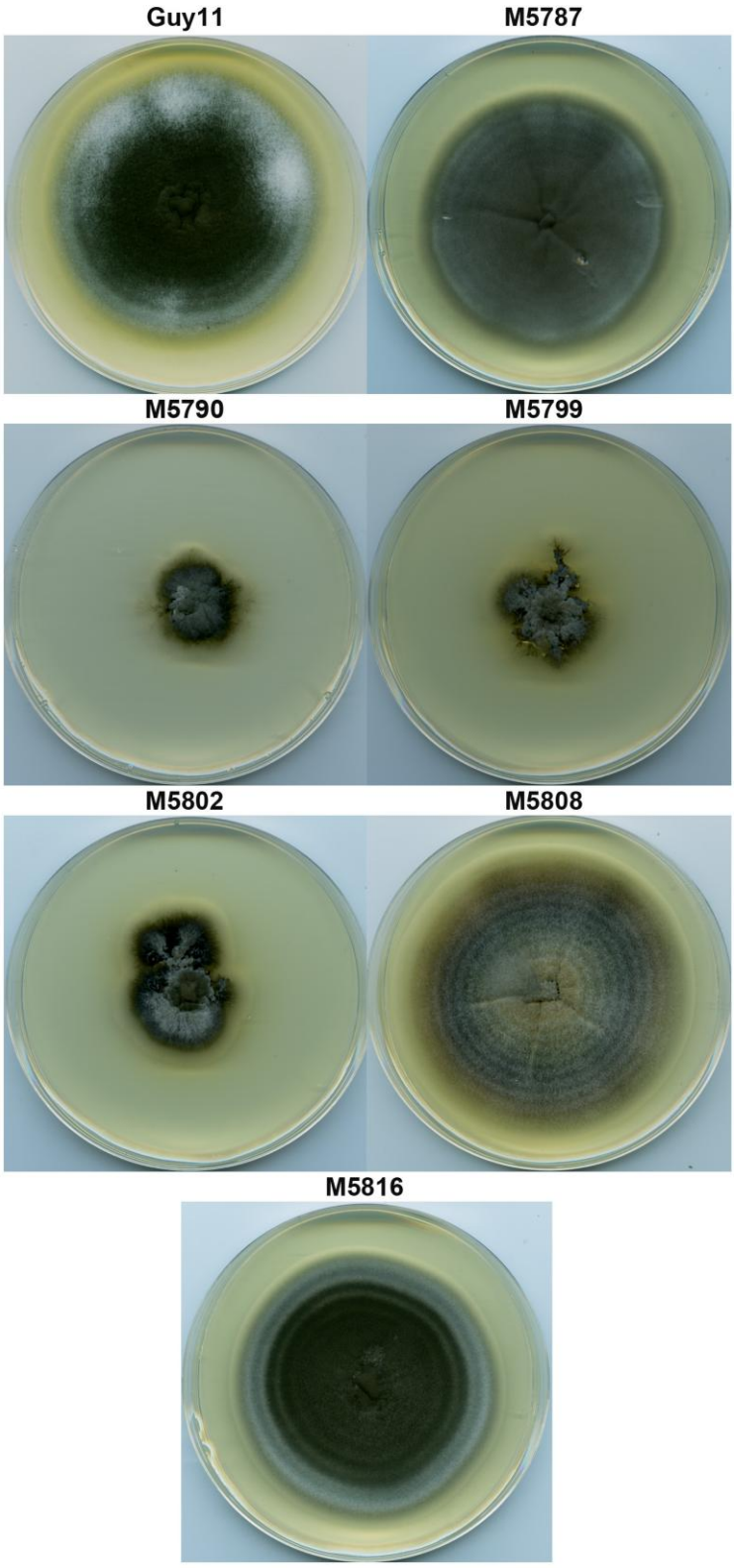

Figure 4.16: Growth and morphology of selected reduced virulence T-DNA mutants of *M. oryzae* grown on CM. Selected reduced virulence T-DNA mutants were grown on complete medium in 9 cm plates and images of the plates were recorded after 12 days of growth at 24°C. Mutants M5790, M5799 and M5802 were reduced in vegetative growth and M5808 grew larger compared to wild-type strain Guy11.

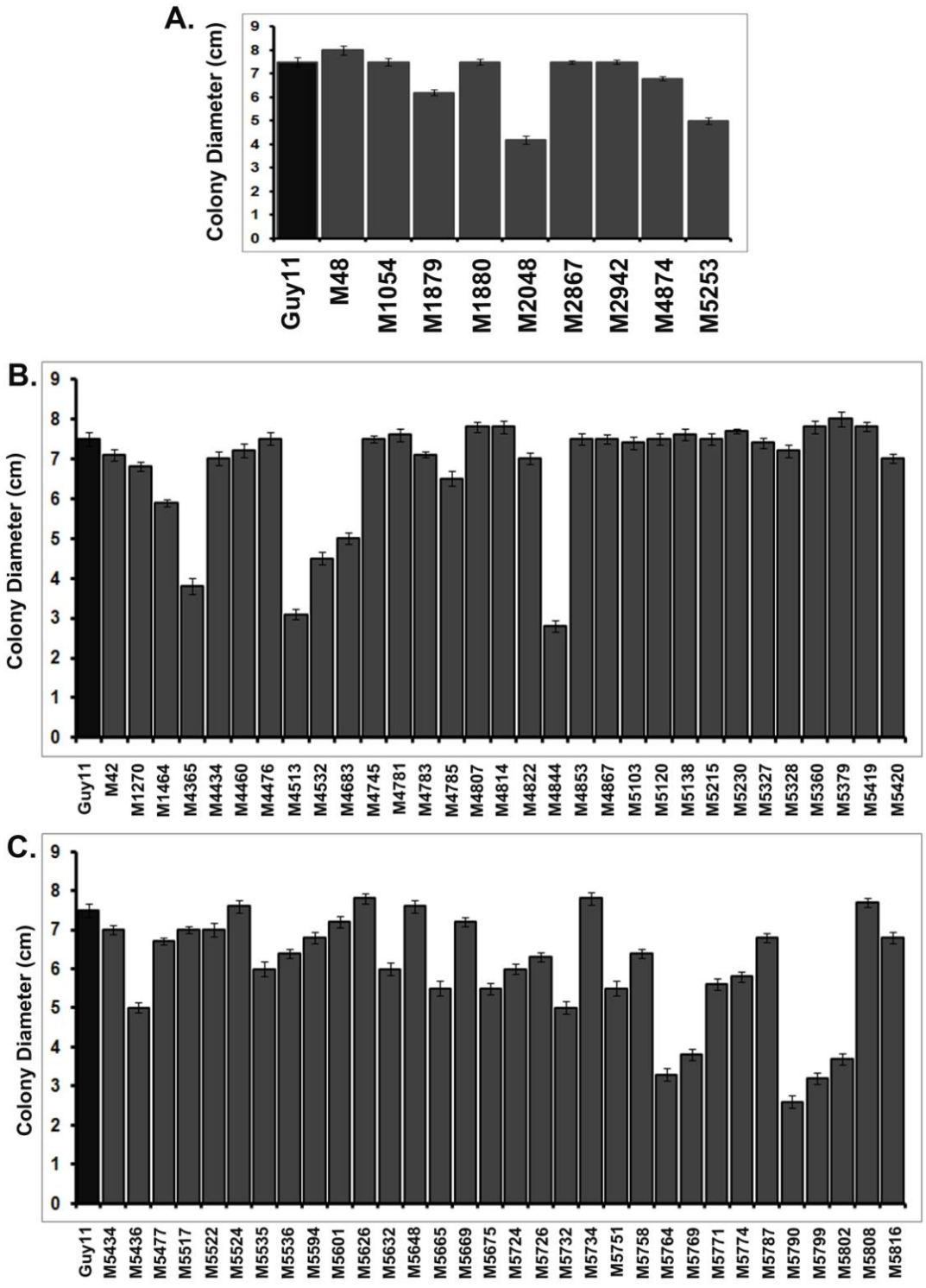

Figure 4.17: Vegetative growth comparison of selected T-DNA mutants of *M. oryzae* on CM. Selected non-pathogenic and reduced virulence T-DNA mutants were grown on complete medium in 9 cm plates and the diameter of colonies measured after 12 days of growth at 24°C. Three replicates were measured for each mutant. Bar charts show the diameter of colony in 9 cm plates. **A.** Three non-pathogenic mutants showed reduction in growth (M1879, M2048 and M5253). **B. & C.** Eight reduced-pathogenic mutants showed very weak growth (e.g. M4513, M4844, M5758, M5790), whereas some of them grew larger than the wild-type Guy11 (e.g. M5379, M5734, M5808).

4.3.2.2 Conidiation, germination and Appressorium Development Assay

In order to assay infection-related development of selected non-pathogenic mutants, we counted conidia for each mutant and observed the frequency of spore germination and appressorium development. Conidia were harvested from three mycelial discs (diameter 1-cm each), suspended in 1 ml sterile water and counted with a haemocytometer by bright field microscopy. Conidial germination and the development of appressoria were monitored over time on borosilicate glass coverslips using a method adapted from Hamer *et al.* (1988). Results showing frequency of conidiation, germination and appressorium development are summarized in Table 4.1.

Mutants M1054 and M1879 produced a dramatically reduced number of conidia. Mutants M1054 and M1879 produced $1.8\pm1.2\times10^3$ and $1.3\pm0.9\times10^3$ conidia mL^{-1} on CM plates, in contrast the wild-type Guy11 produced $6.1\pm0.8\times10^3$ conidia mL^{-1}. Therefore, these two mutants are clearly defective in conidiation ($p<0.05$). None of the mutants except M1879 showed defect in conidial germination. In the appressorium development assay, two mutants M1879 and M2867 showed a significantly reduced ability to develop appressoria (Figure 4.19 and 4.21).

We observed specific stages of appressorium development for all the conidiating non-pathogenic mutants and also three selected reduced virulence mutants (M42, M1270 and M1464). Conidia from 12-day old plates were inoculated onto glass coverslips along with Guy11 as a control. Germination and appressorium development was observed over a period of 24 h using an Olympus IX-81 inverted epifluorescence microscope. Images showing appressorium development are shown in Figure 4.18 - 4.26. Mutant M1879 was delayed in appressorium formation (Figure 4.19). They formed appressoria at 6 h compared to 4 h in

Guy11. Moreover, M1879 produced a high percentage of defective (single or two-celled) conidia which accounted for more than 60% of the conidia observed during appressorium development (Figure 4.19). Those cells also showed aberrant germ tube formation and development of two immature appressoria (Figure: 4.19) which is unusual (Veneault-Fourrey *et al.*, 2006). They also developed germ tube from the basal cells of conidia which showed this mutant was lack in polarity. Reduced virulence mutant M1464 developed very long germ tubes compared to those of Guy11 (Figure 4.26). Furthermore, mutants M1054, M1879 and M2867 were delayed in conidial collapse compared to Guy11 ((Figure 4.18, Figure 4.19 & Figure 4.21). Mutant M1880 failed to form appressoria and instead developed very long germ-tube which is similar to the MAPK deletion mutant Δ*pmk1* of *M. oryzae* (Figure 4.20) (Xu & Hamer, 1996). But M1880 did not show any defect in conidiation and germination (Figure 4.20).

Table 4.2: Comparison of conidiation, germination and appressorium formation for selected non-pathogenic mutants.

Strain	Conidiation ($x10^3$ conidia/mL)	Germination	Appressorium Development
Guy11	6.1±0.8a	95±0.8%a	97.0±1.2%a
M1054	1.8±1.2b	92±2.4%a	92.6±2.6%a
M1879	1.3±0.9b	58±1.2%b	65.0±4.7%b
M1880	5.7±1.7a	91±0.4%a	0
M2867	3.7±1.8b	84.8±1.6%a	74.6±3.8%b
M4874	6.3±1.4a	94.5±0.7%a	95.5±2.8%a

a	Indicates that the values are not significantly different between wild-type and T-DNA mutants (Student t-test, $p<0.05$).
b	Indicates that the values are significantly different between wild-type and T-DNA mutants (Student t-test, $p<0.05$).

Conidiation was measured as the number of conidia on a 1 cm-diameter of culture disc in 1 mL of water. Conidial suspension was counted using a haemocytometer bright field microscopy. Conidia were allowed to germinate and form appressoria on glass coverslips for 24 h. Germination of conidia was counted as the percentage of germinated conidia after 4 h incubation. Appressorium formation was recorded as the percentage of appressorium that developed from germinated conidia after 8 h incubation.

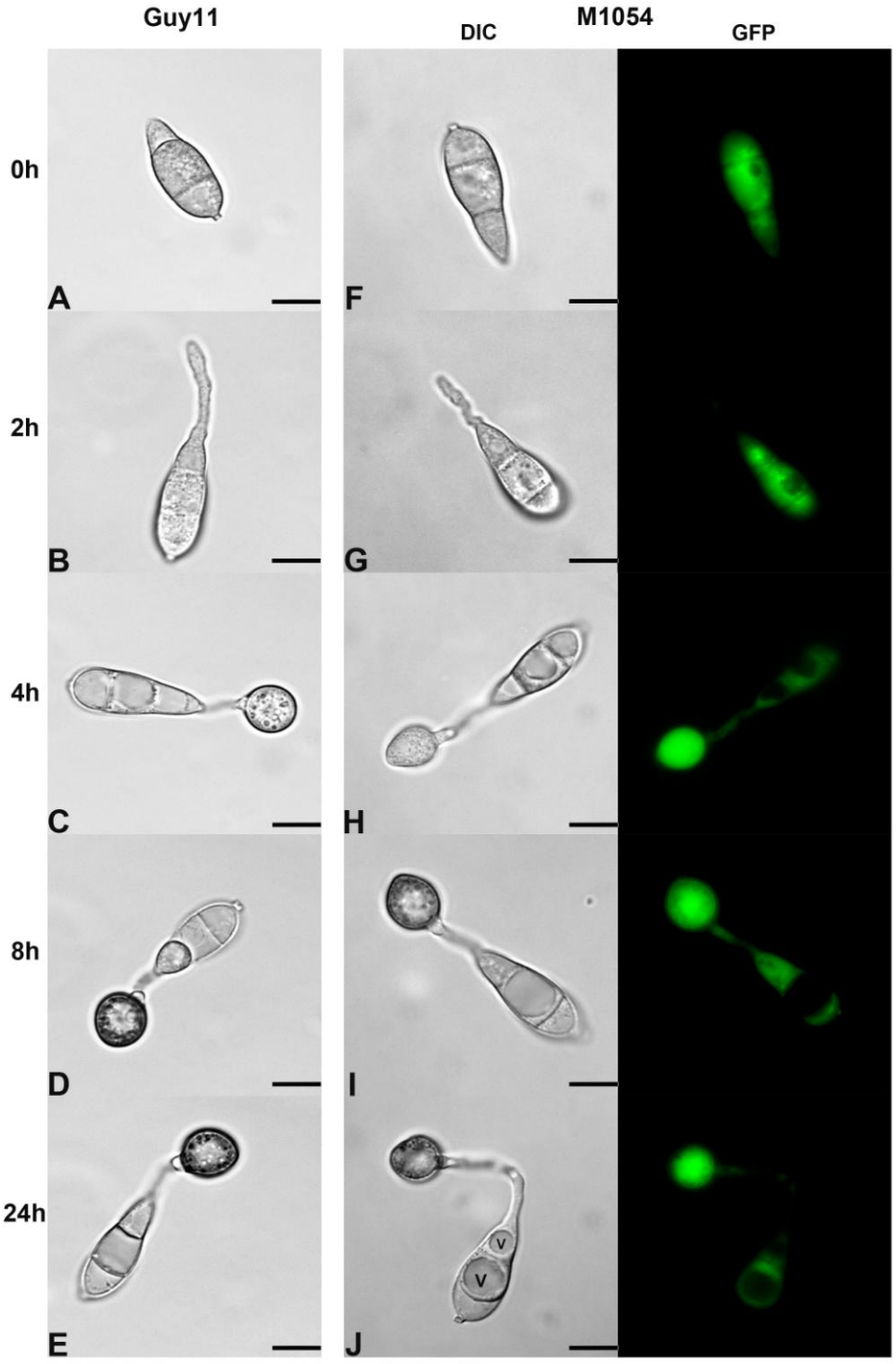

Figure 4.18: Appressorium development of non-pathogenic mutant M1054. Conidia from 12-day old plates of T-DNA mutant M1054 were inoculated onto glass coverslips along with Guy11 as a control. Germination and appressorium development was observed over a period of 24 h using an Olympus IX-81 inverted epifluorescence microscope fitted with HQ^2 camera. Representative DIC (differential interference contrast) and fluorescence images are shown at 0, 2, 4, 8and 24 hpi. M1054 was delayed in conidial collapse. At 24 h, vacuolated **(V)** M1054 conidial cells could not collapse **(J)** compared to the Guy11 conidium which completely collapsed **(E)** by this time point. Scale Bar = 10 µm.

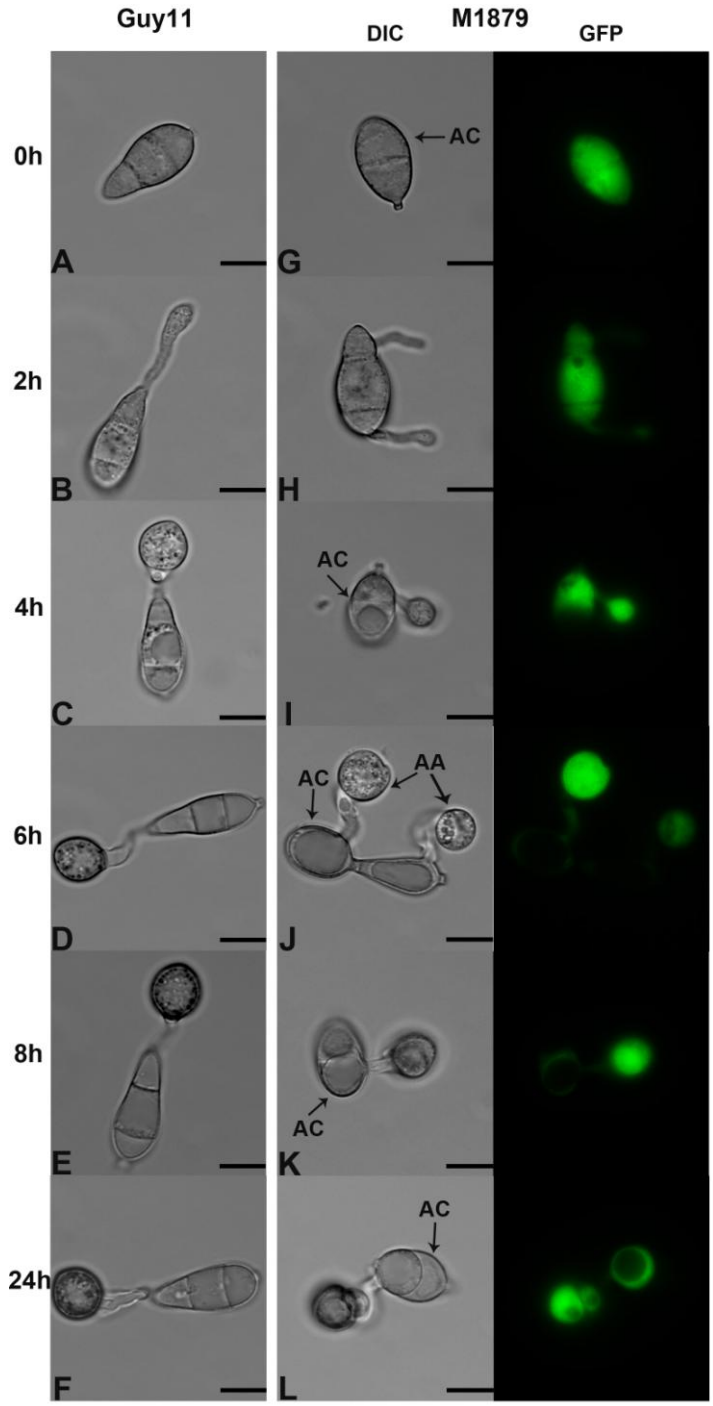

Figure 4.19: Appressorium development of non-pathogenic mutant M1879. Conidia from 12-day old plates of non-pathogenic T-DNA mutant M1879 were inoculated onto glass coverslips along with Guy11 as a control. Germination and appressorium development was observed over a period of 24 h using an Olympus IX-81 inverted epifluorescence microscope fitted with HQ^2 camera. Representative DIC and fluorescence images are shown at 0, 2, 4, 6, 8and 24hpi. M1879 produced a significant percentage (>60%) of abnormal conidia (1-2 cells) which are shown as AC in **G, I, J, K** and **L.** Conidia were delayed in appressorium formation **(I)** and melanization **(K)** compared to Guy11. Aberrant appressorium (AA) was also observed which are shown by arrows. Diameter of the appressorium was smaller than that of Guy11 **(l)**. Scale Bar = 10 µm.

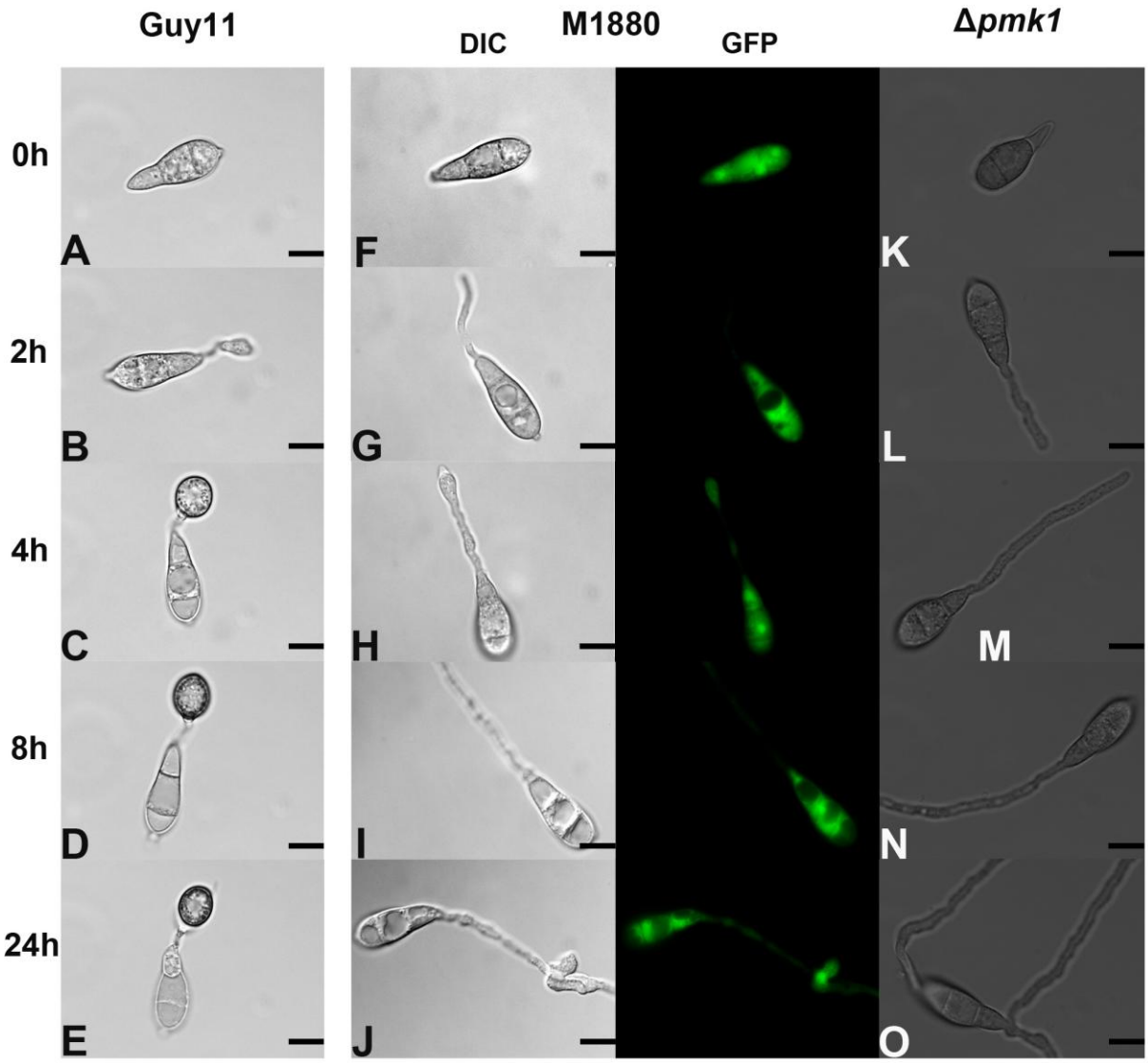

Figure 4.20: Appressorium development of non-pathogenic mutant M1880. Conidia from 12-day old plates of non-pathogenic T-DNA mutant M1880 were inoculated onto glass coverslips along with Guy11 as a control. Germination and appressorium development was observed over a period of 24 h using an Olympus IX-81 inverted epifluorescence microscope fitted with HQ^2 camera. Representative DIC and fluorescence micrographs are shown at 0, 2, 4, 8 and 24hpi. Scale Bar = 10 µm.

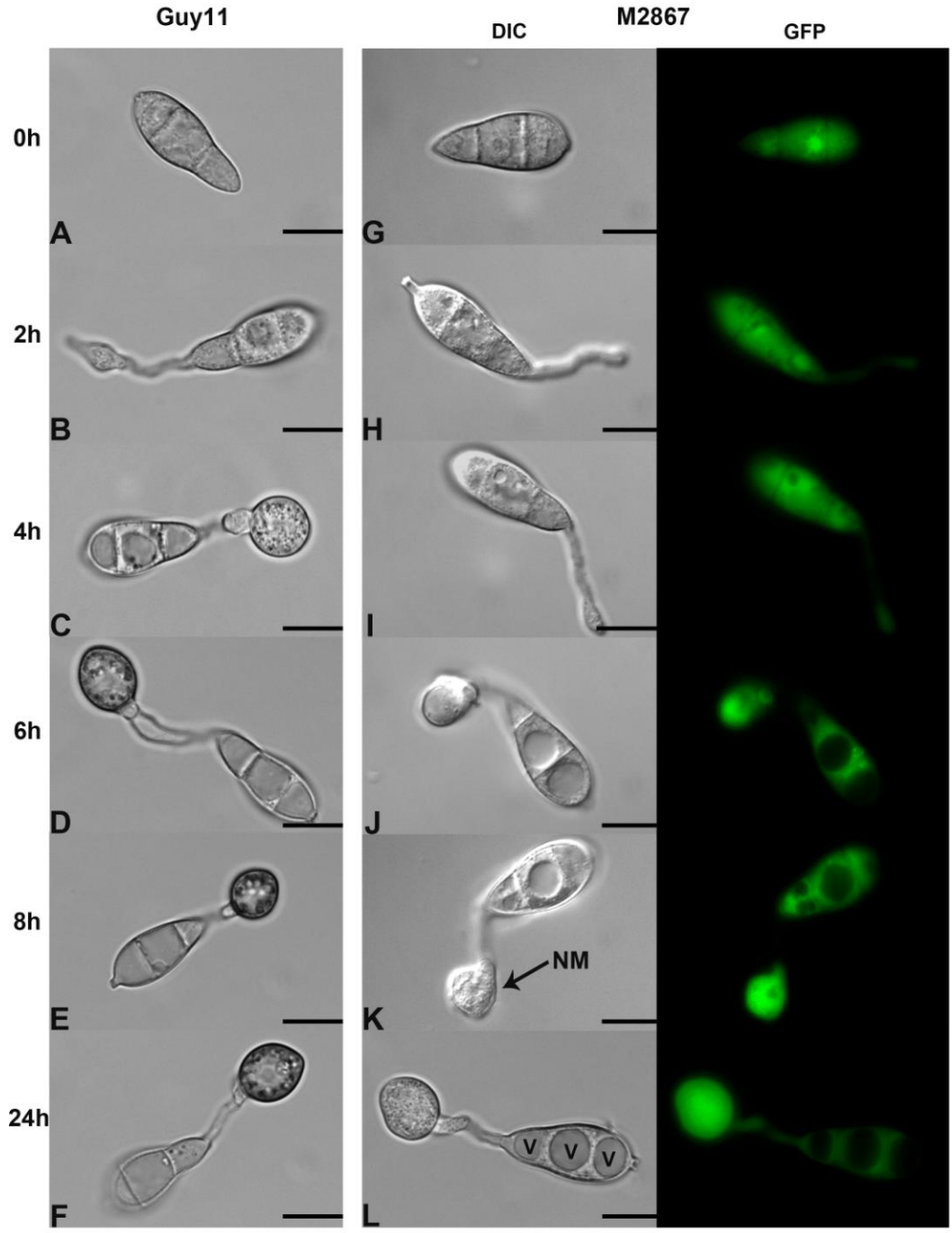

Figure 4.21: Appressorium development of non-pathogenic mutant M2867. Conidia from 12-day old plates of non-pathogenic T-DNA mutant M2867 were inoculated onto glass coverslips along with Guy11 as a control. Germination and appressorium development was observed over a period of 24 h using an Olympus IX-81 inverted epifluorescence microscope fitted with HQ^2 camera. Representative DIC and fluorescence micrographs are shown at 0, 2, 4, 6, 8 and 24hpi. Mutant M2867 was delayed in appressorium morphogenesis **(I)**, conidial collapse **(K & L)** and maturation. M2867 conidia did not collapse and large vacuoles **(V)** were observed in conidial cells **(L)**. It was also defective in appressorium melanization and at 8h non-melanized **(NM)** appressorium is indicted by an arrow. Dark layer of melanin appeared around Guy11 appressoirum at 8 h while M2867 failed to produce so even at 24 h. Scale Bar = 10 µm.

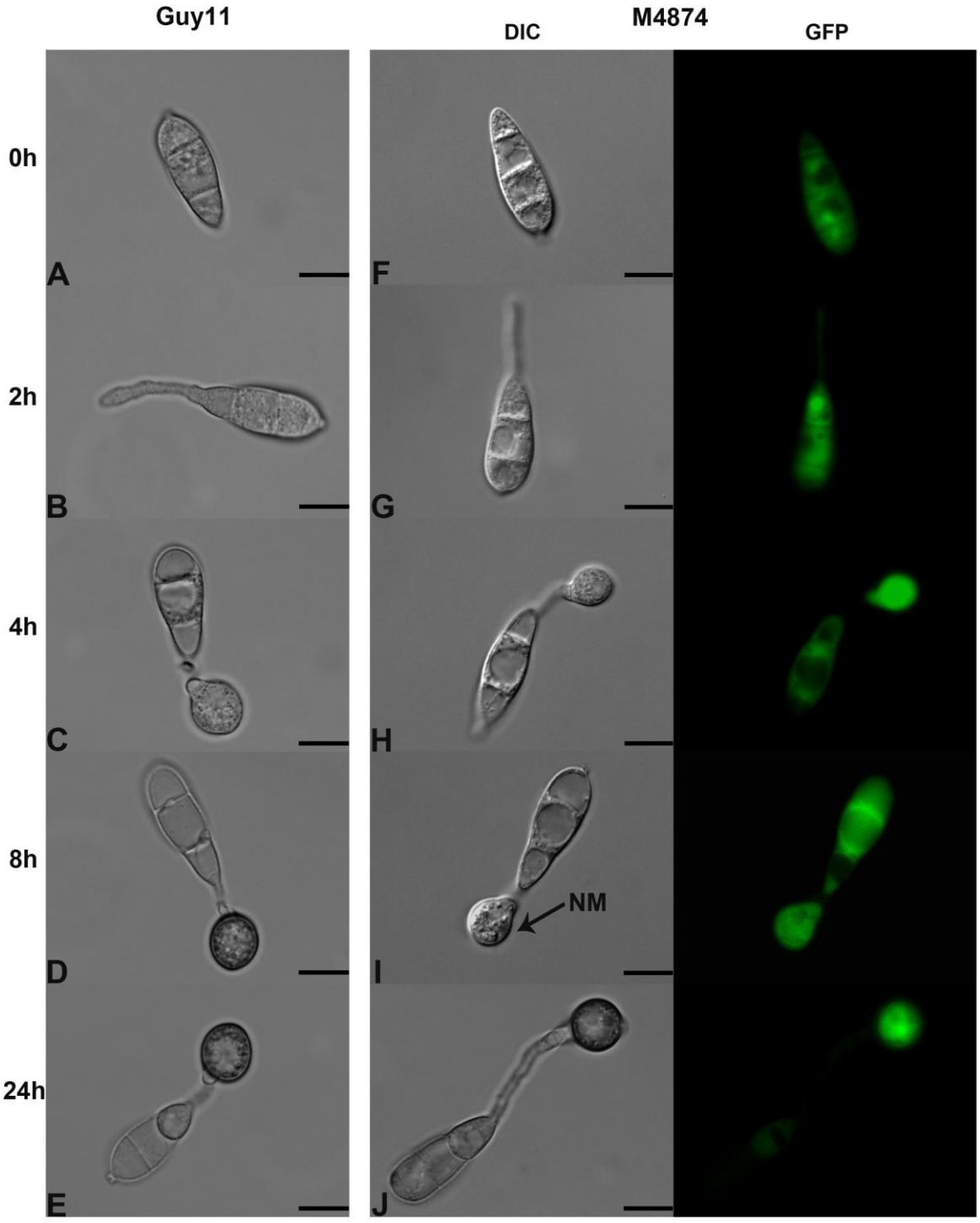

Figure 4.22: Appressorium development of non-pathogenic mutant M4874. Conidia from 12-day old plates of non-pathogenic T-DNA mutant M4874 were inoculated onto glass coverslips along with Guy11 as a control. Germination and appressorium development was observed over a period of 24 h using an Olympus IX-81 inverted epifluorescence microscope fitted with HQ^2 camera. Representative DIC and fluorescence images are shown at 0, 2, 4, 8 and 24hpi. Mutant M4874 was delayed in melanization compared to Guy11. At 8 h Guy11 showed melanization of appressoirum by producing a dark layer around it **(D)** but M4874 was non-melanized (NM) which is indicated by arrow **(I).** M4874 was observed to be melanized later at 24 h **(J)**. Scale Bar = 10 µm.

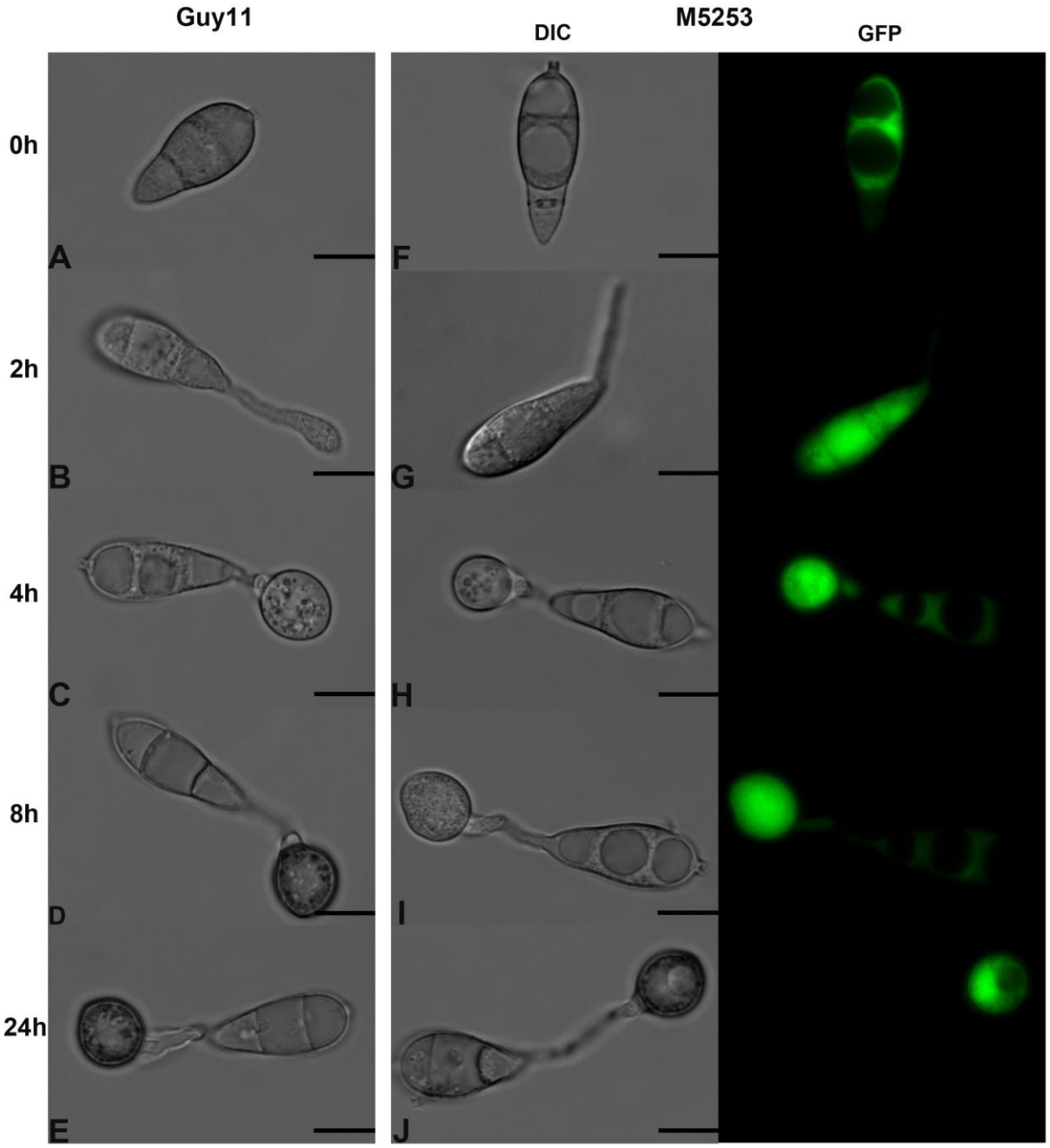

Figure 4.23: Appressorium development of non-pathogenic mutant M5253. Conidia from 12-day old plates of non-pathogenic T-DNA mutant M5253 were inoculated onto glass coverslips along with Guy11 as a control. Germination and appressorium development was observed over a period of 24 h using an Olympus IX-81 inverted epifluorescence microscope fitted with HQ^2 camera. Representative DIC and fluorescence micrographs are shown at 0, 2, 4, 8 and 24hpi. Mutant M5253 was delayed in melanization compared to Guy11. This was observed at 8 h when Guy11 melanized it's appressorium by a dark layer of melanin **(d)** while M5253 appressorium failed to produce it **(i)**. Moreover, conidial collapse and subsequent appressorium maturation were also delayed in M5253. Scale Bar = 10 µm.

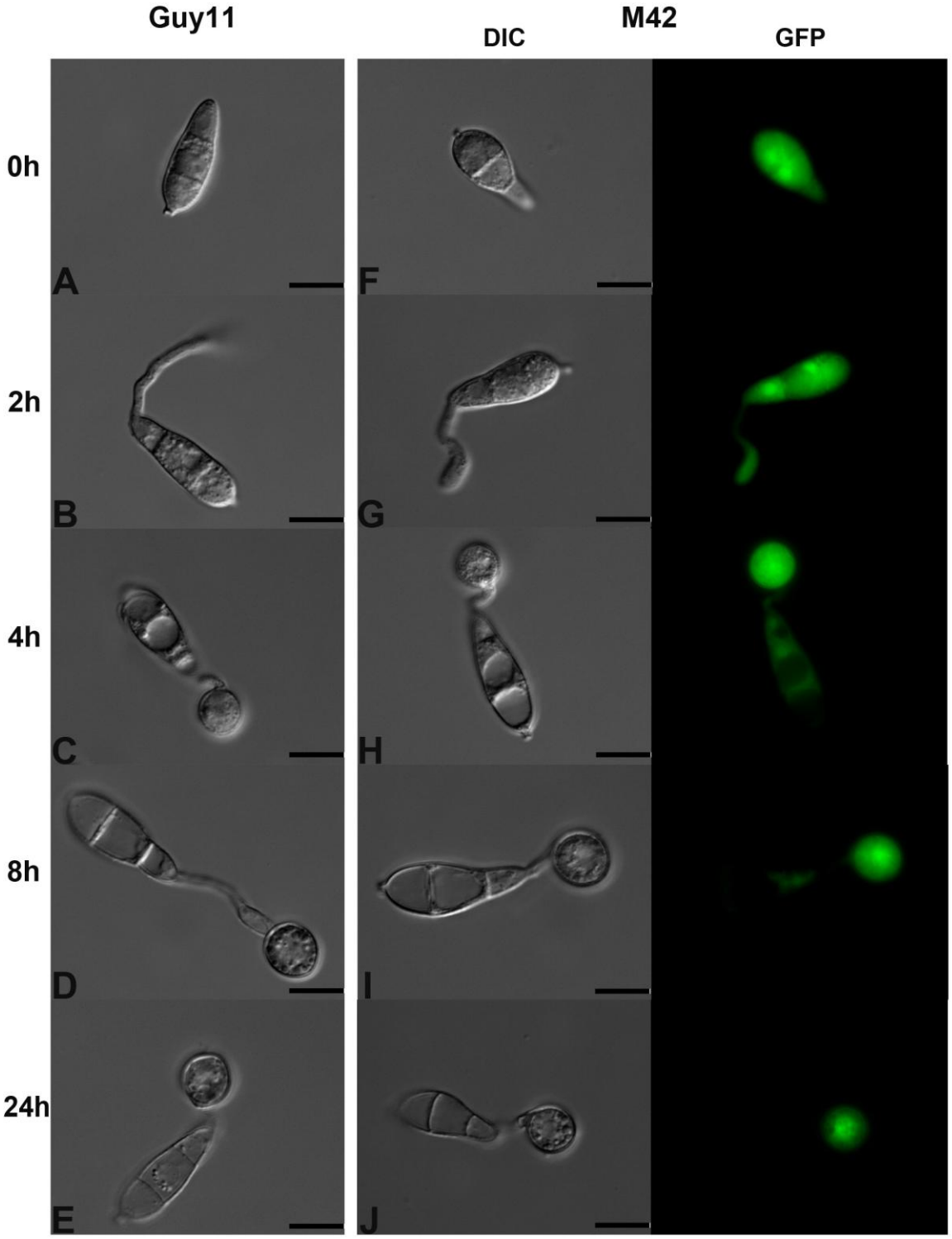

Figure 4.24: Appressorium development of reduced-pathogenic mutant M42. Conidia from 12-day old plates of reduced-pathogenic T-DNA mutant M42 were inoculated onto glass coverslips along with Guy11 as a control. Germination and appressorium development was observed over a period of 24 h using an Olympus IX-81 inverted epifluorescence microscope fitted with HQ^2 camera. Mutant M42 showed similar morphological phenotype as Guy11 during appressorium development. Representative DIC and fluorescence images are shown at 0, 2, 4, 8 and 24hpi. Scale Bar = 10 µm.

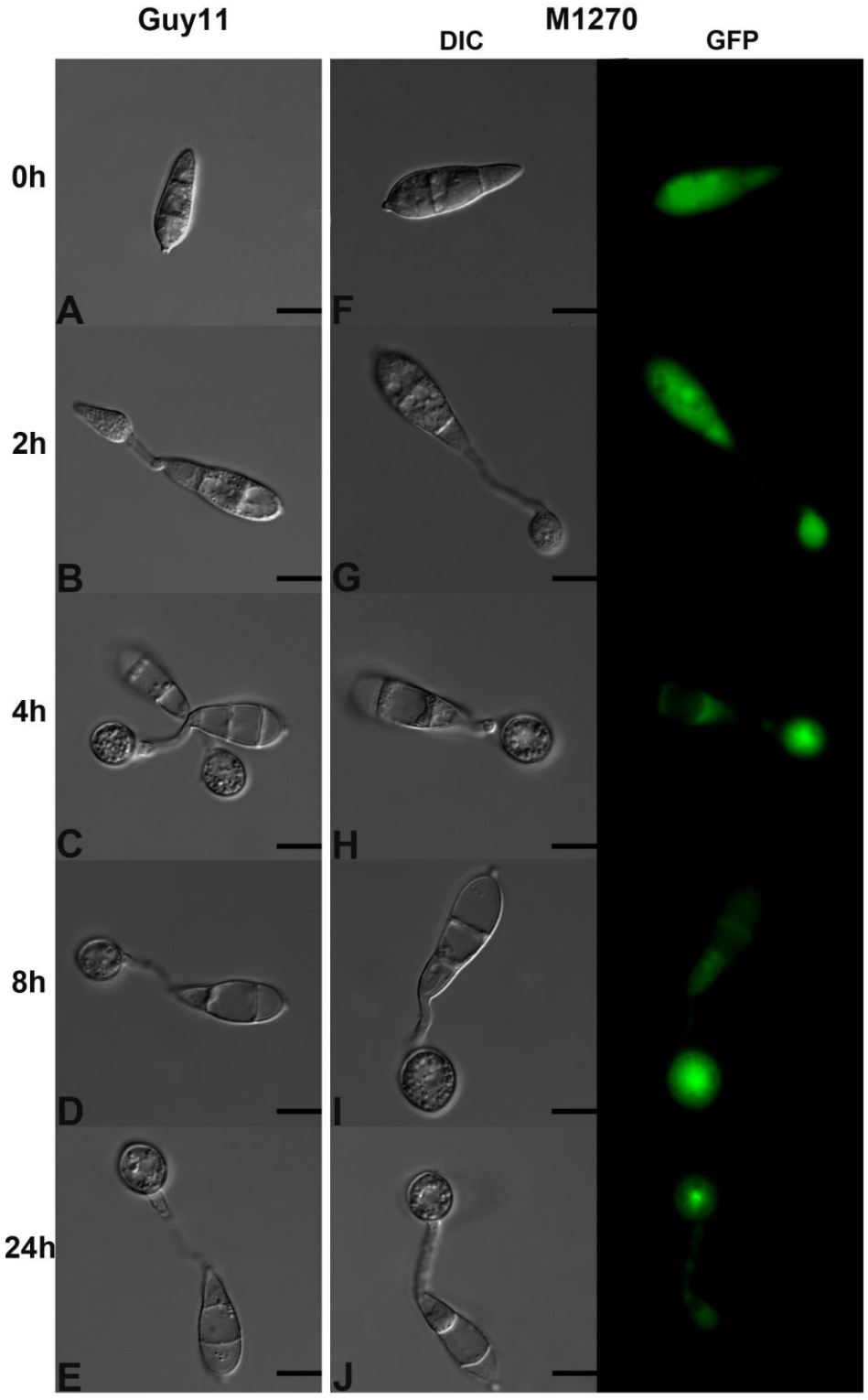

Figure 4.25: Appressorium development of reduced-pathogenic mutant M1270. Conidia from 12-day old plates of reduced-pathogenic T-DNA mutant M1270 were inoculated onto glass coverslips along with Guy11 as a control. Germination and appressorium development was observed over a period of 24 h using an Olympus IX-81 inverted epifluorescence microscope fitted with HQ^2 camera. Representative DIC and fluorescence images are shown at 0, 2, 4, 8 and 24hpi. During appressorium development mutant M1270 showed same morphology as Guy11. Scale Bar = 10 µm.

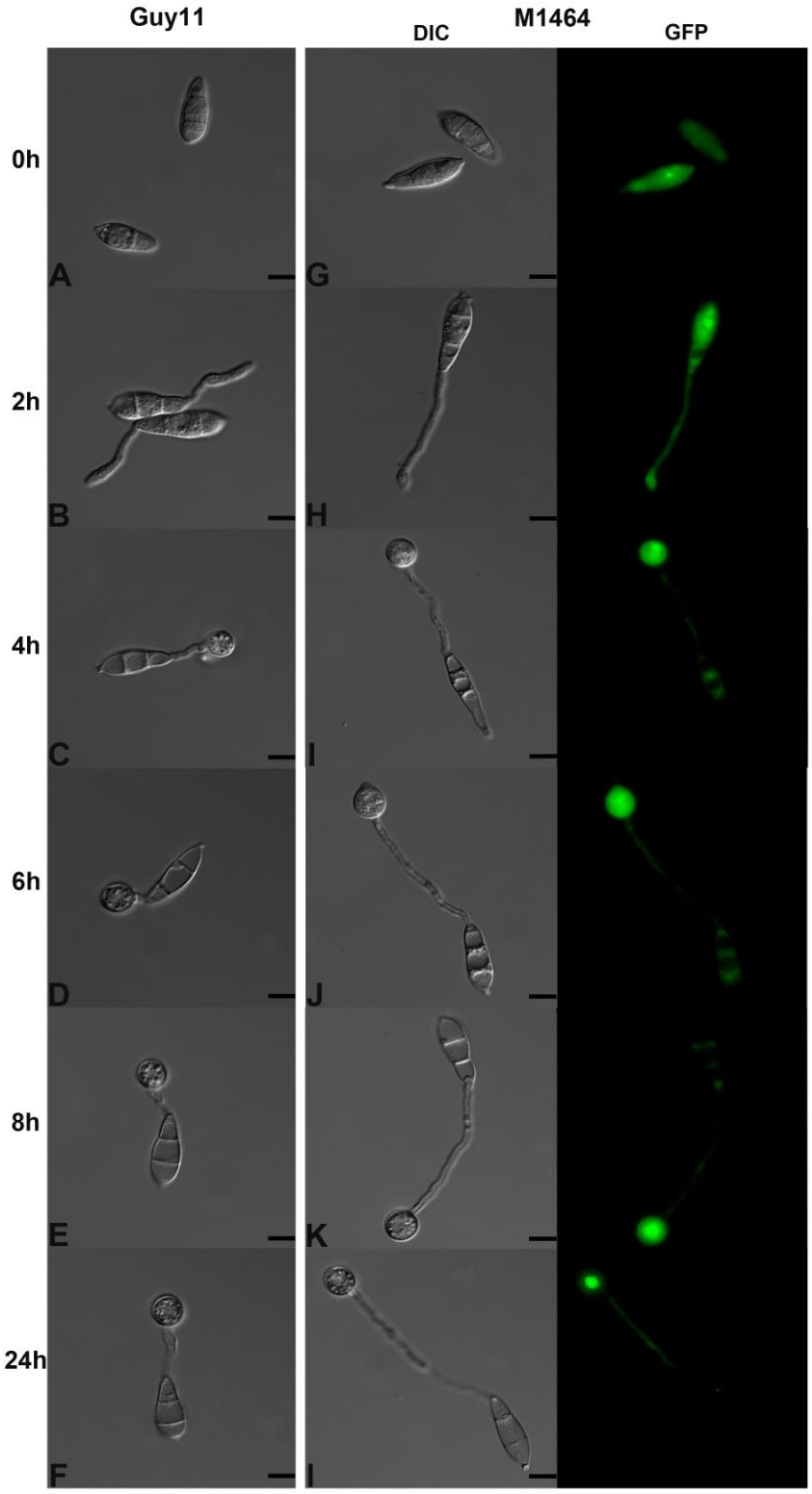

Figure 4.26: Appressorium development of reduced-pathogenic mutant M1464. Conidia from 12-day old plates of reduced-pathogenic T-DNA mutant M1464 were inoculated onto glass coverslips along with Guy11 as a control. Germination and appressorium development was observed over a period of 24 h using an Olympus IX-81 inverted epifluorescence microscope fitted with HQ^2 camera. Representative DIC and fluorescence images are shown at 0, 2, 4, 6, 8 and 24hpi. Much longer germ tubes were observed in M1464. Scale Bar = 10 µm.

4.3.2.4 Appressorium development assay of M1880 in the presence of inducers

One of the non-pathogenic mutants M1880 was unable to from appressoirum (Figure 4.20). We therefore decided to see if appressorium formation could be induced in M1880 by exposure to known inducers of appressorium development. Previous studies have provided evidence that formation of appressoria can be induced by environmental cues, including both physical (Bourett and Howard 1990; Dean 1992; Lee and Dean 1994; Gilbert et al. 1996) and chemical (Gilbert et al. 1996) signals. For instance, the cAMP dependent signal transduction pathway has been shown to be central to appressorium formation (Lee and Dean 1993; Mitchell and Dean 1995; Xu and Hamer 1996; Choi & Dean, 1997). Addition of exogenous cAMP to Δ*mac1* deletion mutants, for example, remediates appressorium development and restores pathogenicity (Adachi & Hamer, 1998). Exogenous cAMP can also induce appressorium development of wild-type *M. oryzae* on normally non-inductive hydrophilic surfaces (Choi & Dean, 1997). In order to see whether appressorium development could be induced in M1880, the fungus was induced to three different inducers. We used the cutin monomer 1, 16-hexadecanediol (hexadecanediol), cAMP and 3-lsobutyl-1-Methylxanthine (IBMX) (Invitrogen). IBMX is an inhibitor of the enzyme phosphodiesterase and increases the levels of intracellular cAMP (Mitchell and Dean 1995; Liu and Dean 1997). Conidia from 12-day old plates were inoculated onto glass coverslips along with Guy11 as a control. Mutant M1880 was allowed to develop appressoria in water without any induction and also in the presence of 10 mM cAMP, 1 μM 1, 16-hexadecanediol or 2.5 mM IBMX (Mitchell and Dean 1995; Liu and Dean 1997). Germination and appressorium development was observed over a period of 24 h by epifluorescence microscopy as shown in Figure 4.27. I found that none of these agents were able to induce appressorium formation in M1880, which suggests that M1880 was not defective either in surface perception or cAMP signaling.

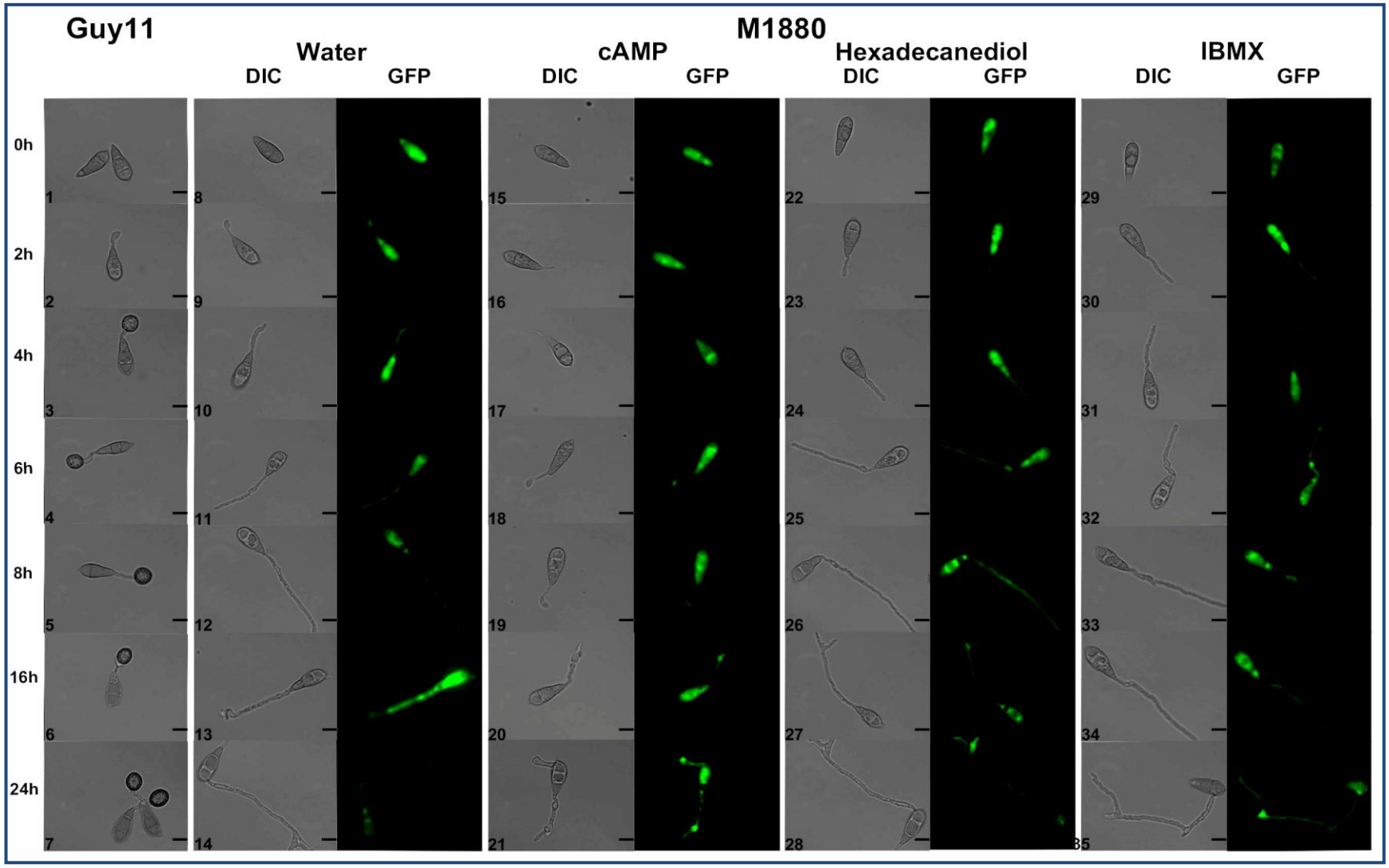

Figure 4.27: Mutant M1880 does not form appressorium in the presence of cAMP, IBMX or Hexadecanediol. Appressorium development was assayed in the presence of different inducers of infection related development. Conidia from 12-day old plates were inoculated onto glass coverslips and allowed to grow in the presence of cAMP (10 mM), hexadecanediol (1 µM) and IBMX (2.5 mM) (Mitchell and Dean, 1995; Liu and Dean, 1997). Conidial germination and appressorium development were observed over 24 h using an Olympus IX-81 inverted epifluorescence microscope fitted with HQ^2 camera. Representative DIC and fluorescence micrographs are shown at 0, 2, 4, 6, 8, 16 and 24hpi. Scale Bar = 10 µm.

4.3.2.5 Penetration assay on onion epidermis

Appressorium-mediated penetration of onion epidermal strips was assessed using a procedure based on that of Chida and Sisler (1987). The frequency of penetration hyphae formation was observed at 24 h and 30 h. The wild-type strain Guy11 penetrated the cuticle by 24 h and had invaded epidermis by 30 h (Figure 4.28-4.32). At 30 h M4874 penetrated the epidermis compared to Guy11 which started growing invasive hyphae (Figure 4.31). Mutants M1054, M1879, M2867 and M5253 failed to penetrate at either time points of observation (Figure 4.28 and Figure 4.30). Mutant M1880 could not form appressoria on onion epidermis and in both time points it had grown superficially (Figure 4.28 and Figure 4.30).

To investigate appressorium-mediated penetration of non-conidiating mutants on onion epidermis, we applied a diluted suspension of mycelium onto epidermis and observed this after 24 hpi. All three non-conidiating mutants had grown a superficial network of hyphae but no other structure was observed (Figure 4.32).

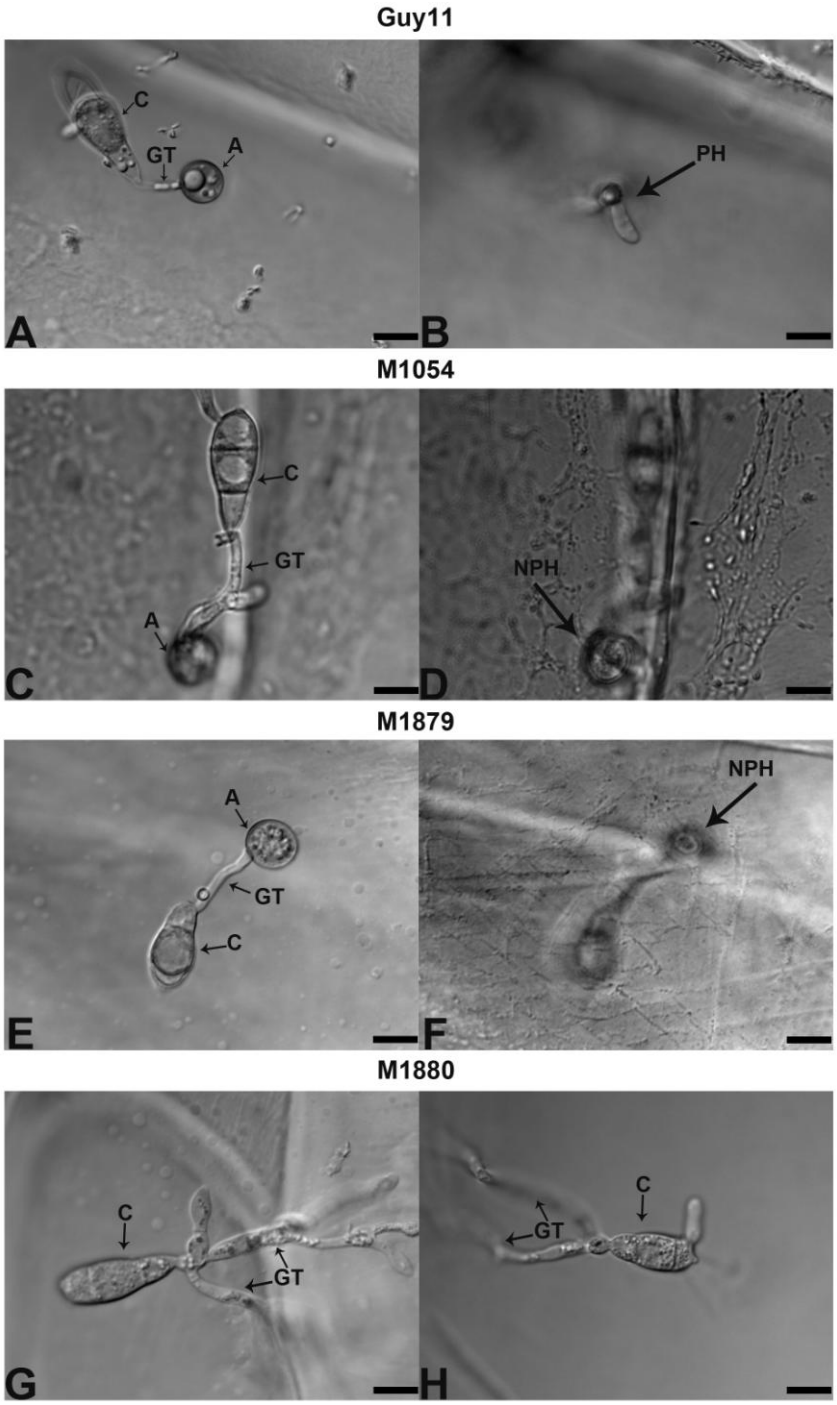

Figure 4.28: Penetration assay of selected non-pathogenic mutants on onion epidermis at 24 h. Conidia from 12-day old plates of non-pathogenic T-DNA mutants M1054, M1879 and M1880 were inoculated on onion epidermis fixed on glass slides. Formation of penetration peg was observed at 24 h using an Olympus IX-81 inverted epifluorescence microscope fitted with HQ^2 camera. Appressoirum (A), germ tube (GT) and conidium (C) are indicated in each micrograph. **A & B** Wild-type Guy11 formed penetration hyphae (PH) at 24 h which is indicated by an arrow. Mutant M1054 (**C & D)** and M1879 (**E & F)** could not penetrate onion epidermis at 24 h. Absence of penetration hyphae are indicated by arrows (NPH= No penetration hyphae). Mutant M1880 (**G & H)** could not form appressorium on onion epidermis and grew elongated germ tube at 24 h. Scale Bar = 10 µm.

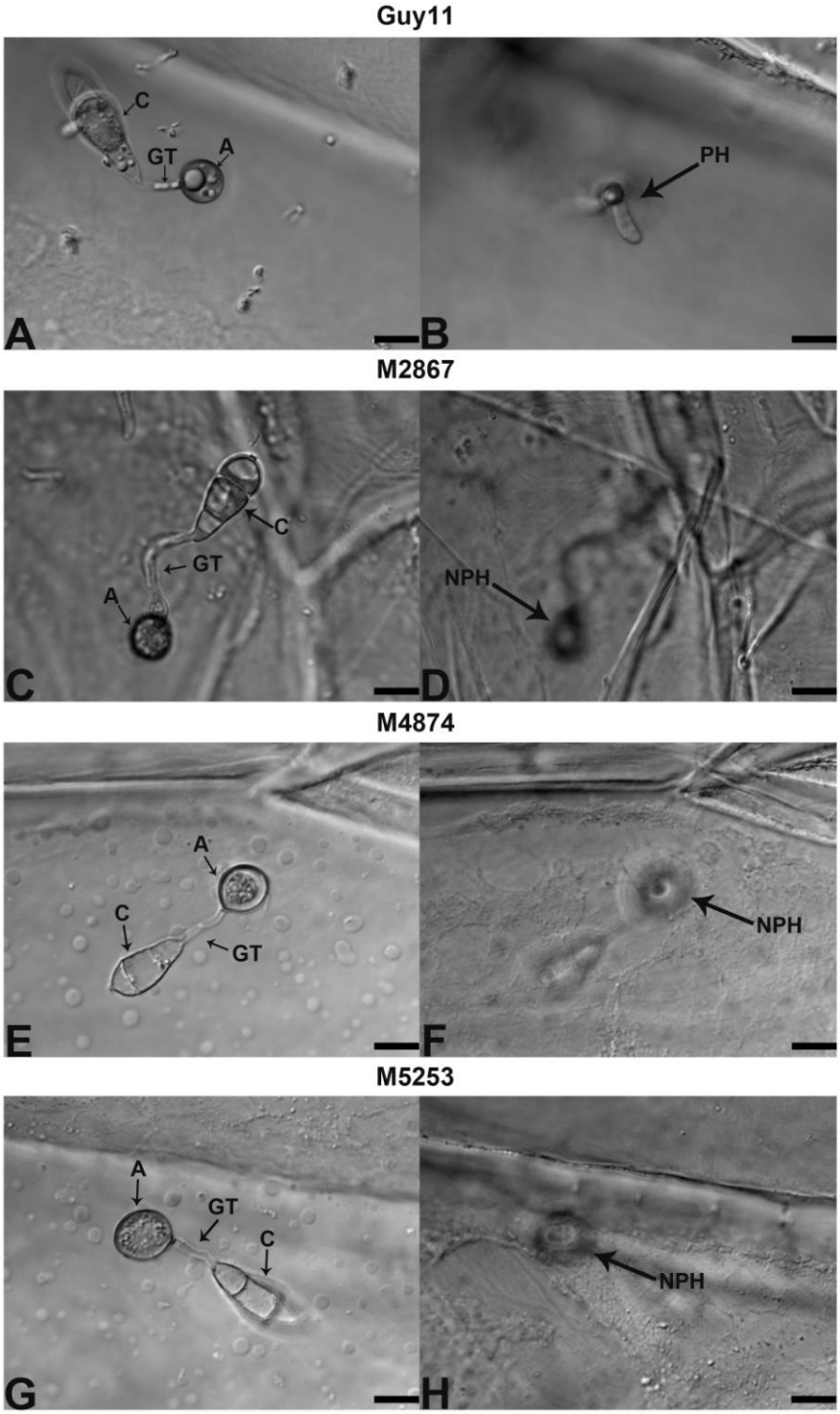

Figure 4.29: Penetration assay of selected non-pathogenic mutants on onion epidermis at 24 h. Conidia from 12-day old plates of non-pathogenic T-DNA mutants M2867, M4874 and M5253 were inoculated on onion epidermis fixed on glass slides. Formation of penetration peg was observed at 24 h using an Olympus IX-81 inverted epifluorescence microscope fitted with HQ^2 camera. Appressoirum (A), germ tube (GT) and conidium (C) are indicated in each micrograph. **A & B** Wild-type Guy11 formed penetration hyphae (PH) at 24 h which is indicated by an arrow. Mutant M2867 (**C & D)**, M4874 (**E & F)** and M5253 (**G & H)** could not penetrate onion epidermis at 24 h. Absence of penetration hyphae are indicated by arrows (NPH= No penetration hyphae). Scale Bar = 10 µm.

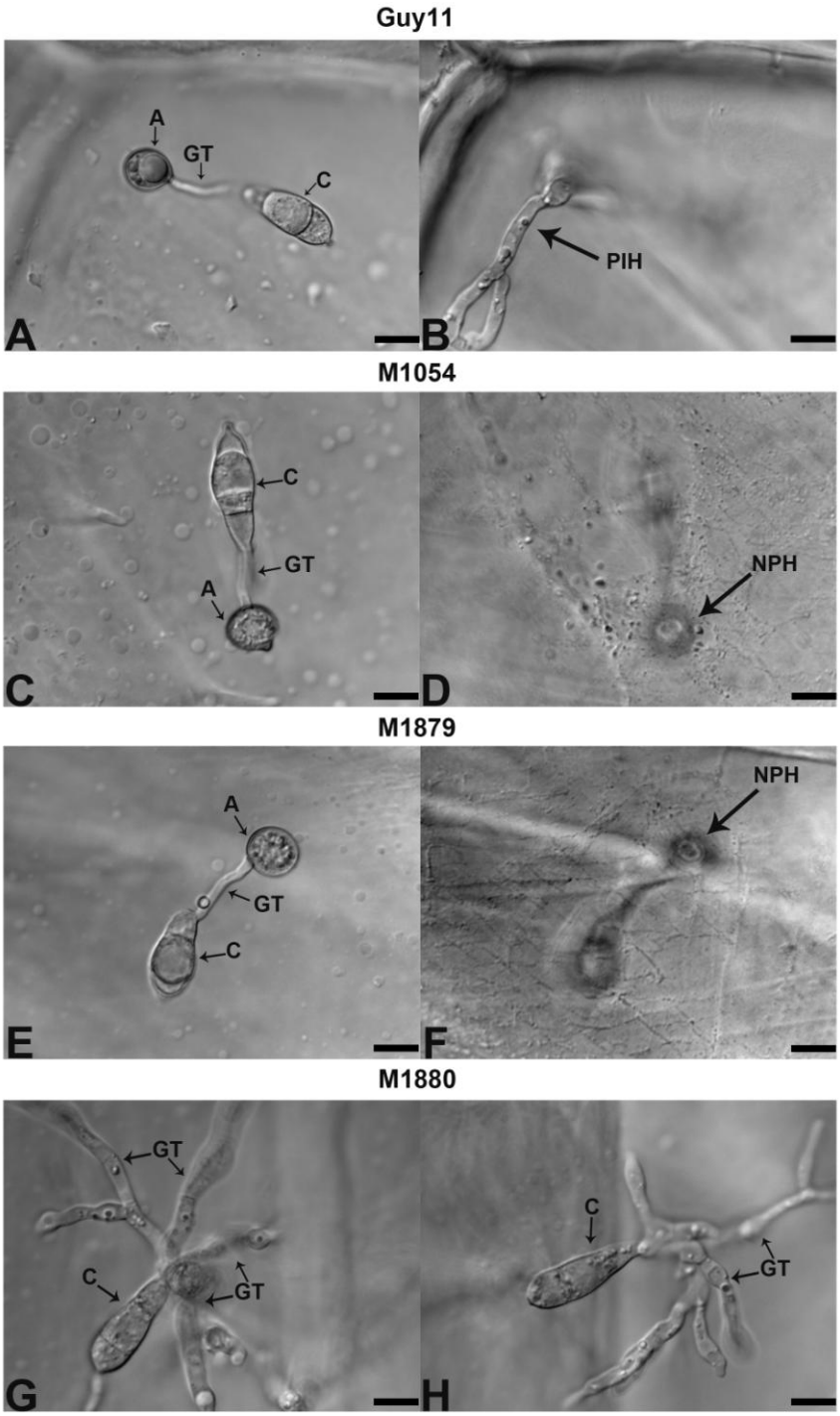

Figure 4.30: Penetration assay of selected non-pathogenic mutants on onion epidermis at 30 h. Conidia from 12-day old plates of non-pathogenic T-DNA mutants M1054, M1879 and M1880 were inoculated on onion epidermis fixed on glass slides. Formation of penetration peg was observed at 30 h using an Olympus IX-81 inverted epifluorescence microscope fitted with HQ^2 camera. Appressoirum (A), germ tube (GT) and conidium (C) are indicated in each micrograph. **A & B** Wild-type Guy11 developed primary invasive hyphae (PIH) by 30 h which is indicated by an arrow. Mutant M1054 (**C & D)** and M1879 (**E & F)** could not penetrate onion epidermis at 30 h. Absence of penetration hyphae are indicated by arrows (NPH= No penetration hyphae). Mutant M1880 (**G & H)** could not form appressoria on onion epidermis and grew elongated germ tube at 30 h. Scale Bar = 10 µm.

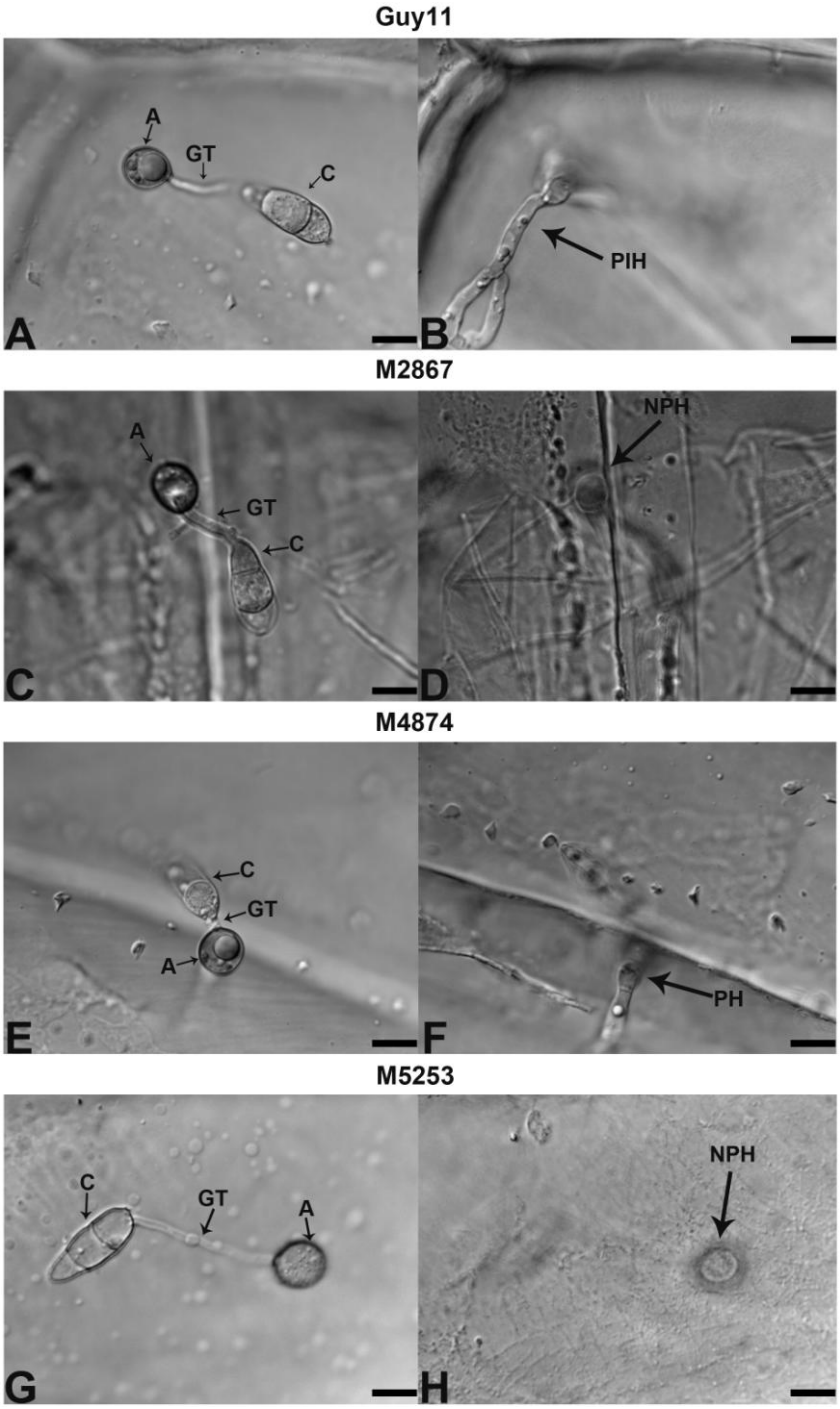

Figure 4.31: Penetration assay of selected non-pathogenic mutants on onion epidermis at 30 h. Conidia from 12-day old plates of non-pathogenic T-DNA mutants M2867, M4874 and M5253 were inoculated on onion epidermis fixed on glass slides. Formation of penetration peg was observed at 30 h using an Olympus IX-81 inverted epifluorescence microscope fitted with HQ^2 camera. Appressoirum (A), germ tube (GT) and conidium (C) are indicated in each micrograph. **A & B** Wild-type Guy11 developed primary invasive hyphae (PIH) by 30 h which is indicated by an arrow. Mutant M2867 (**C & D)** and M5253 (**G & H)** showed no penetration of onion epidermis at 30 h. Absence of penetration hyphae are indicated by arrows (NPH= No penetration hyphae). Mutant M4874 (**E & F)** penetrated onion epidermis at 30 h, which is shown by an arrow. Scale Bar = 10 µm.

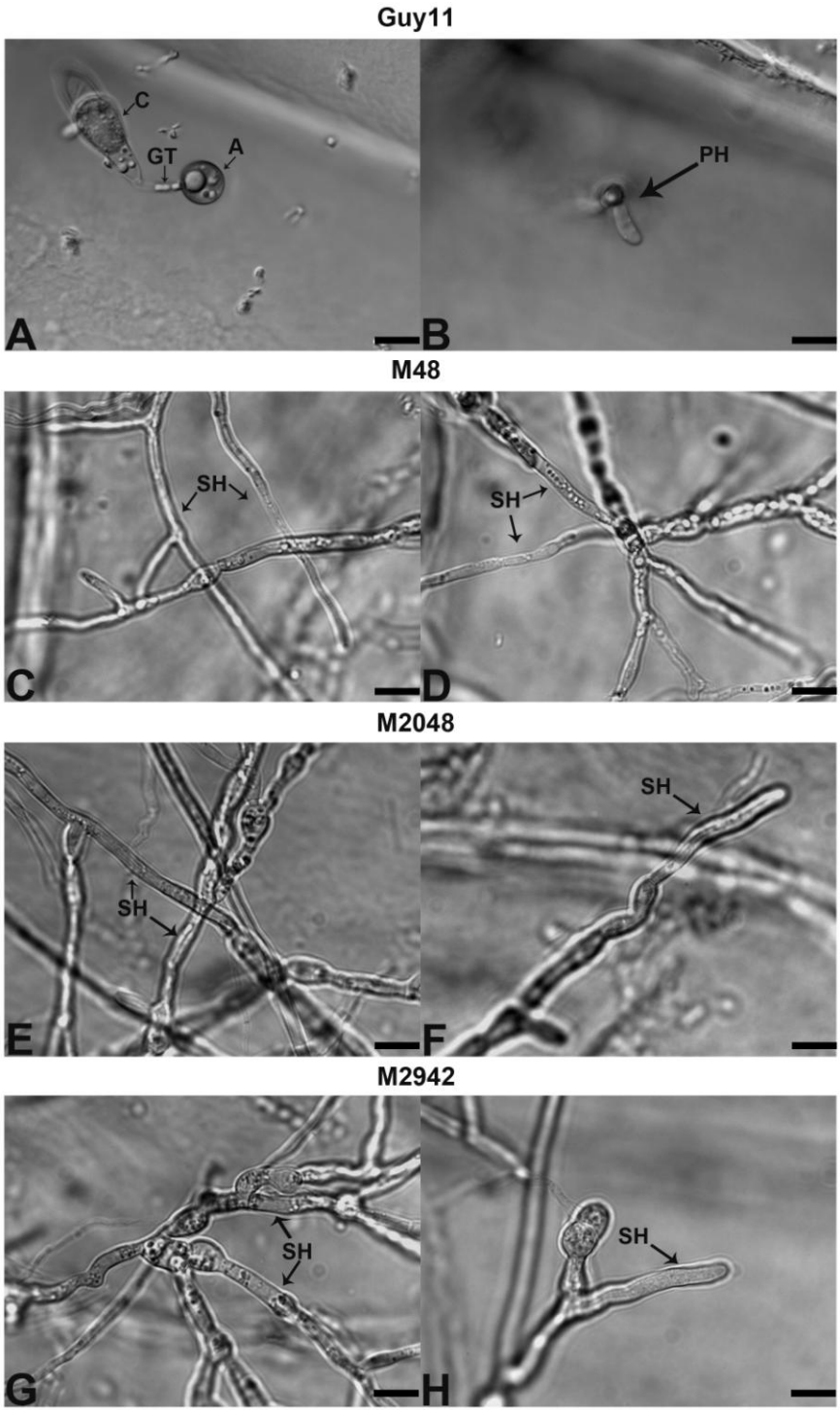

Figure 4.32: Penetration assay of selected non-conidiating mutants on onion epidermis at 24 h. Suspension of mycelium from 12-day old plates of non-conidiating T-DNA mutants M48, M2048 and M2942 were inoculated on onion epidermis fixed on glass slides. Development of mycelium was observed at 24 h using an Olympus IX-81 inverted epifluorescence microscope fitted with HQ^2 camera. **A & B** Wild-type Guy11 spores developed penetration hyphae (PH) at 24 h which is indicated by an arrow. Mutants M48 (**C & D)**, M2048 (**G & H)** and M4874 (**E & F)** showed no other structure formation apart from growing superficially on onion epidermis at 24 h. Surface hyphae (SH) are indicated by arrows. Scale Bar = 10 µm.

4.3.2.6 Penetration assay on rice leaf sheath epidermal layers

Appressorium-mediated penetration of the rice leaf epidermis was assayed using a procedure based on that of Kankanala *et al.* (2007). We observed that none of the mutants were able to penetrate rice leaf sheath layers at 24 h (Figure: 4.33), compared to Guy11 which penetrated and started growing bulbous invasive hyphae. We therefore observed infected leaf sheaths at 30 h. Only mutant M4874 was able to penetrate the leaf epidermis. At 30 h, Guy11 started developing branched and bulbous invasive hyphae (Figure: 4.34). Bulbous Guy11 hyphae infected 2-3 cells by 30 h while M4874 showed nascent invasive hyphae growing from the penetration peg. The leaf sheath assay therefore confirmed that the mutant M4874 was delayed in appressorium-mediated penetration and all of the other non-pathogenic mutants were defective in plant invasion.

To investigate invasive growth of mutant M4874 at later time points we also observed the infected leaf sheath at 36 h and 48 h as shown in Figure 4.35. At 36 h, Guy11 hyphae infected three epidermal plant cells with branched invasive hyphae whereas mutant M4874 was confined to a single cell and developed less branched hyphae. At 48 h, M4874 entered the next cell and started developing branched hyphae compared to Guy11 which infected more cells with heavily branched hyphae. Based on the leaf sheath assay we can conclude that although M4874 was able to penetrate rice cells the fungus was unable to proliferate in the same way as Guy11. To investigate the possible delay in causing plant disease, we carried out the pathogenicity assay again on mutant M4874 and incubated spray-inoculated plants for 8 days at 24 ^{o}C, with high light and 96% humidity. Even after 8 days, the mutant was unable to produce rice blast disease lesions although necrotic flecks were observed (Figure 4.36).

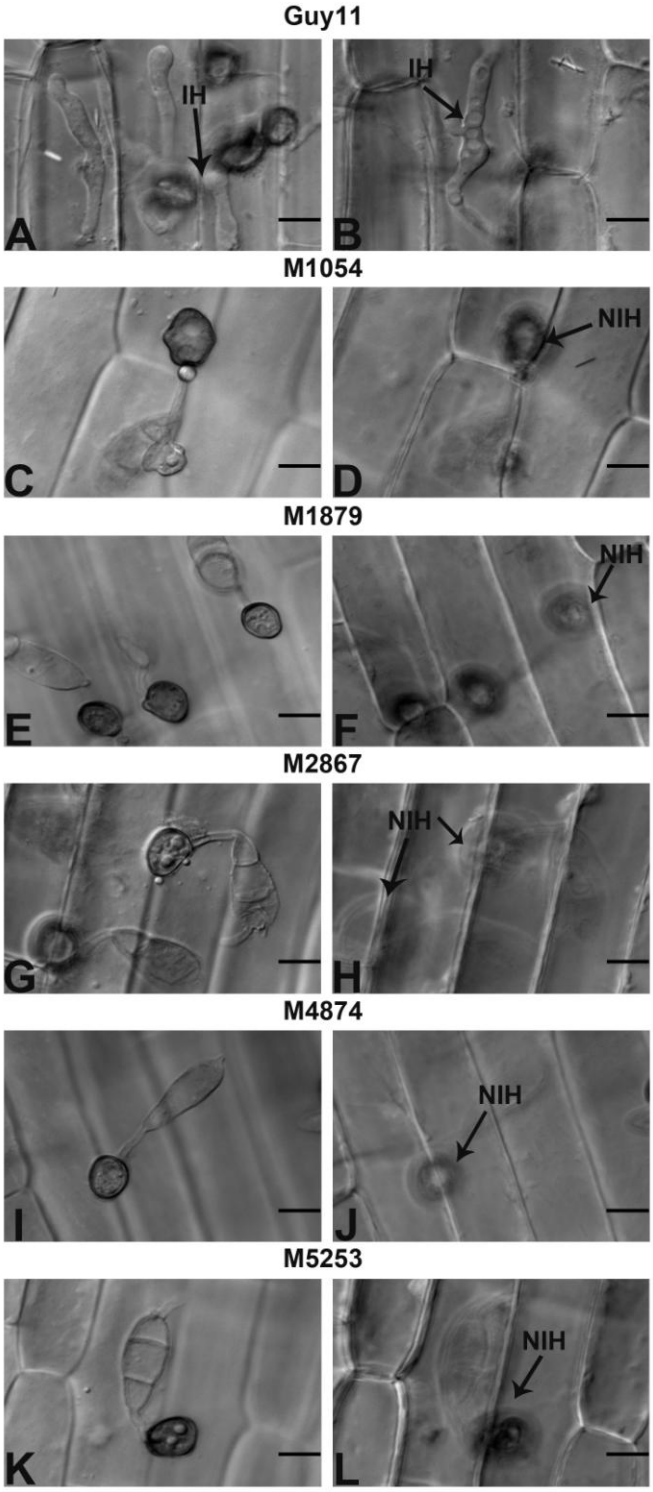

Figure 4.33: Penetration assay of selected non-pathogenic mutants on rice leaf sheath at 24 h. Conidia from 12-day old plates of selected non-pathogenic T-DNA mutants were inoculated on rice leaf sheath. Formation of penetration peg and invasive growth was observed at 24 h using an Olympus IX-81 inverted epifluorescence microscope fitted with HQ^2 camera. **A & B** Wild-type Guy11 penetrated epidermal cells and started growing invasive hyphae (IH) at 24 h which is indicated by an arrow. Mutants M1054, M2867, M4874 and M5253 failed to penetrate rice epidermis at 24 h. Absence of invasive hyphae (NIH) are shown by arrows. Scale Bar = 10 µm.

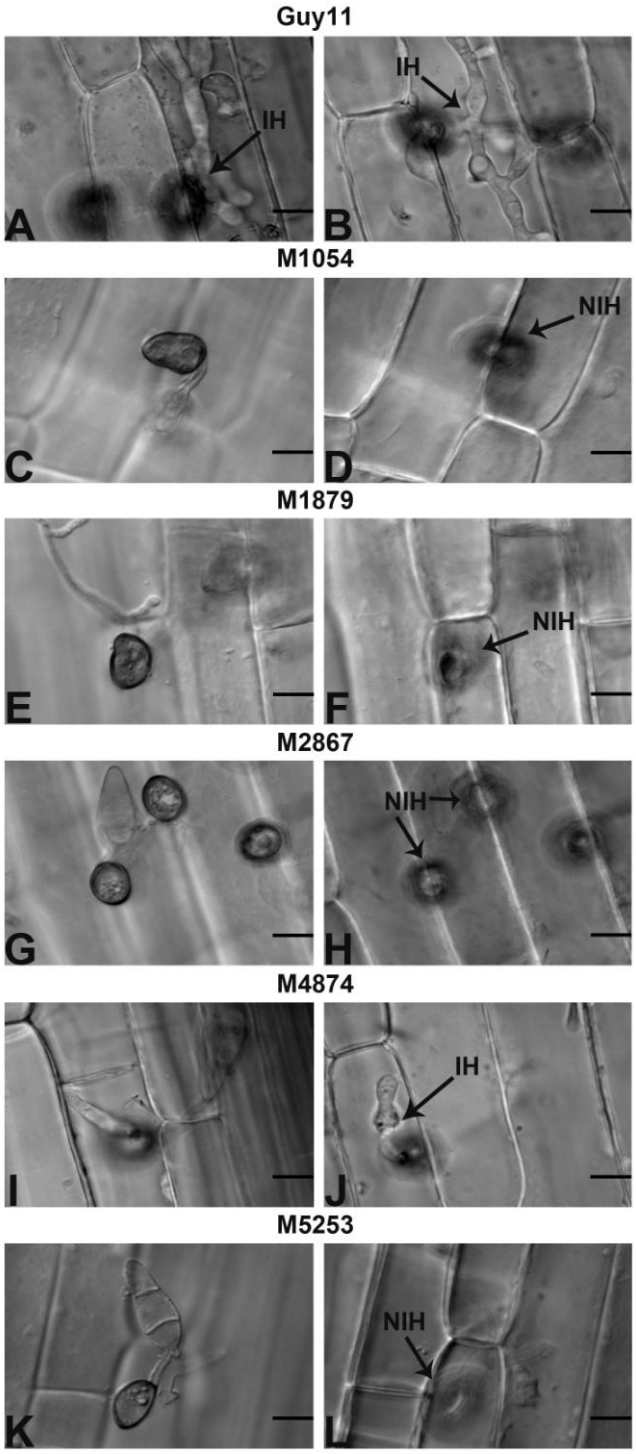

Figure 4.34: Penetration assay of selected non-pathogenic mutants on rice leaf sheath at 30 h. Conidia from 12-day old plates of selected non-pathogenic T-DNA mutants were inoculated on rice leaf sheath. Formation of penetration pegs and invasive growth was observed at 30 h using an Olympus IX-81 inverted epifluorescence microscope fitted with HQ^2 camera. **A & B** Wild-type Guy11 grew bulbous branched invasive hyphae (IH) at 30 h which is indicated by arrow. **I & J.** Mutant M4874 penetrated epidermal rice cells and started growing invasive hyphae at 30 h. M1054, M1879, M2867 and M5253 could not penetrate rice epidermis at 30 h. Absence of invasive hyphae (NIH) are shown by arrows. Scale Bar = 10 µm.

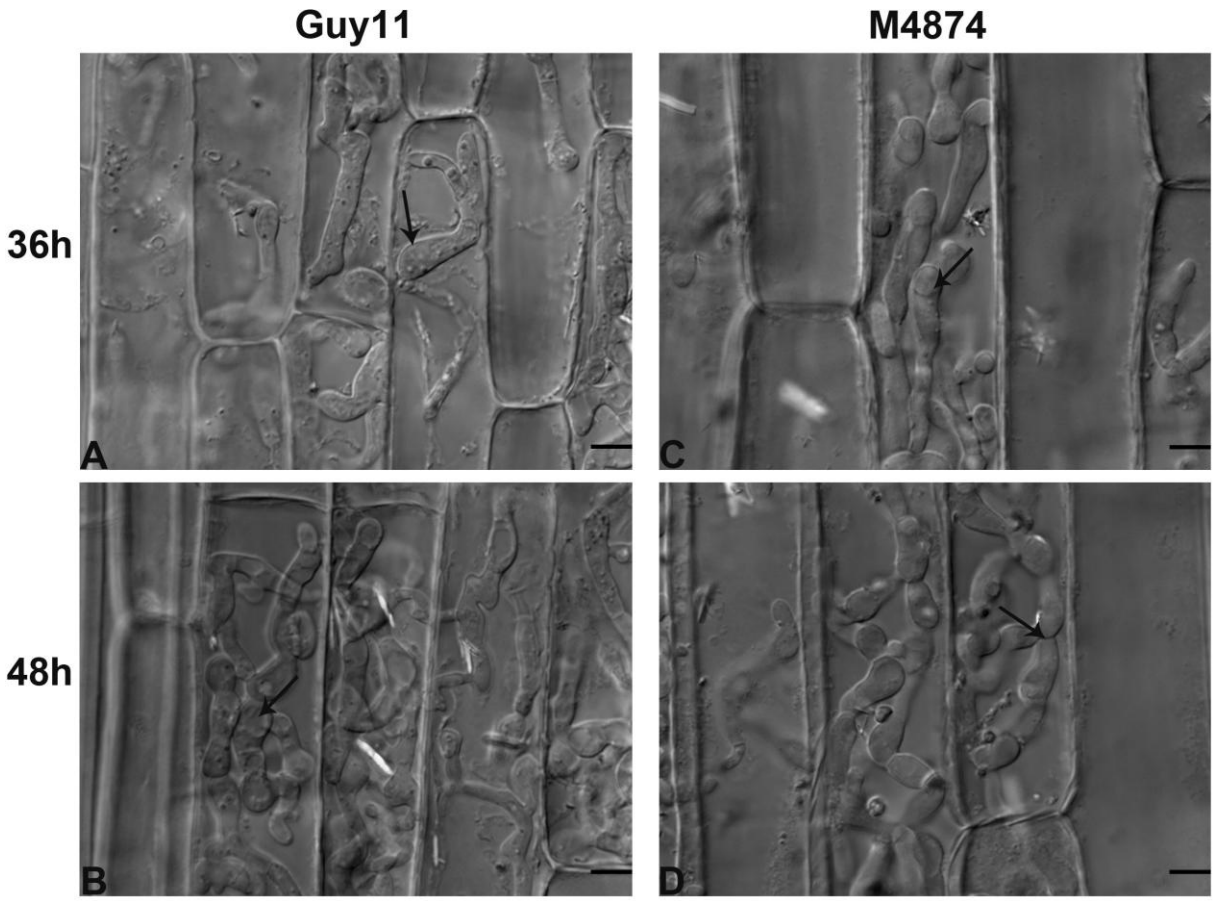

Figure 4.35: *In vivo* invasive growth of mutant M4874 inside epidermal rice cells. Conidia from 12-day old plate culture of non-pathogenic mutant M4874 were inoculated on rice leaf sheath. Invasive growth was observed at 36 h and 48 h using an Olympus IX-81 inverted epifluorescence microscope fitted with HQ^2 camera. **A & B.** The wild-type Guy11 grew bulbous branched invasive hyphae at 36 h and infected 3-5 cells by 48 h. **C.** Mutant M4874 also developed invasive hyphae inside epidermal rice cells by 36 h, but they were less branched. **D.** M4874 started growing inside 2-3 cells, but was delayed compared to Guy11. Scale Bar = 10 µm.

Figure 4.36: Pathogenicity assay of M4874 8 days after inoculation. Two-week old seedlings of rice *cv.* CO-39 were spray inoculated with a conidial suspension at 5 x 10^{-4} conidia mL^{-1} and incubated at 24^{o}C, with high light and 96% humidity for 8 days. Plants were kept in polythene bags for 2 days after inoculation and incubated for another 6 days. Even after 8 days of inoculation, M4874 was unable to produce typical rice blast disease lesions. Some necrotic flecks were observed. M4874 therefore invades epidermal cells but unable to cause disease. This pathogenicity assay was repeated and we obtained uniform results in each round.

4.3.2.7 Incipient cytorrhysis assay

To investigate possible defects in appressorium turgor generation, incipient cytorrhysis assays were performed (de Jong *et al*., 1997; Howard *et al*., 1991). Cytorrhysis assays measure the number of appressorial cells collapsing upon exposure to hyperosmotic solute (usually glycerol or PEG) of varying concentrations. Solutions with high osmotic potential cause the appressoria to collapse allowing an assessment of their internal turgor pressure. I observed that upon exposure 2 M glycerol, 32% of Guy11 appressoria had collapsed compared to 51.7% appressoria of M1054 and 58.5% appressoria of M1879 (Table 4.3). The concentration of glycerol leading to the collapse of 50% of the appressoria was 2 M for the mutants M1054 and M18793 and 3 M glycerol for the wild-type Guy11. M2867 and M4874 did not show any significant difference compared to Guy11. Therefore, the incipient cytorrhysis suggested appressorium turgor was reduced in mutant M1054 and M1879, but not in M2867 and M4874 compared to wild-type Guy11.

Table 4.3: Appressorium turgor assay of selected T–DNA mutants by incipient cytorrhysis analysis. Appressorium turgor was assayed by incipient cytorrhysis analysis. Conidia were allowed to form appressoria on plastic coverslips for 24 h. The cytorrhysis assay measures the percentage collapse of appressoria after exposure to a series of glycerol solution of various concentration (n=300).

Mutant	0.5 M	1.0 M	2.0 M	3.0 M	4.0 M
Guy11	3.0±0.5%a	6.3±2.0%a	32.0±7.2%a	56.0±4.6%a	95.3±1.5%a
M1054	6.5±1.0%b	22..3±3.5%b	51.7±5.6.0%b	81.3±5.9%b	96.3±0.6%a
M1879	8.3±1.6%b	28.7±3.2%b	58.5±6.7%b	88.7±5.1%a	97.0±2.1%a
M2867	3.3±2.1%a	8.7±4.0%a	34.6±8.7%a	61.3±3.5%a	95.0±3.0%a
M4874	4.1±1.6%a	7.3±1.8%a	37.5±4.8%a	60.0±4.2%a	96.0±2.3%a

a	Indicates that the values are not significantly different between wild-type and T-DNA mutants (Student t-test, $p<0.05$).
b	Indicates that the values are significantly different between wild-type and T-DNA mutants (Student t-test, $p<0.05$).

4.3.3 Genetic and molecular analysis of the selected mutants

4.3.3.1 Determination of the T-DNA insertion copy number of selected mutants

The selected non-pathogenic mutants were next analyzed by Southern hybridization to determine the number of T-DNA insertions. Extracted genomic DNA was digested with *Xho*I, fractionated by gel electrophoresis, blotted and probed with a 2.9 kb *Xho*I /*Eco*RI double digested pCAMBGFP fragment. Seven of the non-pathogenic mutants have single copy T-DNA insertions. The only exception was M1879 which showed two T-DNA insertions (Figure 4.37).

4.3.3.2 Rescue of T-DNA flanks by PCR based methods

We selected 8 non-pathogenic mutants for further molecular characterization and gene functional analysis study. Two non-pathogenic mutants M1054 and M1879 were first selected as candidates to identify the gene interrupted by T-DNA insertion and then determine its role in pathogenicity. To do this, we used two conventional PCR-based techniques. First, we used TAIL-PCR (thermal asymmetric interlaced-PCR) (Mullins *et al.*, 2000; Betts *et al.*, 2007; Li *et al.*, 2010a,b; Goh *et al.*, 2011) and 2nd is inverse PCR (iPCR) (Meng *et al.*, 2007; Betts *et al.*, 2007). Inverse PCR (iPCR) was performed following standard methods (Ochman *et al.*, 1988) and modifications described in Meng *et al.* (2007) and (Betts *et al.*, 2007). To rescue T-DNA flanks by high-efficiency thermal asymmetric interlaced (TAIL) polymerase chain reaction (PCR), the standard protocol described by Liu and Whittier (1995) was followed. A commercial TAIL-PCR kit was used in our study to identify T-DNA flanking genomic DNA of selected mutants. The Universal Vectorette™ System (Sigma Aldrich) is a high-efficiency PCR based method for DNA-walking and mapping that uses a form of unidirectional PCR for amplifying and sequencing unknown genomic or large construct DNA.

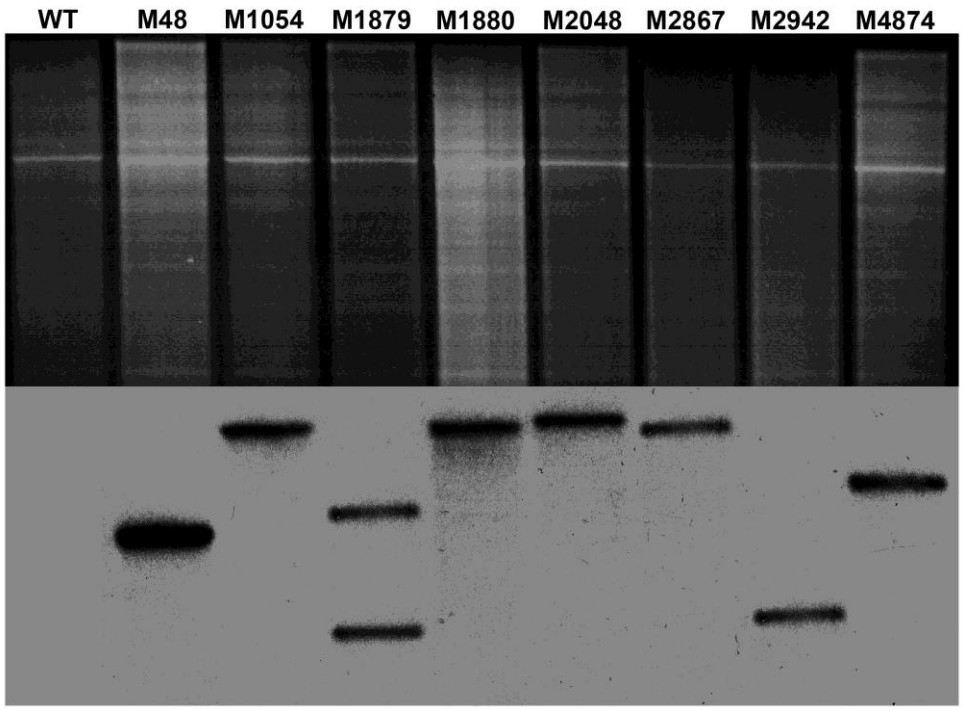

Figure 4.37: Determining the T-DNA insertion copy number of selected non-pathogenic mutants by Southern blot hybridization. Image shows the DNA gel blot analysis of eight selected non-pathogenic mutants. Genomic DNA was digested with *Xho*I, fractionated by gel electrophoresis, blotted and probed with a 2.9 Kb *Xho*I /*Eco*RI double digested pCAMBGFP fragment. The wild-type Guy11 was included as negative control in the first lane (WT). Mutant M1879 showed two T-DNA insertions. Mutants M48, M1054, M1880, M2048, M2942 and M4874 showed single T-DNA insertion.

The principles of the Vectorette TAIL-PCR are explained in Figure: 4.38A. We applied TAIL-PCR on selected mutants M1054 and M1879. One of the results obtained from TAIL-PCR for M1054 is shown in Figure 4.38B. The TAIL-PCR products were cloned and sequenced. Obtained sequences were identified by doing BLAST searches against *M. oryzae* genome sequence. From resulting sequences, we retrieved a 339 bp sequence of the *M. oryzae ATG3* gene flanked by T-DNA right border from M1054. From M1879, we retrieved a 494 bp sequence of the *M. oryzae ATG2* gene flanked by T-DNA right border.

We also applied iPCR to characterize the T-DNA flanks from the same two mutants that were characterized by TAIL-PCR in order to validate the TAIL-PCR result and also establish whether iPCR could be used as a tool for identifying T-DNA flanks in our large-scale study. The principles of iPCR are described schematically in Figure 4.39A. In, Figure 4.39B we explained how we used T-DNA right and left border sequences for amplifying T-DNA flanks from circularized DNA. We just used restriction enzyme *Nco*I to digest genomic DNA because of its double restriction sites within the T-DNA. It facilitated formation of circular DNA with minimum sequences from the T-DNA border for priming without amplifying unnecessary T-DNA sequences. We ligated DNA at low concentration with a high concentration of T4 DNA ligase. In this way, we were able to successfully amplify products from both mutants although multiple bands appeared in case of M1879 which could be results from tandemly ligated linear DNA. Inverse PCR products were cloned and sequenced. From the resulting sequences, we retrieved a 668 bp sequence of the *ATG3* gene flanking the T-DNA left border from M1054. From M1879, we retrieved a 278 bp sequence of the *ATG2* gene flanking the T-DNA left border.

By applying TAIL-PCR and iPCR, we successfully retrieved T-DNA flanking genomic sequences of *M. oryzae* from two T-DNA mutants. Unfortunately, the PCR based methods were unable to identify other expected T-DNA flanks from mutant M1879. The two tagged genes are known to be involved in autophagy in *M. oryzae* and deletion mutant Δ*atg3* and Δ*atg2* have previously been shown to be non-pathogenic (Kershaw and Talbot, 2009). Autophagy is an essential process during infection related development in *M.oryzae* (Veneault-Fourrey *et al.*, 2005). These two genes belongs to a set of 16 genes necessary for non-selective macroautophagy and loss of any of those genes renders the fungus unable to cause rice blast disease, due to impairment of both conidial programmed cell death and appressorium maturation (Kershaw and Talbot, 2009) . Therefore, the two genes we identified have a previously assigned role in pathogenicity. We therefore compared mutants M1054 and M1879 with corresponding deletion strain Δ*atg3* and Δ*atg2* (Kershaw and Talbot, 2009) in terms of vegetative growth and morphology when grown on CM. They showed similar vegetative growth pattern and colony morphology (Figure 4.40). We can conclude that two known autophagic genes were successfully identified from two mutants by PCR based methods. To provide further evidence that these genes were disrupted by T-DNA integration, we decided to investigate the T-DNA integration by RFLP (Restriction fragment length polymorphism) analysis and to complement mutant M1054 for by introducing the cloned *ATG3* gene from *M. oryzae*. We excluded M1879 from this analysis because of the possible ambiguity of its double insertion.

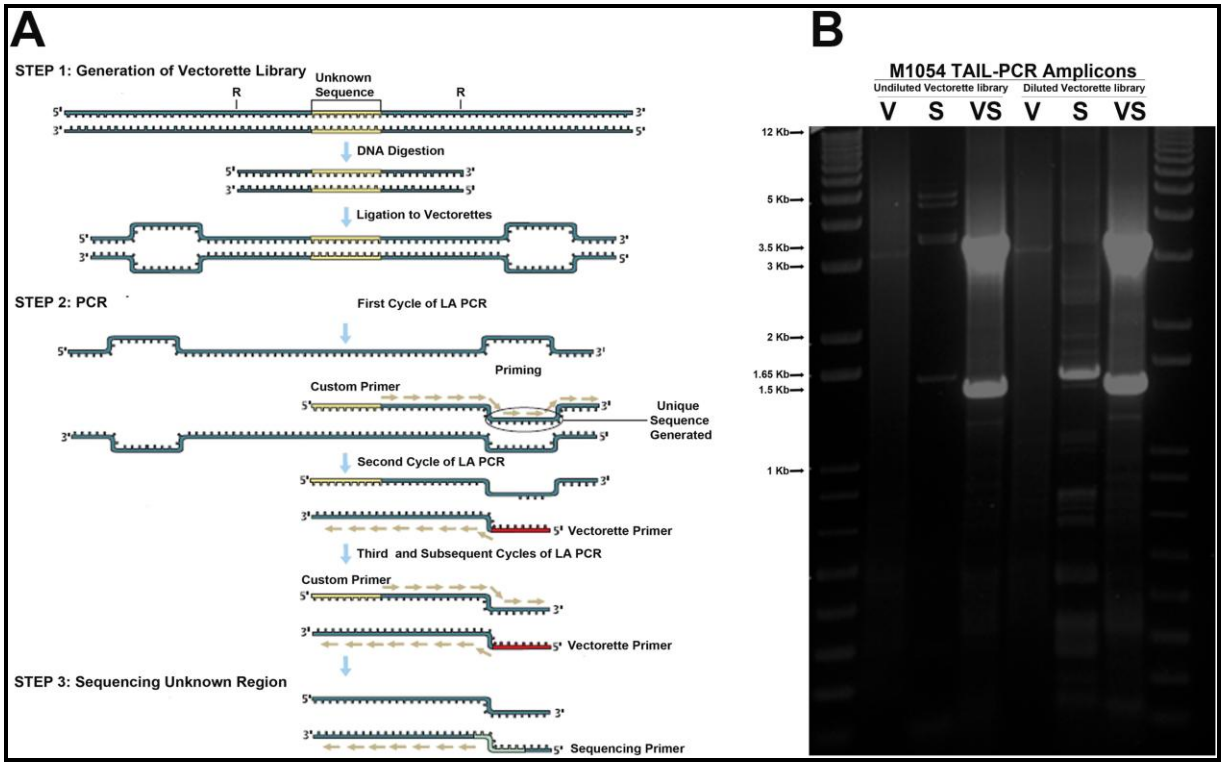

Figure 4.38: Determination of the T-DNA flanks by TAIL-PCR. In order to retrieve T-DNA flanks by high-efficiency thermal asymmetric interlaced (TAIL) polymerase chain reaction (PCR) strategy, the standard protocol described by Liu and Whittier (1995) was followed. **A.** The universal Vectorette™ system (Sigma Aldrich) is shown schematically. In this system a Vectorette unit is employed, which consists of a double stranded linker with an internal mismatched region and a sticky end. A Vectorette library is constructed by restriction digestion of genomic DNA containing the target sequence and ligation of digested fragments with corresponding Vectorette units. PCR is carried out using the Vectorette library from a primer complementary to the mismatched region of the Vectorette unit (Vectorette primer) and a primer specific to the known DNA sequence. Nested PCR can be performed from nested primers are included to increase specificity when amplifying more complex templates. **B.** Agarose gel image of TAIL-PCR amplification. PCR was performed using both the undiluted and diluted Vectorette library constructed from genomic DNA of mutant M1054. TAIL-PCR amplified two distinct DNA fragments from both libraries. Non-specific amplification was found from the diluted library where the Vectorette (V) primer only amplified a 1.6 kb fragment. 3.5 kb and 1.5 kb fragments were amplified from Vectorette-specific (VS) primer pair from both the diluted and undiluted Vectorette libraries. The fragments were amplified from T-DNA right border primers. Amplified fragments was cloned and sequenced. The 3.5 kb band rescued a 339 bp sequence of *M. oryzae ATG3* gene. [Image 4.38A was obtained and modified from Sigma Genomic DNA amplification product handbook]

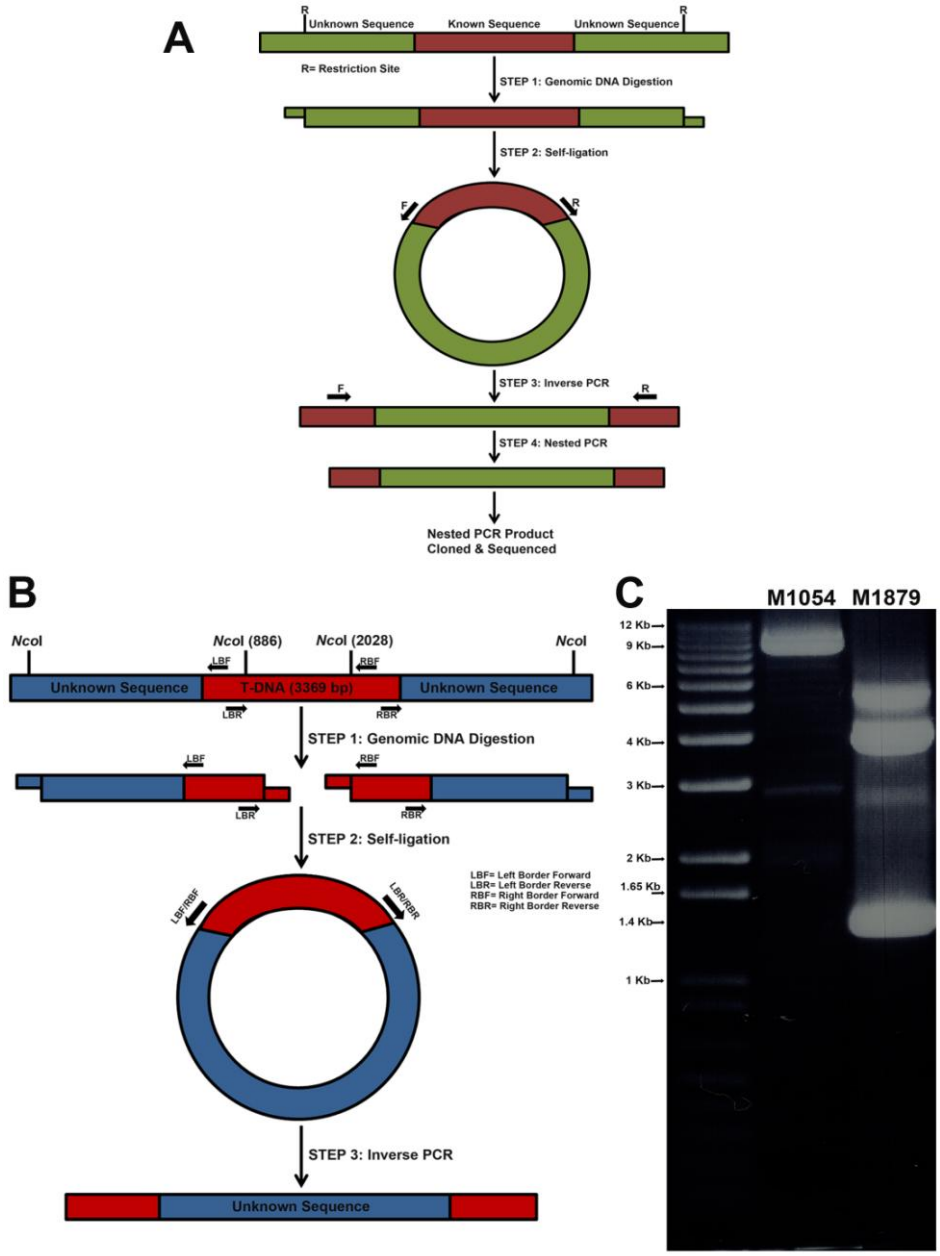

Figure 4.39: Inverse PCR (iPCR) to determine the T-DNA flanking region of *M. oryzae*. **A.** Principles of iPCR are shown schematically. The PCR involves three steps. First, digestion of genomic DNA with restriction enzyme of interest; second, circularization of digested linear DNA at low concentration by high concentration T4 DNA ligase and third, PCR with the primers with inverse direction respect to the original linear DNA. Additionally, a nested PCR can be performed to increase the specificity of amplification. **B.** Schematic representation of the iPCR used in our study. Restriction enzyme *Nco*I was chosen because it has two restriction sites within the T-DNA. It allows smaller circular DNA and amplification from the any of the T-DNA border sequences. Ligation was carried out at a low DNA concentration and PCR was performed with hi-efficiency *Taq* polymerase. **C.** Agarose gel image of iPCR amplification. T-DNA flanks from two mutants were retrieved from the PCR products shown above. Mutant M1054 was identified having an insertion in the *ATG3* locus and M1879 showed a T-DNA insertion within the *ATG2* locus.

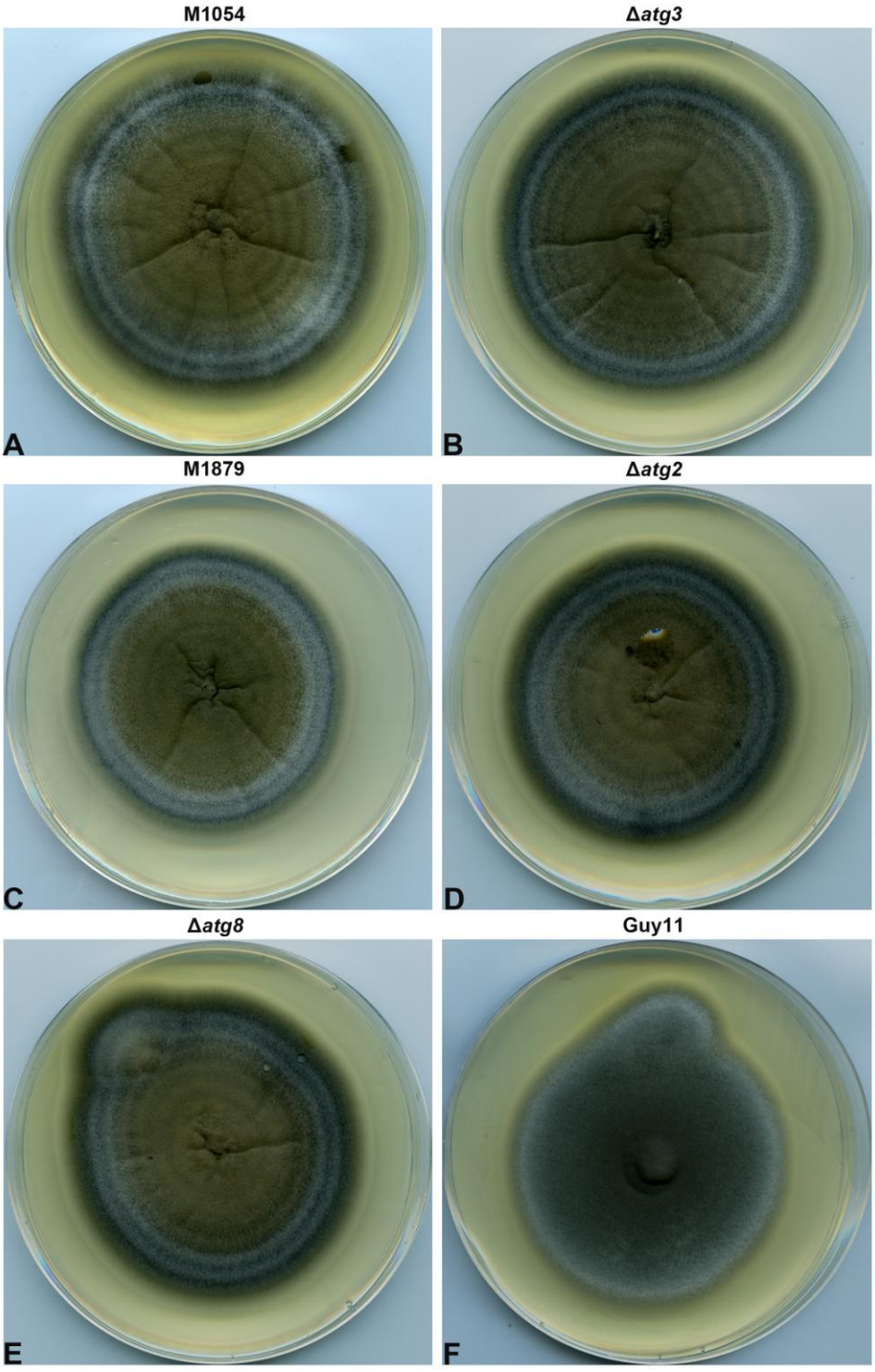

Figure 4.40: Vegetative growth and colony morphology of T-DNA mutants M1054 and M1879 compared to autophagic mutants of *M. oryzae*. Genetic analysis showed that the two non-pathogenic T-DNA insertion mutants M1054 **(A)** and M1879 **(C)** have insertions in the *ATG3* and *ATG2* loci respectively. They showed similar morphology and growth when compared with corresponding deletion strains of *M. oryzae* (Δ*atg3* **(B)** and Δ*atg2* **(D)**). The autophagy mutants showed this morphology was similar to another autophagic deletion strain Δ*atg8* **(E)**. All the strains were grown on CM and images were taken after 12 days of growth in 24°C.

4.3.4 Genetic analysis of the mutant M1054

4.3.4.1 RFLP analysis to confirm the T-DNA Insertion in *ATG3* locus

In order to map the T-DNA insertion in the *ATG3* locus of mutant M1054 by Southern hybridization analysis, a restriction map of the 21.7 kb genomic region (1.7 kb *ATG3* ORF in the middle and 10 kb genomic DNA sequence from 5' and 3' flanks) for wild-type Guy11 was constructed (Figure 4.41A). We also constructed a map of the same genomic region containing the T-DNA inserted within the *ATG3* locus, according to TAIL-PCR and iPCR result and generated a restriction map of the constructed locus (Figure 4.41B). By comparing the two restriction maps, we selected three different restriction enzymes to carry out RFLP analysis. These enzymes were chosen because they are able to produce a differential banding pattern for Guy11 and mutant M1054. We chose *Bam*HI, *Hin*dIII and *Sac*I. The size of the DNA fragments that was expected for both Guy11 and M1054 are summarized in Table: 4.4. Genomic DNA of Guy11 and mutant M1054 was digested with the selected enzymes, fractionated by gel electrophoresis, blotted and probed with a 1 kb *ATG3* gene fragment amplified by PCR. Comparing the band sizes of wild-type Guy11 (Figure: 4.41C) and mutant M1054 (Figure: 4.41D), restriction fragment length polymorphism (RFLP) were found at the *ATG3* locus and confirmed the predicted T-DNA insertion. The T-DNA insertion in M1054 was mapped by the means of *Hin*dIII, *BamH*I and *Sac*I digests. As predicted, *BamH*I and *Sac*I digestion resulted in distinct restriction fragments in M1054 compared to Guy11. Restriction fragment length differences are precisely shown by arrow and the obtained band sizes matched the expected sizes. Therefore, we can conclude that M1054 contains a T-DNA insertion in the *ATG3* locus and this ultimately validated both the TAIL-PCR and iPCR results.

Table 4.4: Expected band sizes from the restriction digestion of selected enzymes used for RFLP analysis at *ATG3* locus in M1054. Three enzymes *Bam*HI, *Hin*dIII and *Sac*I were selected for RFLP analysis of *ATG3* locus in mutant M1054. Among the chosen enzymes two were predicted to generate polymorphic restriction fragment due to T-DNA insertion and one would not show variability. *Bam*HI and *Sac*I show RFLPs in both single and double digests while *Hin*dIII was predicted to generate constant fragments for Guy11 and M1054 both singly and in corresponding double digests with either *Bam*HI or *Sac*I.

Enzyme	Fragment Size (kb)	
	Guy11	M1054
***Bam*HI**	13.5	4.9
***Hin*dIII**	5.8	5.8
***Sac*I**	9.5	6.1
***Bam*HI+ *Hin*dIII**	4	4
***Bam*HI+ *Sac*I**	8.3	4.9
***Hin*dIII+ *Sac*I**	5.2	5.2

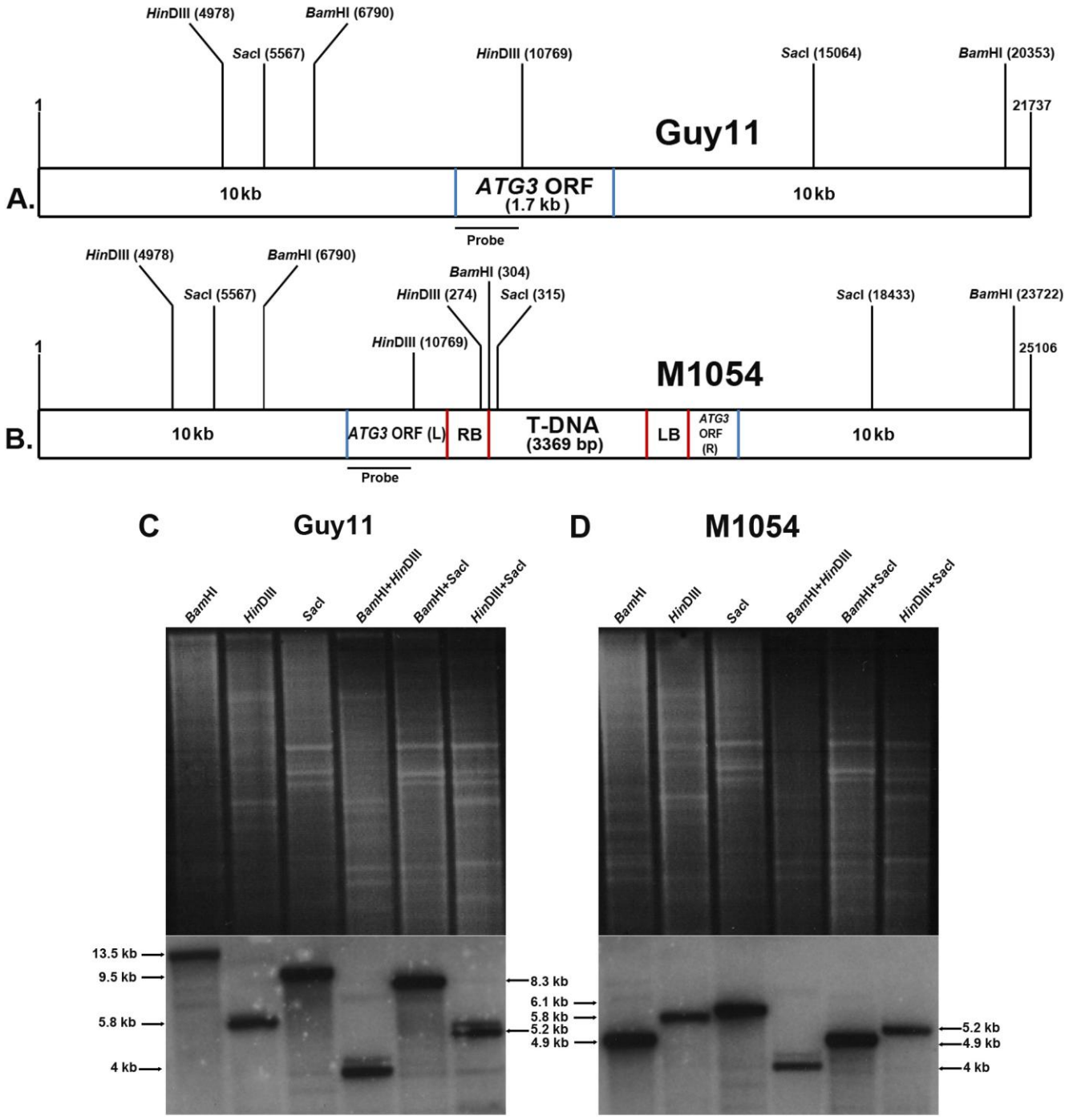

Figure 4.41: Confirmation of a T-DNA insertion in the *ATG3* locus by RFLP analysis. A. A schematic representation of the restriction map of *M. oryzae ATG3* locus. **B.** Restriction map of the *M. oryzae ATG3* locus in mutant M1054. TAIL-PCR result showed a T-DNA insertion in the *ATG3* gene of the mutant M1054. The map was constructed on the basis of retrieved flank sequences from TAIL-PCR. **C. & D.** Three enzymes were chosen for RFLP analysis of the *ATG3* locus in the wild-type Guy11 and mutant M1054. Images show DNA gel blot analysis. Both sample DNA were digested, fractionated by gel electrophoresis, blotted and probed with a 0.75 kb *ATG3* gene fragment amplified by PCR. Wild-type Guy11 **(C)** and mutant M1054 **(D)** showed restriction fragment length polymorphism (RFLP) in the *ATG3* locus. Band sizes are precisely shown by arrow.

4.3.4.2 Construction of *ATG3* complementation vector for the mutant M1054

We confirmed the T-DNA insertion at the *ATG3* locus in mutant M1054 by RFLP analysis and subsequently attempted to complement the mutant with the cloned *ATG3* gene of *M. oryzae*. The complementation vector for M1054 was made using recombination-mediated PCR-directed plasmid construction *in vivo* in yeast (Oldenburg *et al.*, 1997). In this technique, PCR products are transformed directly with the linearized yeast plasmid in a yeast uracil auxotrophic *ura3* (-) strain. The primers used to amplify PCR products have overhangs corresponding to adjacent PCR fragments, or with the yeast plasmid. When the linearized plasmid is mixed with PCR products in appropriate conditions, homologous recombination takes place and joins the PCR amplicons with the vector in the correct orientation to generate the plasmid. The plasmid also contains a *URA3* gene, allowing uracil synthesis and complementation of the uracil (-) auxotrophy. Colonies on selected yeast synthetic dropout media plates were checked for positive clones by colony PCR. Plasmid DNA was extracted from each clone and transformed into *E.coli* to allow large scale plasmid isolation because isolation of the yeast plasmid is inefficient and a large quantity of the plasmid DNA (4 µg) is needed to transform *M. oryzae*.

Four primers were designed to generate the vector. Two primers were designed for each fragment of the sulfonylurea resistance gene cassette or *ILV1* and *ATG3* gene *(*including 1.7 kb promoter, 1.2 kb *ATG3* gene and 0.5 kb 3'-UTR) (Table 4.4). The *ILV1* forward primer was designed with a 5' overhang from the plasmid. *ATG3* forward and reverse primer was designed with 5' overhang from *ILV1* and plasmid respectively (Figure: 4.42A). PCR were carried out using a proofreading polymerase (Fusion, NEB), fractionated by agarose gel electrophoresis and purified from the gel (Figure: 4.42B). Plasmid pNEB1284 was linearized by *Hin*dIII and *Sac*I double digestion, fractionated in agarose gel and purified. An aliquot of

500 ng of each of PCR amplicons were mixed with an equal amount of linearized vector and transformed in the yeast strain following a method described in section 2.4.6. After 2 days, the positive colonies were identified by colony PCR using a primer pair that amplifies a 1.3 kb fragment from promoter to ORF region of *ATG3* gene. Positive clones were selected. Plasmid DNA was extracted and transformed into *E. coli*. (Promega JM109 *end*A1, *rec*A1, *gyr*A96, *thi*, *hsd*R17 (rk–, mk+), *rel*A1, *sup*E44, Δ(*lac-pro*AB), [F´ *tra*D36, *pro*AB, *laq*I^qZΔM15). From the transformed competent cells, positive clones were identified by same primer pair that was used for yeast colonies and complementation vector was finally prepared by plasmid midiperp.

Table 4.5: Primers used for construction of *ATG3* complementation vector

Name	Sequence (5'→3')
ATG3_Comp_F	GATTATTGCACGGGAATTGCATGATCTCACCGCAGCCACCCAAAATGGATGC
ATG3_Comp_R	TTCACACAGGAAACAGCTATGACCATGATTCTGTCTCCAGAGACTGTTACACCG
Sur_F	AACTGTTGGGAAGGGCGATCGGTGCGGGCCCCAACGCCACAGTGCCCCA
Sur_R	CTGTTACTTTTTTCTGTTACTGTTGTCGCTGTGAGAGCATGCAATTCCCGT
ATG3_CPF	GTTACAGGCTTCATTCATCTTTTT
ATG3_CPR	CTGGGGTGACGCTGGCAATA

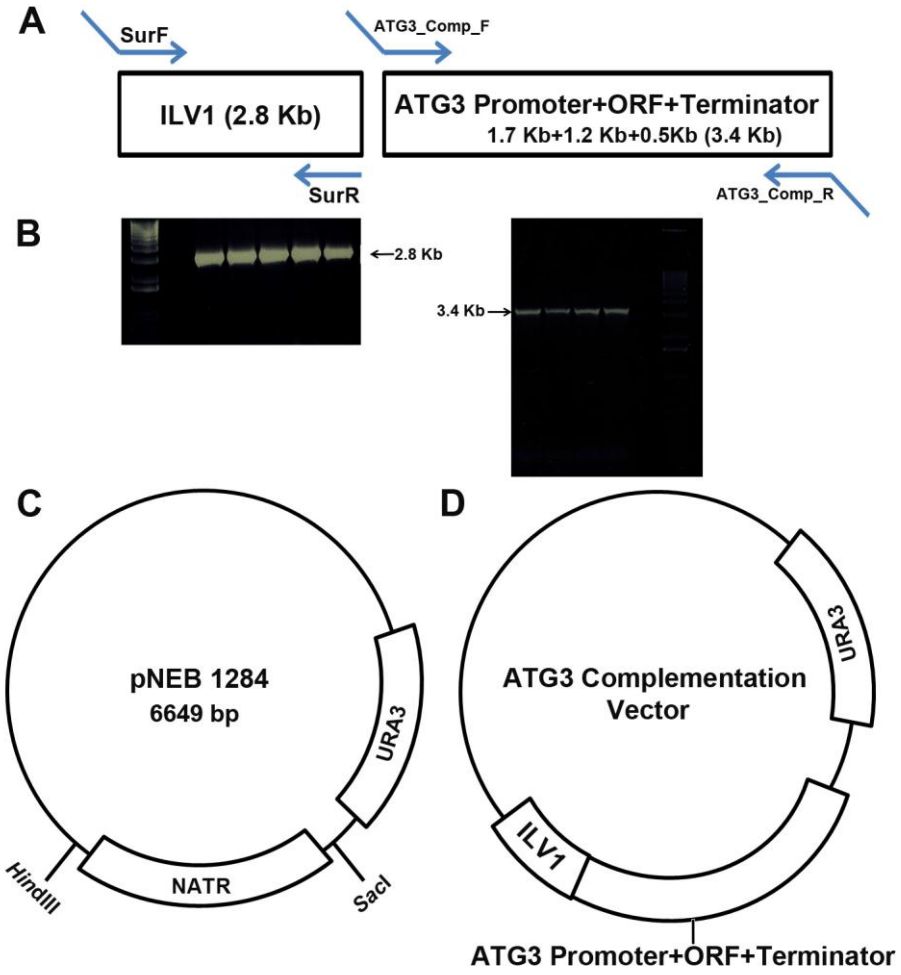

Figure 4.42: Construction of the *ATG3* gene complementation vector. In order to complement mutant M1054, a complementation vector was constructed using the plasmid pNEB1284 by recombination-mediated PCR-directed plasmid construction *in vivo* in yeast (Oldenburg *et al.*, 1997). **A & B.** A 2.8 kb *ILV1* (sulfonylurea resistance gene cassette) and 3.4 kb *ATG3* gene cassette (included 1.7 kb upstream promoter, 1.2 kb *ATG3* ORF and 0.5 kb terminator) was amplified. The primers used to amplify PCR products have overhangs corresponding to adjacent PCR fragments and with the plasmid. **C.** The plasmid was linearized by *Hin*dIII and *Sac*I enzyme double digestion. **D.** When the linearized plasmid is mixed with PCR products and transformed in yeast with appropriate conditions, homologous recombination takes place and joins the PCR amplicons with the vector in the correct orientation to generate the complementation vector.

4.3.4.3 Complementation of the mutant M1054 with *M. oryzae ATG3* gene

The *ATG3* complementation vector was transformed into protoplasts of mutant M1054. Putative transformants were selected for resistance to chloromuron ethyl (sulfonylurea) (100 μg mL^{-1}). Then selected transformants were screened and confirmed for vector integration by Southern blot hybridization analysis. Genomic DNA were digested with *Hind*III enzyme, fractionated by gel electrophoresis, blotted and probed with a 1 kb *ILV1* fragment. The DNA was digested with *Hind*III, because it does not have any restriction site within the *ILV1* cassette. Southern hybridization analysis showed that vector was randomly integrated in the genome (Figure: 4.43 B). Positive transformants were then assayed for pathogenicity by cut-leaf assay. A 50 μL conidial suspension was placed on cut leaves laid on 1% agar plates and incubated for 5 days. Pathogenicity was completely restored in positive mutants when compared with mutant M1054 and wild-type Guy11. Pathogenicity assays for three of the complemented strains are shown in Figure: 4.43C. Complemented strains restored pathogenicity by producing necrotic rice blast lesions. Complemented strains were grown on CM for 12 days and three of them showed distinct growth phenotype compared to M1054 (Figure: 4.43A).

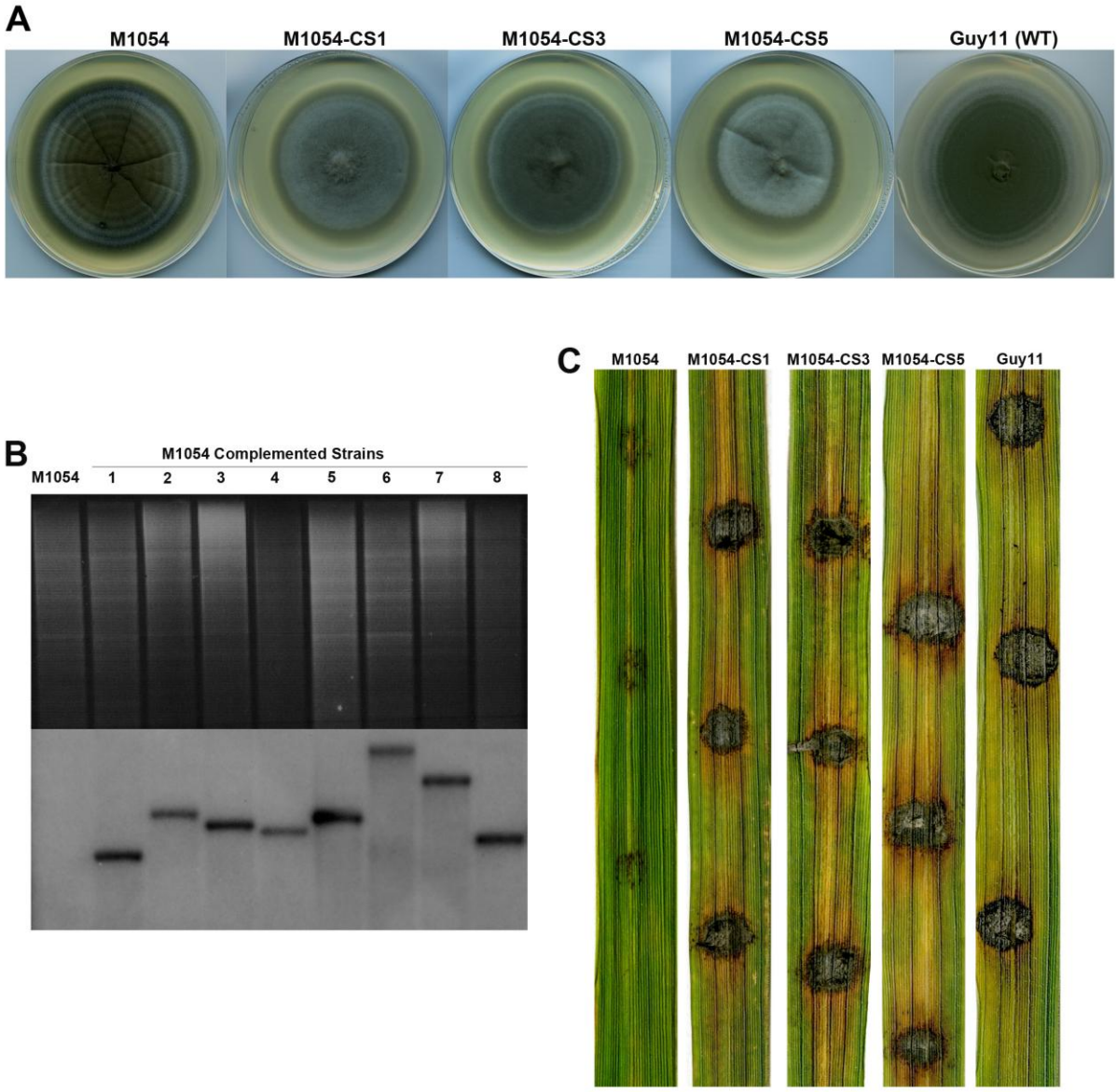

Figure 4.43: Complementation of the mutant M1054 with *M. oryzae ATG3* gene. A. Three complemented strains of mutant M1054 are shown. Morphology of those complemented strains is distinguishable from the autophagic mutant M1054 and their appearance was similar to wild-type Guy11. **B.** Complemented strains were analyzed by Southern blot hybridization to confirm the vector insertion in genomic DNA. Genomic DNA isolated from sulfonylurea resistant transformants was digested with the restriction enzyme *Hin*DIII, fractionated by agarose gel electrophoresis, blotted. The Southern blot was probed with a 1 kb *ILVI* fragment generated by PCR amplification**.** Selected complemented strains showed positive results. **C.** Pathogenicity assay of three selected complemented strains are shown. Complemented strains were able to produce typical necrotic rice blast disease lesions.

4.3.4.4 Construction of plasmid for Atg3p Localization

Although *ATG3* gene is essential for pathogenicity in rice blast disease, the localization of Atg3 protein has not previously been determined in *M. oryzae.* To determine the likely sub-cellular location of Atg3 and the temporal and spatial pattern of *ATG3* expression during appressorium development, an *ATG31:sGFP* C-terminal gene fusion was constructed. The plasmid *ATG3:sGFP:trpC* was made using recombination-mediated PCR-directed plasmid construction *in vivo* in yeast (Oldenburg *et al.*, 1997).The *ATG3* complementation vector was constructed using the same strategy. The C-terminal gene fusion was constructed using the plasmid *AGL1:sGFP:trpC* which was originally constructed from plasmid pNEB1284 (Figure: 4.44B). A 2.9 kb genomic DNA fragment containing the *ATG3* coding region (without stop codon) and 1.7 kb of upstream promoter sequence was amplified (Figure: 4.44A). PCR was carried out using a proofreading polymerase (Fusion, NEB), fractionated in agarose gels and purified from gel (Figure: 4.44A). The primers were modified with overhangs corresponding to the *ILV1* sequence (Forward primer) and the *sGFP* sequence (Reverse primer) in the plasmid. The plasmid was linearized by *Hin*dIII digestion and dephosphorylated with Antarctic phosphatase to prevent self-ligation. *Hin*dIII digestion take out *AGL1* from the plasmid leaving the *sGFP:trpC* intact in the linearized plasmid. When the linearized plasmid was mixed with PCR products in appropriate conditions, homologous recombination took place to join the PCR amplicons with the vector in the correct orientation and generated the C-terminal fusion of *ATG3* in the plasmid. Positive colonies were identified by colony PCR using a primer pair that amplifies a 0.7 kb GFP fragment from the constructed vector. Positive clones were selected. Plasmid DNA was extracted and transformed into *E. coli*. (Promega JM109 *end*A1, *rec*A1, *gyr*A96, *thi*, *hsd*R17 (rk–, mk+), *rel*A1, *sup*E44, Δ(*lac-pro*AB), [F´ *tra*D36, *pro*AB, *laq*I^{q}ZΔM15). From the transformed competent cells, positive

clones were identified by same primer pair that was used for yeast colonies and *ATG3:sGFP:trpC* vector was finally prepared by plasmid midiperp. Following DNA sequence analysis to confirm that the gene fusion was in-frame, the construct was introduced into the wild-type *M. oryzae* strain Guy11. Putative transformants were selected for resistance to chloromuron ethyl (sulfonylurea) (100 μg mL^{-1}) and screened for GFP expression while growing them on selection plates. Selected positive transformants were grown on CM for 12 days and GFP expression during appressorium development was recorded by epifluorescence microscopy.

Table 4.6: Primers used for the construction of *ATG3:sGFP:trpC* plasmid

Name	Sequence (5'→3')
ATG3_GFP_F	GATTATTGCACGGGAATTGCATGATCTCACCGCAGCCACCCAAAATGGATGC
ATG3_GFP_R	GGTGAACAGCTCCTCGCCCTTGCTCACCATGACGCCCATCGTAAAGTCATG
GFP_CPF	GGTGAACAGCTCCTCGCCCTTGCTCACCAT
GFP_CPR	CTTGTACAGCTCGTCCATGCCGTG

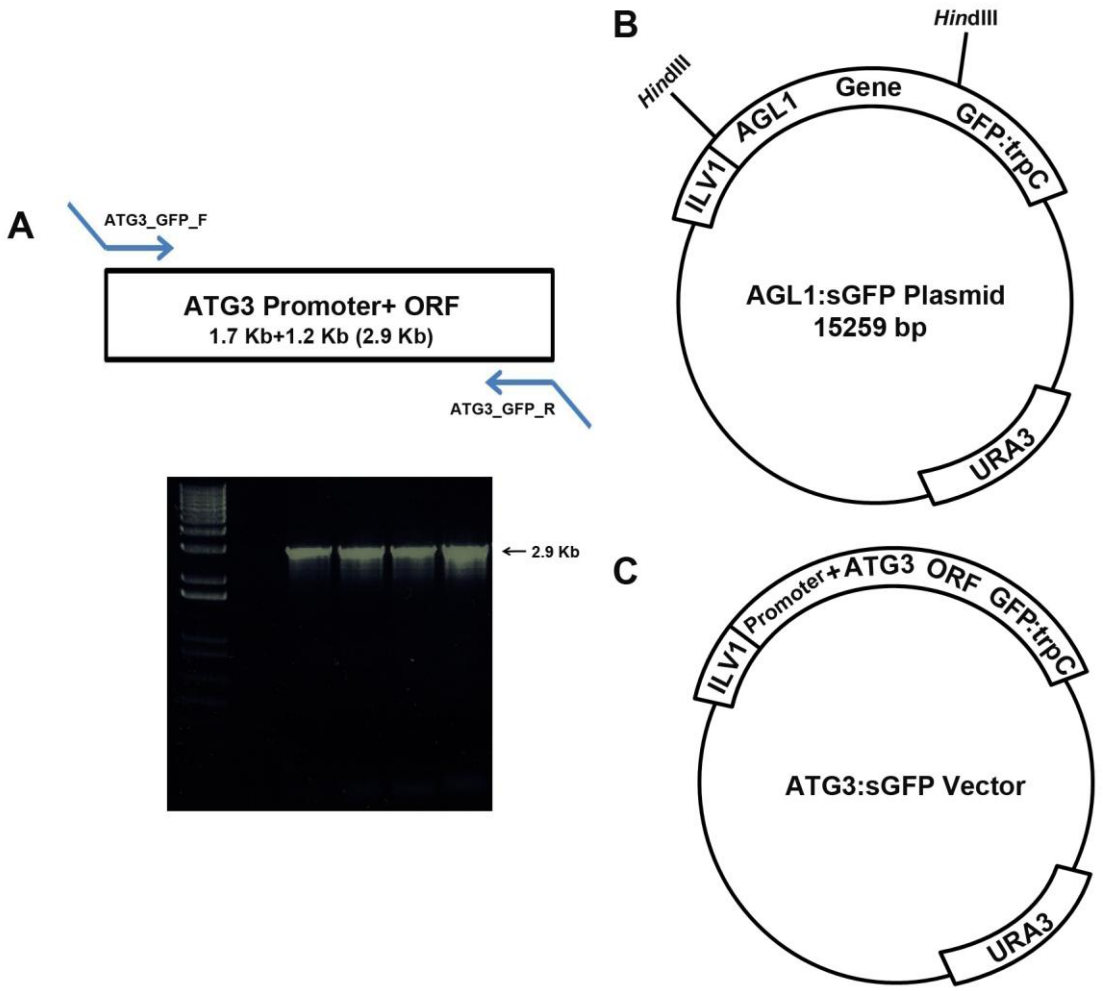

Figure 4.44: Construction of the *ATG3:sGFP* C-terminal gene fusion vector. An *ATG3:sGFP* C-terminal gene fusion was constructed using the plasmid *AGL1:sGFP* (originally constructed from plasmid pNEB1284) by recombination-mediated PCR-directed plasmid construction *in vivo* in yeast (Oldenburg *et al.*, 1997). **A.** A 2.9 kb genomic DNA fragment containing the *ATG3* coding region (without stop codon) and 1.7 kb of upstream promoter sequence was amplified. The primers were modified with overhangs corresponding to *ILV1* sequence and *sGFP* sequence in the plasmid. **B.** The plasmid was linearized by *Hin*dIII digestion. **C.** When the linearized plasmid is mixed with PCR product and transformed in yeast with appropriate conditions, homologous recombination takes place and joins the PCR amplicon with the vector in the correct orientation to generate the vector.

4.5.5 Localization of Atg3-GFP during infection-related development in *M. oryzae*

In order to investigate the sub-cellular location of Atg3 and the temporal and spatial pattern of *ATG3* expression during appressorium formation, conidia expressing *ATG3:sGFP* were inoculated onto borosilicate coverslips and incubated at 24ºC. Examination by epifluorescence microscopy was carried out at 0, 2, 4, 6, 8 and 24 hours from incubation. GFP fluorescence was consistently detected revealing that Atg3 is expressed during conidial germination and appressorium development (Figure 4.45).

In yeast, *ATG3* encodes an ubiquitin E2-like enzyme that conjugates Atg8 with phosphatidylethanolamine (PE) (Tanida *et al.,* 1999, 2000, 2001; Ichimura *et al.,* 2000). Atg3 is composed of three characteristic regions: the E2 core region, the flexible region and the handle region (HR). The latter two regions are necessary for interaction with Atg8, although the mechanism of interaction is not yet known (Yamada *et al.*, 2007). It was shown that Atg3 directly interacts with Atg8 by NMR analyses (Yamaguchi *et al.,* 2010). NMR data together with *in vitro* pull down assays provide evidence for a direct Atg8-Atg3 interaction mediated by HR in Atg3. I*n vitro* conjugation assays also confirmed that that this interaction is important for the formation of Atg8-PE conjugates. Furthermore, it was suggested that that the interaction promotes the transfer of Atg8 from the Atg8-Atg3 thioester intermediate to PE (Yamaguchi *et al.,* 2010).

In conidia, Atg3 localization was very similar to localization of *GFP:ATG8* which is seen in punctate structures in the cytoplasm. Atg8 is localized in autophagosomes throughout the appressorium development (Kershaw and Talbot, 2009). Therefore at 0 h, Atg3p is localized to the autophagosomes where the PE-Atg8 conjugation takes place at the onset of autophagic

process (Figure: 4.45). Autophagosomes accumulate in conidia during germination and subsequently their number steadily decreased during the onset of conidial cell death and appressorium maturation (Kershaw and Talbot, 2009). Similarly at 2 h the punctate structures disappeared and localization of Atg3 was seen in vesicles. At 4 h when appressorium starts to develop Atg3 was localized only in cytoplasm of developing appressorium and conidial expression was no longer detected. At subsequent time points at 6, 8 and 24 h Atg3 expression was observed solely in appressoria. Autophagosomes number within developing appressoria increased during appressorium maturation. Intense autophagic activity and expansion of vacuole was associated with maturation of appressoria which was consistent with previous reports (Kershaw and Talbot, 2009).

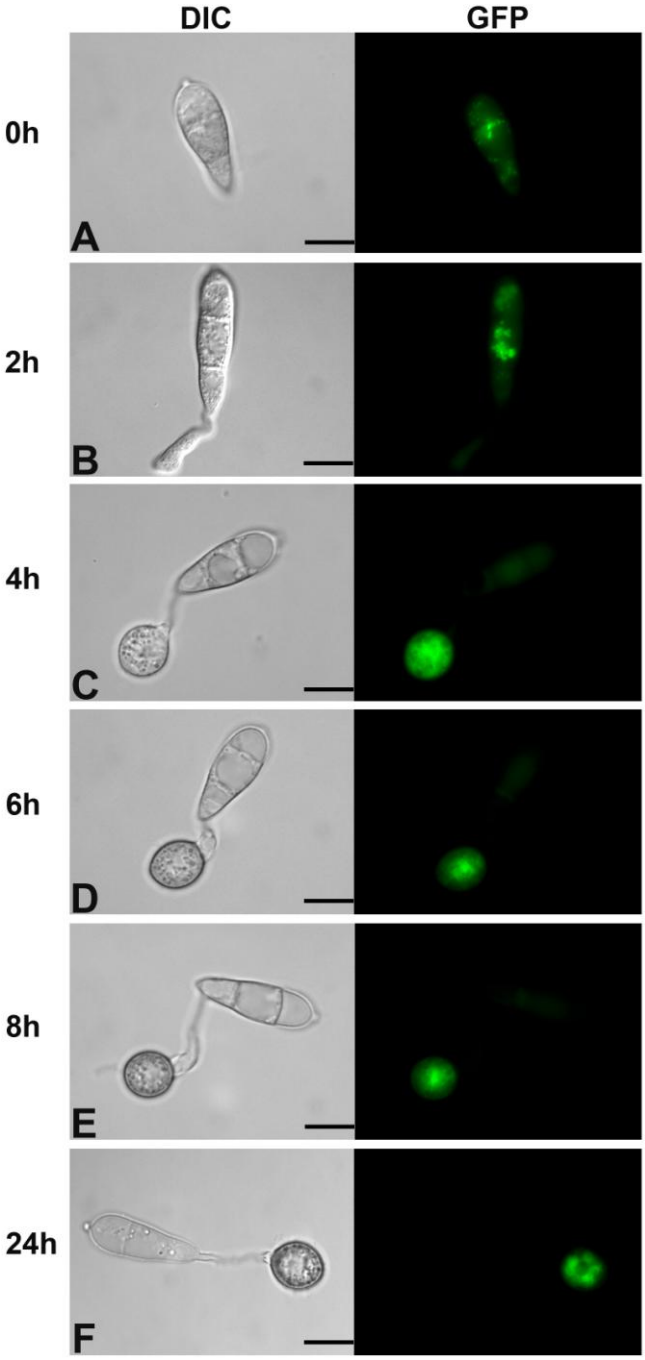

Figure 4.45: Localization of Atg3p fused to Green Fluorescent Protein (GFP) in *M. oryzae* during appressorium development. Conidia from 12-day old plates were inoculated onto glass coverslips. Localization of Atg3p-GFP was observed over a period of 24 h using an Olympus IX-81 inverted epifluorescence microscope fitted with HQ^2 camera. Representative DIC and fluorescence images are shown at 0, 2, 4, 6, 8 and 24 hpi. Atg3p is localized to the autophagosomes where the PE-Atg8 conjugation takes place at the onset of autophagic process. Punctate structures are seen at 0 h **(a)**. At 2 h the punctate structures disappeared from cytoplasm, Atg3p localized in vesicles **(b)** and by 4 h its expression was observed in the developing appressorium **(c)**. At subsequent time points of 6, 8 and 24 h **(d, e and f)**, Atg3p expression were localized solely in the appressoria and conidial expression no longer observed. Scale Bar = 10 µm.

4.4 Discussion

In this chapter I have reported the selection of candidate insertional mutants from the primarily identified cohort of 200 non-pathogenic and reduced pathogenicity mutants. We carried out a comprehensive quantitative screening regime to confirm the pathogenicity phenotype in a reproducible manner, selected mutants that were impaired in pathogenicity and phenotypically characterized them in detail for further molecular, genetic and functional characterization. Simultaneously, I have provided evidence that ATMT mediated insertional mutagenesis is able to tag genes involved in pathogenicity by T-DNA integration.

From the qualitative primary screening, 200 mutants were selected out of 10,200 (1.96%). These showed significant impairment in pathogenicity. These 200 mutants were either non-pathogenic or reduced in their ability to cause disease compared to the isogenic wild-type Guy11. In order to maintain the high-through put of the screen it was not possible to screen them homogenously and quantitatively. Consequently, it was necessary to screen the initially selected mutants in a quantitative procedure before starting phenotypic and molecular characterization. We therefore carried out re-screening on primary selected mutants, scrutinized their consistency in causing disease in a quantitative scale and finally selected mutants for downstream processing. After the first round of quantitative screening we selected 85 mutants for further quantitative screening and discarded more than half of them. Repeated screening was carried out and we identified 9 non-pathogenic mutants showing a consistent disease phenotype. After a comprehensive meticulous lesion count and associated statistical analysis we selected 62 mutants that were reduced in pathogenicity. Mutants were selected which showed ≤50% reduction in pathogenicity. This pool of reduced mutants manifested a diverse array of pathogenic phenotypes. They were reduced in terms of lesion density, size and both. From the rigorous re-screening we were able to identify 3 non-

pathogenic mutants that were actually non-conidiating. Their pathogenicity can be attributed to their aconidial phenotype and it was not possible to identify them without a quantitative re-screening. We screened three mutants for their ability to produce spores by harvesting more than 100 plates and in this way provided evidence that they are completely non-conidiating. Nevertheless, we tested their ability to cause disease in wounded leaves by applying suspension of mycelia on abraded leaf surface. On a wounded leaf the fungus does not need to mechanically breach the tough cuticle by forming appressorium from conidia and able to grow inside plant tissue. All three of them were able to infect plant tissue and caused necrotic lesions. This provides evidence that although they were defective in condition but capability of causing disease was retained. Thus the T-DNA has tagged loci which are involved in conidiogenesis and this opens up scope to investigate the biology of conidiogenesis by determining novel genes in the context of pathogenesis.

We carried out pathogenicity assays on barley and observed the same phenotype for conidiating non-pathogenic mutants. This indicates the identification of general pathogenicity determinants rather than host specificity determinants. We observed the vegetative growth of all the finally selected mutants. Although most of them were similar to Guy11 in terms colony diameter, some of them also grew larger although not significant (statistics not shown). It is noticeable that some of the mutants were very much weak in growth which indicated that genes regulating vegetative growth were disrupted by T-DNA integration.

We set our priority to carry out detailed phenotypic and molecular characterization on non-pathogenic mutants. Therefore, we characterized 8 non-pathogenic mutants in detail. Mutant M1054 was defective in conidiation, but showed abnormal vegetative growth, compared to Guy11. M1054 was defective in turgor generation, but showed normal conidial germination

and appressorium development. Its appressoria do not collapse at 24 hpi during infection related development. It was unable to penetrate either oinion or rice epidermis. Mutant M1879 showed similar phenotype except that it was reduced in conidial germination and appressorium development. Mutant M1880 was very interesting as it showed normal phenotype with respect to conidiation and germination, but was unable to develop appressoria. Moreover, when we tried to induce appressorium development in the presence of exogenous inducers (cAMP, hexadecanediol and IBMX) it failed to develop appressoria. We also tested its ability to develop appressoria on inductive surfaces, such as onion epidermis. On onion M1880 extended long germ tubes as during appressorium development on glass which resembles a MAP kinase mutant Δ*pmk1* (Xu and Hamer, 1996; Zhao *et al.,* 2005). Mutant M2867 was reduced in conidiation and appressorium development but conidial germination was normal. Its conidia did not collapse at 24 hpi during appressorium development. It was impaired in penetrating both onion and rice epidermis. The most interesting non-pathogenic mutant we identified in our repertoire was M4874. It was comparable with Guy11 in terms of conidiation, germination and appressorium development but showed very distinct vegetative growth. It could produce turgor pressure that was not significantly different from Guy11; nevertheless it was delayed in penetration. It penetrated both onion and rice epidermis at 30 h. We investigated its growth in rice tissue at 36 h and 48 h and it showed less-branched invasive hyphae compared to Guy11. Because of its ability to grow in rice tissue, we carried out a pathogenicity assay for M4874 and incubated the infected rice seedlings for 8 days to observe if there is any delay in disease lesion formation. But, no characteristic rice blast disease lesions were detected even after 8 days of infection. Taken together, it can be concluded that the M4874 was not defective in penetration and in planta growth but was defective in causing disease by producing necrotic lesions. These

findings make it the most intriguing mutant to be characterized with the potential to explore the new avenue of necrotic growth and lesion formation determination in *M. oryzae.*

Having the phenotypic data we determined the T-DNA copy number of selected non-pathogenic mutants. Except for M1879 all of the mutants contained single copy T-DNA insertions and this supports the results we generated from copy number analysis that suggested a high percentage of our library is single copy T-DNA insertional mutants. We set out to identify T-DNA tagged genes from the selected mutants. We followed two conventional procedures for retrieving T-DNA flanks. The TAIL-PCR and iPCR were performed on mutants M1054 and M1879 initially. For TAIL-PCR we used a commercial kit (Vectorette system) because of certain advantages. The kit provides a time-efficient way of library construction with a choice of restriction enzymes. Amplicons can be enriched by nested PCR and separate sequencing primer allows sequencing from the Vectorette adaptor end. This kit is well optimized for mapping of promoters, introns, microsatellites, SSRs and STRs and iidentification of flanking genomic sequences of transgenes in transgenic organisms. Therefore, we successfully used it to identify T-DNA tagged genes from both M1054 and M1879. The iPCR also generate the same results. Interestingly we found autophagic genes *ATG3* and *ATG2* were tagged in these mutants. These two genes are known to be essential for infection-related autophagy in *M .oryzae*. They were identified from a genome wide functional analysis study and shown to be essential components of autophagic machinery that is required for causing rice blast disease (Kershaw & Talbot, 2009). But, unfortunately none of the PCR retrieved other T-DNA tagged loci from M1879. Therefore, we excluded it from further gene functional analysis.

We carried out further molecular genetic analysis on M1054. We generated evidence for a T-DNA insertion in the *ATG3* gene of M1054 by RFLP analysis which unequivocally validated

the PCR results. Thereafter, we constructed a complementation vector for *ATG3* gene by cloning it from wild-type Guy11 and were able to complement the mutant for pathogenicity. Although *ATG3* gene was characterized for pathogenicity, by complementation of the mutant M1054 we completed the pipeline for gene discovery and we were able to show that our insertional mutant generated by ATMT has tagged a gene involved in pathogenicity. Furthermore, we took this opportunity to localize the *ATG3* gene product during infection related development in *M. oryzae* which was not investigated in earlier studies.

In summary, I have shown that two autophagic genes were interrupted by T-DNA insertion. Autophagy is a ubiquitous and essential process in eukaryotes to eliminate cellular constituents ranging from soluble proteins to entire organelles (Yorimitsu and Klionsky, 2005; Xie and Klionsky, 2007). Autophagy also appears to play an important role in filamentous fungi impacting upon growth, morphology and development. Recently, it has been shown that non-selective autophagy or macroautophagy is essential for infection-related development and initiation of disease in *M. oryzae* (Veneault Fourrey *et al.*, 2006; Kershaw & Talbot, 2009). This process sequesters cytoplasmic materials into an expanding membranous organelle which is called the phagophore. Later on, the phagophore matures into an autophagosome, which is a double-membrane bound vesicle. The site of autophagosome formation is called the phagophore assembly site (PAS) (Kim *et al.,* 2002; Suzuki *et al.,* 2001). Later in this process autophagosomes fuse with lysosomes, this culminates in lysis and degradation of the membrane and its content. The biogenesis of autophagosome is a tightly regulated process where concerted action of core autophagy machinery proteins leads to its formation and turnover (Yorimitsu and Klionsky, 2005; Xie and Klionsky, 2007). One of the most important constituents of the core machinery proteins is Atg8, an ubiquitin-like protein (Ichimura *et al.,* 2000; Paz *et al.,* 2000). Newly synthesized Atg8 is processed by a cysteine

protease, Atg4, to expose its carboxyl terminal glycine residue (Kirisako *et al.,* 2000; Kim *et al.,* 2001; Hemelaar *et al.,* 2003). It is then conjugated to phosphatidylethanolamine (PE) by the E2-like conjugating enzyme Atg3 (Tanida *et al.,* 1999, 2000, 2001; Ichimura *et al.,* 2000). Atg3 is composed of three characteristic regions: the E2 core region, the flexible region and the handle region (HR). Atg3 HR, which mediates the interaction with Atg8 through the WEDL sequence motif. Initially, a PE-free form of Atg8 binds to the Atg19-Ape1 complex and after that Atg3 and unknown membranes are recruited to the complex and Atg3 conjugates Atg8 to PE in these membrane. Finally, Atg8-PE functions in membrane expansion (Yamada *et al.,* 2007). It was also confirmed that the amino N-terminal region of Atg3 is essential for the interaction with PE in Atg8–PE conjugation (Yamada *et al.,* 2007). Therefore, we constructed a C-terminal GFP fusion for *ATG3* localization. Because of its interaction with Atg8, Atg3 also localizes similarly in the early hour of infection-related development when the autophagic process is initiated (Kershaw and Talbot, 2009). On later time points Atg3 is localized only in appressoria because intense autophagic activity and vacuole expansion are associated with maturation of appressoria. As a consequence, autophagosome number in developing appressoria rise steadily, that was previously shown by Atg8 localization in *M. oryzae* (Kershaw & Talbot, 2009).

In conclusion, T-DNA insertional mutagenesis has been validated as a means of identifying individual genes conditioning the ability of *M. oryzae* to cause disease. The identification of *ATG2* and *ATG3*, which have previously been shown to have some roles in autophagy and are necessary for rice blast disease, validates the procedure set out in the study. We therefore, embarked on a method to identify the remaining genes associated with each of the non-pathogenic mutants selected by insertional mutagenesis.

Chapter 5

Next Generation Sequencing Based Identification of T-DNA Tagged Loci from Insertional Mutants

5.1 Introduction

In this chapter, we set out to test a novel approach for identification of T-DNA tagged loci from selected insertional mutants by next generation sequencing (NGS). Our aim was to establish a rapid and high-throughput identification method of T-DNA flanks by exploiting the advantages of NGS. NGS has revolutionized the realm of sequencing technology by catalyzing the generation of vast and accurate genomic information in a cost and time efficient manner. The automated Sanger method is considered as a 'first-generation' technology and newer methods are referred to as next-generation sequencing (Metzker, 2009). These newer technologies are based on a number of strategies that rely on a combination of template preparation, sequencing and imaging, alignment and assembly methods. Compared to automated Sanger sequencing, NGS platforms have dramatically increased the throughput and decreased the cost and time. The inexpensive production of large volumes of sequence data is the primary advantage over conventional methods (Metzker, 2009). NGS technologies have a wide range of applications and they are under continuous development (Elaine, 2008; Morozova and Marra, 2008; Metzker, 2009; McLean *et al.,* 2009; Zhou *et al.,* 2010; Martin *et al.,* 2011). NGS provides an attractive means to map mutations on a genome-wide scale (Smith *et al.,* 2008) and therefore it offers an attractive approach for localizing the sites of insertions in genome (Smith, 2011). Illumina sequencing is, arguably the most widely applied next-generation sequencing technology. For example, it

has already been used to identify transposon insertions in *Zea mays* (Williams-Carrier *et al.*, 2010). Hence, we decided to use Illumina paired-end (PE) sequencing (sequences of both the beginning and end of a randomly generated DNA fragment) as a means to identify T-DNA tagged loci in insertional mutants.

We took advantage of Illumina PE sequencing because of the enormous throughput short reads (100 bp reads) and they are sequenced from both ends. Instead of a *de novo* genome assembly, we required reads that contained either LB or RB sequence of T-DNA, and at least 15 bases of genomic DNA sequence of *M. oryzae*. A program, Bowtie 0.12.7 (Langmead *et al.*, 2009) can be used to search for reads containing at least 20 bp of LB or RB. After trimming away the T-DNA sequence, reads can then be assembled using automated programme such as Velvet (Zerbino and Birney, 2008). Assembled reads are then ready to identify the sequence matches from *M. oryzae* genome sequence. Therefore, NGS can be used to retrieve T-DNA flanks avoiding the cloning and sequencing steps of the conventional techniques such as TAIL-PCR and iPCR. Moreover, T-DNA flanking sequences can be identified in a high-throughput fashion by multiplexing samples. We therefore, decided to pool genomic DNA of all of the 8 selected non-pathogenic mutants together and made a single barcoded library for paired end sequencing. We reasoned that once the T-DNA flanks were identified, simple PCR could then be used attribute retrieved sequences to the corresponding loci. For a more rigorous confirmation, RFLP analysis can be used to identify tagged loci and compare mutant and wild-type. Complementation of the mutant with the T-DNA tagged loci can then ultimately prove the effect of the T-DNA insertion is associated with the observed phenotype. In this way NGS can be used to facilitate a pipeline of high-throughput T-DNA flank identification. The strategy for NGS mediated T-DNA flanking sequence identification is shown schematically in Figure 5.1.

The Illumina paired-end sequencing involves three steps. First, the sequencing library is constructed by ligating adapters with genomic DNA fragments and enriched by PCR for fragments with adapters ligated at both ends. Then, libraries are amplified to produce clonal clusters by an automated cBot instrument and clusters are finally sequenced using massively parallel synthesis. We used the Illumina HiSeq2000 sequencing system (University of Exeter) for our paired end library sequencing. This system uses Illumina's widely adopted reversible terminator-based sequencing by synthesis (SBS) technology. The principles of SBS technology are based on a proprietary terminator based method that detects fluorescently labelled single bases as they are incorporated during DNA synthesis on template strands. Simultaneously, the reversible terminator which is tagged with the fluorescent label terminates DNA synthesis by blocking DNA polymerase until imaging is completed and subsequently cleaved to resume synthesis by allowing incorporation of the next base. This SBS technology has facilitated sequencing reaction with unprecedented speed, throughput and accuracy.

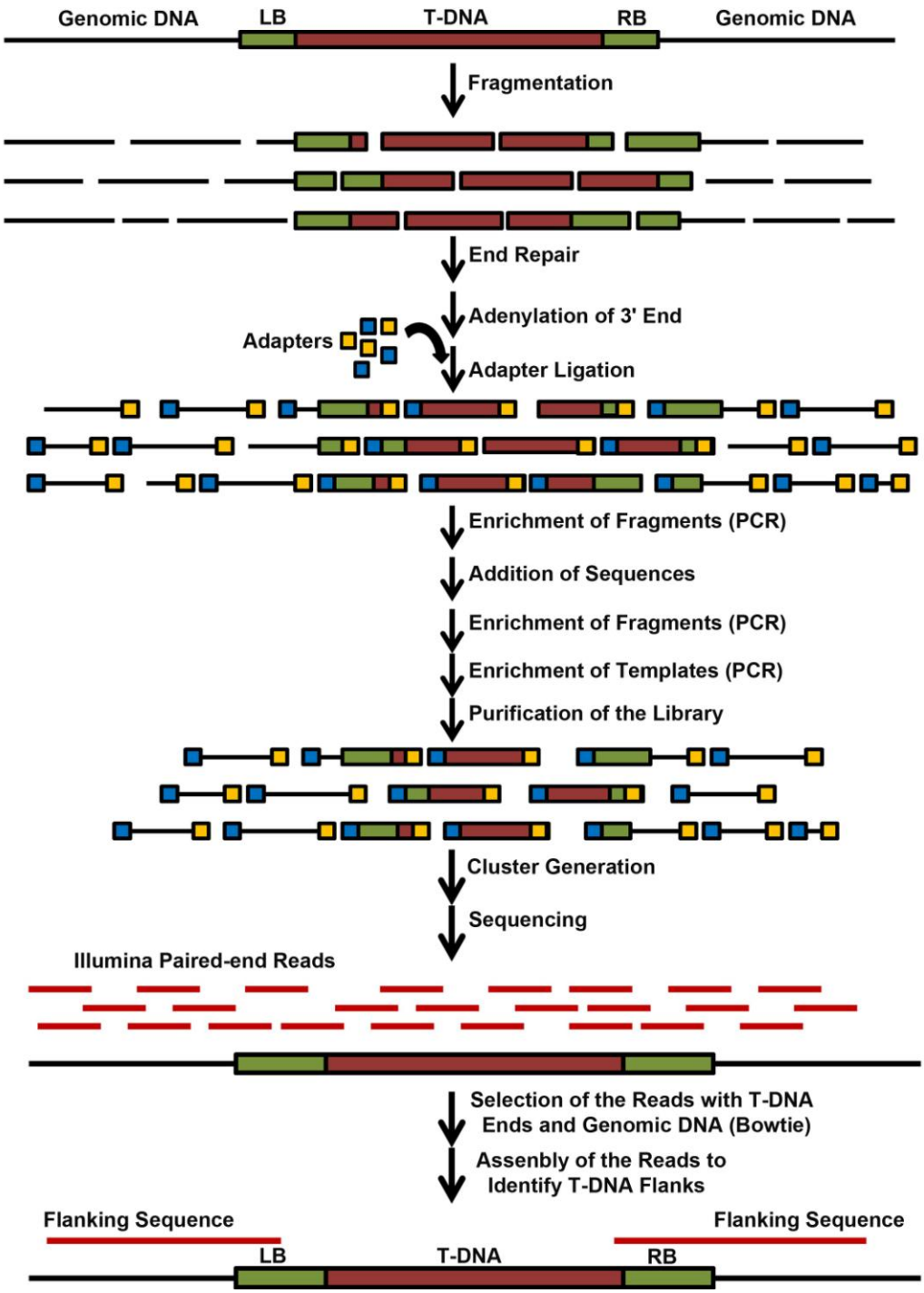

Figure 5.1: An overview of the principles of Illumina paired-end sequencing strategy to retrieve T-DNA flanking sequences from selected insertional mutants. Genomic DNA is fragmented homogenously by nebulization, heterogeneous fragment ends are repaired and adenylated to facilitate the ligation with adapters with 'T' overhangs. DNA fragments with both ends with ligated adapters are enriched by PCR, new sequences added to create primer binding site for sequencing and templates are enriched again by PCR. Purified templates are used for cluster generation and sequencing. From paired-end sequences, reads with at least 20 base pairs from either LB or RB of T-DNA were searched by the programme Bowtie 0.12.7 (Langmead *et al.*, 2009). Those reads were further processed to assemble the flanks. BLASTN was used to find the matches in genome sequence against the retrieved flanks.

5.2 Materials & Methods

5.2.1 NGS by Illumina

Illumina next generation DNA sequencing was carried out by Exeter sequencing service at the University of Exeter. Here we will provide a brief overview of the Illumina NGS technology. For this study paired-end sequencing was performed. The sequencing workflow is schematically shown in Figure 5.1. Information of paired-end sequencing library construction was obtained from the Illumina paired-end sequencing sample preparation guide. The Illumina sequencing workflow is based on three major steps: First, libraries are prepared from nucleic acid sample; second, libraries are amplified to produce clonal clusters and third; clusters are sequenced using massively parallel synthesis.

5.2.1.1 Construction of the paired-end sequencing library for Illumina sequencing

In order to prepare genomic DNA sample for paired end sequencing, standard methods described in Illumina® Paired End Sample Preparation Guide (Illumina) was followed. This protocol explains how to prepare paired- end libraries of genomic DNA (gDNA) for subsequent cluster generation and DNA sequencing using the reagents provided in the Illumina sequencing Kit. The goal of this protocol was to add adapter sequences onto the ends of DNA fragments to generate multiplexed paired end sequencing libraries.

Genomic DNA of the selected mutants was prepared by the large scale fungal DNA extraction (CTAB extraction) procedure described in section 2.3.1.1. DNA samples were prepared and handled with care to avoid any contamination and degradation. Samples were dissolved in TE and treated with RNase at the end of extraction. In order to ensure the quality of prepared genomic DNA, in a 1% agarose gel individual RNase-digested samples

were fractionated by electrophoresis for any degradation or remaining RNA and finally stored at 4°C.

The protocol for paired-end sequencing library construction is optimized for 1-5 μg of input DNA. The ultimate success or failure of a library preparation strongly depends on using an accurately quantified amount of input DNA. For accuracy, DNA quantitation was carried out by fluorescence-based methods in which intercalating fluorescent dyes measure double-stranded DNA. We used a commercial fluorescence based nucleic acid quantitation kit, the Qubit® dsDNA BR assay kits (Invitrogen) in conjunction with the Qubit® 2.0 fluorometer (Invitrogen). Three samples dilutions were made for each sample (1 μL, 5 μL and 10 μL) with the supplied buffer (in a total volume of 200 μL) and then samples measured using the Qubit® 2.0 fluorometer. After correct measurement, 10 μg of genomic DNA from each of the 8 mutants was pooled together in a fresh microfuge tube.

In accordance with the Illumina recommended protocol, nebulization was applied to fragment genomic DNA for paired end library construction. Nebulization fragments DNA into <800 bp size of molecules and generates double-stranded DNA fragments containing 3' or 5' overhangs. Fragmented DNA was assessed in an Agilent BioAnalyzer using a high sensitivity chip. The end repair was then performed which converted fragments into blunt ends using T4 DNA polymerase and Klenow polymerase. The T4 polynucleotide kinase used in this step also phosphorylated the 5' ends of the DNA fragments. In a subsequent 3' adenylation step, a single ‘A’ (adenine) nucleotide was added to the 3' ends of the blunt fragments to facilitate adapter ligation. This overhang was used to ligate fragments with the adapter which contains a complementary T (Thymine) nucleotide on the 3' end. Adapter-added sequences enabled

complimentary primer binding in the flowcell. Adapter-ligated fragments were then purified by gel electrophoresis which removes unligated and excess adapters.

Purified adapter-ligated fragments were PCR amplified to enrich those DNA fragments that have adapter molecules on both ends. The PCR was performed with a PCR primer pair that annealed to the ends of the adapters. The numbers of PCR cycles was optimized to avoid biasing composition of the library. This PCR amplification step also enriched the library by adding sequences to the ends of the adapters and enabled primer hybridization during cluster generation. Products of the PCR ligation reaction were further purified on a gel to select a size-range of templates appropriate for subsequent cluster generation. Illumina paired-end sequencing library preparation is shown as a workflow in Figure 5.2.

For quality control and quantification of DNA library templates, the library was validated following a recommended protocol. To verify the size of PCR-enriched fragments, an aliquot of the enriched library was run on an Agilent Technologies 2100 BioAnalyzer using a high sensitivity DNA chip. For quantification, 10% of the library was loaded on the Agilent high sensitivity DNA chip and the results shown in Figure 5.3.

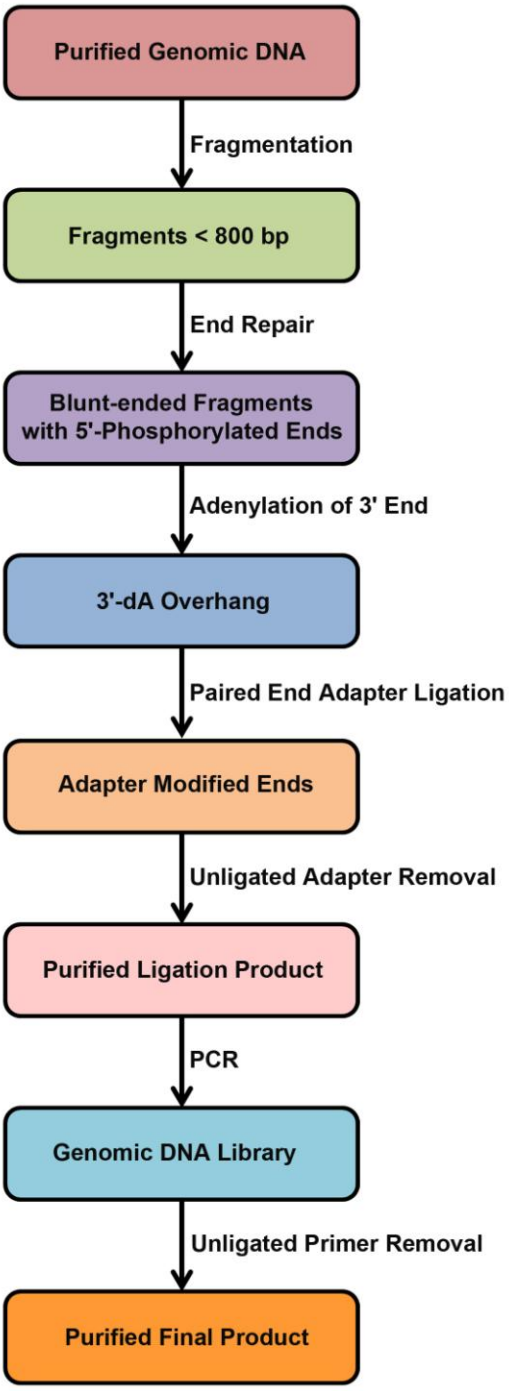

Figure 5.2: Illumina paired-end sequencing library preparation workflow (Image was obtained and modified from Illumina paired-end sequencing sample preparation protocol). This figure depicts the construction of a paired end sequencing library. Genomic DNA was fragmented by nebulization which generated blunt ended and phosphorylated fragments. Adenylation adds a single 'A' nucleotide to the 3' ends of the fragments to facilitate ligation of adapter with 'T' overhang. Adapter ligation adds different sequences at the 5' and 3' ends the genomic DNA fragments. Adapter ligated DNA fragments are gel purified and enriched by PCR for fragments with adapters on both ends. The resulting sample library is again purified. Finally, the purified paired-end library was validated and quantified by Agilent BioAnalyzer prior to cluster generation.

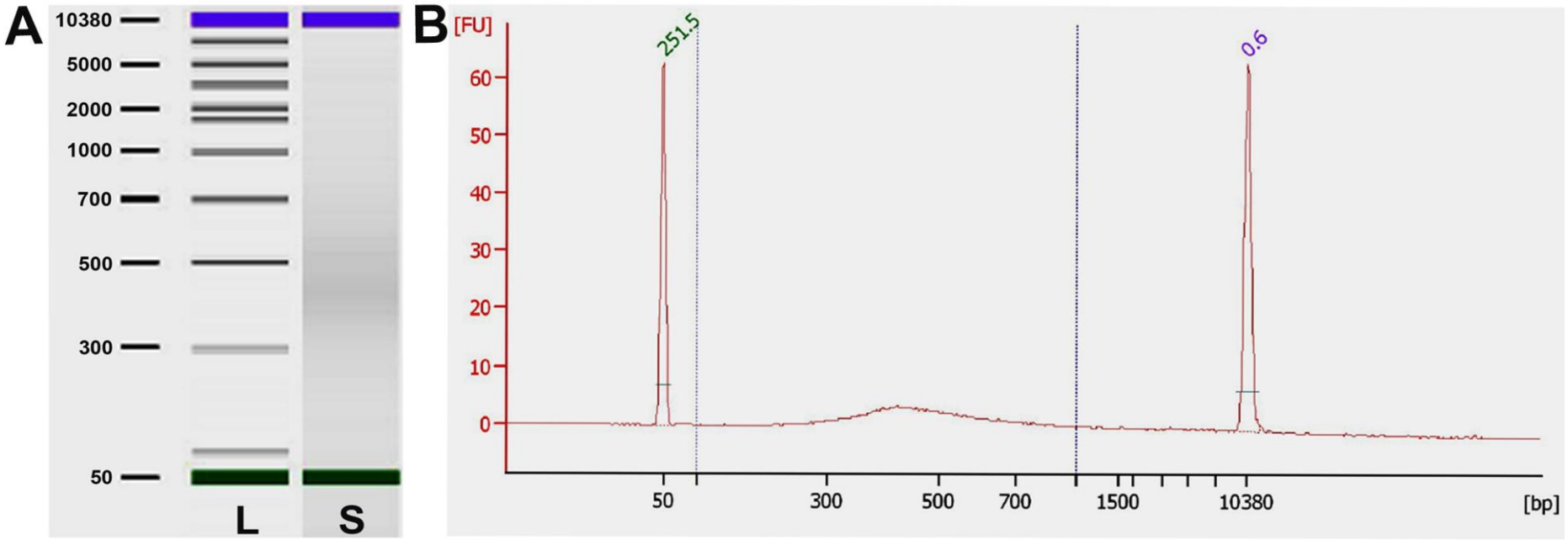

Figure 5.3: Size and distribution of the paired end sequencing library. To verify the size of PCR enriched fragments in the library, template size distribution was checked by running an aliquot of the enriched library on an Agilent 2100 BioAnalyzer using a High Sensitivity DNA chip. A 1:100 dilution of the library was made using water and 1 µL of the diluted library was loaded on a Agilent High Sensitivity DNA chip. **A**. The densitometry plot shows the size of the fragments in the constructed paired end library. **B.** The electropherogram indicates that the library had a DNA template size range of 330-800 bp. The library has a 120 bp of adapter sequence (58bp + 63bp at either end) and therefore, insert sizes ranged from 200-680 bp.

5.2.1.2 Cluster generation

In the HiSeq2000 sequencing platform (Illumina), clonal clusters of template DNA are generated by the fully automated cBOT instrument. This process involves multiplication of the constructed library on an oligo-decorated solid support in a flowcell (Elaine, 2008). Cluster generation is an automated clonal amplification process that takes place in multi-well plates (96-well plates) in a single flow cell. The flow cell is an 8-channel micro-fabricated sealed glass device and amplification of DNA takes place on its surface by DNA polymerase. Resultant multiple DNA copies, or clusters represent the single molecule that initiated the cluster amplification (Elaine, 2008).

The principles of cluster generation are explained diagrammatically in Figure 5.4. The entire process is accomplished in three simple steps. First, millions of DNA templates are hybridized to the covalently-attached forward and reverse primers on the flow cell surface. After amplification, templates are denatured which are immobilized on the flow cell surface. In the second step, the templates are hybridized to adjacent oligonucleotides and amplification occurs from the hybridized oligonucleotides to form dsDNA bridges. After this isothermal bridge amplification, dsDNA are denatured to form ssDNA strands. The process is repeated by cycles of isothermal denaturation and amplification to create millions of individual dense clonal clusters. At the final step, denaturation of clusters of dsDNA bridges leaves only the forward DNA and the reverse strand removed by specific base cleavage. In order to prevent interference with the DNA sequencing reaction, flow cell-bound oligonucleotides and 3' ends of the DNA strands are blocked. During the sequencing reaction, the primer is hybridized to the complementary sequence on the Illumina adapter on unbound ends of the templates in the clusters.

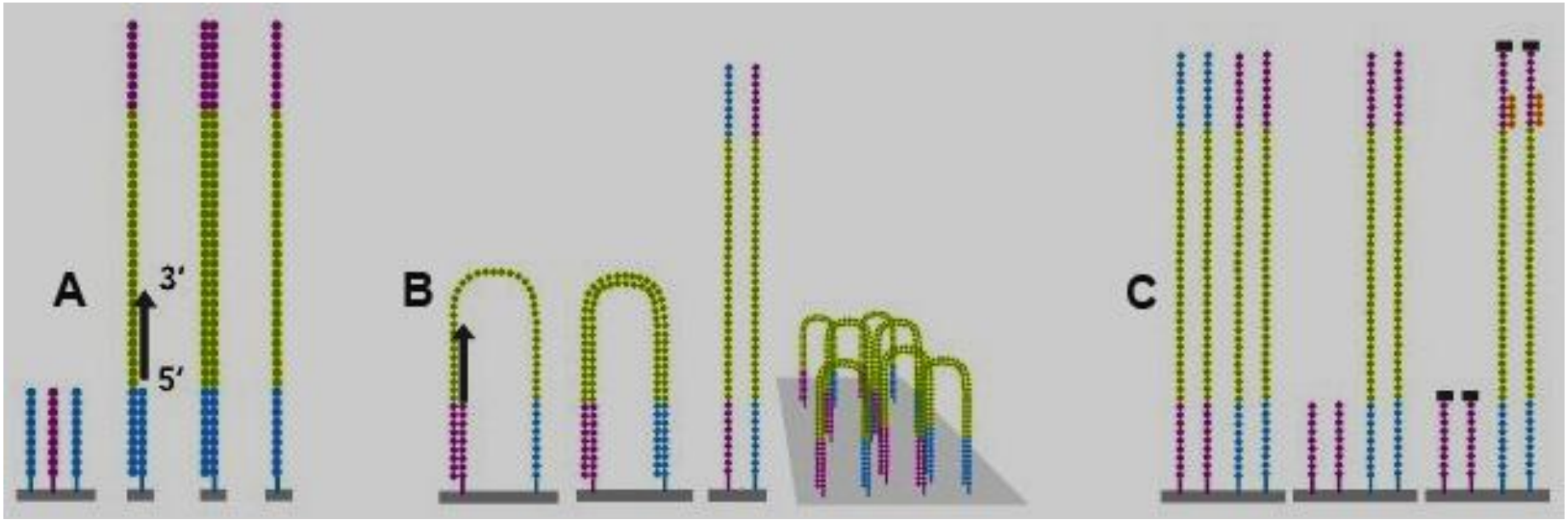

Figure 5.4: Schematic representation of the cluster generation process from paired-end genomic DNA library (Image was obtained and modified from Illumina Cluster Generation Protocol). Cluster generation forms single molecule DNA template within the sealed Illumina flowcell on the cBot instrument and involve three steps. **A. Immobilization of single-molecule DNA templates.** Templates are hybridized to oligonucleotides immobilized on the flow cell surface. The templates are copied from the hybridized primers by 3' extension using a high-fidelity DNA polymerase and then denatured. **B. Isothermal bridge amplification.** The templates are hybridized to adjacent oligonucleotides and DNA polymerase copies the templates from the hybridized oligonucleotides to form dsDNA bridges. They are denatured to form ssDNA and the process is repeated to create millions of individual dense clonal clusters. **C. Linearization and primer hybridization.** Finally, clusters are denatured and the reverse strand removed. In order to facilitate sequencing primer hybridization and avoid mispriming, unbound ends of the DNA strands and flow cell-bound oligonucleotides are blocked.

5.2.1.3 Next generation DNA sequencing by Illumina HiSeq™ 2000 system

The HiSeq™ 2000 sequencing system from Illumina was used for genome sequencing. Illumina sequencing is based on sequencing by synthesis (SBS) technology. The reversible terminator-based method is at the core of this technology, which uses dye-labelled modified nucleotides. These fluorescently-labelled nucleotides are specifically incorporated after priming and the remaining unincorporated nucleotides are washed away. Subsequently, DNA synthesis is terminated by a reversible terminator present in the modified nucleotide. After fluorescence imaging these fluorophores, along with the terminator are efficiently cleaved, washed off and this allows incorporation of the next base (Metzker, 2009). Four different nucleotides fluoresce at four different wavelengths that are detected by total internal reflection fluorescence (TIRF) imaging using two lasers (Metzker, 2009).

5.2.2 Construction of the complementation vectors

Bioinformatic analysis of the NGS data was carried out by Darren Soanes of the school of Biosciences, University of Exeter. A detail description of the strategy will be described in the section 5.3.1.

5.2.2 Construction of the complementation vectors

Complementation vectors for each T-DNA mutant were made using recombination-mediated PCR-directed plasmid construction *in vivo* in yeast (Oldenburg *et al.*, 1997), as described in Section 4.4.3. Primers were designed for the sequence information obtained from *M. oryzae* genome database (version 8) at the Broad Institute website (http://www.broadinstitute.org/annotation/genome/magnaporthe_grisea/MultiHome.html). Construction of the complementation vectors is explained in Figure 5.5.

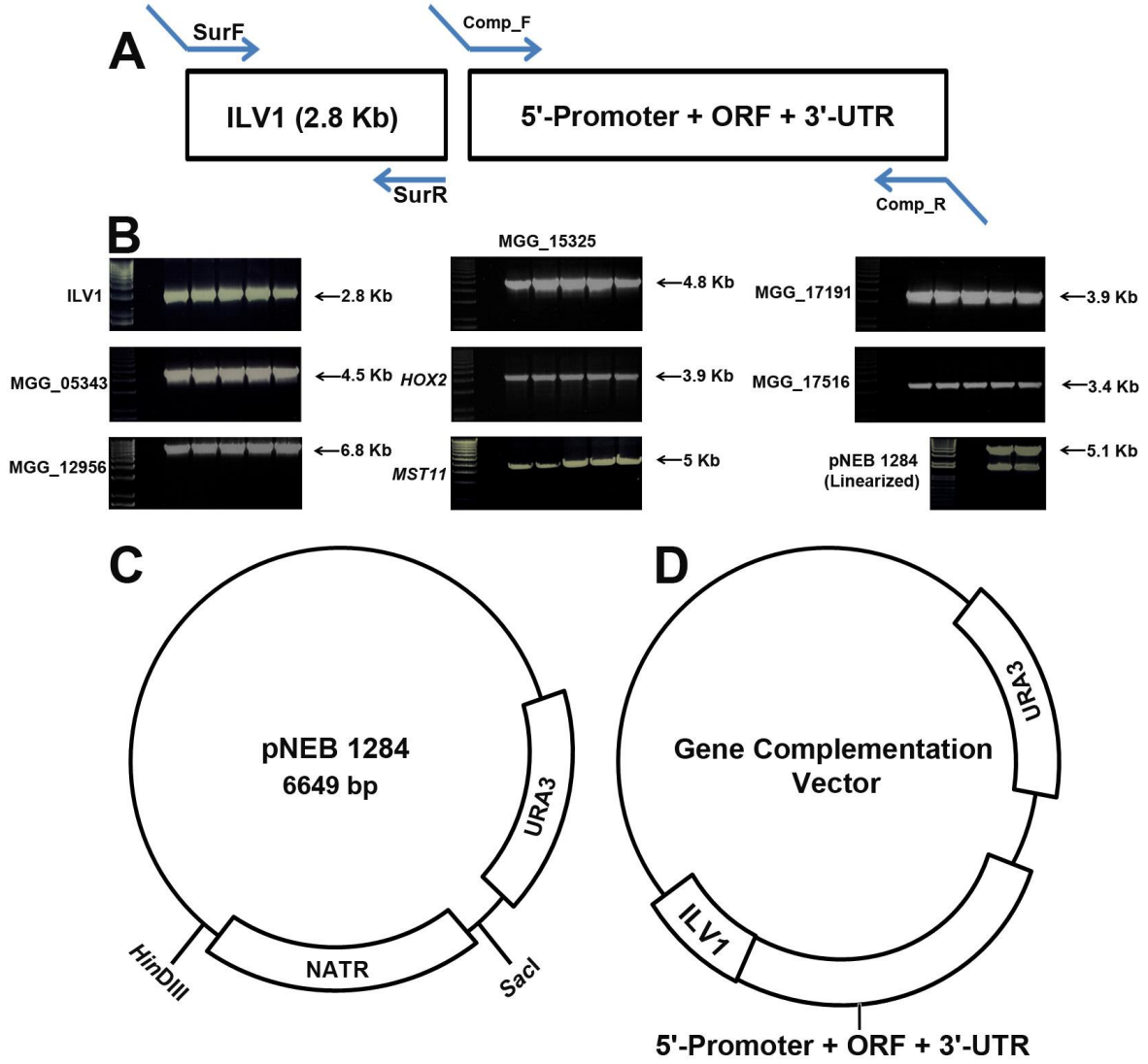

Figure 5.5: Construction of the complementation vectors. In order to complement selected mutants, complementation vectors were constructed using plasmid pNEB1284 by recombination-mediated PCR-directed plasmid construction *in vivo* in yeast (Oldenburg *et al.*, 1997). **A.** A 2.8 kb *ILV1* (sulfonylurea resistance gene cassette) and the identified gene to be complemented were amplified for each complementation vectors. For each gene at least 1.5 kb of 5' promoter and 0.5 kb of 3' UTR were amplified along with the ORFs. The primers used to amplify PCR products have overhangs corresponding to adjacent PCR fragments and with the plasmid **B.** Fragments amplified for the vector construction included a 2.8 kb *ILV1* gene cassette and 7 identified gene constructs (respective gene number shown). **C.** The plasmid was linearized by *Hin*dIII and *Sac*I double digestion. **D.** The linearized plasmid was mixed with PCR products and transformed into yeast under appropriate conditions. Complementation vectors were generated by homologous recombination between the PCR amplicons and the linearized plasmid.

Table 5.1: Primers used in the study to construct the complementation vectors.

Name	Sequence (5'→3')
Sur_F	AACTGTTGGGAAGGGCGATCGGTGCGGGCCCCAACGCCACAGTGCCCCA
Sur_R	CTGTTACTTTTTTCTGTTACTGTTGTCGCTGTGAGAGCATGCAATTCCCGT
MGG05343_CF	TGCACGGGAATTGCATGCTCTCACGTCGACCATACCGGTAGTGAAAGCCCA
MGG05343_ CR	TTCACACAGGAAACAGCTATGACCATGATTCAAGTCCGCCGCTACAATCAC
MGG15325_CF	TGCACGGGAATTGCATGCTCTCACGTCGACTTGATGCTGGCACACCCCGTT
MGG15325_ CR	TTCACACAGGAAACAGCTATGACCATGATTTGTGTTGATTGGCCCATCCCG
MGG00184_CF	TGCACGGGAATTGCATGCTCTCACGTCGACTCGCATCAACTCTTCTCGTGG
MGG00184_ CR	TTCACACAGGAAACAGCTATGACCATGATTAAAGCGAAATGCCACCTCCAG
MGG12956_CF	TGCACGGGAATTGCATGCTCTCACGTCGACTGAGGACAGCCACAGACACGG
MGG12956_CR	TTCACACAGGAAACAGCTATGACCATGATTCGGGAGTGGCGTTAAGCTGGA
MGG14847_CF	TGCACGGGAATTGCATGCTCTCACGTCGACGCTTTCGTCTCGTTCTTTGTCG
MGG14847_CR	TTCACACAGGAAACAGCTATGACCATGATTTCTGTTTTCGCTGGACCCTTCC
MGG17516_ CF	TGCACGGGAATTGCATGCTCTCACGTCGACAGGTAAGGAGAGGGAGAGAGG
MGG17516_ CR	TTCACACAGGAAACAGCTATGACCATGATTCTGCAAAGAGACGCCATAATC
MGG17191_CF	TGCACGGGAATTGCATGCTCTCACGTCGACGACTGTAGCGGCTCTTCTTGC
MGG17191_CR	TTCACACAGGAAACAGCTATGACCATGATTCAGGTGAAAAGAAGCGATGGT

5.2.3 Construction of the mutant allele of MGG_05343 and MGG_15325 (*IME2*)

A number of mutant alleles were generated for MGG_05343 and MGG_15325 (*IME2*) using recombination-mediated PCR-directed plasmid construction *in vivo* in yeast (Oldenburg *et al.*, 1997), as described in section 4.4.3.

5.2.3.1 Construction of the mutant alleles of MGG_15325

Three point mutations constructs and one null construct were made for MGG_15325 (*IME2*). A two-step fusion PCR was applied to generate point mutations in the TTY motif and also to replace the TTY motif with AAA. For amplification, a high-fidelity *Phusion* polymerase (NEB) was used. The mutant *ime2*^{T212A} allele was constructed by assembly of two 2.4 kb fragments carrying the T212A mutation. These two fragments were generated by PCR with the primer pairs IME2_MutF1/IME2_Thr212R1 and IME2_Thr212F2/IME2_MutR2. The 4.8 kb PCR fragment generated by the IME2_MutF1/IME2_MutR2 primer pair was used to construct the pNEB- *ime2*^{T212A} plasmid. Similarly, two other point mutation constructs, *ime2*^{T213A} and *ime2*^{Y214A} were generated. For *ime2*^{T213A} construct two primer pairs were, IME2_MutF1/IME2_Thr213R1 and IME2_Thr213F2/IME2_MutR2 and for *ime2*^{Y214A} construct two primers pairs were, IME2_MutF1/IME2_Tyr214R1 and IME2_Tyr214F2/IME2_MutR2. Each of the 4.8 kb fusion PCR fragment was used to construct the pNEB- *ime2*^{T213A} and pNEB- *ime2*^{Y214A} plasmid. The entire TTY motif was replaced by AAA in a similar manner by using the primer pairs, IME2_MutF1/IME2_MutR1 and IME2_MutF2/IME2_MutR2 for the 1st round products. The 4.8 kb fusion PCR product was used to construct the *ime2*$^{TTY\text{-}AAA}$ plasmid. Construction of the *ime2*$^{TTY\text{-}AAA}$ plasmid is explained in Figure 5.6.

Table 5.2: Primers used in the study to construct mutant alleles of MGG_15325.

Name	Sequence (5'→3')
Sur_F	AACTGTTGGGAAGGGCGATCGGTGCGGGCCCCAACGCCACAGTGCCCCA
Sur_R	CTGTTACTTTTTTCTGTTACTGTTGTCGCTGTGAGAGCATGCAATTCCCGT
IME2_MutF1	TGCACGGGAATTGCATGCTCTCACGTCGACTTGATGCTGGCACACCCCGTT
IME2_MutRI	CTCGTTGAGACGGCGGCGGCGTATGGGAGTTTCGAATGCGTTTCTCTTGCCA
IME2_MutF2	AACTCCCATACGCCGCCGCCGTCTCAACGAGATGGTACCGCGCACCCGAAGT
IME2_MutR2	TTCACACAGGAAACAGCTATGACCATGATTGCCATCCCTTCCCAGTAAAGGA
IME2_Thr212RI	CTCGTTGAGACGTAGGTGGCGTATGGGAGTTTCGAATGCGTTTCTCTTGCCA
IME2_Thr212F2	AACTCCCATACGCCACCTACGTCTCAACGAGATGGTACCGCGCACCCGAAGT
IME2_Thr213RI	CTCGTTGAGACGTAGGCCGTGTATGGGAGTTTCGAATGCGTTTCTCTTGCCA
IME2_Thr213F2	AACTCCCATACACGGCCTACGTCTCAACGAGATGGTACCGCGCACCCGAAT
IME2_Tyr214RI	CTCGTTGAGACGGCGGTCGTGTATGGGAGTTTCGAATGCGTTTCTCTTGCCA
IME2_Tyr214F2	AACTCCCATACACGACCGCCGTCTCAACGAGATGGTACCGCGCACCCGAAT

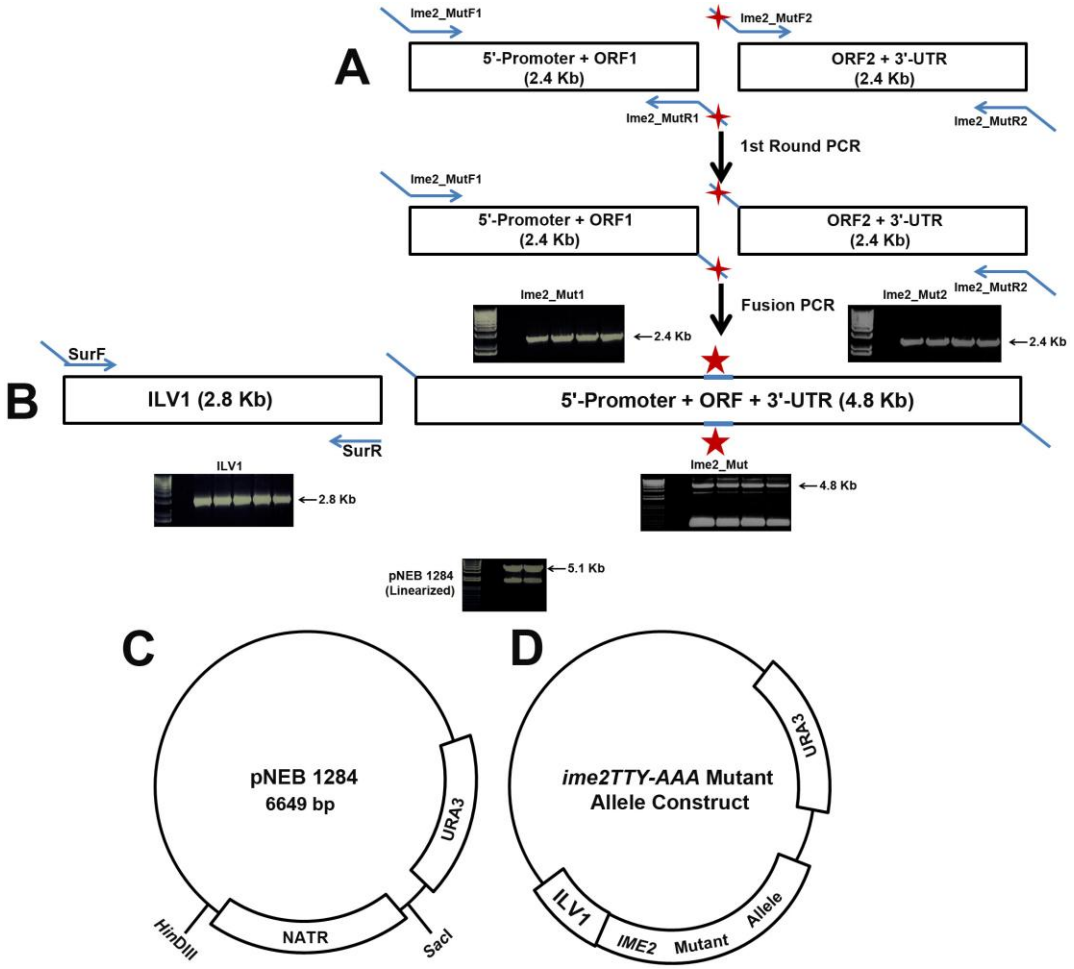

Figure 5.6: Construction of the mutant alleles of MGG_15325 of *M. oryzae*. In order to complement mutant M4874, complementation vectors were constructed containing mutant MGG_15325 (*IME2*). Point mutations were introduced in the TTY motif and the entire TTY motif was mutated by replacement with AAA. All the vectors were constructed using the plasmid pNEB1284 by recombination-mediated PCR-directed plasmid construction *in vivo* in yeast (Oldenburg *et al.*, 1997). The figure diagrammatically explains the construction process of the *ime2*$^{TTY\text{-}AAA}$ plasmid and three point mutation constructs were generated by similar strategy. **A.** The mutant *ime2*^{T212A} allele was constructed by the assembly of two 2.4 kb fragments carrying the TTY-AAA mutation. In the first round these were generated by PCR with primer pairs IME2_MutF1/IME2_MutR1 and IME2_MutF2/IME2_MutR2. Primer IME2_MutR1 and IME2_MutF2 contained the mutation in their overhangs. **B.** Two 2.4 kb fragments amplified in the first round were fused in the second round by PCR with IME2_MutF1/IME2_MutR2 primer pair and generated a 4.8 kb fusion PCR fragment containing the mutation. This 4.8 kb *ime2*$^{TTY\text{-}AAA}$ gene cassette (included 1.6 kb 5'- promoter, 2.5 kb *IME2* ORF and 0.7 kb 3'-terminator) was used to construct the pNEB- *ime2*^{T212A} plasmid. A 2.8 kb *ILV1* (sulfonylurea resistance gene cassette) was amplified as a selectable marker. The primers used to amplify PCR products have overhangs corresponding to adjacent PCR fragments and the plasmid. **C.** The plasmid was linearized by *Hin*dIII and *Sac*I enzyme double digestion. **D.** The linearized plasmid was mixed with the PCR products and transformed into yeast with appropriate conditions. Homologous recombination-mediated joining of PCR amplicons with the linearized plasmid generated the *ime2*$^{TTY\text{-}AAA}$ vector.

5.2.3.2 Construction of the mutant alleles of MGG_05343

For the Zn2C6 zinc finger encoding protein MGG_05343, a mutant allele was generated with complete replacement of the HRRK motif in the C6 zinc finger domain. A two-step fusion PCR method was applied to replace the HRRK motif with AAAA. For amplification, a high-fidelity *Phusion* DNA polymerase (NEB) was used. In this procedure (explained schematically in Figure 5.7), two fragments were amplified in the first step by using primers with appropriate overhangs and replacement of codons were designed in the overhangs. In the second step, forward primer of the first fragment and reverse primer of the second fragment were used to fuse two PCR fragments and generate mutant alleles of MGG_05343. In the first step the 1.65 kb fragment was generated by C6TF_MutF1/C6TF_MutR1 primer pairs and the 2.9 kb fragment was generated by C6TF_MutF2/C6TF_MutR2 primer pairs. They were then assembled in a 4.5 kb fusion PCR product (fused by amplification C6TF_MutF1/ C6TF_MutR2 primer pair) containing the AAAA motif instead of HRRK motif was used to construct the plasmid as explained in Figure 5.7.

Table 5.3: Primers used in the study to construct the mutant allele of MGG_05343.

Name	Sequence (5'→3')
Sur_F	AACTGTTGGGAAGGGCGATCGGTGCGGGCCCCAACGCCACAGTGCCCCA
Sur_R	CTGTTACTTTTTTCTGTTACTGTTGTCGCTGTGAGAGCATGCAATTCCCGT
C6TF_MutF1	TGCACGGGAATTGCATGCTCTCACGTCGACCATACCGGTAGTGAAAGCCCA
C6TF_MutRI	GCATTTGACGCCGCCGCCGCCGCAGGCGTCTGTTGGTTGCAATCACCAAGG
C6TF_MutF2	GACGCCTGCGGCGGCGGCGGCGTCAAATGCGACGGCATCAACCCGTGCAG
C6TF_MutR2	TTCACACAGGAAACAGCTATGACCATGATTCAAGTCCGCCGCTACAATCAC

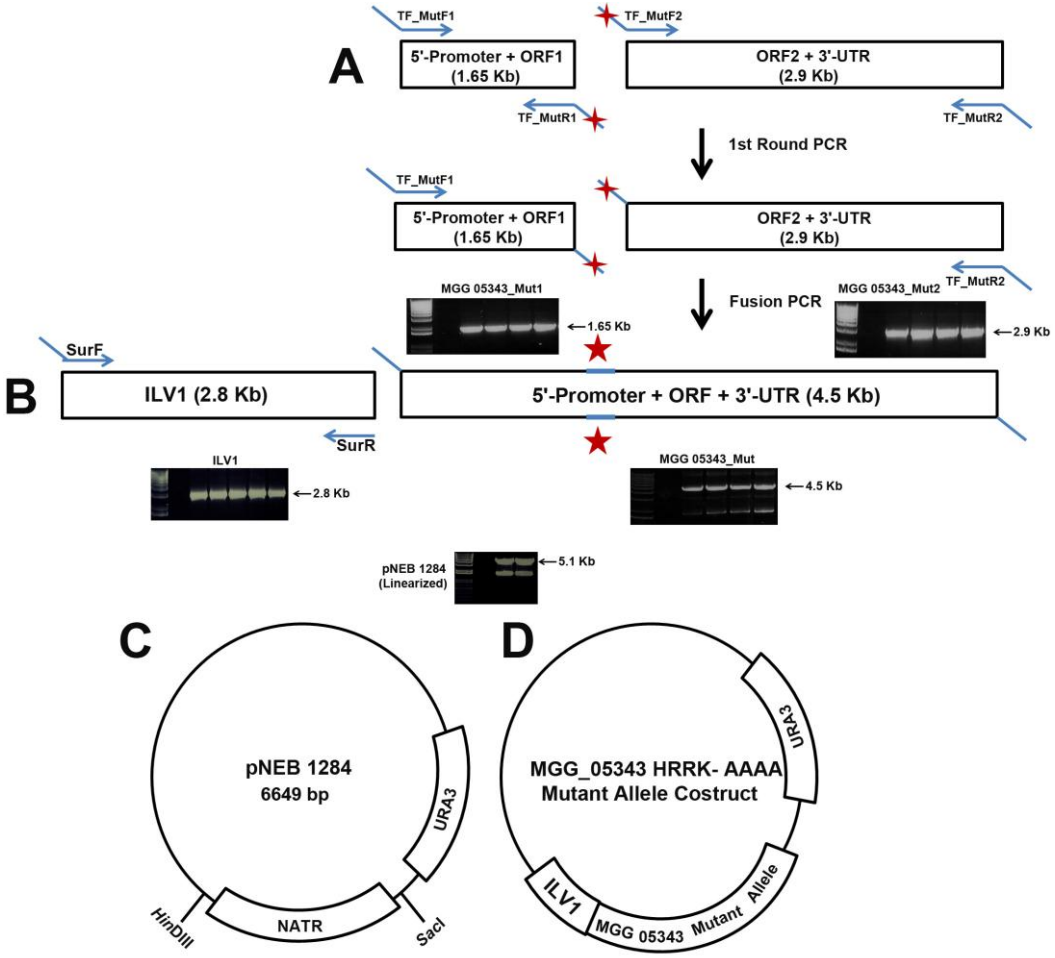

Figure 5.7: Construction of the mutant allele of MGG_05343 which putatively encodes a Zn2Cys6 binuclear cluster DNA-binding domain containing protein. In order to complement the mutant M2942, complementation vectors were constructed containing mutant alleles of MGG_05343. The entire HRRK motif replaced with AAAA. The vector was constructed using the plasmid pNEB1284 by recombination-mediated PCR-directed plasmid construction *in vivo* in yeast (Oldenburg *et al.*, 1997). The figure diagrammatically explains the construction process of HRRK-AAAA plasmid. **A.** The mutant allele was constructed by the assembly of two fragments carrying the HRRK-AAAA mutation. In the first round a 1.65 kb and a 2.9 kb fragment were generated by PCR with primer pairs C6TF_MutF1/C6TF_MutR1 and C6TF_MutF2/C6TF_MutR2 respectively. Primer C6TF_MutR1 and C6TF_MutR2 contained the mutation in their overhangs. **B.** Two fragments amplified in the first round were fused in the second round by PCR with C6TF_MutF1/C6TF_MutR2 primer pair and they generated a 4.5 kb fusion PCR fragment containing the mutation. This 4.5 kb mutant gene cassette (included 1.5 kb 5'- promoter, 2.5 kb MGG_05343 ORF and 0.5 kb 3'-terminator) of MGG_05343 was used to construct the pNEB- HRRK-AAAA plasmid. A 2.8 kb *ILV1* (sulfonylurea resistance gene cassette) was amplified as a selectable marker. The primers used to amplify PCR products have overhangs corresponding to adjacent PCR fragments and the plasmid. **C.** The plasmid was linearized by *Hin*dIII and *Sac*I enzyme double digestion. **D.** The linearized plasmid was mixed with PCR products and transformed in yeast with appropriate conditions. The vector containing the mutant gene construct of MGG_05343 was generated by homologous recombination which joins the PCR amplicons with the vector.

5.2.4 Targeted deletion of C6 zinc finger transcription factor MGG_05343

The split marker gene deletion method was used to carry out a targeted deletion of MGG_05343 (Catlett *et al.*, 2003). This is a rapid PCR-based method that overcomes the need for cloning s in order to delete targeted gene sequences within the genome. The method is explained diagrammatically in Figure 5.8 and involves two rounds of PCR. Six gene-specific primers and four selectable marker-specific primers were used for each gene deletion (Table 5.4). In the first round of PCR, a 1 kb fragment of the 5' and 3' flanking sequence of the gene coding region (named LF and RF respectively) was amplified using C6TF_UF/ C6TF_m13F and C6TF _DR/ C6TF _m13R primers in combination, from genomic DNA of wild-type Guy11 (Figure 5.8A). C6TF_m13F and C6TF _m13R primers were designed with additional 5´ sequences, corresponding to the M13F/M13R primers. This additional sequence enabled fusion PCR to be carried out in the second round. In a parallel reaction, the selectable marker (the hygromycin resistance gene in this case) was amplified in two unequal halves using M13F/HySplit and M13R/YgSplit primer pairs from the hygromycin resistance gene cassette [cloned in pBluescript plasmid (Stratagene)](Figure 5.8A) (Carroll *et al*., 1994; Sweigard *et al.*, 1997). These two products named HY (1142 bp) and YG (789 bp) have an overlapping sequence of 464 bp. The *HPH* gene, which encodes for hygromycin phosphotranferase confers resistance to hygromycin B (Carroll *et al*., 1994). In the second round of PCR, each flank was fused with one half of the selectable marker (LF/HY and RF/YG) using primers C6TF_NstUF / HYSplit and C6TF_NstDR / YGSplit (Figure 5.8B). Nested primers from LF and RF were used for efficient amplification on the 2nd round. The resulting fusion products (Figure 5.8B) were gel purified and used in equal amounts to transform the Δ*ku*70 strain of *M. Oryzae* (Kershaw & Talbot, 2009)**.** Homologous recombination between the overlapping regions of the selectable marker and chromosomal DNA results in targeted deletion of the gene, as shown in Figure 5.8C. (Catlett *et al.*, 2003).

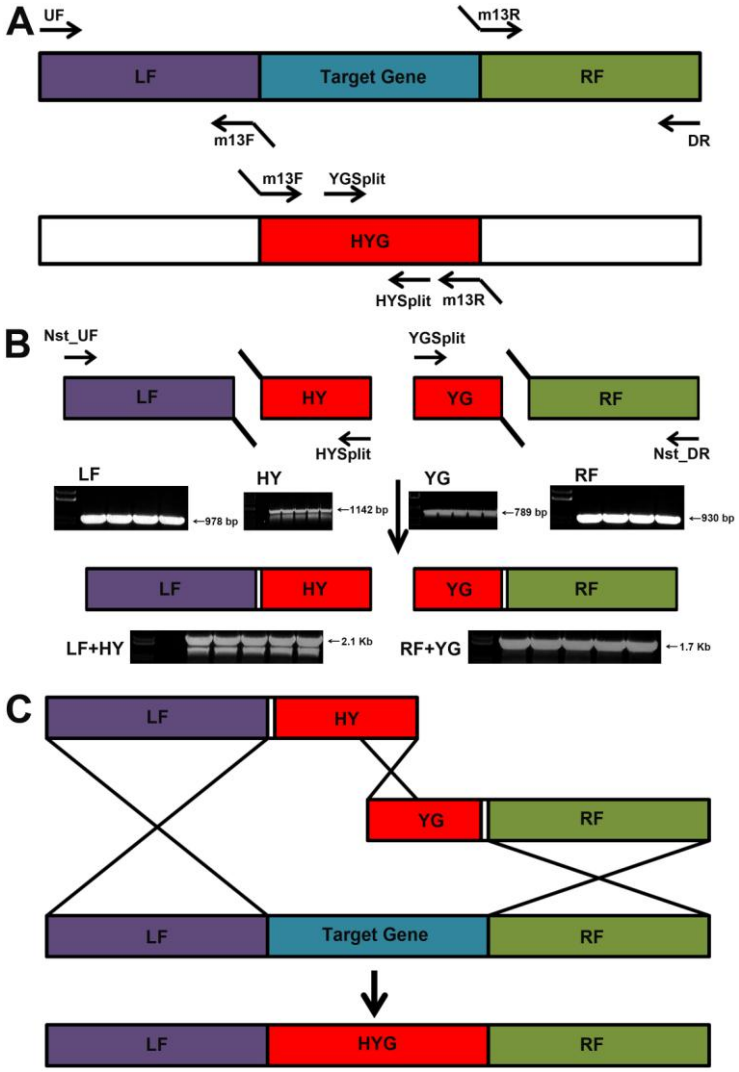

Figure 5.8: A schematic representation of the targeted deletion of C6 zinc finger transcription factor MGG_05343 by the split-marker deletion method. A. In the first round of PCR, ~1 kb of the 5' and 3' flanks of the MGG_05343 open reading frame (ORF) was amplified with primers C6TF_UF/ C6TF_m13F and C6TF_DR/ C6TF_m13R. In parallel, as selectable marker, hygromycin resistance gene (*HPH*) was amplified in two overlapping halves using primers M13F/HYSplit and M13R/YGSplit. The primers for 5' and 3' inner flanks were designed to include an extension complementary to the tail of the fragments of selectable marker. Therefore, primers C6TF_m13F and C6TF_m13R contained complementary sequences at their 5´ end corresponding to M13F and M13R respectively. **B**. In a second round of PCR, the flanks of (LF and RF) were fused with overlapping selectable marker fragments HY and YG respectively. In the fusion PCR, nested primers from the flanks were used to fuse each half of the selectable marker with flanks (LF and RF). C6TF_NstUF / HYSplit primer pairs fused LF with HY and C6TF_NstDR / YGSplit primer pair fused YG with RF. All the PCR amplicons are shown and their sizes are indicated. **C**. The two fusion PCR products are used in equimolar amount to transform the Δ*ku*70 strain of *M. oryzae*. Homologous recombination between the flanking regions and chromosomal DNA and between the overlapping regions of the hygromycin phosphotranferase cassette resulted in a targeted deletion of the gene (Catlett *et al.*, 2003). This schematic diagram is not drawn to scale. LF= Left Flank, RF= Right Flank.

Table 5.4: Primers used to carry out targeted gene deletion of MGG_05343.

Name	Sequence (5'→3')
C6TF_UF	ATACCACGTTCATGTCGTCCC
C6TF _NstUF	GTCCCATCCAATTTACGGTTGTG
C6TF_m13F	GTCGTGACTGGGAAAACCCTGGCGGCTAAAACGATCGGTGCCTTG
C6TF_m13R	TCCTGTGTGAAATTGTTATCCGCTGGTCAAGGTCTCCTCGAAGC
C6TF_DR	ATTGCTTGCAGGGCTCCCGA
C6TF _NstDR	GGGCTCCCGACCTACTAACTA
M13F	CGCCAGGGTTTTCCCAGTCACGAC
M13R	AGCGGATAACAATTTCACACAGGA
HYSplit	GGATGCCTCCGCTCGAAGTA
YGSplit	CGTTGCAAGACCTGCCTGAA

5.3 Results

5.3.1 Identification of T-DNA tagged loci from Illumina paired end sequence reads

Genomic DNA from 8 selected non-pathogenic T-DNA mutants was pooled and sequenced using Illumina HiSeq2000 based NGS. We then identified sequences that contained either LB or RB sequence of T-DNA and at least 15 bases of genomic DNA sequence of *M. oryzae*. The program that was used to search for reads containing LB or RB sequences was Bowtie 0.12.7 (Langmead *et al.*, 2009). A sequence of 20 bp from LB and 20 bp from RB was used to search expected reads (up to two-base mismatch allowed). Custom perl scripts were then used to identify reads containing at least 15 bp of genomic DNA sequence and to trim away the T-DNA sequence. Trimmed reads were assembled using the programme Velvet (version 1.1) (Zerbino and Birney, 2008). BLASTN was used to identify the sequence matches from *M. oryzae* genome sequence (version 8) at the Broad Institute genome sequence database and T-DNA insertions were positioned on the basis of sequence information.

Among 8 mutants both of the RB and LB flanks were identified unequivocally for 3 insertions. The RB flanks were identified for 3 additional insertions and a LB flank was identified for a single insertion. Therefore, 7 insertion sites were found in the pooled DNA sequence in total. Six T-DNA insertions were found within the ORFs of a corresponding locus while and one integration was found within the promoter of the locus. Table 5.5 summarizes each identified locus, the types of insertions and the respective T-DNA border sequence from which the flanks were retrieved.

Table 5.5: Summary of the T-DNA tagged loci identified by NGS strategy. On the basis of NGS data, a systemic PCR analysis was carried out to assign an identified T-DNA tagged locus to each mutant. The Table summarizes each identified locus in each mutant where T-DNA was inserted. Six out of seven confirmed T-DNA insertions occurred within an ORF. Both LB and RB flanking sequences were identified for 3 insertions. Only RB flanks were identified for 3 insertions and only LB flank was identified for a single insertion. All of the seven different insertions were validated by PCR (Figure 5.9) and orientations of the T-DNA in each locus are shown schematically (Figure 5.10).

Mutant	Locus where insertion was identified	Insertion Type	Flank Retrieved
M48	MGG_17516 (Unknown)	ORF	LB & RB
M1054	MGG_17909 (*ATG3*)	ORF	LB & RB
M1879	MGG_16734 (*ATG2*)	ORF	RB
M1880	MGG_17191 (Unknown)	ORF	RB
M2048	MGG_12956 (Unknown)	ORF	RB
M2942	MGG_05343 (Unknown)	ORF	LB & RB
M4874	MGG_15325 (Unknown)	Promoter	LB

5.3.2 PCR confirmation of the T-DNA tagged loci

A systemic PCR analysis was carried out to assign an identified T-DNA tagged locus to each mutant. To confirm the T-DNA insertion in the corresponding locus by PCR, primers were designed both from the T-DNA LB and RB sequences. Using the retrieved flanking sequences, T-DNA insertions were positioned and a primer pair designed for each insertion. A primer was designed from either LB or RB of T-DNA and another one was designed from corresponding retrieved flanking sequence. For the entire RB flanking sequences, reverse primers were designed from the retrieved genomic DNA sequences and forward primer was designed from the RB sequences (RBCPF). For the entire LB flanking sequences, forward primers were designed from the retrieved genomic DNA sequences and reverse primer was designed from the LB (LBCPR). Primers were designed to amplify a fragment of ~1 kb containing T-DNA sequence and retrieved *M. oryzae* genomic DNA sequence (Table 5.6). For unbiased elucidation of the T-DNA flanks from genomic DNA, all of the 8 selected mutants were used for the amplification from each set of primer pairs. PCR was performed following the standard PCR protocol described in section 2.3.2.3. The results of this systemic PCR analysis are shown in Figure 5.9.

PCR results confirmed T-DNA insertions in each mutant except mutant M2867. Truncation of the T-DNA border sequence or genome rearrangement in the insertion site can be attributed to failiure to recover T-DNA flanks in mutant M2867. As a result, in case of M2867, PCR failed to provide evidence for any T-DNA flanking sequence. Systematic PCR analysis however validated the NGS data. Based on the NGS identified flanking sequences we then constructed the maps of T-DNA insertions in the tagged loci. Figure 5.10 show the orientation of inserted T-DNA in each locus in the respective mutants.

Table 5.6: Primers used in the study confirm the T-DNA insertion in mutants by PCR.

Name	Sequence (5'→3')
RBCPF	ACCCTGGTGAACCGCATCGAG
ATG3_CPR	GATCAGGAGGTTGCCATTCGGG
ATG2_CPR	ATCGACCTCCTGAATCTTGGCG
MGG17516_CPR	CGGACGGCAGACAAGCAGAGA
MGG05343_CPR	CCTACGCACGCCATACAACGC
MGG12956_CPR	GAAGCCCCGAGGCCAAAATCAT
MGG17191_CPR	GCGAGTGGCTGCCTTGATTGAT
ATG3_CPF	CCACTCGAGGGGTTCGATACG
MGG05343_CPF	GTTGTTTCGAGCATCAGCCAGC
MGG00183_CPF	AATCAACGGCCAAAAGTCGCGG
MGG15325_CPF	AAGCGGGTTCAACGGGGTGTG
LBCPR	ATGCTTTGGGCCGAGGACTGC

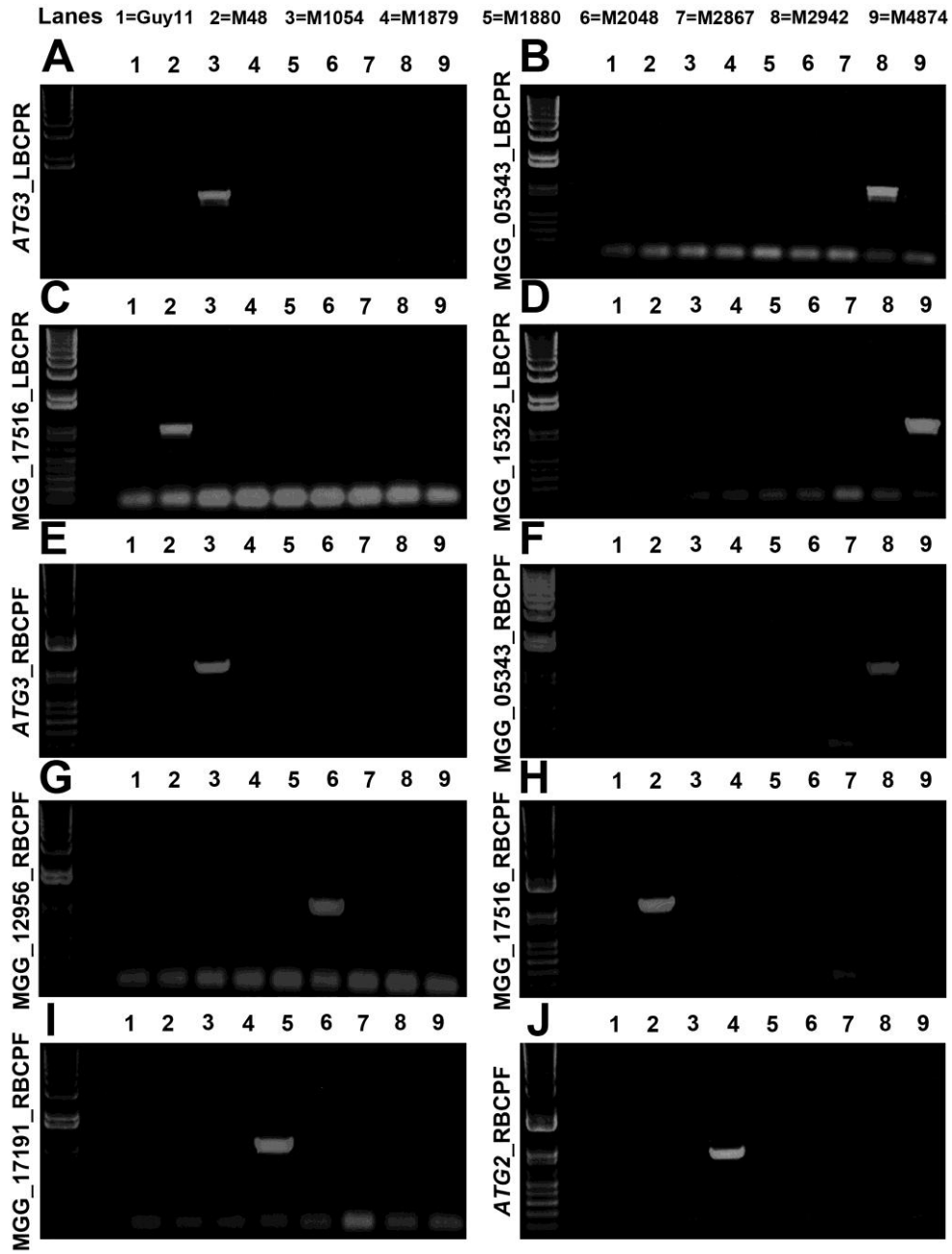

Figure 5.9: Confirmation of the T-DNA tagged loci by PCR. To confirm the T-DNA insertions by systemic PCR analysis, primers were designed both from the T-DNA LB and RB sequences. Identified flanking sequences were used to position the T-DNA insertions and a primer was designed for each insertion. For the entire RB flanking sequences, reverse primers were designed and a forward primer was designed from the RB (RBCPF). For the entire LB flanking sequences, forward primers were designed and a reverse primer was designed from the LB (LBCPR). Primers were designed to amplify a fragment of ~ 1Kb containing T-DNA sequence and retrieved *M. oryzae* genomic DNA sequence. To elucidate the T-DNA flanks in an unbiased manner, all of the 8 selected mutant genomic DNA was used for the amplification from each set of primer pair. Each gel image **(A-J)** shows a ~1 kb band amplified in only one lane and the number of the lane represent the mutant which was positive for that particular primer pair. ID of the locus and type of the border primer (RBCPF or LBCPR) used are shown on the left of each gel image.

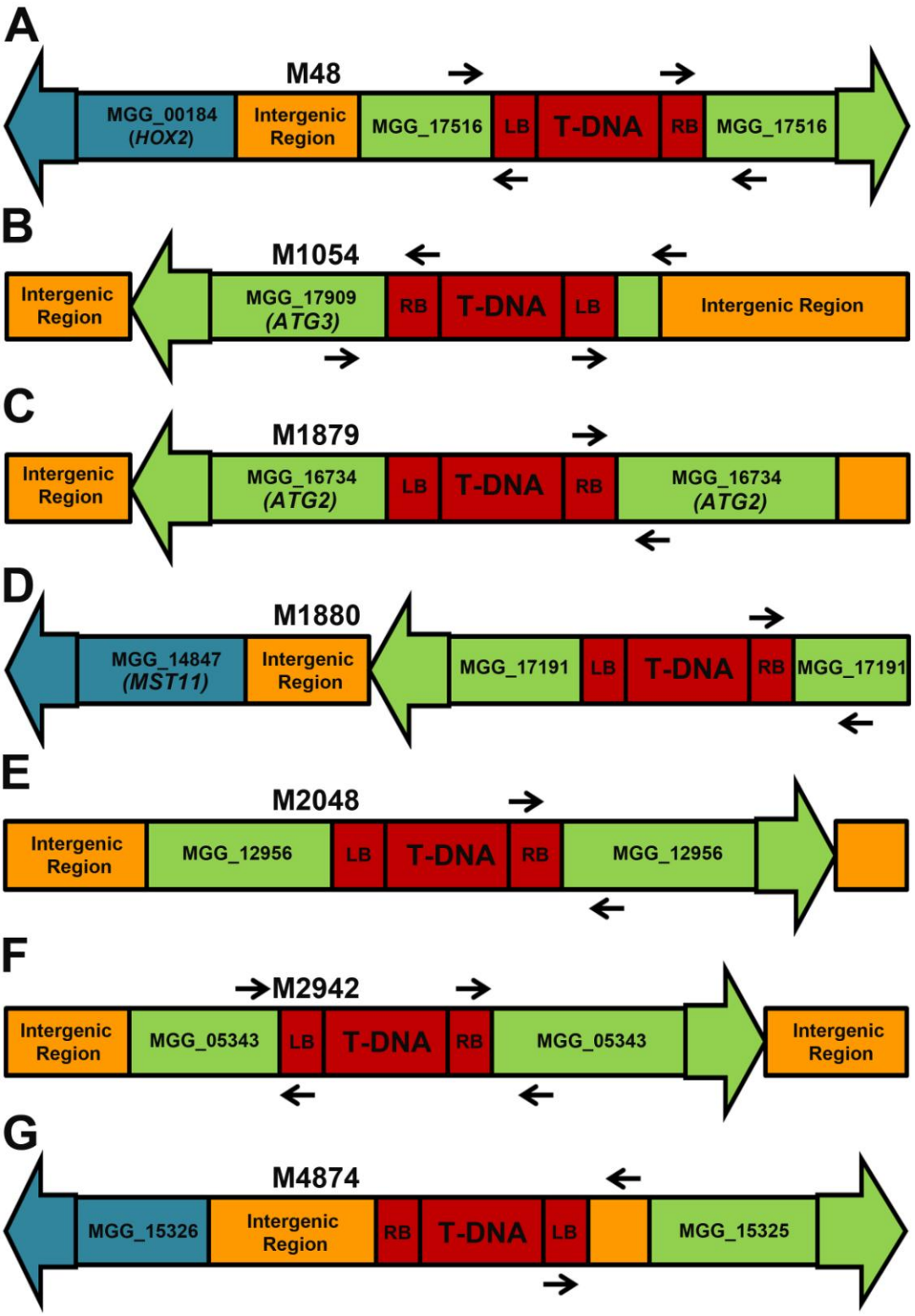

Figure 5.10: T-DNA insertion maps predicted from NGS data. A systemic PCR analysis allowed us to validate the NGS retrieved T-DNA flanking sequences and identify the putative tagged locus in each mutant. We constructed the map of each locus where orientation of the integrated T-DNA is shown. **A-G.** Images show the T-DNA tagged locus in each mutant and arrows indicate the position of primers designed to validate the insertion by PCR. These maps were not drawn to scale.

5.3.3 Expression profiles of the putative identified genes during appressorium development of *Magnaporthe oryzae*

To gain clues to the likely function of each gene potentially corresponding to a T-DNA tagged insertion mutant, we looked at identified gene expression profiles during appressorium development. Out of 8 selected mutants, we mapped 7 T-DNA insertions and only M2867 could not be attributed any T-DNA insertion from the PCR. From PCR analysis 6 mutants were found to have T-DNA insertions in the ORF of the putative tagged loci (M48, M1054, M1879, M1880, M2048 and M2942). Only M4874 showed a promoter insertion. Among the genes two encoded hypothetical proteins (M17516 and M17191) (Figure 5.10). Therefore, we also took into consideration genes downstream that could potentially be affected by the T-DNA insertion. Considering these facts, we constructed an expression profile of the putative genes likely to be disrupted by the T-DNA insertions in selected mutants. The profile was constructed from a database generated during a previous study on global patterns of gene expression during appressorium development by *M. oryzae*. (Soanes *et al.*, 2012). The HT-SuperSAGE data described in this study can be accessed from a publicly accessible online database (http://cogeme.ex.ac.uk/supersage/), as part of the suite of COGEME databases. Entry into the database of any *M. oryzae* gene ID will provide HT-SuperSAGE data for the time course of appressorium development. This enriched repository allows evaluation of the expression profiles of more than 96% of the *M. oryzae* genome (10,591 genes) during infection-related development (Soanes *et al.*, 2012). Therefore, this provides the most comprehensive coverage of the transcriptome in *M. oryzae* published studies. HT-SuperSAGE results in longer 26 base tags generated from sample cDNA and sequencing by NGS. When sequence tags are aligned with the reference genome, tags are matched to gene sequences without ambiguity (Matsumura *et al.*, 2010). The number of tags from each gene is calculated to measure expression of gene. In this study, total RNA was extracted from conidia

germinated on a hydrophobic glass slide for 4, 6, 8, 14 and 16 h, respectively (Figure 5.10). HT-SuperSAGE measured transcript abundance, representing individual genes at each time point (Soanes *et al.*, 2012). These time points can be broadly dissected into two stages; an appressorium developmental phase from 4 to 8 h and the appressorium maturation phase from 8 to 16 h.

We constructed an expression profile including 9 genes which were likely to be affected by T-DNA insertions in the corresponding mutants. MGG_17516 is a hypothetical gene containing a T-DNA insertion within coding region and is flanked by MGG_00184 which is the *HOX2* locus. MGG_14847 is the MAPKK, *MST11* gene in *M. oryzae* and this flanks another hypothetical gene MGG_17191 which showed T-DNA insertion within the ORF. MGG_05343 is a putative novel transcription regulator and MGG_12956 is a putative unknown signalling protein, and both of them were found to be disrupted by T-DNA insertions within ORFs. MGG_15325 is a putative novel kinase which was tagged by T-DNA insertion within its upstream promoter. Interestingly, two autophagy genes, MGG_17909 (*ATG3*) and MGG_16734 (*ATG2*) were tagged by T-DNA insertions in the coding regions. From the expression profile, data we found that two genes MGG_17516 and MGG_17191 are down-regulated throughout the time course of appressorium development. MGG_14847 and MGG_05343 showed up-regulation throughout the time course. Two of the genes, MGG_15325 and MGG_12956 showed a similar pattern of up-regulation during appressorium development but down-regulation during appressorium maturation. The two autophagy genes, *ATG2* (MGG_16734) and *ATG3* (MGG_17909) showed up-regulation during appressorium maturation when conidia undergo autophagic cell death (Wilson and Talbot, 2009). MGG_00184 was down-regulated throughout all the time points (Kim *et al.*, 2009).

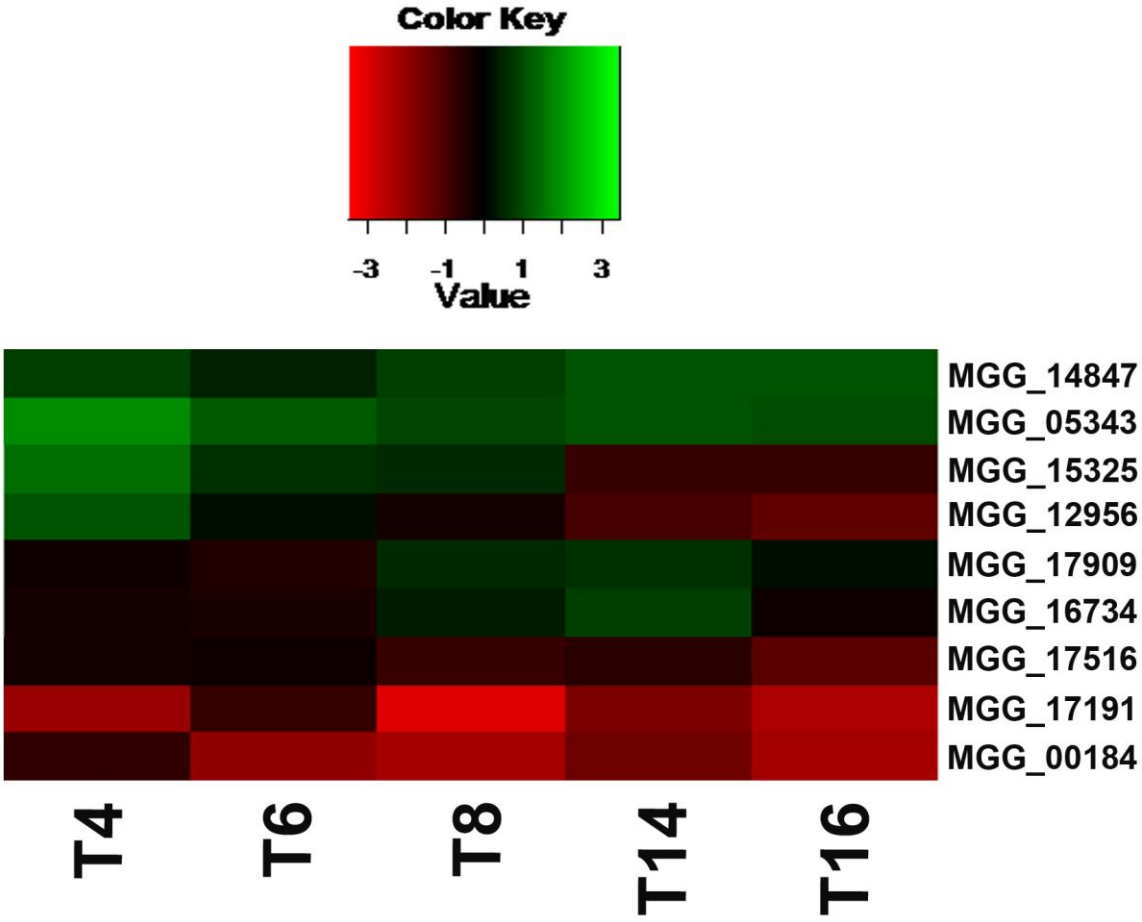

Figure 5.11: Heatmap showing relative levels of transcript abundance during the time course of appressorium development. This Heatmap shows transcript levels of genes during a time course of appressorium development. The genes correspond to these assigned to each T-DNA insertion. Levels of expression are represented as moderated $\log_2$ ratio of transcript abundance compared to mycelium grown in complete medium. Values are from 4 h (T4) to 16 h (T16) after conidia were incubated on a hydrophobic surface. MGG_14847 is the MAPKK, *MST11* gene in *M. oryzae* and this flanks the hypothetical gene MGG_17191 which showed T-DNA insertion within the coding region. MGG_17516 is a hypothetical gene containing a T-DNA insertion within the ORF and is flanked by MGG_00184 which is the *HOX2* gene. MGG_05343 is a putative novel transcription regulator and MGG_12956 is a putative unknown signalling protein, and both of them were found to be disrupted by T-DNA insertions in ORFs. Two autophagic genes, MGG_17909 (*ATG3*) and MGG_16734 (*ATG2*) were tagged by T-DNA insertions in the coding regions. MGG_15325 is a putative novel kinase which was tagged by T-DNA insertion in its upstream promoter. [The HT-SuperSAGE data was accessed from a publicly accessible online database (http://cogeme.ex.ac.uk/supersage/), as part of the suite of COGEME databases]

5.3.4 Mapping of T-DNA insertions by RFLP analysis

NGS retrieved T-DNA flanks from 7 of the mutants were detected and these were validated by RFLP analysis of the respective locus following PCR confirmation. RFLP at *ATG3* locus in M1054 is shown in the Section 4.4.1. In order to confirm and map the T-DNA in corresponding locus, a systemic RFLP analysis was carried out for remaining five mutants (Figure 5.11-5.16). RFLP analysis provided a rigorous confirmation of the sites of T-DNA insertion at each identified locus.

5.3.4.1 RFLP analysis to confirm the T-DNA insertion in the MGG_17516 locus

In mutant M48, T-DNA was found to be inserted within a gene that encoded a hypothetical protein of unknown function. In order to map the T-DNA insertion in the MGG_17516 locus of mutant M48 by Southern hybridization analysis, a restriction map of the 21.1 kb genomic region (1.1 kb MGG_17516 ORF in the middle and 10 kb genomic DNA sequence from 5' and 3' flanks) for wild-type Guy11 was constructed (Figure 5.11A). We also constructed a restriction map of the same genomic region containing the T-DNA insertion within the MGG_17516 locus according to NGS data and subsequent PCR result (Figure 5.12B). By comparing the two restriction maps, we selected four different restriction enzymes to use to carry out RFLP analysis. These enzymes were chosen because they were predicted to produce a differential restriction fragment pattern for Guy11 and mutant M48. We chose *Eco*RI, *Hin*dIII, *Sph*I and *Xba*I. The size of the DNA fragments expected for both Guy11 and M48 are summarized in Table 5.7. Genomic DNA of Guy11 and M48 was digested with the selected enzymes, fractionated by gel electrophoresis, blotted and probed with a ~1 kb 5' flanking gene fragment amplified by PCR. By comparing the band sizes of wild-type Guy11 (Figure 5.12C) and mutant M48 (Figure 5.12D), restriction fragment length polymorphisms (RFLP) were found at the MGG_17516 locus and confirmed the predicted T-DNA insertion. The T-DNA

insertion in M48 was mapped by means of *Eco*RI, *Hin*dIII, *Sph*I and *Xba*I digests. As predicted, all of those digestions resulted in distinct restriction fragments in M48 compared to Guy11. Restriction fragment length differences are precisely shown by arrows and the obtained fragment sizes matched the expected sizes (Table 5.7). Therefore, we can conclude that M48 contains a T-DNA insertion in the MGG_17516 locus and this ultimately validated both the PCR result (Figure 5.8C & H) and mapping of the loci based on NGS data (Figure 5.9A).

Table 5.7: Expected sizes of restriction fragments after digestion with selected enzymes for RFLP analysis at MGG_17516 locus in mutant M48. Four enzymes *Eco*RI, *Hin*dIII, *Sph*I and *Xba*I were selected for RFLP analysis at MGG_17516 locus in mutant M48. For Guy11, the restriction map was constructed by including 10 kb upstream and downstream genomic DNA sequence of the MGG_17516 ORF. For mutant M48, restriction map of the locus was constructed on the basis of PCR validated retrieved NGS data. All of the chosen enzymes were predicted to generate polymorphic restriction fragment in both single and double digests due to a T-DNA insertion in the locus.

Enzyme	Fragment Size (kb)	
	Guy11	M48
***Eco*RI**	>13.6	6.4
***Hin*dIII**	5.6	7.9
***Sph*I**	6.7	2.3
***Xba*I**	12.5	10.9
***Eco*RI + *Hin*dIII**	4.2	6.4
***Eco*RI + *Sph*I**	6.7	2.3
***Eco*RI + *Xba*I**	8.0	6.4
***Hin*dIII + *Sph*I**	2.5	2.3
***Hin*dIII + *Xba*I**	5.6	7.8
***Sph*I + *Xba*I**	6.3	2.3

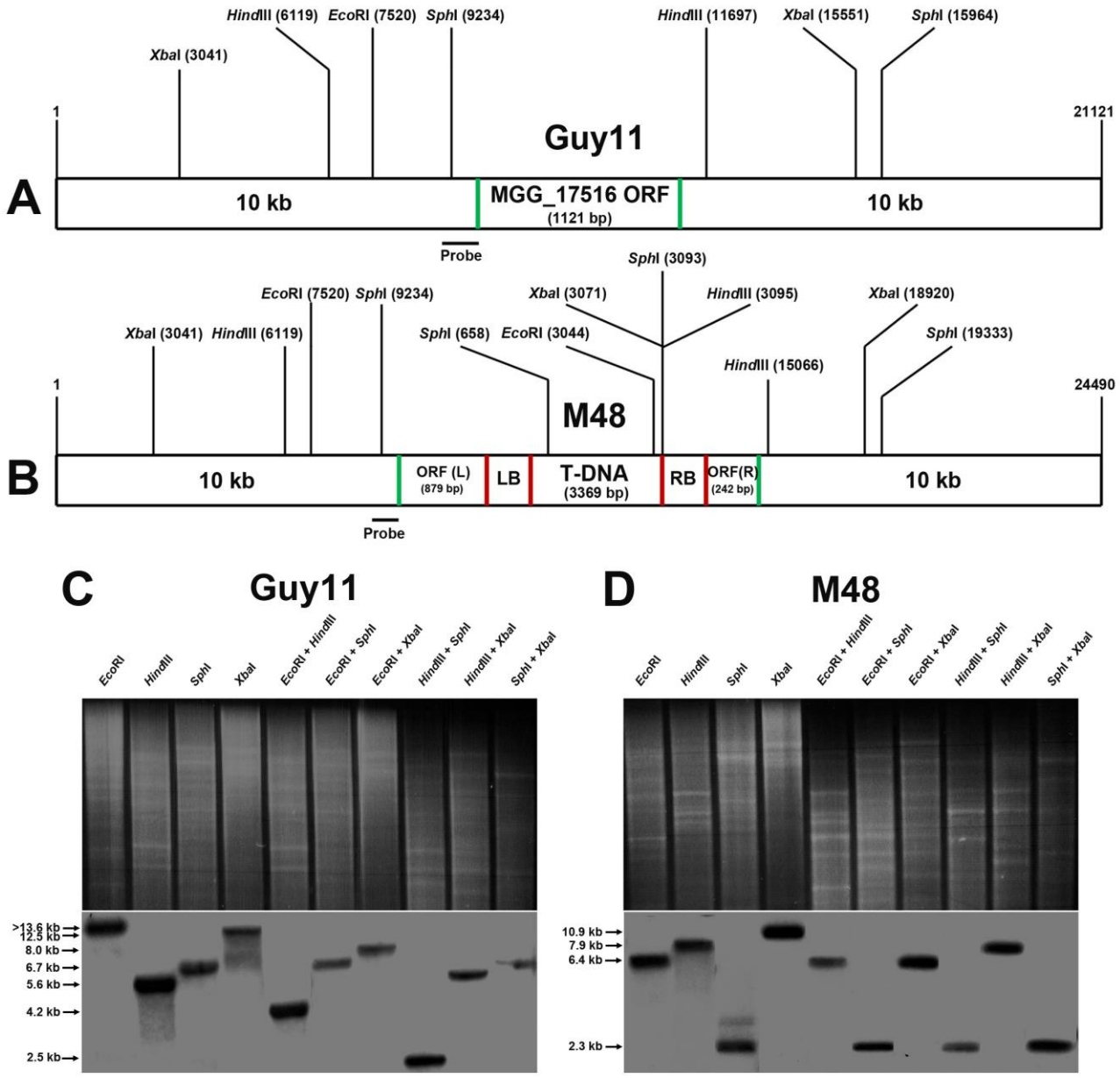

Figure 5.12: Confirmation of a T-DNA insertion in the MGG_17516 locus by RFLP analysis. A. A schematic representation of the restriction map of *M. oryzae* MGG_17516 locus. Positions of the restriction sites are indicated by nucleotide numbers in a 21.1 kb genomic DNA sequence. **B.** Restriction map of the *M. oryzae* MGG_17516 locus in mutant M48. NGS data showed a T-DNA insertion in the MGG_17516 gene of the mutant M48 and the map was constructed according to the orientation of retrieved flank sequence from NGS. Positions of the restriction sites are indicated by numbers in a 24.5 kb genomic DNA sequence. Positions of the T-DNA restriction sites are shown as distance from the left border. **C. & D.** Four enzymes *Eco*RI, *Hin*dIII, *Sph*I and *Xba*I were selected for RFLP analysis at MGG_17516 locus in wild-type Guy11 and mutant M48. Images show DNA gel blot analysis. Genomic DNA was digested, fractionated by gel electrophoresis, blotted and probed with a ~1 kb 5' flanking gene fragment amplified by PCR. Wild-type Guy11 **(C)** and mutant M48 **(D)** showed polymorphic restriction fragments from single and double digestions of the selected restriction enzymes. Fragment sizes are precisely shown by arrows.

5.3.4.2 RFLP analysis to confirm the T-DNA insertion in the MGG_17191 locus

In mutant M1880, T-DNA was inserted within a hypothetical gene MGG_17191. To map the T-DNA insertion in this locus of mutant M1880 by Southern blot hybridization analysis, a restriction map of the 21.5 kb genomic region (1.5 kb MGG_17191 ORF in the middle and 10 kb genomic DNA sequence from 5' and 3' flanks) for wild-type Guy11 was constructed (Figure 5.13A). We also constructed a restriction map of the same genomic region containing the T-DNA insertion in M1880 (Figure 5.13B). By comparing the two restriction maps, we selected four different restriction enzymes to carry out RFLP analysis. These enzymes were chosen because they were predicted to produce a differential banding pattern for Guy11 and mutant M1880. We chose *Hin*dIII, *Sac*I, *Sac*II and *Xho*I. The size of the DNA fragments that was expected for both Guy11 and M1880 are summarized in Table 5.8. Genomic DNA of Guy11 and M1880 was digested with the selected enzymes, fractionated by gel electrophoresis, blotted and probed with a ~1 kb 5' flanking gene fragment amplified by PCR. A comparison between the restriction fragment sizes of wild-type Guy11 (Figure 5.13C) and mutant M1880 (Figure 5.13D) revealed restriction fragment length polymorphism (RFLP) at the MGG_17191 locus and consequently confirmed the predicted T-DNA insertion. As expected, all of those digestions resulted in distinct restriction fragments in M1880, compared to Guy11. Restriction fragment length differences are precisely shown by arrows and the obtained restriction fragment sizes matched the predicted sizes (Table 5.8). Therefore, we conclude that M1880 contains a T-DNA insertion at the MGG_17191 locus that validates mapping of the T-DNA based on NGS data (Figure 5.10D) and also the PCR result (Figure 5.9I).

Table 5.8: Expected sizes of restriction fragments after digestion with selected enzymes used for RFLP analysis at MGG_17191 locus in mutant M1880. Four enzymes, *Hin*dIII, *Sac*I, *Sac*II and *Xho*I were selected for RFLP analysis at MGG_17191 locus in mutant M1880. For Guy11, the restriction map was constructed to include 10 kb upstream and downstream genomic DNA sequence of the MGG_17191 locus. For mutant M1880, a restriction map of the locus was constructed on the basis of PCR-validated retrieved NGS data. All of the chosen enzymes were predicted to generate polymorphic restriction fragment in both single and double digests due to a T-DNA insertion in the locus.

Enzyme	Fragment Size (kb)	
	Guy11	M1880
***Hin*dIII**	4.0	6.5
***Sac*I**	6.5	8.4
***Sac*II**	3.4	6.8
***Xho*I**	6.4	5.8
***Hin*dIII + *Sac*I**	4.0	6.5
***Hin*dIII + *Sac*II**	3.4	5.9
***Hin*dIII + *Xho*I**	4.0	3.6
***Sac*I + *Sac*II**	3.4	5.9
***Sac*I + *Xho*I**	6.0	5.5
***Sac*II + *Xho*I**	3.4	2.8

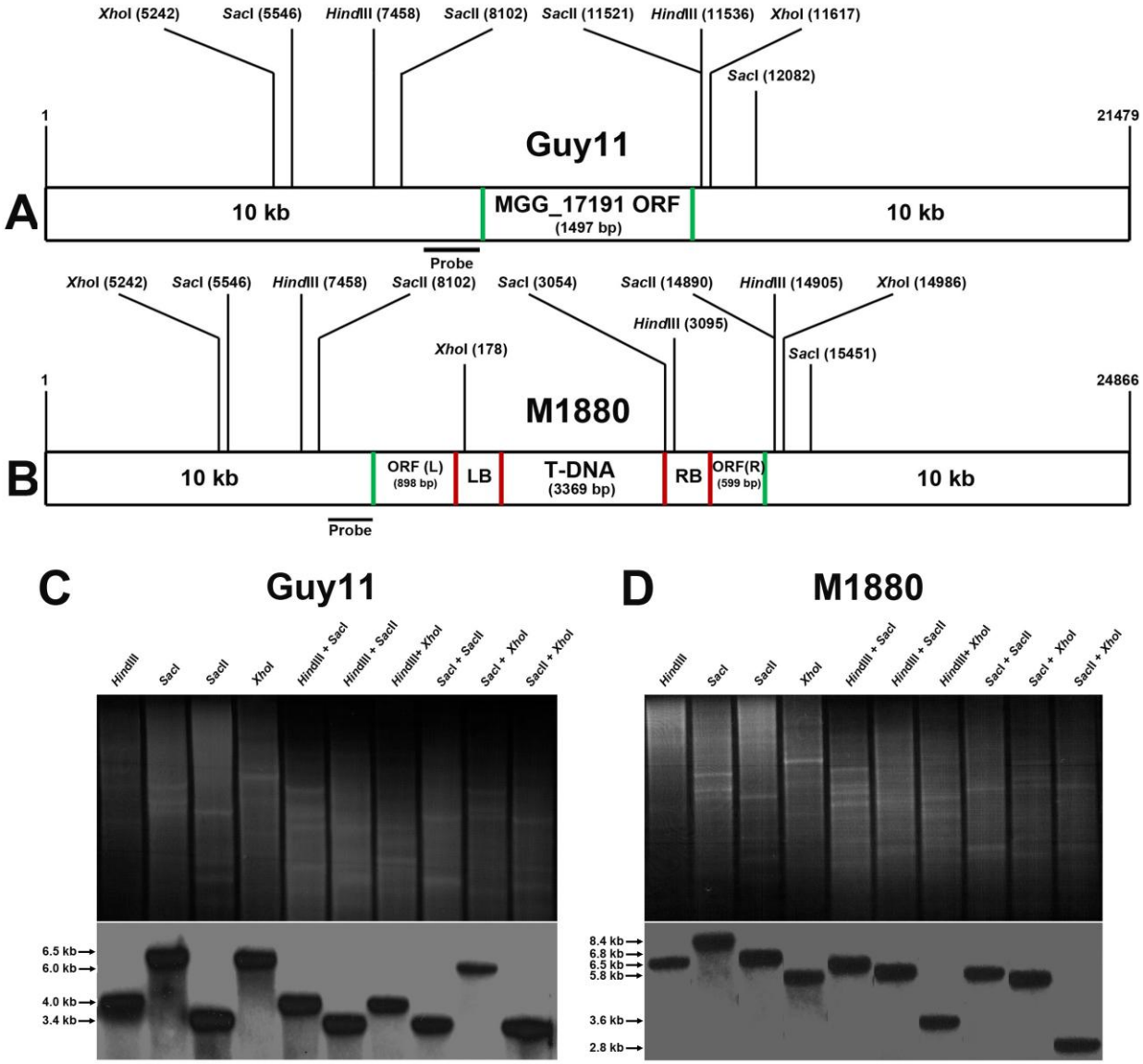

Figure 5.13: Confirmation of T-DNA insertion in the MGG_17191 locus by RFLP analysis. A. A schematic representation of the restriction map of *M. oryzae* MGG_17191 locus. Positions of the restriction sites are indicated by numbers in a 21.5 kb genomic DNA fragment. **B.** Restriction map of the *M. oryzae* MGG_17191 locus in mutant M1880. PCR validated NGS data proved a T-DNA insertion in the MGG_17191 gene of the mutant M1880 and the map was constructed according to the orientation of the retrieved flank sequence from NGS. Positions of restriction sites are indicated by numbers in a 24.5 kb genomic DNA sequence. Location of T-DNA restriction sites are shown as distance from the left border. **C. & D.** Four enzymes *Hin*dIII, *Sac*I, *Sac*II and *Xho*I were selected for RFLP analysis at the MGG_17191 locus in wild-type Guy11 and mutant M1880. Images show DNA gel blot analysis. Genomic DNA was digested, fractionated by gel electrophoresis, blotted and probed with a ~1 kb 5' flanking gene fragment amplified by PCR. Wild-type Guy11 **(C)** and mutant M48 **(D)** showed polymorphic restriction fragments from single and double digestions of the selected restriction enzymes. Fragment sizes are precisely shown by arrows.

5.3.4.3 RFLP analysis to confirm the T-DNA insertion in the MGG_12956 locus

In mutant M2048, T-DNA was found to be inserted within the gene MGG_12956. In order to map the T-DNA insertion in the MGG_12956 locus of mutant M2048 by Southern blot hybridization analysis, a restriction map of the 25.7 kb genomic region (5.7 kb MGG_12956 ORF in the middle and 10 Kb genomic DNA sequence from 5' and 3' flanks) for wild-type Guy11 was constructed (Figure 5.14A). A restriction map of the same genomic region containing the T-DNA insertion within the MGG_12956 locus was also constructed according to NGS data and subsequent PCR results (Figure 5.14B). By comparing the two restriction maps, we selected four different restriction enzymes to carry out RFLP analysis, *Hin*dIII, *Xba*I, *Xma*I and *Xmn*I were selected. These enzymes were chosen because they were predicted to produce a differential restriction pattern for Guy11 and mutant M2048. The size of the DNA fragments that was expected for both Guy11 and M48 are summarized in Table 5.9. Genomic DNA of Guy11 and M2048 was digested with the selected enzymes, fractionated by gel electrophoresis, blotted and probed with a ~1 kb gene fragment amplified by PCR. Comparing the band sizes of wild-type Guy11 (Figure 5.14C) and mutant M2048 (Figure 5.14D), restriction fragment length polymorphisms (RFLP) were found at the MGG_12956 locus and confirmed the predicted T-DNA insertion. The T-DNA insertion in M2048 was mapped by the means of *Hin*dIII, *Xba*I, *Xma*I and *Xmn*I digests. As predicted, all of those digestions resulted in distinct restriction fragments in M2048 compared to Guy11. Restriction fragment length differences are precisely shown by arrows and the obtained fragment sizes matched the expected sizes (Table 5.9). RFLP evidences suggest that M2048 contains a T-DNA insertion in the MGG_12956 locus and this ultimately validated both the PCR result (Figure 5.9G) and mapping of the loci based on NGS data (Figure 5.10E).

Table 5.9: Expected sizes of restriction fragments after digestion with selected enzymes used for RFLP analysis at MGG_12956 locus of the mutant M2048. Four enzymes *Hin*dIII, *Xba*I, *Xma*I and *Xmn*I were selected for RFLP analysis at the MGG_12956 locus in mutant M2048. For Guy11, the restriction map was constructed to include 10 kb upstream and downstream genomic DNA sequence of the MGG_12956 ORF. For mutant M2048, a restriction map of the locus was constructed on the basis of PCR validated retrieved NGS data. All of the chosen enzymes were predicted to generate polymorphic restriction fragment in all single and some double digests due to a T-DNA insertion in the locus. Among six double digests, four were expected to show size differences and two were expected to produce no differences (*Xmn*I digestion with *Xba*I and *Xma*I respectively).

Enzyme	**Fragment Size (kb)**	
	Guy11	**M2048**
***Hin*dIII**	7.7	6.7
***Xba*I**	6.4	9.4
***Xma*I**	16.6	9.3
***Xmn*I**	6.7 & 9.4	6.7 &12.8
***Hin*dIII + *Xba*I**	3.7	6.6
***Hin*dIII + *Xma*I**	7.7	6.6
***Hin*dIII + *Xmn*I**	4.5 & 3.2	3.2 & 3.5
***Xba*I + *Xma*I**	6.3	9.3
***Xba*I + *Xmn*I**	6.0	6.0 & 3.4
***Xma*I + *Xmn*I**	5.9 & 9.4	5.9 & 3.4

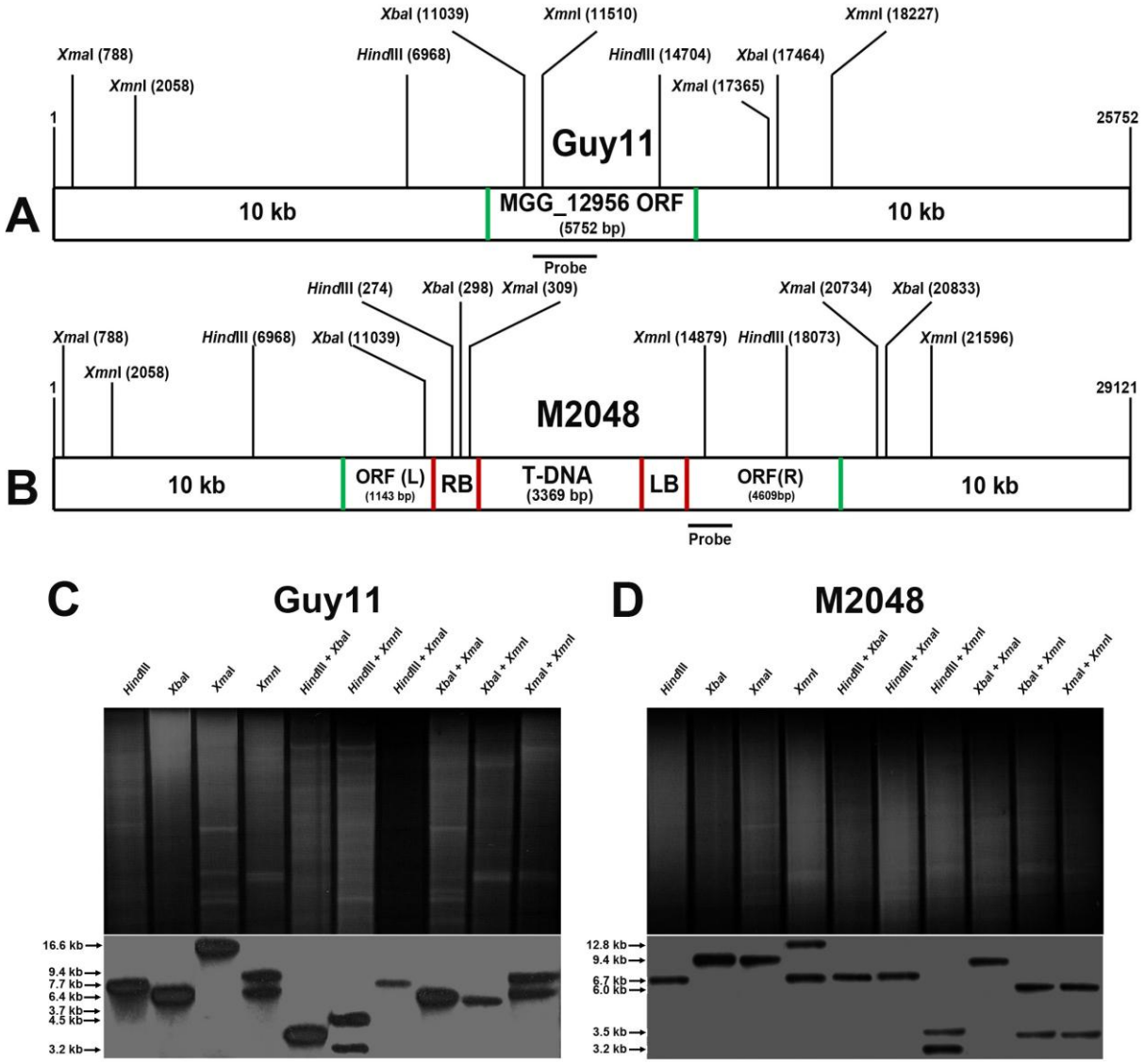

Figure 5.14: Confirmation of T-DNA insertion in the MGG_12956 locus by RFLP analysis. A. A schematic representation of the restriction map of *M. oryzae* MGG_12956 locus. Positions of the restriction sites are indicated by numbers in a 25.7 kb genomic DNA sequence. **B.** Restriction map of the *M. oryzae* MGG_12956 locus in mutant M2048. NGS data showed a T-DNA insertion in the MGG_12956 gene of the mutant M2048 and the map was constructed following the orientation of the retrieved flank sequence from NGS. Positions of restriction sites are indicated by numbers in a 29.1 kb genomic DNA sequence. Location of T-DNA restriction sites are shown as distance from the right border. **C. & D.** Four enzymes *Hin*dIII, *Xba*I, *Xma*I and *Xmn*I were selected for RFLP analysis at MGG_12956 locus in wild-type Guy11 and mutant M2048. Images show DNA gel blot analysis. DNA was digested, fractionated by gel electrophoresis, blotted and probed with a ~1 kb gene fragment amplified by PCR. Wild-type Guy11 **(C)** and mutant M48 **(D)** showed polymorphic restriction fragments from single and double digestions of the selected restriction enzymes. Fragment sizes are precisely shown by arrows.

5.3.4.4 RFLP analysis to confirm the T-DNA insertion in the MGG_05343 locus

Mutant M2942 integrated T-DNA within the gene MGG_05343. To map the T-DNA insertion in the mutant by Southern blot hybridization analysis, a restriction map of the 23.7 kb genomic region (3.7 kb MGG_05343 ORF in the middle and 10 kb genomic DNA sequence from 5' and 3' flanks) for wild-type Guy11, was constructed (Figure 5.15A). A restriction map of the same genomic region containing the T-DNA insertion within the MGG_05343 locus was also constructed according to NGS data and the subsequent PCR result (Figure 5.15B). By comparing the two restriction maps, we selected four different restriction enzymes to carry out RFLP analysis with *Hin*dIII, *Sph*I, *Xma*I and *Xcm*I. These enzymes were chosen because they were predicted to show a differential banding pattern for Guy11 and mutant M2942. The sizes of DNA fragments that were expected for both Guy11 and M2942 are summarized in Table 5.10. Genomic DNA of Guy11 and M2942 was digested with the selected enzymes, fractionated by gel electrophoresis, blotted and probed with a 1 kb gene fragment amplified by PCR. Comparing the fragment sizes of wild-type Guy11 (Figure 5.15C) and mutant M2942 (Figure 5.15D), restriction fragment length polymorphism (RFLP) were found at the MGG_05343 locus and confirmed the predicted T-DNA insertion. The T-DNA insertion in M2942 was mapped by *Hin*dIII, *Xba*I, *Xma*I and *Xmn*I digests. As predicted, all of those digestions resulted in distinct restriction fragments in M2942 compared to Guy11. Restriction fragment length differences are precisely shown by arrows and the obtained restriction fragment sizes matched the expected sizes (Table 5.10). Therefore, based on RFLP we conclude that mutant M2942 contains a T-DNA insertion in the MGG_05343 locus and this RFLP also validates previously shown PCR result (Figure 5.9B & F) and mapping of the loci based on NGS data (Figure 5.10F).

Table 5.10: Expected sizes of restriction fragments after digestion with selected enzymes used for RFLP analysis at MGG_05343 locus of the mutant M2942. Four enzymes, *Hin*dIII, *Sph*I, *Xma*I and *Xcm*I were selected for RFLP analysis at MGG_05343 locus of the mutant M2942. For Guy11, the restriction map was constructed including 10 kb upstream and downstream genomic DNA sequence of the MGG_05343 coding region. For mutant M2942, a restriction map of the locus was also constructed on the basis of PCR-validated, retrieved NGS data. All of the chosen enzymes were predicted to generate polymorphic restriction fragment in all single and some double digests due to a T-DNA insertion in the locus. All four enzymes were predicted to show polymorphic restriction fragment in corresponding single and double digests of Guy11 and M2048.

Enzyme	Fragment Size (kb)	
	Guy11	M2942
***Hin*dIII**	11.3	3.8
***Sph*I**	9.5	8.8
***Xma*I**	5.2	1.9
***Xcm*I**	3.3	6.7
***Hin*dIII + *Sph*I**	4.5	3.8
***Hin*dIII + *Xma*I**	5.2	1.9
***Hin*dIII + *Xcm*I**	3.3	2.6
***Sph*I + *Xma*I**	2.6	1.9
***Sph*I + *Xcm*I**	3.3	2.6
***Xma*I + *Xcm*I**	2.5	1.9

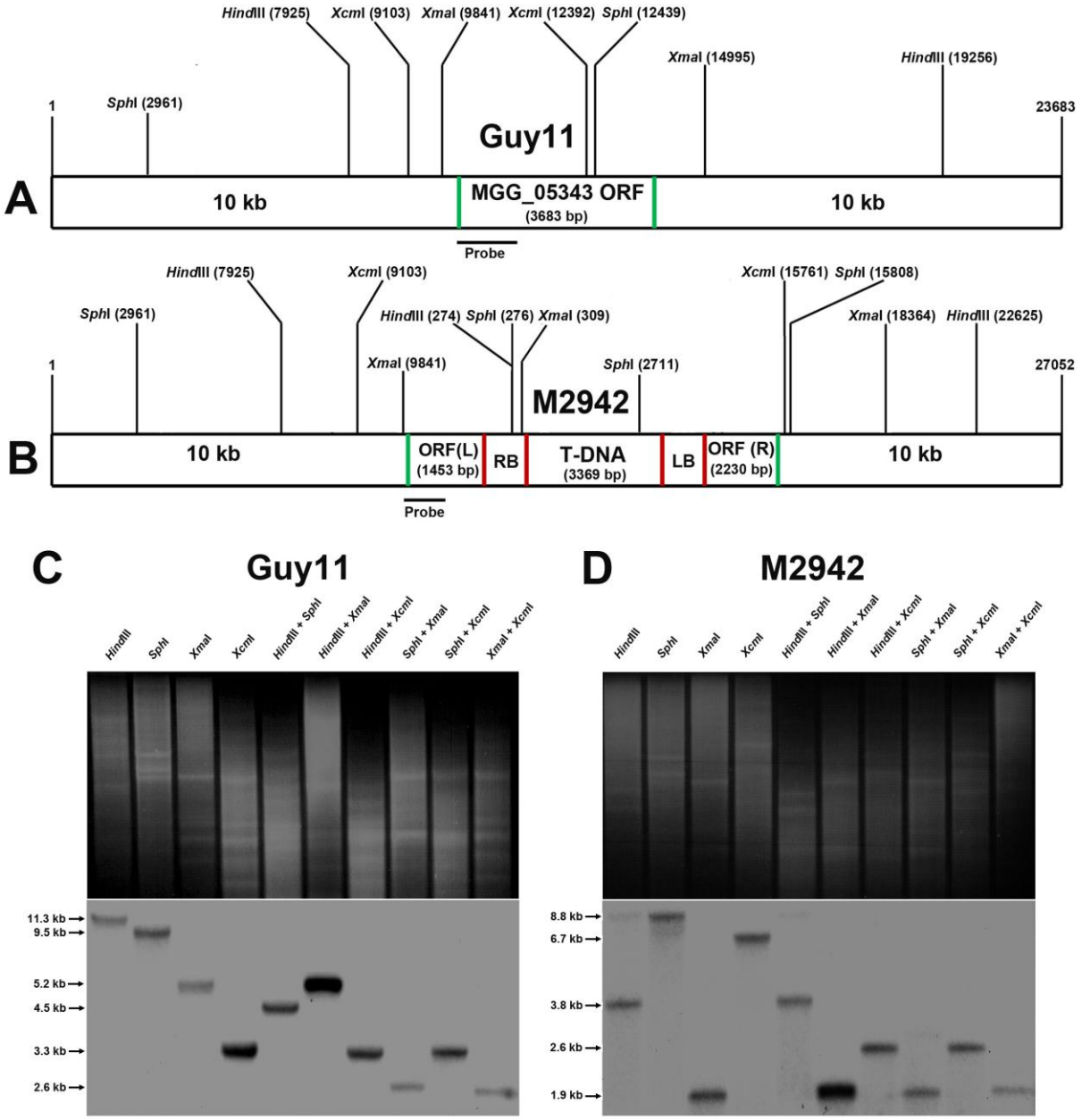

Figure 5.15: Confirmation of T-DNA insertion in the MGG_05343 locus by RFLP analysis. A. A schematic representation of the restriction map of *M. oryzae* MGG_05343 locus. Positions of the restriction sites are indicated by numbers in a 23.7 kb genomic DNA sequence. **B.** Restriction map of the *M. oryzae* MGG_05343 locus in the mutant M2942. NGS data showed a T-DNA insertion in the MGG_05343 gene of the mutant M2942 and the map was constructed according to the retrieved flank sequence from NGS. Location of restriction sites are indicated by numbers in a 27 kb genomic DNA sequence. Positions of T-DNA restriction sites are shown as distance from the right border. **C. & D.** Four enzymes *Hin*dIII, *Sph*I, *Xma*I and *Xcm*I were selected for RFLP analysis at MGG_05343 locus in wild-type Guy11 and mutant M2942. Images show DNA gel blot analysis. Genomic DNA was digested, fractionated by gel electrophoresis, blotted and probed with a 1 kb gene fragment amplified by PCR. Wild-type Guy11 **(C)** and mutant M48 **(D)** showed polymorphic restriction fragments from single and double digestions of the selected restriction enzymes. Restriction fragment sizes are precisely shown by arrows.

5.3.4.5 RFLP analysis to confirm the T-DNA insertion in the MGG_15325 locus

In mutant M4874, T-DNA was inserted within a gene MGG_15325. To map the T-DNA insertion in this locus of mutant M4874 by Southern blot hybridization analysis, a restriction map of the 24.9 kb genomic region (4.9 kb MGG_15325 ORF in the middle and 10 kb genomic DNA sequence from 5' and 3' flanks) for wild-type Guy11 was constructed (Figure 5.16A). We also constructed a restriction map of the same genomic region containing the T-DNA insertion within the MGG_15325 locus following data derived from NGS and subsequent PCR result (Figure 5.16B). By comparing the two restriction maps, we selected four different restriction enzymes to carry out RFLP analysis. These enzymes were chosen because they were expected to produce a differential restriction fragment pattern for Guy11 and mutant M4874. We chose *Sac*II, *Xcm*I, *Xma*I and *Xho*I. The size of the DNA fragments that was expected for both Guy11 and M4874 are summarized in Table 5.11. Genomic DNA of Guy11 and M4874 was digested with the selected enzymes, fractionated by gel electrophoresis, blotted and probed with a ~1 kb 5' flanking gene fragment amplified by PCR. A comparison between the band sizes of wild-type Guy11 (Figure 5.16C) and mutant M4874 (Figure 5.16D) showed restriction fragment length polymorphism (RFLP) at the MGG_15325 locus and consequently confirmed the predicted T-DNA insertion. As expected, all of those digestions resulted in distinct restriction fragments in M4874 compared to Guy11. Restriction fragment length differences are precisely shown by arrows and the obtained fragment sizes matched the predicted sizes (Table 5.11). Therefore, it was clear that M4874 contains a T-DNA insertion in the MGG_15325 locus and this in turn validates mapping of the T-DNA based on NGS data (Figure 5.10G) and also the PCR result (Figure 5.9D).

Table 5.11: Expected sizes of restriction fragments after digestion with selected enzymes used for RFLP analysis at MGG_15325 locus in mutant M4874. Four enzymes *Sac*II, *Xcm*I, *Xma*I and *Xho*I were selected for RFLP analysis at the MGG_15325 locus in mutant M4874. For Guy11, the restriction map was constructed to include 10 kb upstream and downstream genomic DNA sequence of the MGG_15325 coding region. A restriction map of the locus was constructed for mutant the M4874, on the basis of PCR-validated NGS data. All of the chosen enzymes were predicted to generate polymorphic restriction fragment in both single and double digests due to a T-DNA insertion in the locus.

Enzyme	Fragment Size (Kb)	
	Guy11	M4874
***Sac*II**	6.7	10.0
***Xcm*I**	4.3	7.7
***Xma*I**	4.1	7.0
***Xho*I**	10.1	2.5
***Sac*II + *Xcm*I**	3.6	7.0
***Sac*II + *Xma*I**	1.7	4.5
***Sac*II + *Xho*I**	6.7	1.7
***Xcm*I + *Xma*I**	2.4	5.3
***Xcm*I + *Xho*I**	4.3	2.4
***Xma*I + *Xho*I**	2.5	2.5

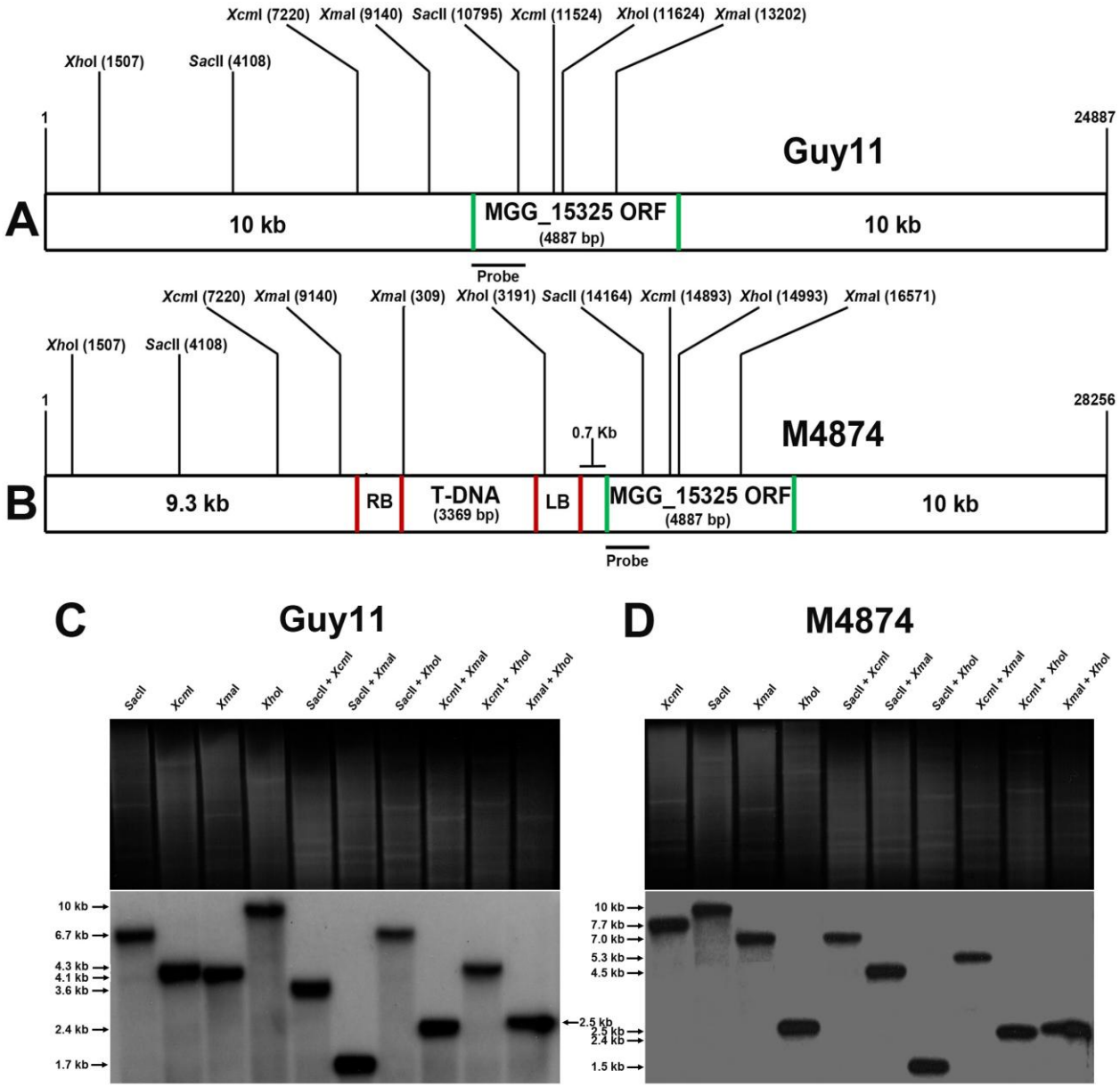

Figure 5.16: Confirmation of T-DNA insertion in the MGG_15325 locus by RFLP analysis. A. A schematic representation of the restriction map of *M. oryzae* MGG_15325 locus. Positions of the restriction sites are indicated by numbers in a 24.9 kb genomic DNA sequence. **B.** Restriction map of the *M. oryzae* MGG_15325 locus in mutant M4874. NGS data showed a T-DNA insertion in the MGG_15325 gene of the mutant M4874 and the map was constructed according to the orientation of retrieved flank sequence from NGS. Positions of restriction sites are indicated by numbers in a 28.25 kb genomic DNA sequence. Location of the T-DNA restriction sites are shown as distance from the right border. **C. & D.** Four enzymes *Sac*II, *Xcm*I, *Xma*I and *Xho*I were selected for RFLP analysis at the MGG_15325 locus in wild-type Guy11 and mutant M4874. Images show DNA gel blot analysis. Genomic DNA was digested, fractionated by gel electrophoresis, blotted and probed with a ~1 kb 5' flanking gene fragment amplified by PCR. Wild-type Guy11 **(C)** and mutant M4874 **(D)** showed polymorphic restriction fragments from single and double digestions of the selected restriction enzymes. Restriction fragment sizes are precisely shown by arrows.

5.3.5 Complementation of the mutants with putative identified genes

All the complementation vectors were constructed by recombination-mediated PCR-directed plasmid construction *in vivo* in yeast (Oldenburg *et al.*, 1997). The complementation vectors were systemically transformed into protoplasts of corresponding mutants. Putative transformants were selected for resistance to chloromuron ethyl (sulfonylurea) (100 μg mL^{-1}). Selected transformants were screened and confirmed for vector integration by Southern blot hybridization analysis. Genomic DNA was digested with *Xho*I, fractionated by gel electrophoresis, blotted and probed with a 1 kb *ILV1* fragment. The DNA was digested with *Xho*I, because it does not have any restriction site within the *ILV1* cassette. Positive transformants were then assayed for pathogenicity by cut-leaf assay. Complemented strains were grown on CM for 12 days and a 50 μL conidial suspension was placed on cut leaves laid on 1% agar plates and incubated for 5 days. Restoration of pathogenicity was confirmed by comparing with wild-type Guy11 and for each mutant, pathogenicity assays for three of the complemented strains are shown (Figure 5.17-5.22).

The list of genes that complemented the mutants is presented in Table 5.12. Not all the mutants were complemented by the T-DNA tagged genes as predicted from PCR and RFLP based confirmation. For mutant M2048, M2942 and M4874, the predicted genes MGG_12956, MGG_05343 and MGG_15325 complemented pathogenicity, respectively. In contrast, M48 and M1880 were not complemented by the genes MGG_17516 and MGG_17191 respectively despite the fact that T-DNA integration was confirmed within the corresponding ORFs. Their inability to complement those mutants was unexpected but was consistent with SuperSAGE data (Figure 5.11). These two genes were for example down-regulated throughout a time course of the appressorium development. The insertion of T-DNA in these genes might have however affected downstream genes at each locus. Figure

5.10 shows the downstream genes of MGG_17516 and MGG_17191 which are *HOX2* (MGG_00184) and *MST11* (MGG_14847) respectively. Mutant M48 was therefore complemented by *HOX2* (Figure 5.17) and mutant M1880 was complemented by *MST11* (Figure 5.19). It is noteworthy that these two mutants (M48 and M1880) were phenotypically very much similar to *HOX2* (Kim *et al.*, 2009; Liu *et al.*, 2010) and *MST11* (Zhao *et al.*, 2005) deletion mutants respectively. Furthermore, we also complemented the Δ*hox*2 mutant using the cloned *HOX2* gene from wild-type Guy11 and the deletion strain (deletion strain was made in wild-type KJ201) was complemented (Figure 5.18). We therefore, unequivocally proved that in the mutant M48, the T-DNA affected gene was *HOX2*. Thus, T-DNA integration in MGG_17516 and MGG_17191 in fact affected downstream genes. Both of the genes are well characterized. *HOX2* is for example, one of the eight homeobox genes in *M. oryzae* and essential for conidiogenesis and pathogenicity (Kim *et al.*, 2009; Liu *et al.*, 2010). *MST11* is the yeast *STE11* homolog in *M. oryzae*. This is an upstream activator of the Pmk1 MAPK pathway and its activation occurs through Mst7 protein which is the MEK or ERK kinase in the MAP kinase cascade (Zhao *et al.*, 2005).

Table 5.12: List of the complemented mutants with identified putative *M. oryzae* genes. This table shows the list of *M. oryzae* genes cloned to complement the selected mutants in a systematic way. From PCR and RFLP analysis, insertion into the corresponding loci was confirmed. Cloned *M. oryzae* genes from each locus (Including 5'-promoter and 3'-UTR) were used to construct complementation vectors and these were transformed into the respective mutants. Mutants M48 was transformed with an annotated hypothetical gene MGG_17516 because the T-DNA was inserted within its ORF. But it failed to complement mutant M48 and hence we complemented the mutant with the flanking *HOX2* gene. Similarly, M1880 was complemented with annotated hypothetical gene MGG_17191 and the T-DNA was inserted within the ORF. As it failed to complement the mutant, we therefore cloned the flanking *MST11* gene and the mutant was complemented for pathogenicity. Mutant M2048 and M2942 were complemented with MGG_12956 and MGG_05343 respectively and both genes have T-DNA inserted within the ORFs. MGG_12956 and MGG_05343 are homologs of yeast *BUD4* and *PUT3* transcription factor, respectively. Mutant M4874 was complemented with MGG_15325 because of the T-DNA insertion in its promoter and this is a homolog of yeast meiosis regulatory kinase *IME2*.

Mutants	***M. oryzae* genes complemented the mutant**
M48	MGG_00184 (*HOX2*)
M1880	MGG_14847 (*MST11*)
M2048	MGG_12956 (Bud4 homolog)
M2942	MGG_05343 (Put3 homolog)
M4874	MGG_15325 (Ime2 homolog)

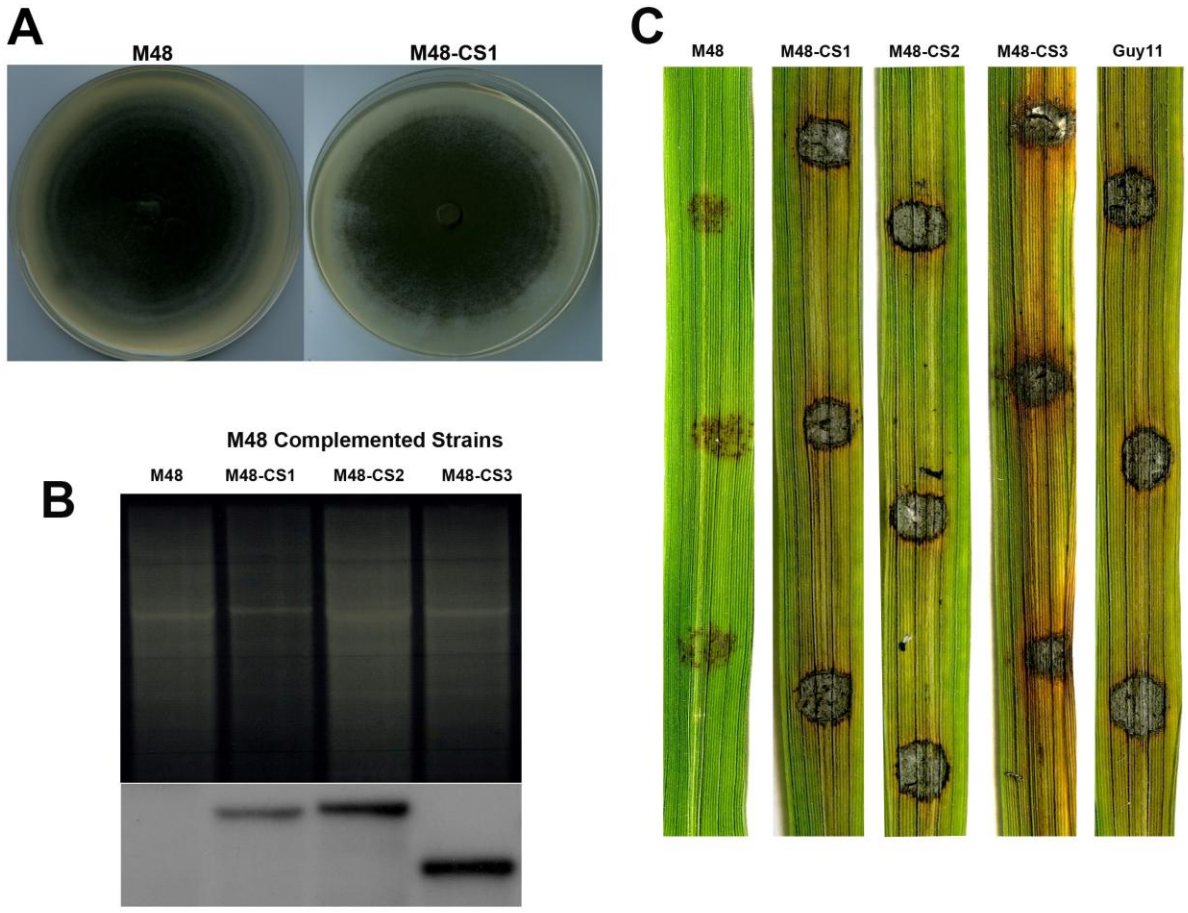

Figure 5.17: Complementation of the mutant M48 with *M. oryzae HOX2* gene. Mutant M48 was transformed with cloned MGG_17516 and *HOX2* gene, respectively. MGG_17516 failed to complement the mutant (results not shown) whereas *HOX2* gene complemented the mutant for pathogenicity and conidiation. **A.** A complemented transformants of mutant M48, M48-CS1 is shown. Complemented strains restored conidiation. **B.** Complemented strains were analyzed by Southern blot to confirm the vector insertion in genomic DNA. Genomic DNA isolated from sulfonylurea resistant transformants was digested with the restriction enzyme *Xho*I, fractionated by agarose gel electrophoresis and blotted. The Southern blot was probed with a 1 kb *ILVI* fragment generated by PCR amplification**.** Selected complemented strains showed positive results. **C.** Pathogenicity assay of three selected complemented strains are shown. Complemented strains (M48-CS1, CS2 and CS3) were able to produce typical necrotic rice blast disease lesions. Thus, pathogenicity was restored upon introduction of *HOX2* gene in mutant M48 and confirming that T-DNA insertion disrupted *HOX2* gene function.

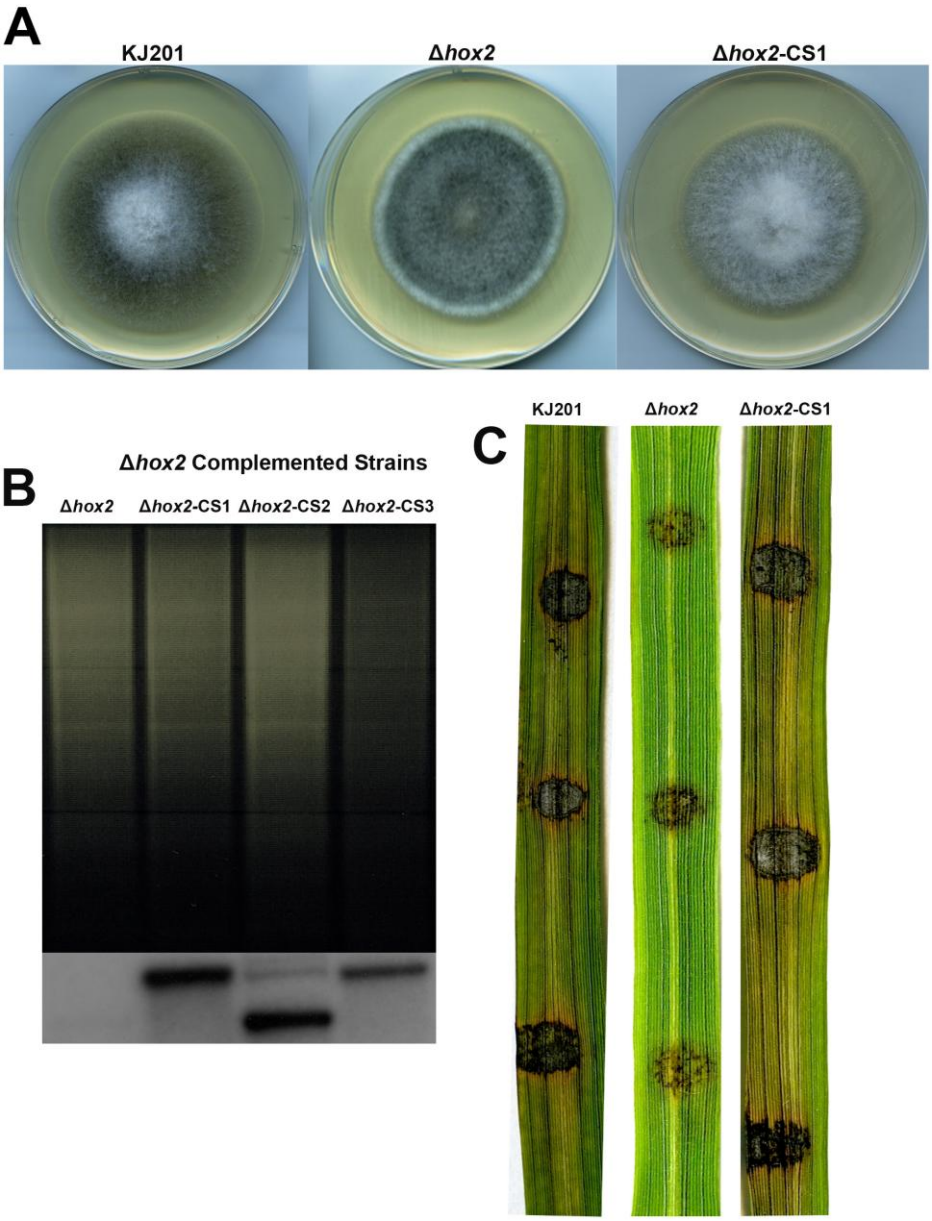

Figure 5.18: Complementation of Δ*hox2* deletion mutant with the *M. oryzae HOX2* gene. The Δ*hox2* deletion mutant was generated in the isogenic wild-type strain KJ201 (Kim *et al.*, 2009). It was complemented with the *HOX2* complementation construct which was used to complement the mutant M48. **A.** Wild-type strain KJ201, Δ*hox2* deletion mutant and a complemented strain is shown. The wild-type strain KJ201 and complemented strain showed similar vegetative growth phenotype. The Δ*hox2* is non-conidiating but the complemented strain restored conidiation. **B.** Complemented strains were analyzed by southern blot to confirm the vector insertion in genomic DNA. Genomic DNA isolated from sulfonylurea resistant transformants was digested with the restriction enzyme *Xho*I, fractionated by agarose gel electrophoresis, blotted and probed with a 1 kb *ILVI* fragment generated by PCR amplification**.** Selected complemented strains showed vector integration in genomic DNA. **C.** Pathogenicity assay of one complemented strain is shown. The Δ*hox2* strain is non-pathogenic and unable to cause disease. In contrast, he complemented strain was pathogenic and produced necrotic rice blast disease lesions.

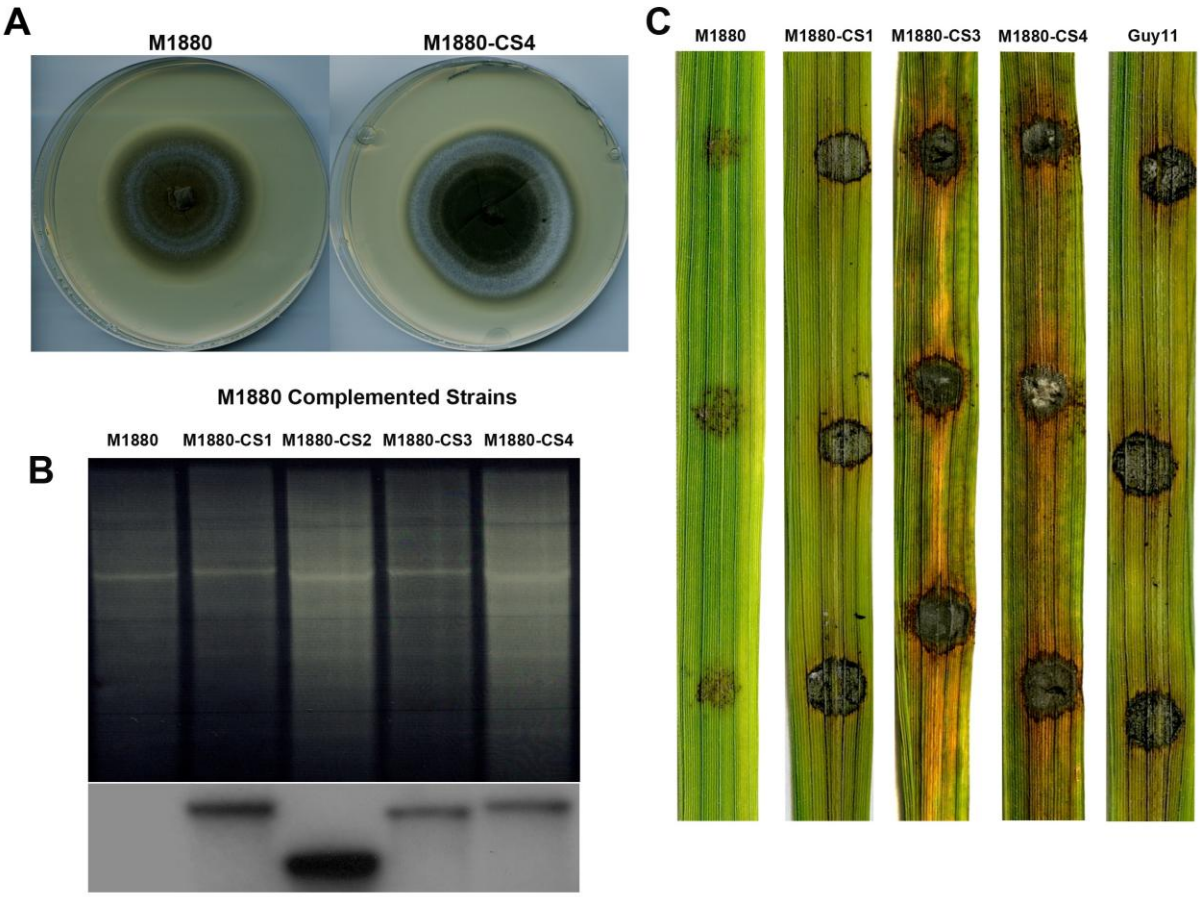

Figure 5.19: Complementation of mutant M1880 with the *M. oryzae MST11* gene. Mutant M1880 was transformed with MGG_17191 and *MST11* complementation vector respectively. The *MST11* gene complemented the mutant for pathogenicity and appressorium formation while MGG_17191 failed to complement the mutant. **A.** A complemented transformant M1880-CS4 is shown and which restored wild-type vegetative growth. **B.** Complemented strains were analyzed by Southern blot to confirm vector insertion in genomic DNA. Genomic DNA isolated from sulfonylurea resistant transformants was digested with the restriction enzyme *Xho*I, fractionated by agarose gel electrophoresis and blotted. The Southern blot was probed with a 1 kb *ILVI* fragment generated by PCR amplification**. C.** Pathogenicity assay of three selected complemented strains are shown. Complemented strains restored pathogenicity by producing necrotic rice blast disease lesions.

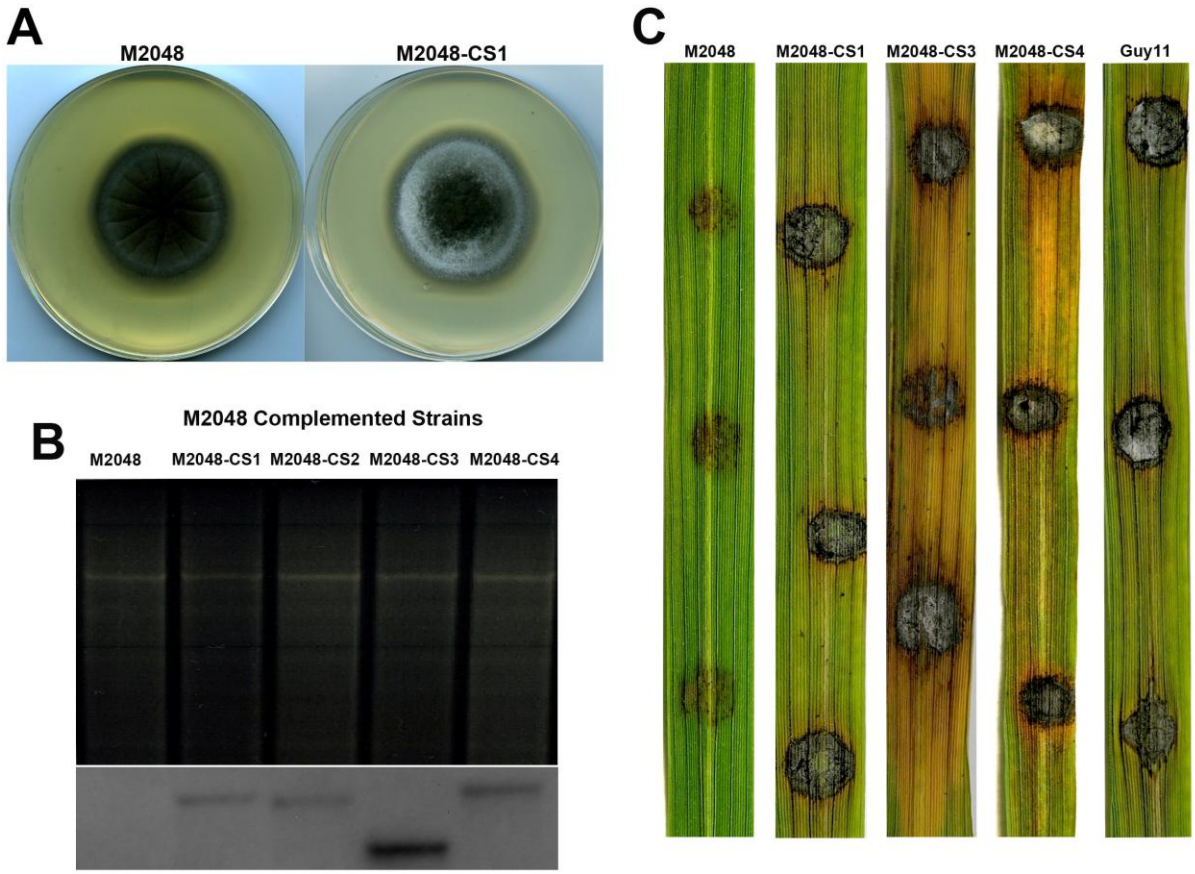

Figure 5.20: Complementation of mutant M2048 with the *M. oryzae* gene MGG_12956. Mutant M2048 was transformed with MGG_12956 and this complemented the mutant for pathogenicity. **A.** A complemented strain M2048-CS1 is shown with distinguishable vegetative growth compared to mutant M2048. **B.** Complemented strains were analyzed by Southern blot to confirm the vector insertion in genomic DNA. Genomic DNA isolated from selected transformants was digested with the restriction enzyme *Xho*I, fractionated by agarose gel electrophoresis, blotted and probed with a 1 kb *ILVI* fragment generated by PCR amplification**. C.** Pathogenicity assay of three selected complemented strains are shown. Restoration of pathogenicity in complemented strains was exemplified by necrotic rice blast disease lesions.

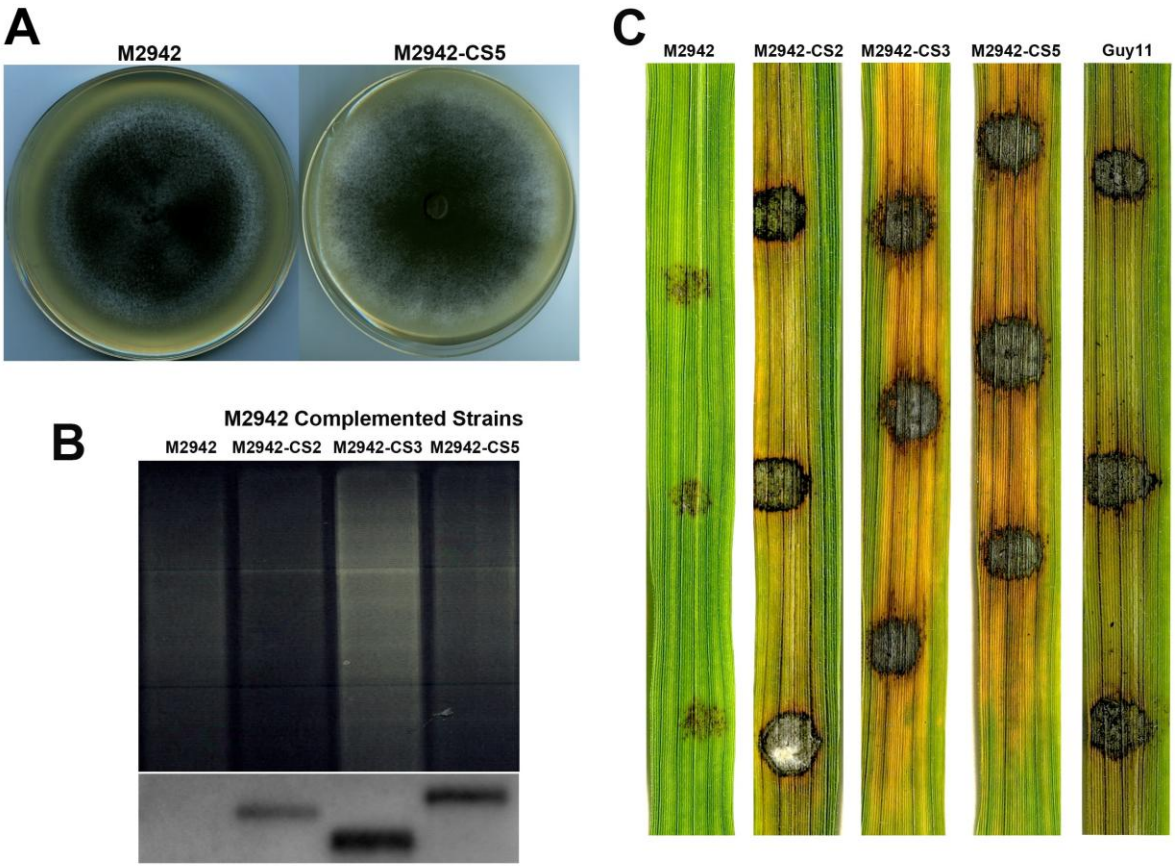

Figure 5.21: Complementation of mutant M2942 with the *M. oryzae* gene MGG_05343. Mutant M2942 was transformed with MGG_05343 and it complemented the mutant for pathogenicity and conidiation. **A.** A complemented transformant (M294-CS5) of mutant M2942 is shown and conidiation was restored in complemented starins. **B.** Complemented transformants were analyzed by Southern blot to confirm vector insertion in genomic DNA. Genomic DNA isolated from sulfonylurea resistant transformants was digested with the restriction enzyme *Xho*I, fractionated by agarose gel electrophoresis, blotted and probed with a 1 kb *ILVI* fragment generated by PCR amplification**. C.** Pathogenicity assay of three selected complemented strains are shown. Pathogenicity was restored in complemented strains and they produced necrotic rice blast disease lesions.

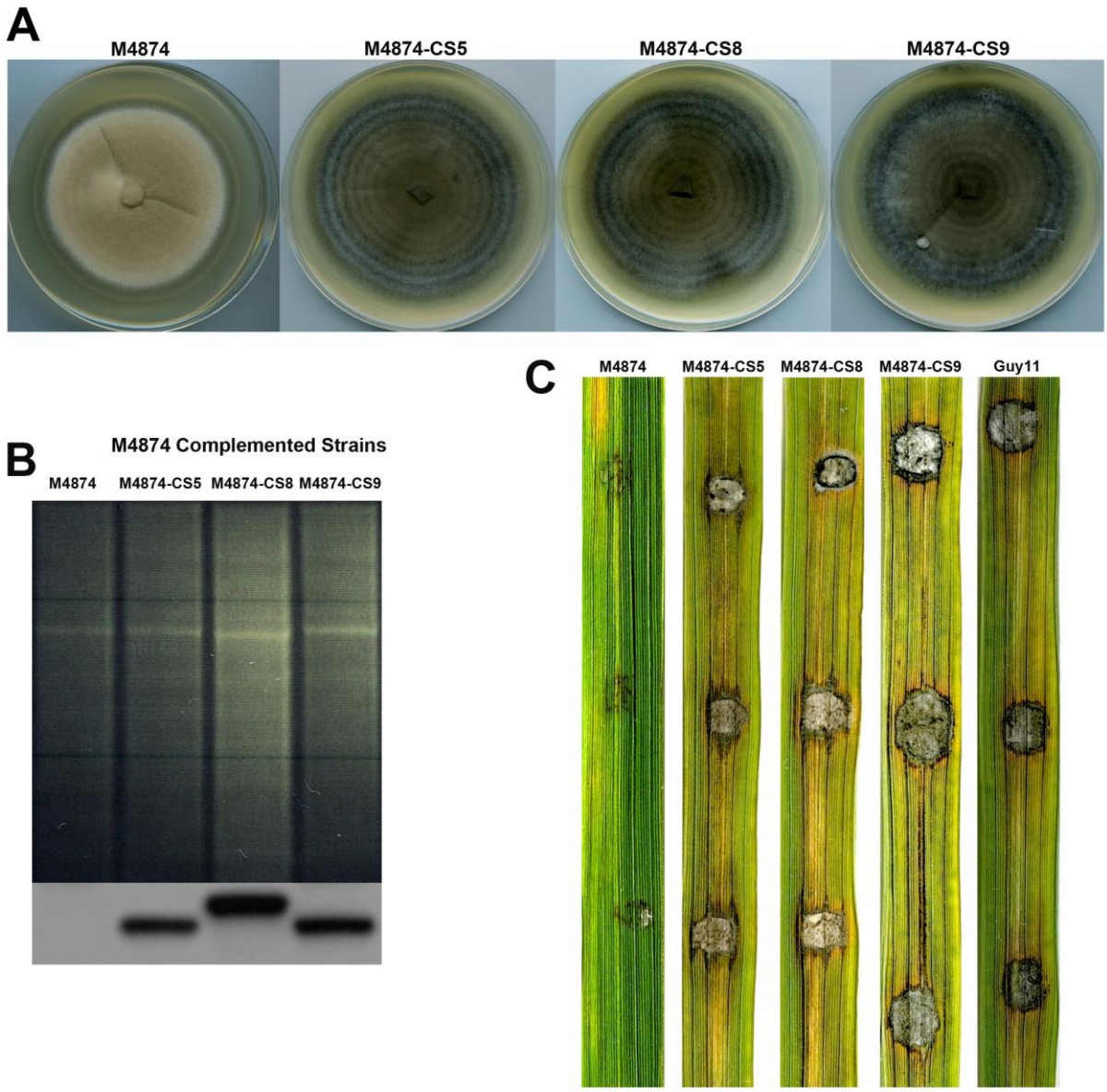

Figure 5.22: Complementation of the mutant M4874 with MGG_15325. Mutant M4874 was complemented by MGG_15325 complementation construct. **A.** Three complemented strains of mutant M4874 are shown. All the complemented transformants showed distinguishable vegetative morphology compared to mutant M4874. **B.** Complemented strains were analyzed by Southern blot to confirm vector insertion in genomic DNA. Genomic DNA isolated from sulfonylurea resistant transformants was digested with the restriction enzyme *Xho*I, fractionated by agarose gel electrophoresis, blotted and probed with a 1 kb *ILVI* fragment generated by PCR amplification**. C.** Pathogenicity assay of three selected complemented strains showed complete restoration of pathogenicity which produced necrotic rice blast disease lesions on rice leaves.

5.3.6 Domain structures of the putative novel genes

From the systematic complementation analysis of the selected non-pathogenic mutants three novel genes were unequivocally confirmed to be involved in pathogenicity. The genes responsible for pathogenicity were MGG_12956 in M2048, MGG_05343 in M2942 and MGG_15325 *(IME2*) in M4874, respectively. We searched for conserved domains (CD) in those identified proteins from NCBI CDD (conserved domain database) (Marchler-Bauer *et al.*, 2011). Domain organization of three putative protein products of these genes is shown diagrammatically in Figure 5.23.

MGG_12956 was confirmed as a determinant of conidiation and pathogenicity in M2048. The putative protein product has one anillin domain (Field and Alberts, 1995) and a pleckstrin homology (PH) domain in the C-terminal region (Mayer *et al.*, 1993; Haslam *et al.*, 1993; Yoon *et al.*, 1994). The lengths of these two domains are 96 aa and 129 aa respectively.

MGG_05343 putatively encodes a transcription factor responsible for conidiation and pathogenicity in M2942. The protein contains a N-terminal GAL4-like Zn2Cys6 binuclear cluster DNA-binding domain which is found in transcription regulators such as, GAL4 (Baleja *et al.*, 1992; Kraulis *et al.*, 1992). This domain consists of two α helices organized around a Zn2Cys6 motif. This protein also has a fungal transcription factor regulatory middle homology region (Fungal_TF_MHR) and this regulatory module is present in the large family of fungal zinc cluster transcription factors that contain an N-terminal GAL4-like C6 zinc binuclear cluster DNA-binding domain. The lengths of these two domains are 36 aa and 410 aa respectively.

A novel kinase, MGG_15325 was shown to be the determinant of pathogenicity in mutant M4874. This is the putative yeast *IME2* homolog in *M. oryzae*. *IME2* belongs to a novel sub-family of MAP kinases (Hamel *et al.*, 2012). The conserved protein kinase (PK) domain showed homology with serine-threonine kinases (STKs). Its kinase domain is 283 aa in length which consists of a catalytic site, ATP binding site, substrate binding site and an activation loop.

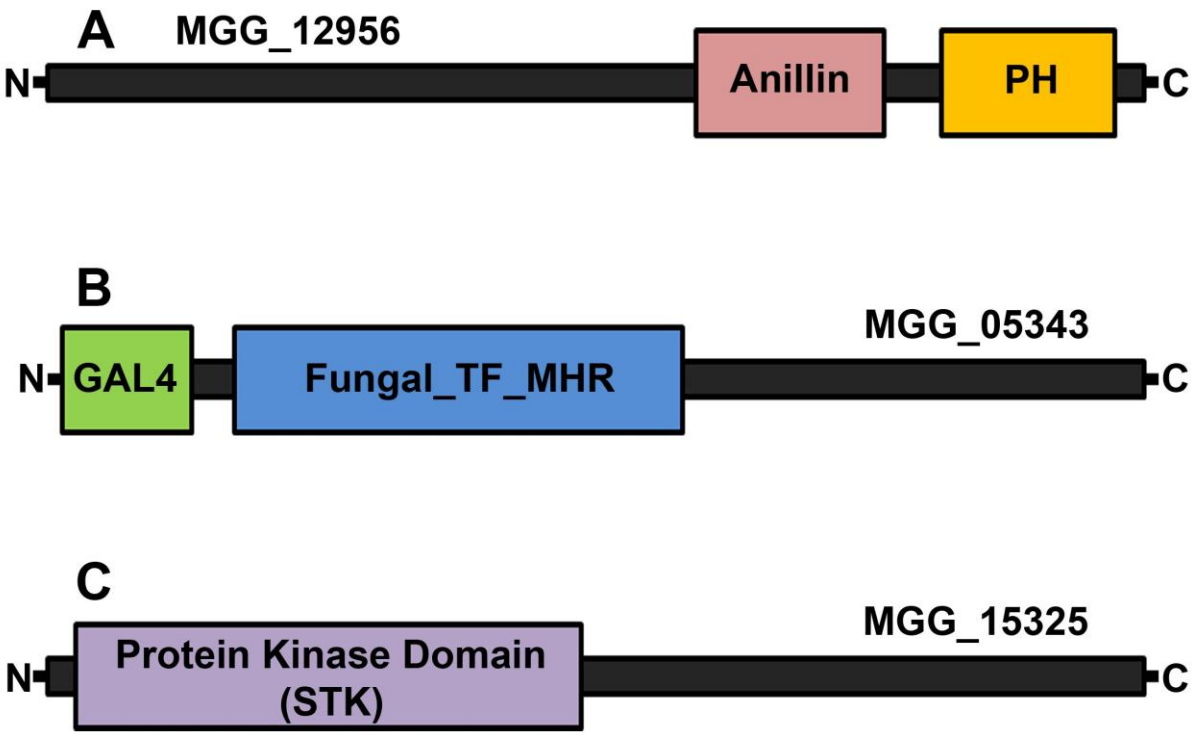

Figure: 5.23 Domain architectures of three putative novel proteins identified from T-DNA insertional mutants. Conserved domains (CD) were found in each of these three novel proteins responsible for pathogenicity from NCBI CDD. **A.** MGG_12956 was the determinant for conidiation and pathogenicity in M2048. The protein has one anillin domain (Field and Alberts, 1995) and a pleckstrin homology (PH) domain in the C-terminal region (Yoon *et al.*, 1994). **B.** Transcription factor MGG_05343 complemented conidiation and pathogenicity in M2942. The protein contains a N-terminal GAL4-like Zn2Cys6 binuclear cluster DNA-binding domain which is found in transcription regulators like GAL4 (Baleja *et al.*, 1992; Kraulis *et al.*, 1992). This domain consists of two α helices organized around a Zn2Cys6 motif. This protein also has a fungal transcription factor regulatory middle homology region (Fungal_TF_MHR) and this regulatory module is present in the large family of fungal zinc cluster transcription factors that contain an N-terminal GAL4-like C6 zinc binuclear cluster DNA-binding domain. **C.** The putative yeast *IME2* homolog in *M. oryzae* is MGG_15325 which was confirmed as the pathogenicity determinant in mutant M4874. Ime2 is a serine-threonine kinase with a conserved protein kinase (PK) domain and belongs to a novel sub-family of MAP kinases (Hamel *et al.*, 2012). Its kinase domain consists of catalytic site, ATP binding site, substrate binding site and an activation loop.

5.3.7 Phylogenetic analysis of the putative novel genes

Phylogenetic analyses of three putative novel genes were carried out using amino acid sequences from homologous fungal genes. Phylogenetic trees were constructed for the C6 zinc finger transcription factor MGG_05343, PH domain (Plecstrin homology domain) containing protein MGG_12956 and MGG_15325. Protein sequences were aligned using MUSCLE version 3.8.31 (Edgar *et al.*, 2004). Divergent and poorly aligned regions of the resulting multiple sequence alignment were removed using Gblocks (Talavera and Castresana, 2007). Default parameters were used for both of these programs. Maximum likelihood phylogenies were estimated from the curated alignment with PhyML version 3.0 (Guindon *et al.*, 2010) using the following parameters: number of substitution rate categories =8, gamma distribution parameter = estimated, proportion of invariable sites = estimated, 100 bootstraps. The most appropriate protein substitution model was selected using Model Generator (Keane *et al.*, 2006). The Phylogenetic trees are shown Figure 5.24 – 5.26. Phylogenetic trees show the homologous genes in different fungal species. Figure 5.24 shows the family of C6 zinc finger transcription factors in different fungi carrying the same functional C6 domain as MGG_05343. Figure 5.25 prrsents some of the homologues of MGG_12956 and *S. cerevisiae* Bud4 is one that is well known among them. Figure 5.26 is a family tree of kinases where a number of MAPKs shring homology with MGG_15325 is shown. This tree essentially shows that having hallmark of MAPKs, similar domain structure and significant sequence homology, MGG_15325 can be classified as novel MAPK in *M. oryzae*.

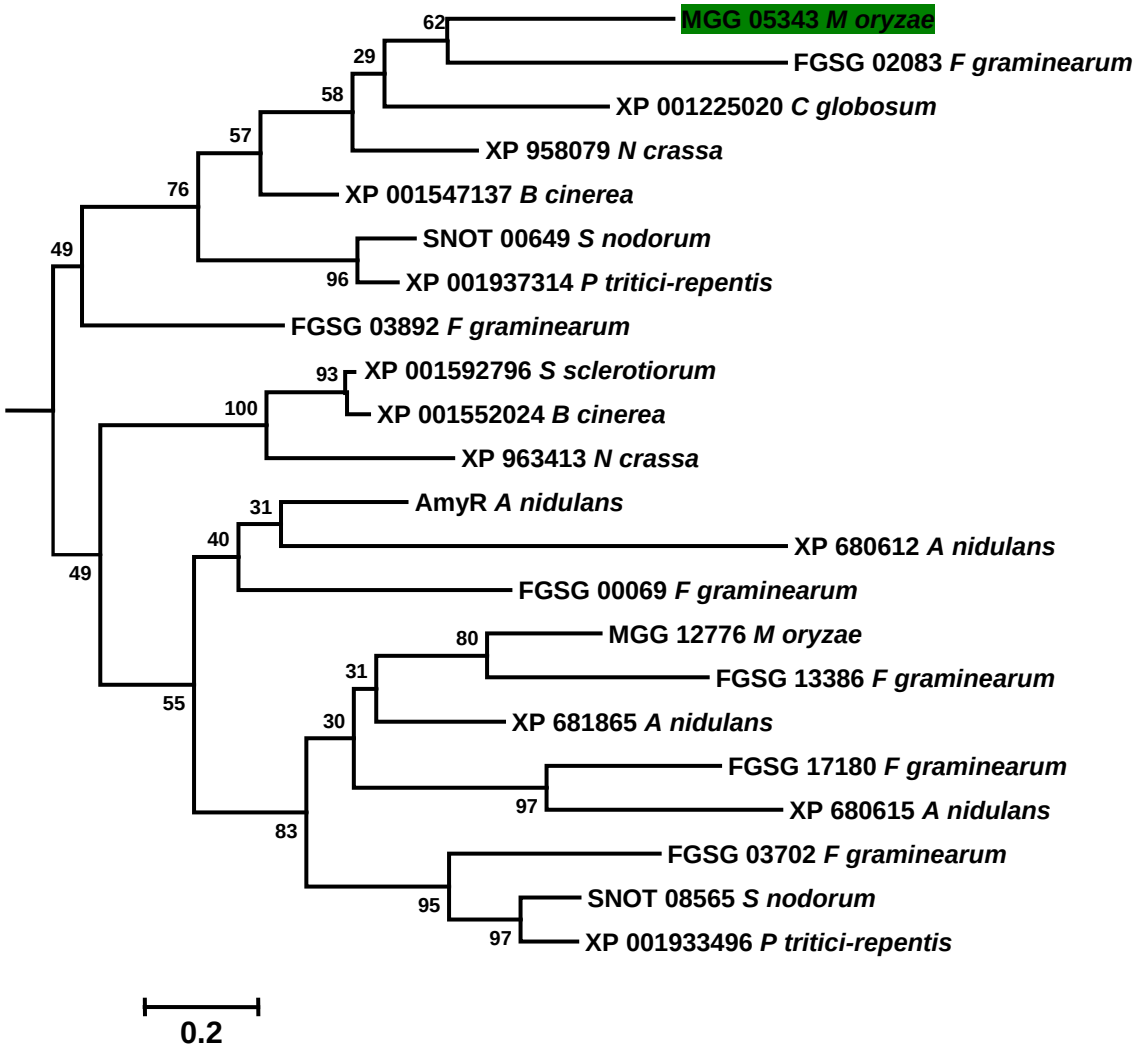

Figure 5.24: Phylogenetic analysis of C6 zinc finger protein MGG_05343. Protein sequences were aligned using MUSCLE version 3.8.31 (Edgar *et al.*, 2004). Maximum likelihood phylogenies were estimated from the curated alignment with PhyML version 3.0 (Guindon *et al.*, 2010). The most appropriate protein substitution model was selected using Model Generator (Keane *et al.*, 2006). This gene is part of a major clade of ascomycete-specific C6 zinc finger encoding genes.

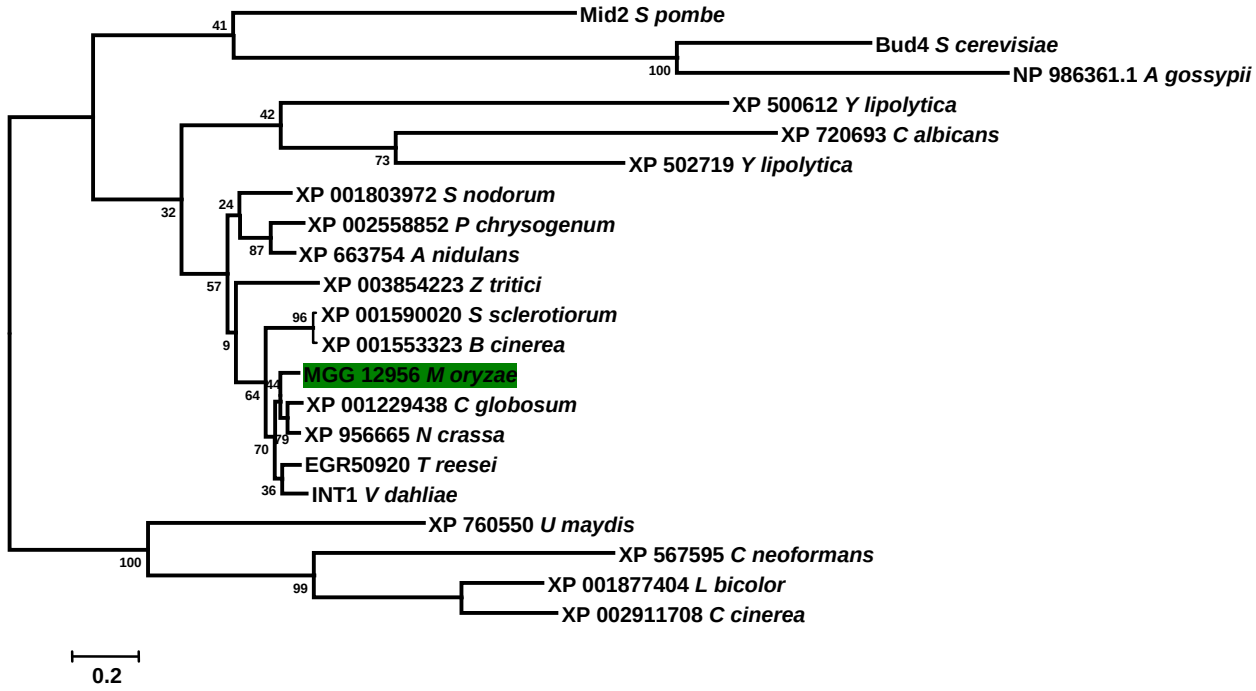

Figure 5.25: Phylogenetic analysis of PH domain containing protein MGG_12956. Protein sequences were aligned using MUSCLE version 3.8.31 (Edgar *et al.*, 2004). Maximum likelihood phylogenies were estimated from the curated alignment with PhyML version 3.0 (Guindon *et al.,* 2010). The most appropriate protein substitution model was selected using Model Generator (Keane *et al.*, 2006). The closest known relative of this protein is Bud4 of *Saccharomyeces cerevisiae.*

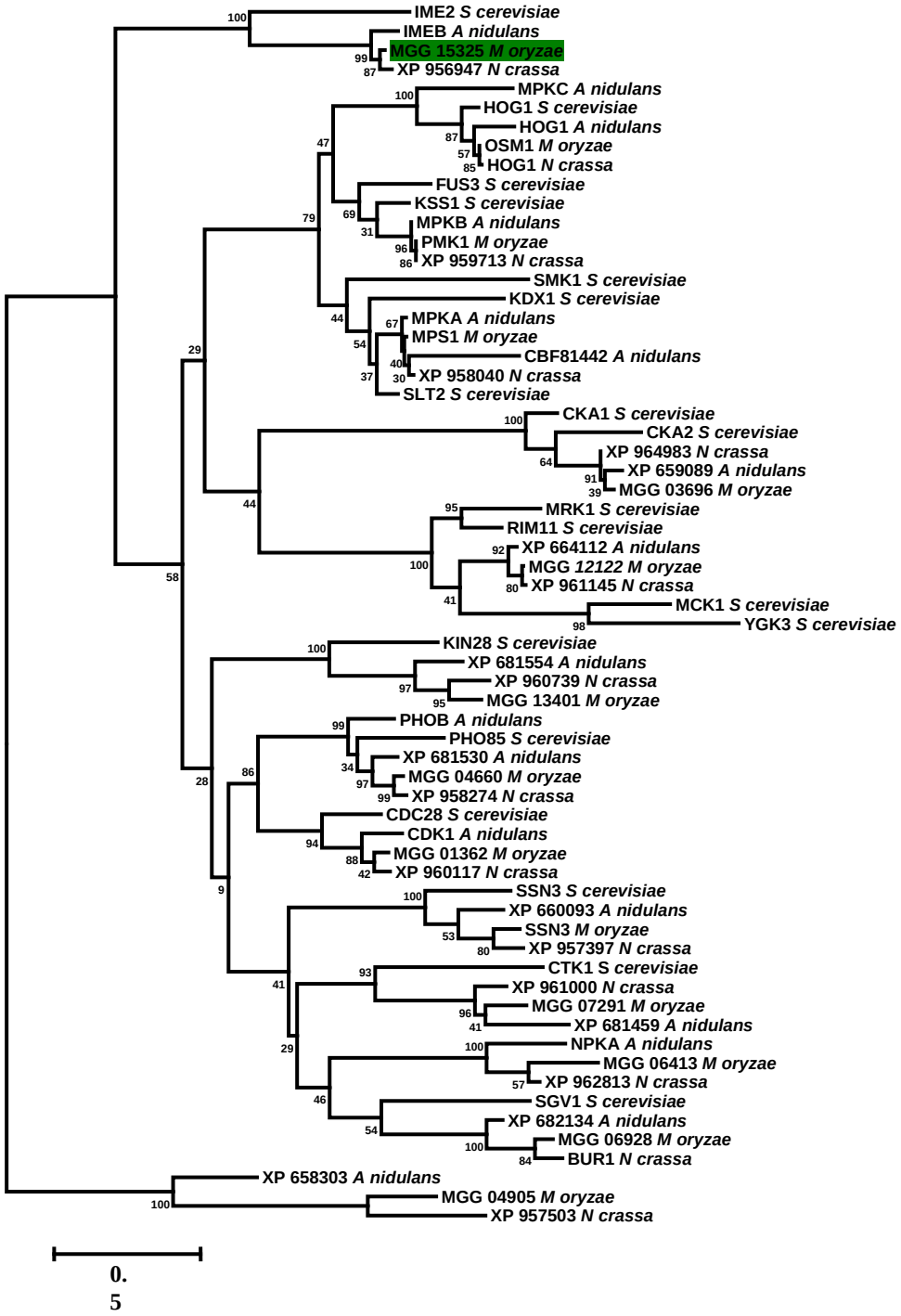

Figure 5.26: Phylogenetic analysis of the novel kinase encoding gene MGG_15325. Protein sequences were aligned using MUSCLE version 3.8.31 (Edgar *et al.*, 2004). Maximum likelihood phylogenies were estimated from the curated alignment with PhyML version 3.0 (Guindon *et al.*, 2010). The most appropriate protein substitution model was selected using Model Generator (Keane *et al.*, 2006). This protein belongs to the family of MAP kinases and the closest known homologous genes in its clade are *IME2* of *Saccharomyeces cerevisiae* and *IMEB* of *Aspergillus nidulans.*

5.3.8 Mutation of the DNA binding motif of novel transcription factor MGG_05343

The putative MGG_05343 protein is a GAL4-like transcription factor that consists of an N-terminal Zn2Cys6 binuclear cluster DNA-binding domain and a fungal transcription factor middle homology region (Fungal_TF_MHR). The latter is the regulatory module present in a large family of fungal zinc cluster transcription factors which contain a Zn2Cys6 binuclear cluster DNA-binding domain (DBD). Sequence alignment of the DBD of MGG_05343 with similar proteins from different fungi shows that there are conserved, positively-charged amino acid residues in the domain (Figure 5.27A). There is a conserved RRK (arginine and lysine) motif (shown in Red) preceded by H (histidine) in the MGG_05343 (the motif is HRRK). The closest homolog of this protein in *S. cerevisiae* is Put3. In Put3, the positively charged motif is RKRH and all these four positively charged residues are critical for DNA binding (Walters *et al.*, 1997). There are other conserved residues (shown in blue) and cysteine in the most essential one for binding the ligand Zn to form the characteristic tertiary structure.

Two putative 3-D structural models of the complex of the Put3 transcription factor from *S. cerevisiae* were constructed using the PyMOL molecular graphics system, version 1.2 (Schrodinger). Figure 5.27B-C shows the Put3 protein bound to its cognate DNA sequence. Figure 5.27B shows the protein (green) and DNA (orange/grey) in the cartoon format, with zinc ions shown as grey spheres. Figure 5.27C shows a close-up of the DNA-binding region, with conserved basic region (RKRH) shown with the side chains as sticks (carbon atoms coloured yellow, nitrogen atoms coloured blue). The cysteine side chains co-ordinating the zinc atoms are shown as lines, with carbon atoms coloured green, sulfur atoms coloured orange. This highlights that these conserved residues include residues that are intimately contacting the DNA. Therefore, mutation in this region is very likely to abolish function.

On the basis of 3-D structure of homolog Put3, we predicted that a mutant allele of MGG_05343 with an altered basic HRRK motif might be crucial for its function. Therefore, we constructed a mutant allele of MGG_05343 with HRRK motif replaced by AAAA (alanine). The mutant version of the protein was cloned and used to complement the Mutant M2942. As predicted, the mutant allele failed to complement the mutant M2942 (Figure 5.28). Thus, it was proved that these four positively charged residues are an essential component of the N-terminal Zn2Cys6 DBD of the transcription factor MGG_05343. This is consistent with the DNA binding activity of the protein being required for its function.

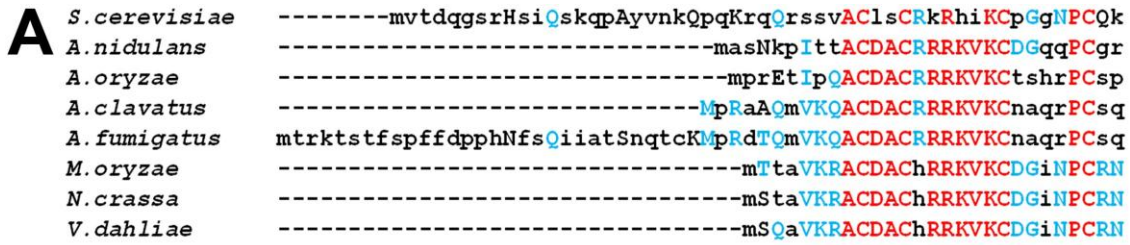

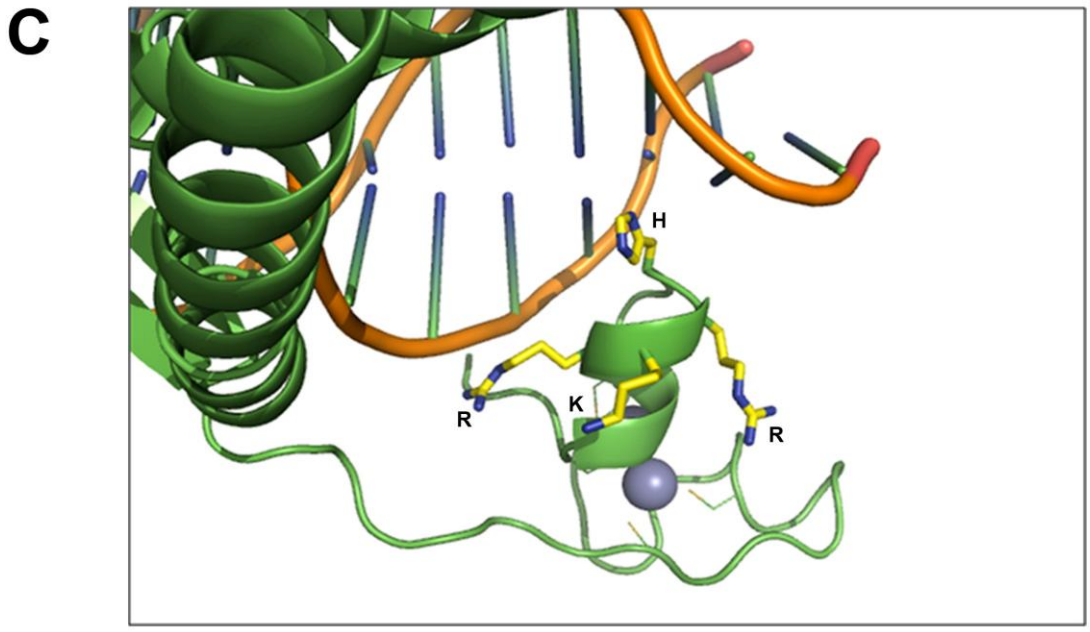

Figure 5.27: Sequence alignment of the putative DNA-binding domain of MGG_05343 with similar proteins and schematic representation of its predicted structure. A. Sequence alignment of the N-terminal Zn2Cys6 binuclear cluster DNA-binding domain of

MGG_05343 with similar proteins from different fungi. Sequence alignment shows that there are conserved, positively charged amino acid residues in the domain. There is a conserved RRK (arginine and lysine) motif (shown in Red) preceded by H (histidine) in the MGG_05343 (the motif is HRRK). In contrast the yeast homolog Put3 possesses a RKRH motif (Siddiqui & Brandriss, 1989; des Etages, 1996; Walters *et al.*, 1997) and all these four positively charged residues are critical for DNA-binding activity. There are other conserved residues (shown in blue) and cysteine in the most essential to form the characteristic structure by binding the ligand Zn. **B & C.** Two structural images of the complex of the Put3 transcription factor (Walters *et al.*, 1997) from *S. cerevisiae*, bound to its cognate DNA sequence (PDB code: 1ZME). This is the top hit from BLAST of the protein data bank with the protein MGG_05343 that shows the complex with DNA. Both images were made using the PyMOL molecular graphics system, version 1.2 (Schrodinger). Figure 5.27B shows the protein (green) and DNA (orange/grey) in the cartoon format, with zinc ions shown as grey spheres. Figure 5.27C shows a close-up of the DNA binding region, with the conserved basic region (RKRH in this case) shown with the side chains as sticks (carbon atoms coloured yellow, nitrogen atoms coloured blue). The cysteine side chains co-ordinating the zinc atoms are shown as lines, with carbon atoms coloured green, sulfur atoms coloured orange. This highlights that these conserved residues include residues that are intimately contacting the DNA and so mutation in this region was very likely to abolish the function of the protein.

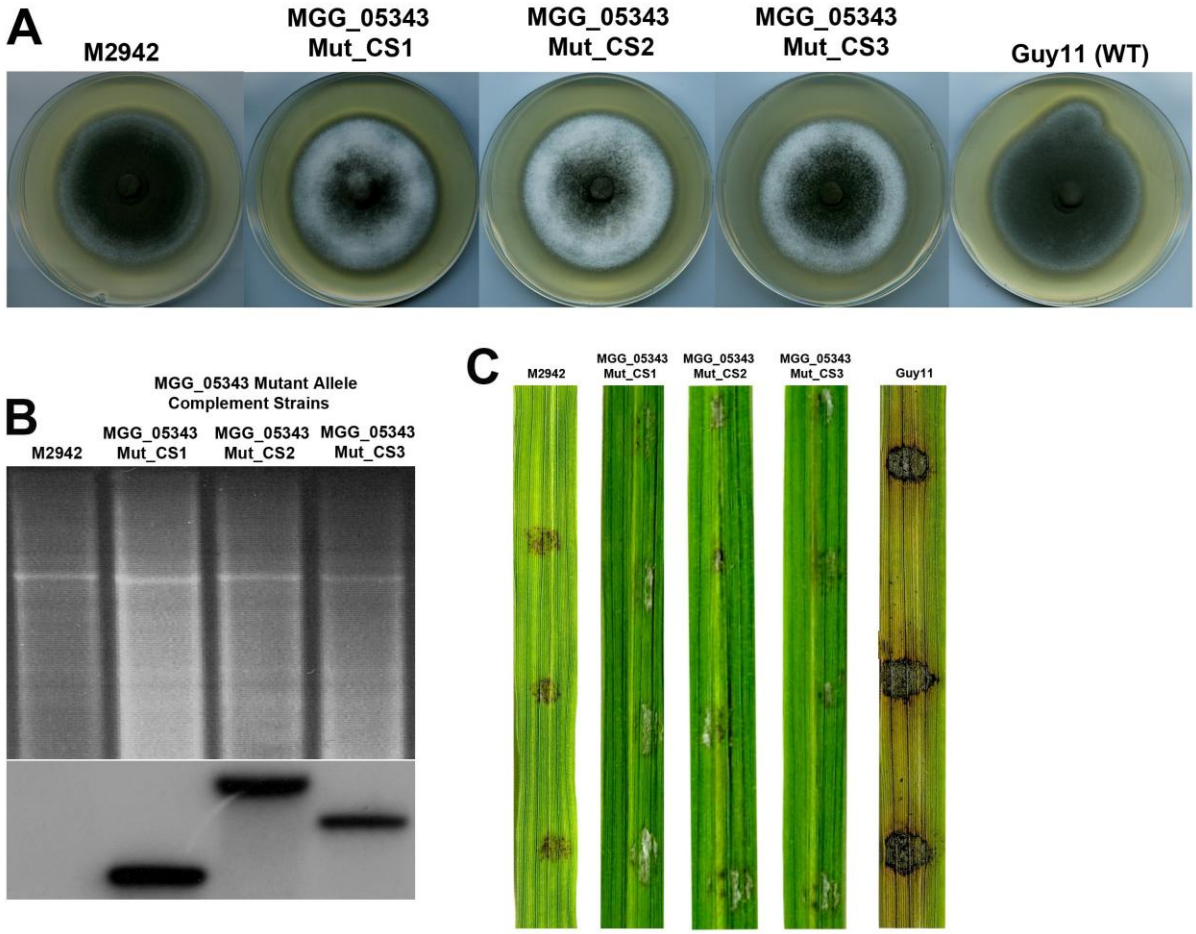

Figure 5.28: Transformation of mutant M2942 with a mutant allele of MGG_05343. Mutant M2942 was transformed with a mutant allele of MGG_05343 protein with HRRK-AAAA substitution. The mutant allele failed to complement the mutant M2942 for pathogenicity and conidiation. Thus, the HRRK motif is essential for the function of this putative transcription factor. **A.** Three complemented strains of mutant M2942 are shown. Complemented strains were assayed for conidiation and none of them produced conidia. **B.** Complemented strains were analyzed by southern blot to confirm the vector insertion in genomic DNA. Genomic DNA isolated from sulfonylurea resistant transformants was digested with the restriction enzyme *Xho*I, fractionated by agarose gel electrophoresis, blotted and probed with a 1 kb *ILVI* fragment generated by PCR amplification**. C.** Pathogenicity assay of three selected complemented strains are shown which was carried out by cut-leaf assay. The strains were unable to produce characteristic rice blast disease lesion which indicates the mutant allele of the gene MGG_05343 failed to complement the mutant M2942.

5.3.9 Introduction of point mutations in the functional motif of novel kinase encoding gene MGG_15325 (*IME2*)

We carried out a comprehensive phylogenetic analysis of the novel kinase MGG_15325, which is classified as a novel kinase in the family of MAP kinases (Figure 5.26). Protein sequence alignment with the Ime2 of *Saccharomyeces cerevisiae* (Smith and Mitchell, 1989; Yoshida *et al*., 1990) and ImeB of *Aspergillus nidulans* (Bayram *et al*., 2009) showed very strong homology between these proteins. Highly conserved N-terminal parts of the proteins showed 40% identity. In yeast, the catalytic domain of the Ime2 is located in the N-terminal region (Honigberg, 2004). The catalytic domain of MGG_15325 showed a highly conserved region with a TXY motif. The TXY motif is found in the catalytic domain of MAP kinases which is highlighted in the Figure 5.29. TXY motifs are highly conserved in the activation loop of MAP kinases and are known to be phosphor-acceptor sites for MAP kinase kinases (Payne *et al*., 1991). Therefore, the novel kinase MGG_15325 may be classified in the family of MAP kinases and predicted to be a potential Ime2 ortholog in *Magnaporthe oryzae*.

MGG_15325 contains the sequence motif TTY which corresponds to the characteristic TXY motif in its kinase domain. Previously, it was shown that dual phosphorylation on tyrosine and threonine residues are a prerequisite for kinase activation (Payne *et al*., 1991). To test the role of this motif in the activation of the predicted Ime2 kinase, we decided to introduce point mutations in the TTY motif with alanine and test the ability of these mutant alleles to complement corresponding insertion mutant M4874. We generated the mutant alleles containing T212A, T212A and Y214A point mutations. We also generated a version of MGG_15325 having TTY motif replaced with AAA (Figure 5.6). All these mutant alleles were cloned in the plasmid pNEB1284 by recombination-mediated PCR-directed plasmid construction *in vivo* in yeast (Oldenburg *et al.*, 1997) and transformed in mutant M8474.

Integration of each construct into the genome was determined by Southern blot hybridization analysis (Figure 5.30B) and selected transformants were assayed for pathogenicity by cut-leaf assay. None of the mutants were able to restore pathogenicity in mutant M4874 compared to the wild-type MGG_15325 allele which complemented the mutant (Figure 5.22C). We observed that even a single substitution in the TTY motif of the protein MGG_15325 inactivates the catalytic domain and failed to complement the phenotype. These point mutations provided evidence to support a crucial role of the TTY motif of MGG_15325 and hence established that the protein is probably a functional kinase of *M. oryzae*. We therefore conclude that the TTY motif is indispensable for kinase activity of the protein MGG_15325 and any mutation in this motif confers null activity on the protein.

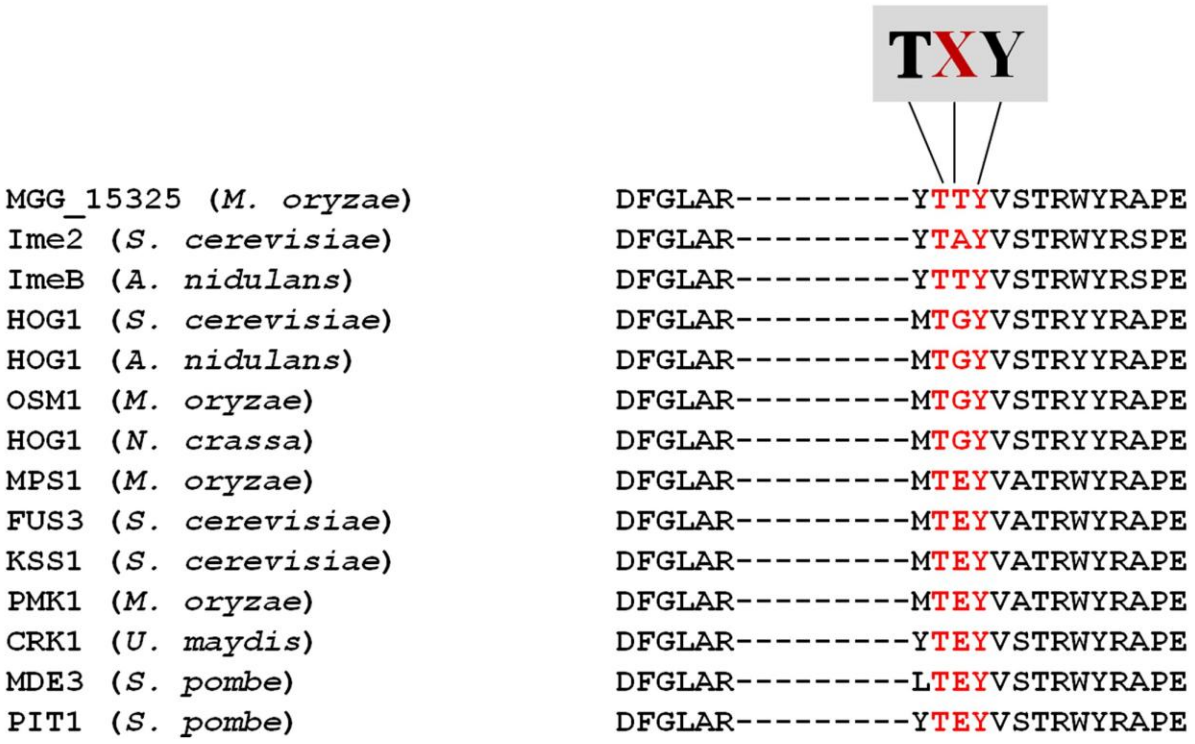

Figure 5.29: **Sequence alignment of conserved MAPK motifs from different organisms.**

From the phylogenetic analysis it was determined that the novel kinase MGG_15325 belongs to the family of MAP kinase. This protein consists of 808 amino acids and alignment with the Ime2 of *Saccharomyces cerevisiae* (Smith and Mitchell, 1989; Yoshida *et al*., 1990) and ImeB of *Aspergillus nidulans* (Bayram *et al*., 2009) showed very strong homology between these proteins. The N-terminal parts of the proteins are highly conserved, with 40% similarity between them. In yeast, the catalytic domain of the Ime2 is located in the N-terminal region (Honigberg, 2004). Sequence alignment of the catalytic domain of MGG_15325 with other related proteins from different organisms revealed a highly conserved region containing the TXY motif. The TXY motif is the hallmark of MAP kinases and it is highlighted in the image. TXY motifs are highly conserved in the activation loop of MAP kinases and known as phosphor-acceptor sites for MAP kinase kinases (Payne *et al*., 1991). Thus, MGG_15325 was predicted to be a potential Ime2 ortholog in *Magnaporthe oryzae* and it belongs to a family of MAP kinase like proteins conserved across eukaryotes.

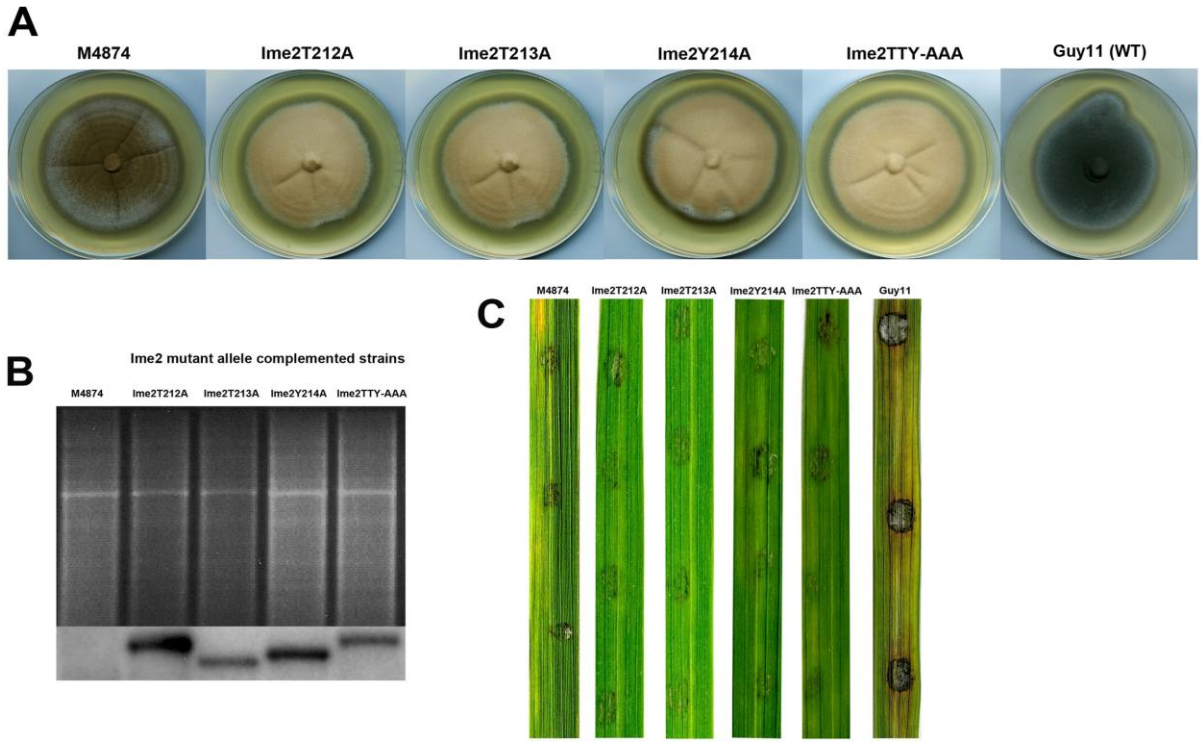

Figure 5.30: Transformation of mutant M4874 with mutant alleles of MGG_15325 (*IME2*). Three point mutation constructs (*ime2*^{T212A}, *ime2*^{T213A}, *ime2*^{Y214A}) and one complete replacement of the TXY motif of *IME2* (*ime2*$^{TTY\text{-}AAA}$) was constructed, cloned and transformed into M4874 to test the ability of mutant alleles to complacent the mutant. All the mutant alleles failed to complement the mutant. **A.** Four complemented strains of mutant M4874 are shown for each mutant allele. Vegetative growth of those mutants was similar to M4874 and it provided evidence that the point mutations and TXY mutant allele of *IME2* gene are null alleles. **B.** Complemented strains were analyzed by Southern blot hybridization to confirm vector insertion in genomic DNA. Genomic DNA isolated from sulfonylurea resistant transformants was digested with the restriction enzyme *Xho*I, fractionated by agarose gel electrophoresis, blotted and probed with a 1 kb *ILVI* fragment generated by PCR amplification. In this blot a strain for each mutant allele are shown. And the selected complemented strains showed positive results. **C.** Pathogenicity assay of four selected complemented strains are shown. Pathogenicity of the selected strains was assayed by cut leaf assay. Pathogenicity was not restored in the mutant M4874 by any of the mutant alleles which were shown by their inability to cause the disease. Therefore, the TXY motif is essential for *IME2* function and any mutation in this motif leads to the failure to complement mutant M4874.

5.3.10 Targeted deletion of the novel transcription factor MGG_05343

Reverse genetics was applied in order to validate the T-DNA tagging of a gene involved in conidiogenesis and pathogenicity. Targeted deletion of the C6 zinc finger transcription factor encoding gene MGG_05343 was carried out by the split marker deletion method (Catlett *et al.*, 2003). Following transformation, *M. oryzae* transformants were screened by resistance to hygromycin B (Carroll *et al*., 1994). Transformants were then screened for conidiation because it was already known that the T-DNA mutant M2942 is impaired in conidiation in which the T-DNA insertion has disrupted the MGG_05343 gene. Five non-conidiating transformants were selected and DNA was extracted. Transformants were confirmed by two sets of Southern blot hybridization analysis. Genomic DNA of the transformants, along with the wild-type were digested with *Xho*I for each set and fractionated in a 0.8% agarose gels by electrophoresis. The DNA was transferred to a Hybond-N membrane (GE Healthcare) and probed with a ~1 kb 5' flanking sequence (left flank) of the MGG_05343 locus and 1.4 kb hygromycin resistance gene cassette respectively. Figure 5.31C shows the blot probed with the left flank (~1 kb) of the MGG_05343 locus. All investigated transformants were deletion mutants as they produced a predicted 8.2 kb band compared to a predicted 1.9 kb band produced by the wild-type strain. The second blot was probed with a 1.4 kb hygromycin resistance gene cassette and the transformants showed positive results indicated by an 8.2 kb bands and an absence of band in the wild-type (Figure 5.31D). Vegetative morphology of the MGG_05343 deletion strain was similar to T-DNA mutant M2942. The targeted deletion starin failed to produce conidia and was found non-pathogenic when pathogenicity was assayed (Figure 5.32).

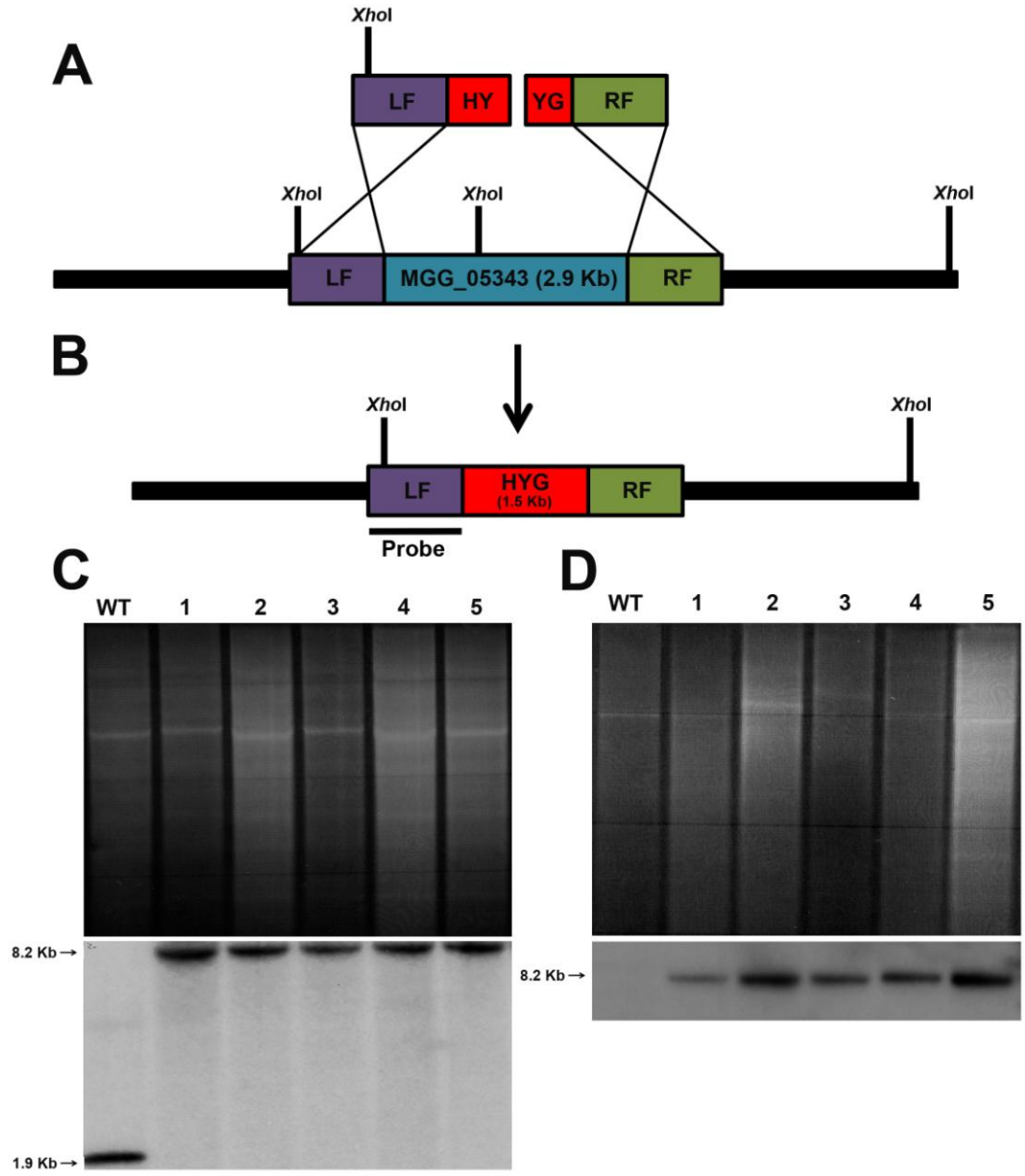

Figure 5.31: Targeted gene deletion of the novel transcription factor MGG_05343. **A.** Organization of the MGG_05343 locus showing the restriction sites. Targeted gene replacement constructs for gene deletion shows the mechanism of insertion by homologous recombination and generation of null mutants. **B.** The selectable marker gene (HYG, hygromycin phosphotranferase) replaced the MGG_05343 ORF in deletion mutant and restriction sites of the locus are shown. **C.** DNA gel blot analysis of MGG_05343 deletion mutant. DNA was digested with *Xho*I, fractionated, blotted and probed with a 1 kb LF (left flank). The wild-type produced a 1.9 kb band but the deletion mutants showed an 8.2 kb band because of the alteration of restriction site by the insertion of hygromycin resistance gene cassette. **C**. DNA gel blot analysis of MGG_05343 deletion mutant. DNA was digested with *Xho*I, fractionated, blotted and probed with a 1.4 kb *HPH* gene cassette. All of the deletion mutants showed positive results.

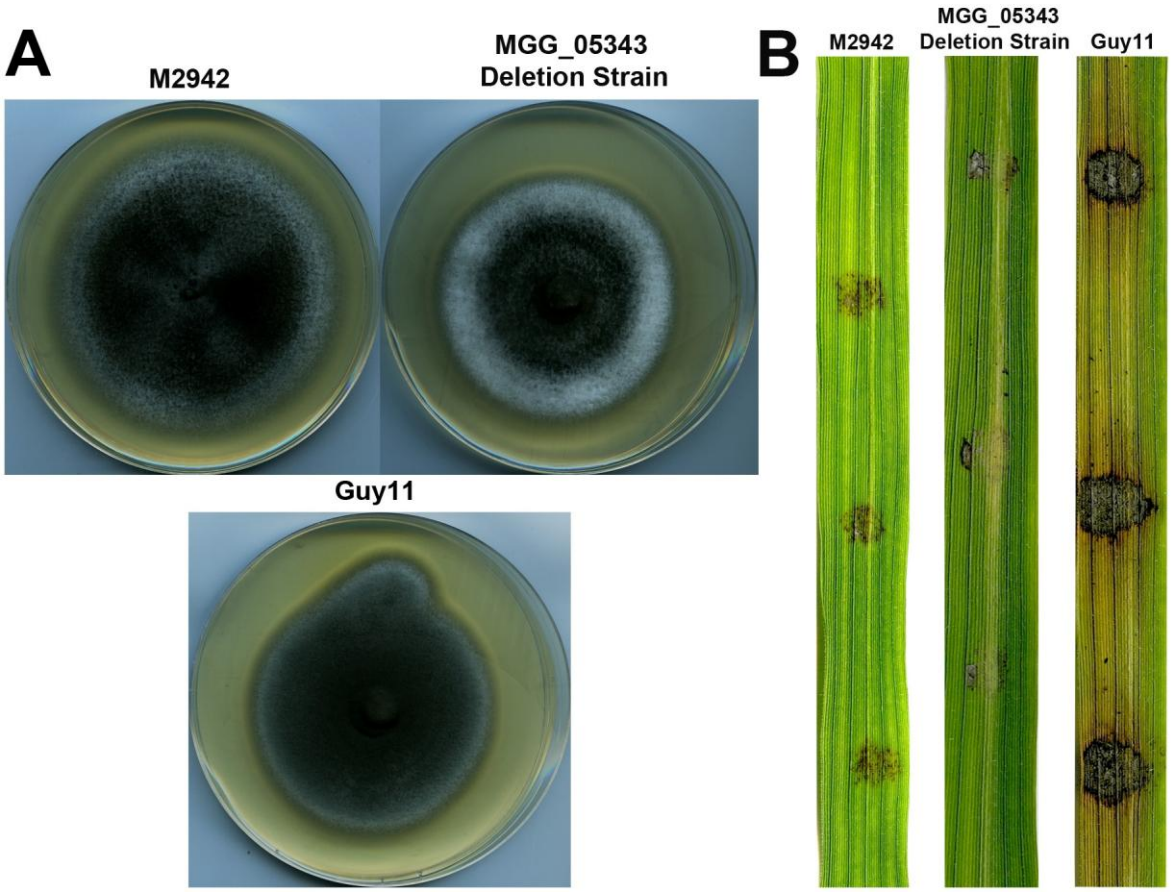

Figure 5.32: Targeted deletion mutant of *Magnaporthe oryzae* MGG_05343 and pathogenicity assay. **A.** Vegetative growth phenotype of the deletion mutant of MGG_05343 gene was similar to T-DNA insertional mutant M2942. Like M2942, the deletion mutant was also impaired in conidiogenesis. **B.** A 50 µL aliquot of diluted suspension of mycelium of the deletion strain was applied on rice leaf in order to assay its ability to cause disease. The deletion mutant showed the same result as M2942 and failed to produce any lesion when compared with Guy11.

5.4 Discussion

Here I have described the successful application of next generation sequencing in order to identify T-DNA flanks of insertion mutants. We managed to determine the T-DNA tagged loci in a high-throughput manner from a multiplexed sample of selected mutants, validated the insertions in each respective mutant by molecular genetic analysis and finally complemented the mutants with the cloned identified wild-type loci from *M. oryzae*. In this way, I was able to identify three novel genes from a pool of eight selected *M. oryzae* mutants. Thus, we have shown the advantages of NGS over conventional techniques to determine the T-DNA flanking sequences and demonstrate its potentiality in facilitating the pipeline for discovery of novel genes in a large scale forward genetics study.

To our knowledge, this is the first time NGS has been applied to identify T-DNA flanking sequences of insertion mutants generated by ATMT in fungi. Although application of NGS to identify transposon tagged sites have been reported in plants. For example, NGS was first reported to be used for identification of *Mutator (Mu)* transposon insertion sites of maize in a forward genetics study (Williams-Carrier *et al.*, 2010). Recently, Illumina sequencing has also been applied to identify T-DNA insertion loci in activation-tagged *Arabidopsis thaliana* plants (Polko *et al.*, 2012). But, no report has been published NGS as a method of high-throughput insertion site identification in fungi up to date. Therefore, we established Illumina based NGS as a tool for rapid identification of T-DNA tagged loci of fungal insertional mutants. We have shown the advantage and efficiency of this novel approach for large scale forward genetic study and subsequent identification of novel pathogenicity determinants from ATMT mutants of *M. oryzae*.

NGS technologies have a growing number of applications and the list consciously upgrading (Shendure & Ji, 2008; Elaine, 2008; Morozova and Marra, 2008; Metzker, 2009; McLean *et al.*, 2009). For instance, NGS was applied to map mutations on a genome-wide scale (Smith *et al.*, 2012) and therefore it is an efficient method for localizing the site of insertion (Smith, 2011). At present, Illumina sequencing is the most widely used NGS platform and we utilized its capability of generating millions of reads through massively parallel sequencing. In the chapter we mainly showed how Illumina paired-end sequencing was carried out to identify T-DNA tagged genes from some of the candidate mutants.

In Chapter 4, I reported selection of 8 non-pathogenic T-DNA mutants from comprehensive pathogenicity screening and phenotypic analysis. We identified two T-DNA tagged genes (*ATG2* and *ATG3* from mutant M1879 and M1054 respectively) by conventional methods i.e. TAIL-PCR and iPCR. Then we decided to retrieve the T-DNA flanking sequences from these 8 selected mutants by a novel high-throughput approach of Illumina sequencing. We pooled high-quality genomic DNA of eight non-pathogenic T-DNA mutants and paired-end sequencing library was constructed from the multiplexed sample for sequencing by Illumina HiSeq2000 system. From the mass of sequenced short reads (100 bp), those containing at least 15 bp sequence of *M. oryzae* genomic DNA sequences and 20 bp of T-DNA LB or RB sequences were identified with the help of programme Bowtie 0.12.7 (Langmead *et al.*, 2009). After trimming away the T-DNA sequences, the identified reads were then assembled using the programme Velvet (version 1.1) (Zerbino and Birney, 2008). *M. oryzae* genomic DNA sequence matches were identified using BLASTN against assembled sequence reads. Table 5.6 represents a summary of the type of insertions, identified locus and the T-DNA border sequence from which the flanks were retrieved.

By analysing all the assembled reads, we designed primers from the retrieved genomic DNA sequences and respective T-DNA border sequences (LB or RB) in order to validate the insertions in each respective locus. PCR confirmed seven insertions for seven mutants and we summarized the results of PCR in Table 5.6. We sequenced eight mutants but only seven insertions were found. We failed to attribute any insertion to mutant M2867 and an expected second insertion for mutant M1879 (M1879 showed a double T-DNA insertion which was shown in Figure 4.37. One of them was confirmed as the *ATG2* locus). In previous studies, truncation of T-DNA borders during integration has been reported ((Bundock and Hooykaas, 1996; de Groot *et al.*, 1998; Mullins *et al.*, 200; Combier *et al.*, 2003; Michielse *et al.*, 2004; Betts *et al.*, 2007b). Therefore, truncation of either of the T-DNA borders could be a potential reason that is why we failed to identify the expected flank from the reads with the search parameters we used. Sequence matches were found in *ATG3* and *ATG2* gene which in turn validated the results of TAIL-PCR and iPCR (Figure 4.38 &4.39). In fact, these two insertions worked as a control for the sequencing strategy undertaken. The remaining five T-DNA insertions were *M. oryzae* locus MGG_17516 in M48, MGG_17191 in M1880, MGG_12956 in M2048, MGG_05343 in M2942 and MGG_15325 in M4874.

By applying PCR, we were not only able to validate the insertion but also determined the orientation of T-DNA in the respective loci (Figure 5.10). We constructed the map of T-DNA insertions and set out to validate the insertions in even more elegant way of RFLP analysis. Restriction maps of the respective loci of T-DNA insertions were constructed for both wild-type and mutant locus was constructed. Restriction enzymes were chosen from the maps to generate a set of restriction fragments from single and double digestion of the enzymes and visualize them by Southern hybridization analysis. A systematic RFLP analysis was carried out for five loci of insertions (MGG_17516 in M48, MGG_17191 in M1880, MGG_12956 in

M2048, MGG_05343 in M2942 and MGG_15325 in M4874.) (*ATG3* was shown in chapter 4 and *ATG2* was excluded). Polymorphic restriction fragments observed from wild-type Guy11 and corresponding mutant matched the predicted fragment sizes and confirmed the T-DNA insertions in the identified *M. oryzae* loci.

Subsequently, after confirming the insertions unequivocally, we cloned five respective loci from the wild-type *M. oryzae* strain Guy11 and transformed them into the five corresponding mutants to test their ability to complement gene function. All the genes were systematically cloned including upstream promoter and downstream terminator sequences by using recombination-mediated PCR-directed plasmid construction *in vivo* in yeast (Oldenburg *et al.*, 1997). Resulting transformants were analyzed by Southern blot hybridization for vector insertions and positive transformants were assayed for pathogenicity. Three of the cloned genes MGG_12956, MGG_05343 and MGG_15325 complemented mutants M2048, M2942 and M4874, respectively. Two cloned genes, MGG_17516 and MGG_17191 failed to complement the mutants M48 and M1880 respectively. Although, these two genes were confirmed by.PCR and RFLP analysis to have T-DNA insertions within the ORF but they were unable to complement the candidate mutants.

MGG_17516 and MGG_17191 were annotated as encoding hypothetical proteins in the version 8 of the *M. oryzae* genome but they did not exist in the previous versions. Therefore, we assumed that they could be untranscribed genes or pseudogenes. This assumption was supported by the expression profile of putative identified genes. The expression profile (Figure 5.11) was constructed from a resource that was derived from a previous study on global patterns of gene expression during appressorium development by *M. oryzae* (Soanes *et al.*, 2012). It was observed that MGG_17516 and MGG_17191 are down-regulated

throughout the time course of appressorium development. Considering the facts, we assumed that the downstream genes of these two loci could be responsible for the observed phenotypes with T-DNA being in their promoter region. We cloned MGG_00184 and MGG_14847 as downstream genes of MGG_17516 and MGG_17191 respectively (Figure 5.10) and transformed in corresponding mutants M48 and M1880. Both of the genes were able to complement the mutants and each of them is already known to be involved in pathogenicity in rice blast disease. MGG_14847 is known as *MST11* (Zhao *et al.*, 2005) and mutant M1880 is phenotypically quite similar to Δ*mst11*. M1880 failed to develop appressoria similar to Δ*mst11*. *MST11* is the yeast *STE11* homolog in *M. oryzae* which acts as an upstream activator of Pmk1 MAPK cascade (Zhao *et al.*, 2005). Therefore, this gene is essential for pathogenicity. MGG_00184 is the putative *HOX2* gene which belongs to the group of eight homeobox domain containing genes in *M. oryzae* (Kim *et al.*, 2009; Liu *et al.*, 2010). *HOX2* is essential for conidiogenesis and Δ*hox2* mutants failed to produce conidia ((Kim *et al.*, 2009; Liu *et al.*, 2010). Similarly, mutant M48 was impaired in conidiation and upon introduction of cloned *M.oryzae HOX2* gene complementation occurred. Complemented were able to produce conidia and cause necrotic rice blast lesions. Moreover, the cloned *HOX2* complementation construct was also transformed into the Δ*hox*2 mutant (Kim *et al.*, 2009), which was generated in wild-type KJ201 strain. The deletion mutant was also complemented and ultimately proved that *HOX2* gene function was affected by T-DNA insertion in *mutant* M48. From the scenario of these two mutants, we conclude that T-DNA integration in MGG_17516 and MGG_17191 in fact affected the downstream genes *HOX2* and *MST11* respectively by interrupting the function of promoter.

In essence, by complementation we actually confirmed three novel genes out of eight candidate non-pathogenic mutants. MGG_05343 was found to be responsible for impaired conidiogenesis and pathogenicity in mutant M2942 and this was also confirmed by generating a corresponding deletion mutant. Targeted deletion of the *M. oryzae* MGG_05343 resulted in mutant defective in conidiation and pathogenicity. MGG_12956 was confirmed as the gene interrupted in M2048 which resulted in impaired conidiogenesis, reduced growth and consequent loss of pathogenicity. In mutant M874, MGG_15325 locus was found to be affected by T-DNA integration within its promoter that resulted in characteristic appearance of M4874 and non-pathogenic phenotype. We identified putative functional domain of these three novel proteins involved in pathogenicity. Protein MGG_12956 has one anillin domain which is found in cell division protein anillin and a pleckstrin homology (PH) domain in the C-terminal region (Mayer *et al.*, 1993; Haslam *et al.*, 1993; Yoon *et al.*, 1994; Field and Alberts, 1995). MGG_05343 contains an N-terminal GAL4-like Zn2Cys6 binuclear cluster DNA-binding domain (DBD) (Baleja *et al.*, 1992; Kraulis *et al.*, 1992). This domain consists of two helices organized around a Zn2Cys6 motif. This protein also has a regulatory module found in the family of fungal zinc cluster transcription factors that contain a GAL4-like Zn2Cys6 binuclear cluster DNA-binding domain. Therefore, MGG_05343 is a putative transcription regulator controlling gene expression. MGG_15325 was found to be a kinase containing a conserved protein kinase (PK) domain and homologous domains are putative functional module of serine-threonine kinases (STKs).

In order to classify the novel genes and predict their potential function, detailed phylogenetic analysis was carried out for three putative novel proteins. The best known homolog of MGG_12956 is Bud4 in budding yeast *Saccharomyces cerevisiae*. Bud4 is an anillin domain containing GTP-binding protein required for bud-site selection and necessary for axial

budding pattern (Chant and Herskowitz, 1991; Sanders and Herskowitz, 1996). During mitosis it localizes with septins to the bud neck (Sanders and Herskowitz, 1996) acting as a landmark for the initiation of budding (Chant and Herskowitz, 1991). Bud4 is also involved in septin organization (Eluere *et al.*, 2012). In addition, MGG_12956 contains a Pleckstrin homology domain (PH) in its C-terminus that is found in diverse class of proteins including serine/threonine and tyrosine kinases, phospholipase C, GTPase activating proteins, nucleotide exchange factors and cytoskeletal elements (Mayer *et al.*, 1993; Haslam *et al.*, 1993; Musacchio *et al.*, 1993; Shaw, 1993; Parker *et al.*, 1993; Gibson *et al.*, 1993). Depending on the specificity, PH domain can bind number of ligands including phosphatidylinositol lipid constituents of membranes (Wang & Shaw, 1995) and proteins such as protein kinase C (Yao *et al.*, 1994) and the βγ-subunits of heterotrimeric G proteins (Wang *et al.*, 1994). The main function of PH domains include, targeting proteins to appropriate cellular compartments and facilitating interaction with other components of the signalling pathways (Pitcher *et al*., 1992; Koch *et al*.; 1993; Cifuntes *et al*., 1993; Davis and Bennett, 1994; Ingley and Hemmings; 1994). These suggest that MGG_12956 may have important role in signal transduction which is involved in regulating vegetative growth and also essential for conidiogenesis.

MGG_05343 complemented the mutant M2942 which is a transcription factor that consists of a Zn2Cys6 binuclear cluster DNA-binding domain (DBD) in its N-terminal and another regulatory module. This domain containing protein are also named as GAL4-like transcription factor after the name of yeast GAL regulon regulatory gene *GAL4* (Keegan *et al.*,1986; Johnston, 1987; Johnston *et al.*, 1987; Severne *et al.*, 1988; Freedman *et al.*,1988). The trace element zinc is required for the function of a large number of proteins and predominantly they are transcription factors named zinc finger proteins. They form one of the

largest families of transcriptional regulators and are categorized into various classes according to zinc-binding motifs **(**MacPherson *et al.*, 2006). The best homolog of this protein in yeast *S. cerevisiae* is Put3 which is the activator of the proline utilization pathway (des Etages *et al.*; 1996**).** PUT3 regulates expression of the genes encoding the enzymes PUT1 and PUT2 that convert proline to glutamate (Siddiqui and Brandriss, 1989). It contains a positively charged motif RKRH (Walters *et al.*, 1997). Predicted 3-D structures showed that all these four positively charged residues are critical for DNA binding. In MGG_05343, the DBD contains a similar positively charged motif which is HRRK. To determine the role of this DNA binding motif, we constructed a mutant allele by replacing the HRRK with AAAA and transformed into mutant M2942 to test its ability to complement. The mutant allele of MGG_05343 failed to complement the mutant M2942 which proved HRRK motif is essential for its function. Thus, MGG_05343 belongs to the class of Zn2Cys6 transcription factor.

The putative novel kinase, MGG_15325 complemented the mutant M4874. From a comprehensive phylogenetic analysis we showed that MGG_15325 is the putative Ime2 homolog of *S. cerevisiae* (Smith and Mitchell, 1989; Yoshida *et al*., 1990) and ImeB of *Aspergillus nidulans* (Bayram *et al*., 2009). N-terminal catalytic domain of the protein is highly conserved and possesses a TXY motif in its activation loop which is consistent with the MAPK family of kinases. Therefore, this novel kinase MGG_15325 could be classified as a Ime2 type MAP kinase (Hamel *et al.*, 2012). It was shown in a previous study that a dual phosphorylation on tyrosine and threonine of this TXY motif is a prerequisite for kinase activation (Payne *et al*., 1991). We showed that the TXY motif of MGG_15325 (the sequence element is TTY) is essential for function of this protein. A complete replacement of this motif and single amino acid substitution resulted in inactive kinases and all of them failed to complement the corresponding mutant M4874. In yeast, Ime2 regulates the meiotic cell cycle

(Guttmann-Raviv *et al.*, 2002). Interestingly, studies on homologous protein in various fungal species indicates that Ime2 kinases are also essential for a number of processes, including ascospore formation, pseudohyphal growth and sexual reproduction in response to light and nutrient deprivation (Irniger, 2011). A noteworthy example is the Ime2 homolog Crk1 of corn smut fungus *U. maydis* which is involved in mating and virulence (Garrido *et al.*, 2004 2003). Considering the diverse role of Ime2 homologs, the novel kinase MGG_15325 of *M. oryzae* could be regarded as the most intriguing determinant of pathogenicity we have obtained in this insertional mutagenesis study.

In conclusion, we demonstrated the advantages of NGS technology for high-throughput identification of T-DNA tagged loci from candidate mutants. We identified three novel genes from right selected mutants, which indicate a 37.5% probability of identifying novel determinants from our selected cohort of mutants. In chapter 4, I selected 62 reduced virulence T-DNA mutants from exhaustive screening procedure and T-DNA tagged genes of these mutants can be identified in high-throughput manner by applying this NGS based strategy we have shown. Depending on the obtained rate of identified novel genes, a number of novel virulence genes could be expected from the remainder of mutants.

Chapter 6

General Discussion

The main purpose of this study was to use an unbiased means of identifying novel determinants of pathogenicity in the rice blast fungus *M. oryzae*. Identification of new virulence determinants in the rice blast fungus has shown rapid progress in recent years (Wilson and Talbot, 2009; Li *et. al.*, 2012). In parallel, *M. oryzae* has emerged as a highly tractable experimental fungus for studying host-pathogen interactions. Development of new strategies for gene functional analysis has facilitated the emergence of *M. oryzae* as a model and also catalyzed investigation of the most serious threats to global food security. The availability of a complete genome sequence of *M. oryzae* has provided unprecedented opportunities to apply high-throughput methods for gene functional analysis, ranging from gene identification to genome-wide expression profiling and proteomics (Wilson & Talbot, 2009). However, the investigation of the biology of plant infection in rice blast disease has been dominated by the reverse genetic approaches. Targeted gene deletion analysis has been used to identify most of the genes involved in pathogenicity to date and has therefore provided significant insight into morphogenesis of the appressorium, major signalling pathways for appressorium development (e.g. MAP kinase cascade, cAMP signalling), turgor generation, infection-related autophagy, cell cycle control, appressorium-mediated plant infection, invasive growth, the physiology of plant infection and evasion of plant defences (Wilson & Talbot, 2009).

These studies have provided a conceptual framework for understanding the disease. Nonetheless, most of the genes identified and studied by reverse genetics are functional equivalent of homologous genes in other organisms. Therefore, the identification of

completely novel determinants of pathogenicity by targeted gene knockout is difficult. In contrast, forward genetic approaches uncover genes necessary for pathogenesis in an unbiased manner. Hence, completely novel virulence determinants can be identified by forward genetic screens. Insertional mutagenesis is an effective forward genetics tool to discover novel genes. Insertional mutagenesis screens aims to achieve an efficient random disruption of the genome and subsequent retrieval of tagged genes from the mutant of interest (Michielse *et al.*, 2005). The low efficiency of DNA-mediated transformation has, however largely precluded insertional mutagenesis as an effective method for gene identification. However, this limitation was overcome by application of *Agrobacterium tumefaciens*-mediated random insertional mutagenesis in order to construct large mutant collections in *M. oryzae*. A large scale T-DNA tagging study for example, generated a collection of 21,070 *M. oryzae* mutants and showed coverage of 61% of the *M. oryzae* genome. This mutant collection allowed identification of more than 200 novel loci required to cause rice blast disease (Jeon *et al.*, 2007). A similar study by Betts *et al.* (2007) has generated >39,000 *M. oryzae* transformants by ATMT in a library of >56,000 insertional strains. This has been the most comprehensive ATMT-mediated insertional mutagenesis studies to date and identified more than 200 novel mutants of *M. oryzae*. Moreover, this study also showed the manifold efficiency and advantages of ATMT by comparing the method with conventional plasmid transformation as an insertional mutagenesis tool for novel gene discovery (Betts *et al.*, 2007).

In the current project, we adopted T-DNA tagging to identify novel determinants of pathogenicity in rice blast disease. Advantages of ATMT include high efficiency transformation, random insertions in the genome and a high percentage of single copy insertions (de Groot *et al.*, 1998; Chen *et al.*, 2000; Mullins et al. 2001; Rho et al.2001; Betts

et al., 2007; Michielse *et al.,* 2009). By applying ATMT, a library of 10,200 M. *oryzae* T-DNA tagged mutants was generated at the beginning of this study and subsequently we determined that 84% of the mutants generated were a single T-DNA copy mutant which is consistent with previous studies (Betts *et al.,* 2007). We developed a high-throughput screening system that enabled us to screen the mutants for pathogenicity in a systematic way. Although laborious, we decided to carry out whole plant infection assays by spray inoculation because this is arguably a better way to produce realistic pathogenicity phenotypes compared to cut-leaf, or test tube assays. From primary screening of this library, 200 mutants were identified impaired in pathogenicity which represents the 1.96 % of the library. Considering the annotated 12,827 genes (version 8) of *M. oryzae* and the random nature of T-DNA insertion it can be assumed that a maximum of ~2 % of genes associated with virulence have been tagged in these mutants selected from primary pathogenicity screening. Primary selection included the non-pathogenic and reduced virulence mutants compared to the isogenic wild-type strain Guy11. These mutants were re-screened by quantitative plant infection assays to allow assessment of the consistency and reproducibility of observed phenotypes. After rigorous re-screening, I confirmed 9 non-pathogenic mutants and 62 reduced-virulence mutants that were selected on the basis of a threshold of ≤50% reduction in pathogenicity. Finally, I selected 8 non-pathogenic mutants for gene functional analysis.

In this study, I applied a novel approach for identifying T-DNA tagged loci of selected mutants. Next generation sequencing (NGS) was used for the first time in an insertional mutagenesis study in fungi to retrieve T-DNA flanking sequences in a high-throughput manner. NGS facilitated the identification of 7 tagged loci from the 8 selected mutants which suggests an 87.5 % recovery of T-DNA tagged genes. Such a high recovery rate justifies the efficiency of NGS as a method to aid insertional mutagenesis studies. All of the insertions

were unequivocally validated by PCR and RFLP analysis. Among the 7 identified loci, 4 loci had T-DNA inserted within gene coding regions and 3 have T-DNA insertions in putative promoter regions. This finding confirmed the random nature of T-DNA insertion. Application of NGS allowed discovery of 3 novel genes from 8 non-pathogenic mutants, which indicates a 37.5 % probability of tagging novel genes from selected mutants. We selected a total of 71 mutants on the basis of a stringent threshold for the pathogenicity phenotype and 63 potential mutants have yet to be studied. If the current rate of finding novel genes (37.5 %) is taken into account, then a maximum of 25 novel genes could be expected from the remainder of these unidentified mutants, assuming random T-DNA integration.

Among the identified genes, four have previously been shown to be determinants of pathogenicity in rice blast disease. Interestingly, two genes involved in infection-related autophagy were tagged by T-DNA in the library. *ATG3* and *ATG2* genes are essential for infection-related autophagy which leads to conidial cell death and culminates in formation of functional appressorium necessary for plant infection. (Kershaw & Talbot, 2009). We also identified the homeobox gene *HOX2*, which is essential for conidiogenesis and pathogenicity (Kim *et al.*, 2009; Liu *et al.*, 2010). Furthermore, a MAPK kinase gene *MST11* was also tagged by T-DNA insertion, which is the upstream activator of the *PMK1* encoded MAP kinase which is required for appressorium development (Zhao *et al.*, 2005). Phenotypic characterization of these four non-pathogenic mutants was consistent with the previously characterized gene deletion mutants. Tagging these four previously reported genes confirms the efficiency and randomness of ATMT as an insertional mutagenesis tool for identification of virulence genes required for pathogenicity in *M. oryzae*.

6.1 Novel genes involved in pathogencity identified in this study

Among the novel genes, we identified MGG_05343 from mutant M2942, which putatively encodes a transcription factor involved in conidiogenesis. The putative protein contains an N-terminal Zn2Cys6 binuclear cluster DNA-binding domain (DBD) which is found in many transcription regulators. Proteins containing this domain are classified as GAL4-like transcription factors after yeast GAL regulon regulatory gene *GAL4* (Keegan *et al.*,1986; Johnston, 1987; Johnston *et al.*, 1987; Severne *et al.*, 1988; Freedman *et al.*,1988; Baleja *et al.*, 1992; Kraulis *et al.*, 1992). The MGG_05343 protein belongs to a large family of fungal zinc cluster transcription factors that also possess a fungal transcription factor regulatory middle homology region (Fungal_TF_MHR). Zinc ions are required for co-ordinate formation of the characteristic DBD and therefore are referred to as zinc finger proteins. Zinc finger proteins are categorized into various classes according to zinc-binding motifs **(**MacPherson *et al.*, 2006). A homolog of the MGG_05343 product in yeast *S. cerevisiae* is Put3 which the activator of the proline utilization pathway and contains a positively charged motif RKRH (des Etages *et al.* 1996; Walters *et al.*, 1997)**.** The 3-D structure suggests that these four positively charged residues are critical for DNA binding and therefore, we tested the function of a similar positively charged motif HRRK in the DBD of MGG_05343. A constructed mutant allele failed to complement the mutant M2942 consistent with the predicted function of MGG_05343 as a Zn2Cys6 transcription factor. *M. oryzae* genome encodes 453 putative transcription factors and among them 228 are zinc-finger transcription factors (Dean *et al.*, 2005). In spite of such a large number of zinc binding transcription factors in the genome, few have been studied in detail.

A limited number of transcription factors have been identified that regulate conidiogenesis. The first morphogenetic locus identified in *M. oryzae* was *smo* (spore morphology locus) that

affects conidial shape but not the ability to sporulate (Hamer *et al.*, 1989). Shi and Leung (1994, 1995) identified several genetic loci, such as *CON1-7*, that control each stage of conidiogenesis. Most of these loci have not been characterized in detail, therefore mechanism whereby they regulate conidiogenesis is not very well understood. The *CON7* gene was studied in more detail which identified it as a transcription factor but its role in regulating conidiation has not been revealed (Odenbach *et al.*, 2007). Homeobox domain-containing proteins were also shown to be involved in conidiogenesis and interestingly, we identified *HOX2* in our study (Kim *et al.*, 2009; Liu *et al.*, 2010). In the model filamentous ascomycete fungus *Neurospora crassa*, a Zn2Cys6 transcription factor gene *FL* (fluffy) has been described as a regulator of genes involved in conidiogenesis (Rerngsamran *et al.*, 2005). Recently, a zinc finger transcription factor encoding gene *COS1* was identified by T-DNA tagging in *M. oryzae* and regulates genes involved in conidiophore development and production of conidia. Interestingly, this gene is dispensable for pathogenicity (Zhou *et al.*, 2009). We observed the same phenotype in the case of M2942 which showed necrotic lesion formation by infecting wounded leaves (Figure 4.10). This is consistent with the predicted role for MGG_05343 in conidiogenesis, but not plant tissue invasion. Later, we also confirmed the non-conidial phenotype by generating a targeted gene deletion strain for MGG_05343. The deletion mutant showed the ability to infect wounded leaves and cause disease, but consistently showed impairment in sporulation (data not shown). However, transcriptional profiling data showed up-regulation of MGG_05343 throughout a time course of appressorium development. This suggests that the transcription factor may have additional gene regulatory functions during appressorium development coupled to conidiogenesis but dispensable for plant infection. Activity of Zinc finger transcription factors is dependent on some important features. For example, their ability to bind DNA depends on recognizing conserved DNA sequence elements containing trinucleotide sequences in single or repeat

forms such as CGG triplets. Large variations within these binding elements can however be found (MacPherson *et al.*, 2006). Chromatin immunoprecipitation (ChIP-Seq) could be used in future to information about target binding sites of MGG_05343. A GFP translational fusion protein should also be constructed and expressed in *M. oryzae* to observe localization of the gene product in conidiophores and during appressorium morphogenesis. GFP-Trap method followed by mass spectrometry may also facilitate identification of interacting proteins of this transcription factor (Dagdas *et al.*, 2012). It is known that zinc finger proteins potentially interact with other zinc finger proteins and chromatin remodelling proteins for example (MacPherson *et al.*, 2006). Zinc finger proteins require activation by phosphorylation within C-terminus. Site-directed mutagenesis experiment that we applied to confirm the DBD could also be applied to examine activation by phosphorylation. Moreover, this class of transcription factors may act as a monomer or dimer. NMR spectroscopy and X-ray crystallography could therefore be applied to investigate whether MGG_05343 forms a dimer (MacPherson *et al.*, 2006). The suggested experiments could provide insight into its potential role in condiogenesis.

Locus MGG_12956 was the second gene confirmed as a determinant of conidiation and reduced hyphal growth in mutant M2048. The putative protein product of gene MGG_12956 has one anillin domain, named after the cell division protein anillin (Field and Alberts, 1995) and a pleckstrin homology (PH) domain in its C-terminal region (Mayer *et al.*, 1993; Haslam *et al.*, 1993; Yoon *et al.*, 1994). The Anillin domain was first identified in the highly-conserved, multidomain cell division protein anillin, which is involved in septin organisation, interacting with cytoskeletal components such as actin, myosin and microtubules. It also a plays a crucial role in cytokinesis and maintaining cell shape. Moreover, anillin has been implicated as a scaffold protein that mediates interaction with other associated proteins.

(Piekny and Maddox, 2010). In *M. oryzae* there are 19 PH-domain containing proteins including the transporter protein Sec73 and guanine nucleotide exchange factor Rho1 (Dean *et al.*, 2005). PH domains are found in diverse signalling proteins including serine/threonine and tyrosine kinases, lipid associated enzymes, phospholipase C, GTPase activating proteins, nucleotide exchange factors, adaptors and cytoskeletal elements (Mayer *et al.*, 1993; Haslam *et al.*, 1993; Musacchio *et al.*, 1993; Shaw, 1993; Parker *et al.*, 1994; Gibson *et al.*, 1994). PH-domains have little sequence conservation, but all share a common fold. PH domains also have diverse functions. For example, they bind to many important ligands such as phosphatidylinositol rich lipid constituents of membranes and this depends on specificity of the domain. Specificity is determined by the loop regions or insertions in the N-terminus of the domain, which are not conserved across all PH domains (Wang & Shaw, 1995). PH domains can also bind a number of proteins such as protein kinase C (Yao *et al.*, 1994) and βγ-subunits of heterotrimeric G proteins (Wang *et al.*, 1994). The main assigned role of PH domains include targeting proteins to different membrane domains or appropriate cellular compartments and to facilitate interaction with other components of signal transduction pathways (Pitcher *et al*., 1992; Koch *et al*.; 1993; Cifuentes *et al*., 1993; Davis and Bennett, 1994; Ingley and Hemmings; 1994). From phylogenetic analysis we found that the most well known homolog of MGG_12956 is the *BUD4* in budding yeast *Saccharomyces cerevisiae*. Bud4 is an anillin domain-containing GTP-binding protein involved in bud-site selection and therefore, is necessary for axial budding pattern. This protein was found to be co-localized with septins to the bud neck during mitosis acting as a landmark for budding (Chant and Herskowitz, 1991; Sanders and Herskowitz, 1996). Bud4 have also been implicated in septin organization (Eluere *et al.*, 2012).

Considering the myriad roles of Anillin and PH domain, we assume that the MGG_12956 may serve an important role in cellular signaling involved in vegetative growth and condiogenesis. Recently, it has been shown that appressorium-mediated plant infection by *M. oryzae* is a septin-dependent mechanism. Septins are involved in organizing a toroidal actin network via direct phosphoinositide links plasma membrane to the cortical actin cytoskeleton (Dagdas *et al.*, 2012). Since this novel protein has the potential to interact with septins therefore it would be interesting to identify interactors by yeast two-hybrid screening or co-immunoprecipitation. Construction of a GFP fusion would also be very useful in identifying potential interactors as well as providing evidence for its sub-cellular localization. SuperSAGE data suggested that the MGG_12956 gene is up-regulated at the onset of appressorium development but its expression gradually declines as the appressorium matures (Figure 5.11) consistent with a signalling function during appressorium development. Similarly, the protein might play a role in invasive growth of *M. oryzae* during plant infection, because the mutant M2048 showed a reduced ability to cause lesion formation (Figure 4.10). Furthermore, the mutant was also reduced in vegetative growth and impaired in conidiation. Future investigation will be necessary to determine the role of this novel signalling protein which affects conidiogenesis, growth and virulence and therefore has broad function in growth and development.

The most intriguing gene identified from this insertional mutagenesis study was, however a putative MAP kinase encoding gene *IME2* (MGG_15325). Comprehensive phylogenetic analysis showed that MGG_15325 is the likely homolog of Ime2 of *Saccharomyces cerevisiae* (Smith and Mitchell, 1989; Yoshida *et al*., 1990) and ImeB of *Aspergillus nidulans* (Bayram *et al*., 2009). This protein contains an N-terminal kinase domain with a TXY motif in its activation loop, which is the hallmark of MAP kinase family of protein kinases. This

gene complemented mutant M4874 for pathogenicity and subsequently we tested function of the TXY motif by introducing point mutations. Mutagenesis provided evidence that MGG_15325 encodes a functionally-active kinase and therefore, this novel kinase *IME2* could be potentially classified as a new member of the family of Ime2 type MAP kinases (Hamel *et al.*, 2012).

In budding yeast *Saccharomyces cerevisiae*, Ime2 was first identified as a regulator for induction of meiosis and sporulation (Smith and Mitchell 1989). This protein serves both early and late roles in meiosis, including the initiation of meiosis, meiotic DNA replication, meiotic divisions I and II, and ascospore formation (Benjamin *et al.*, 2003; Honigberg 2004; Brush *et al.*, 2012).The major role of Ime2 is activation of the major middle meiotic transcription factor NDT80 by phosphorylation. (Pak and Segall 2002; Sopko *et al.*, 2002; Shubassi *et al.*, 2003; Shin *et al.*, 2010). Ime2 also positively regulates spore morphogenesis by activating a MAPK-related kinase Smk1 which is required for the formation of the outer spore wall layer (Krisak *et al*., 1994; Huang *et al*., 2005). Although the function of Ime2 was believed to be strictly limited to meiosis and ascospore formation, but recently it has been assigned an additional function of pseudohyphal formation in yeast (Strudwick *et al.*, 2010). Ime2 acts a regulator of the dimorphic transition in yeast (Strudwick *et al.*, 2010). Characteristics of pseudohyphal cells include elongated cell shape, budding from either axial buds in haploids or the opposite pole in diploids and the adhesion of cells after cell division (Inringer, 2011).

In filamentous fungi, Ime2 homologs appear to serve diverse roles apart from meiosis. In *Aspergillus nidulans*, the Ime2 homolog ImeB inhibits light-dependent sexual development. It is necessary for production mycotoxin sterigmatocystin and ImeB regulates the

sterigmatocystin gene cluster. Ime2 homolog Crk1 of the corn smut fungus *U. maydis* is involved in mating and virulence. Mating and virulence are tightly linked in *U. maydis* and therefore, Crk1 is required for pathogenicity (Garrido *et al.*, 2004, 2003). By contrast, the Ime2 homologue Crk1 in the human pathogen *Cryptococcus neoformans* negatively regulates mating (Liu and Shen, 2011). Very recently, Ime2 has also been implicated to have role in non-self recognition, programmed cell death and mitochondrial homeostasis in *Neurospora crassa* (Hutchison *et al.*, 2012).

In *M. oryzae*, Ime2 homologs have not yet been identified and studied. We identified a putative Ime2 homologue in the rice blast fungus and this protein is a determinant of pathogenicity. The challenge will now be to elucidate its role in rice blast disease. From detailed phenotypic characterization it was found that the corresponding T-DNA tagged mutant M4874 is normal in appressorium development, turgor generation and appressorium melanization. Interestingly, the mutant is completely non-pathogenic but is able to penetrate and colonize plant tissue although it is delayed in penetration compared to the wild-type Guy11. This observation inevitably gives rise to the question of why Ime2 mutant is unable to produce characteristic disease lesion even after extensively colonizing rice plant tissue. This warrants investigation of the precise nature of invasive hyphae observed when M4874 colonizes plant tissue. It may be possible for instance that colonization rates differ or that development of invasive hyphae is subtly altered.

To address the role of Ime2 in *M. oryzae*, generation of a targeted deletion strain will be necessary. We tagged Ime2 by T-DNA insertion within the promoter of the gene. Therefore, a very weak or residual expression of the gene in mutant M4874 is not unlikely but need to be confirmed. If it is the case then the delay in penetration and delay in plant tissue colonization

must be confirmed in a deletion mutant. In parallel, measuring the transcript level of Ime2 in M4874 will confirm whether it is altered in expression or not. However, mutant M4874 was not able to produce disease lesions, 8 days after inoculation which implies that Ime2 is involved in defining the nature of invasive hyphae in *M. oryzae*. It is very well known that primary penetration hyphae differentiate into bulbous branched infectious hyphae once the fungus gains entry to plant tissue. These rapidly colonizing invasive hyphae (IH) resemble yeast pseudohyphae (Talbot, 2003). Considering the role of Ime2 in formation of yeast pseudohypahe it may be worth speculating that Ime2 plays a similar function in *M. oryzae*. This question could be addressed by observing the formation of the biotrophic interfacial complex (BIC) in Δ*ime2* mutant (Khang *et al.*, 2010). Effectors such as *PWL2* and *BAS1* have been found to be BIC-localized suggesting a putative role of BICs in effector secretion. *BAS4* is another secreted protein that is localized in the plant derived extrainvasive hyphal membrane (EIHM) (Khang *et al.*, 2010). Localization of these fluorescently tagged effectors (e.g. *PWL2:RFP*, *BAS4:GFP*) during plant infection should therefore be observed in a Δ*ime2* mutant. This may provide significant information because BIC development is coupled to differentiation of invasive hyphae and this switching is a prerequisite for disease development (Veses and Gow, 2009). Therefore, elucidating the role of Ime2 in pseudohyphal transitions and its regulation of BIC formation will be the most pressing question to be answered.

Mutant M4874 also showed a distinct vegetative colonial phenotype. The colour of the spores and mycelium during vegetative growth resembles melanin deficient mutant *rsy* that suggested melanin biosynthesis defects although the appressorium showed melanization as Guy11. Consequently, appressorium turgor was also normal in M4874. Therefore, mutant M4874 may have defect in melanin deposition or cell wall biogenesis. Defects in cell wall biogenesis could be assessed in future by calcoflour white staining and this may give some

clue as to whether Ime2 has additional role in maintaining cell wall integrity. From transcriptional profiling data, Ime2 was found to be up-regulated at the onset of appressorium development and gradually becomes down-regulated as the appressorium matures. Therefore, the role of Ime2 during appressorium development is also quite significant. Finding interactors, for example will be very useful to resolve the potential role of Ime2 during infection-related development and invasive growth. Interactors of the protein could be found by yeast two-hybrid analysis initially. Furthermore, in *U. maydis*, the Ime2 homolog Crk1 is phosphorylated in its TXY motif by Ste7 which stimulates mating and virulence. Crk1 also physically interacts with the Pmk1 homolog Kss1-1 and activation of Crk1 is dependent on this MAPK. These suggest a tight linkage of the Crk1 and Kss1-1 MAPK cascade (Garrido *et al.*, 2004). Therefore, in *M. oryzae,* interplay between the Pmk1 MAPK cascade and the Ime2 kinase could be investigated by phosphoproteomic analysis and interaction studies. Any relationship between these two kinases will provide new insight into the regulation of appressorium morphogenesis and invasive hyphae development in *M. oryzae.* Simultaneously, it will develop our understanding of temporal regulation of these two processes and how they are ultimately regulated by perception of environmental cues from the plant host. In future, there are many more avenues to study Ime2 could be adopted to discover what other important functions it has been assigned in *M. oryzae*.

In this study, I demonstrated utility of ATMT based insertional mutagenesis for identification of novel virulence determinants in rice blast disease. By combining the efficiency of T-DNA tagging with the advantages of NGS technology for high-throughput identification of T-DNA tagged loci form candidate mutants, I was able to identify 3 novel genes out of 8 selected mutants from a collection of 10,200 original transformants. Further novel determinants of pathogencity are expected from the remainder of the selected mutants that can be identified

by the novel approach of NGS in future. This merger of insertional mutagenesis and NGS may become a widespread approach for applying large scale insertional mutagenesis study to emerging fungal phytopathogens. Application of NGS for T-DNA tagging of mutants will therefore add a new dimension to the arena of insertional mutagenesis. Significantly, the three novel genes we identified will be able provide fresh insight into the biology of *M. oryzae* and pathology of rice blast disease.

Bibliography

Abuodeh, R. O., Orbach, M .J., Mandel, M. A., Das, A., Galgiani, J. N. (2000). Genetic transformation of *Coccidioides immitis* facilitated by *Agrobacterium tumefaciens*. J. Infect. Dis. **181**:2106-2110.

Adachi, K., Hamer, J. E. (1998). Divergent cAMP signaling pathways regulate growth and pathogenesis in the rice blast fungus *Magnaporthe grisea*. Plant Cell. **10**:1361–1373.

Agrios, G. N. (2005). Plant Pathology 4th Edition. Academic Press.

Agrios, G.N. (1997). Plant Pathology, 4th edition. (Burlington, Massachusetts: Harcourt/Academic Press).

Akamatsu, H., Itoh, Y., Kodama, M., Otani, H. and Kohmoto, K. (1997). AAL-toxin deficient mutants of Alternaria alternate tomato pathotype by restriction enzyme-mediated integration. Phytopathology **87**: 967–972.

Albright, L. M., Huala, E., Ausubel, F. M. (1989). Prokaryotic signal transduction mediated by sensor and regulator protein pairs. Annu. Rev. Genet. **23:**311-336.

Alonso, J.M., Stepanova, A.N., Leisse, T.J., Kim, C.J., Chen, H.M., Shinn, P., Stevenson, D.K., Zimmerman, J., Barajas, P., Cheuk, R., Gadrinab, C., Heller, C., Jeske, A., Koesema, E., Meyers, C.C., Parker, H., Prednis, L., Ansari, Y., Choy, N., Deen, H., Geralt, M., Hazari, N., Hom, E., Karnes, M., Mulholland, C., Ndubaku, R., Schmidt, I., Guzman, P., Aguilar-Henonin, L., Schmid, M., Weigel, D., Carter, D.E., Marchand, T., Risseeuw, E., Brogden, D., Zeko, A., Crosby, W.L., Berry, C.C., and Ecker, J.R. (2003). Genomewide Insertional mutagenesis of *Arabidopsis thaliana*. Science. **301:**653-657.

Altschul, S. F., Madden, T. L., Schäffer, A. A., Zhang, J., Zhang, Z., Miller, W., Lipman, D. J. (1997). Gapped BLAST and PSI-BLAST: a new generation of protein database search programs. Nucleic Acids Res. **25(17)**:3389-3402.

Amey RC, Athey-Pollard A, Burns C, Mills PR, Bailey A, Foster GD. (2002). PEG-mediated and *Agrobacterium* mediated transformation in the mycopathogen *Verticillium fungicola*. Mycol. Res. **106**:4–11.

Andrea Pitzschke1, Heribert Hirt. (2010). New insights into an old story: Agrobacterium induced tumour formation in plants by plant transformation. The EMBO Journal **29**, 1021–1032.

Arencibia, A., Molina, P. de la Riva, G., Selman-Housein, G. (1995). Production of transgenic sugarcane (*Saccharum officinarum* L.) plants by intact cell electroporation. Plant Cell Reports **14**: 305-309.

Asakura, M., Ninomiya, S., Sugimoto, M., Oku, M., Yamashita, S., Okuno, T., Sakai, Y., Takano, Y. (2009). Atg26-Mediated Pexophagy Is Required for Host Invasion by the Plant Pathogenic Fungus *Colletotrichum orbiculare*. Plant Cell **21(4)**: 1291-1304.

Ash, C., Jasny, B. R., Malakoff, D. A., Sugden, A. M. 2010. Feeding the Future. Science. **327:** 797.

Ashizawa T., Zenbayashi K., Sonoda R. (2005). Effects of preinoculation with an avirulent isolate of *Pyricularia grisea* on infection and development of leaf blast lesions caused by virulent isolates on near-isogenic lines of Sasanishiki rice. J. Gen. Plant Pathol. **71**: 345–350.

Babujee, L., Gnanamanickam, S.S. (2000). Molecular tools for characterization of rice blast pathogen, *Magnaporthe grisea*, population and molecular marker-assisted breeding for disease resistance. Curr. Sci. **78**, 248–257.

Baker, B., Zambryski, P., Staskawicz, B., Dinesh-Kumar, S. P. (1997). Signalling in plant-microbe interactions. Science. **276**:726-733.

Baleja, J. D., Marmorstein, R., Harrison, R. C., Wagner, G. (1992). Solution structure of the DNA-binding domain of Cd_2-GAL4 from *S. cerevisiae*. Nature. **356**:450 – 453.

Balhadére, P. V., Foster, A. J., Talbot, N. J. (1999). Identification of pathogenicity mutants of the rice blast fungus *Magnaporthe grisea* by insertional mutagenesis. Mol. Plant Microbe Interact. **12**: 129–142

Balhadére, P. V., Talbot, N. J. (2000). Fungal pathogenicity-establishing infection. Molecular Plant Pathology, Annual Plant Reviews, Volume 4. Edited by Matthews Dickinson.

Ballini, E., Morel, J. B., Droc, G., Price, A., Courtois, B., Notteghem, J. L., Tharreau, D. (2008). A genome-wide meta-analysis of rice blast resistance genes and quantitative trait loci provides new insights into partial and complete resistance. Mol. Plant Microbe Interact. **21:** 859–868.

Banuett, F. (1992). *Ustilago maydis*, the delightful blight. Trends Genet. **8(5):**174-80.

Banuett, F. (1998). Signalling in the yeasts: an informational cascade with links to the filamentous fungi. Microbiol Mol Biol Rev. **62(2)**: 249-274.

Baron, C., Zambryski, P. C. (1996). Plant transformation: A pilus in *Agrobacterium* T-DNA transfer. Curr Biol. **6**:1567-1569.

Barrett, C. B. (2010). Measuring food insecurity. Science. **327(5967)**: 825-828.

Baulcombe, D. (2010). Reaping benefits of crop research. Science. **327(5967)**: 761.

Bayram, O., Sari, F., Braus, G.H., Irniger, S. (2009). The protein kinase ImeB is required for light-mediated inhibition of sexual development and for mycotoxin production in *Aspergillus nidulans*. Mol. Microbiol. **71**:1278–1295.

Bechinger, C., Giebel, K. F., Schnell, M., Leiderer, P., Deising, H. B. & Bastmeyer, M., (1999). Optical measurements of invasive forces exerted by appressoria of a plant pathogenic fungus.Science. **285**: 1896-1899.

Benjamin, K. R., Zhang, C., Shokat, K. M., Herskowitz, I. (2003). Control of landmark events in meiosis by the CDK Cdc28 and the meiosis-specific kinase Ime2. Genes Dev. **17**:1524–1539.

Betts MF, Tucker SL, Galadima N, Meng Y, Patel G, Li L, Donofrio N, Floyd A, Nolin S, Brown D, Mandel MA, Mitchell TK, Xu JR, Dean RA, Farman ML, Orbach MJ. **(**2007**).** Development of a high throughput transformation system for insertional mutagenesis in Magnaporthe oryzae. Fungal Genet Biol. **44(10)**:1035-49.

Boland, B., Nixon, R. A. (2006). Neuronal macroautophagy: from development to degeneration. Mol. Aspects Med. **27**:503–519.

Bölker, M. (1998). Sex and crime: heterotrimeric G proteins in fungal mating and pathogenesis. Fungal Genet. Biol. **25:** 143–56.

Bölker, M., Böhnert, H. U., Braun, K. H., Görl, J., Kahmann R. (1995). Tagging pathogenicity genes in *Ustilago maydis* by restriction enzyme-mediated integration (REMI). Mol. Gen. Genet. **248:** 547–552.

Bolton, G. W., Nester, E. W., Gordon, M. P. (1986). Plant Phenolic-Compounds Induce Expression of the *Agrobacterium tumefaciens* Loci Needed for Virulence. Science. **232:**983-985.

Bonman, J.M., Estrada, B.A & Bandong, J.M. 1989. Leaf and neck blast resistance in tropical lowland rice cultivars. Plant disease. **73(5)**: 388-390.

Bonman, J.M., Khush G. S., Nelson R.J. (1992) Breeding rice for resistance to pests. Annu. Rev. Phytopathol. **30**:507–528.

Bourett, T. M., Howard, R. J. (1990). *In vitro* development of penetration structures in the rice blast fungus *Magnaporthe grisea*. Can. J. Botany. **68:** 329-342.

Bowyer, P. (1999). Plant disease caused by fungi: phytopathology. In: Molecular Fungal Biology. (Oliver R. P., Schweizer, M. eds.) Cambridge: Cambridge University Press.

Brandriss, M. C. (1987). Evidence for positive regulation of the proline utilization pathway in Saccharomyces cerevisiae. Genetics. **117(3)**:429-35.

Brefort, T., Doehlemann, G., Mendoza-Mendoza, A., Reissmann, S., Djamei, A., Kahmann, R. (2009). *Ustilago maydis* as a Pathogen. Annu. Rev. Phytopathol. **47:** 423–45.

Brewster, J. L., de Valoir, T., Dwyer, N. D., Winter, E., Gustin, M. C. (1993). An osmosensing signal transduction pathway in yeast. Science. **259**: 1760–1763.

Brown, J. S., Aufauvre-Brown, A., Holden, D.W. (1998). Insertional mutagenesis of Aspergillus fumigatus. Mol. Gen. Genet. **259:**327-35.

Brown, J.S., Holden, D.W. (1998). Insertional mutagenesis of pathogenic fungi. Curr. Opin. Microbiol. **1:**390-394.

Brush, G. S., Najor, N. A., Dombkowski, A. A., Cukovic, D., Sawarynski, K. E. (2012). Yeast *IME2* functions early in meiosis upstream of cell cycle-regulated SBF and MBF targets. PLoS ONE. **7**: e31575.

Bundock, P., Dulk-Ras, A., Beijersbergen, A., Hooykaas, P.J. (1995). Trans-kingdom T-DNA transfer from Agrobacterium tumefaciens to Saccharomyces cerevisiae. EMBO J **14**:3206–3214.

Bundock, P., Hooykaas, P.J. (1996). Integration of *Agrobacterium tumefaciens* T-DNA in the *Saccharomyces cerevisiae* genome by illegitimate recombination. Proc. Natl. Acad. Sci. USA. **93(26)**:15272–15275.

Bundock, P., Mroczek, K., Winkler, A. A., Steensma, H. Y., Hooykaas, P. J. (1999). T-DNA from Agrobacterium tumefaciens as an efficient tool for gene targeting in *Kluyveromyces lactis*. Mol. Gen. Genet. **261**:115–121.

Bundock, P., van Attikum, H., den Dulk-Ras, A., Hooykaas, P.J. (2002). Insertional mutagenesis in yeasts using T-DNA from *Agrobacterium tumefaciens*. Yeast. **19(6)**:529–536.

Campoy, S., Perez, F., Martin, J. F., Gutierrez, S., Liras, P. (2003). Stable transformants of the azaphilone pigment-producing Monascus purpureus obtained by protoplast transformation and *Agrobacterium* mediated DNA transfer. Curr Genet. **43**:447–452.

Caracuel-Rios, Z., Talbot, N. J. (2008). Silencing the crowd: high-throughput functional genomics in *Magnaporthe oryzae*. Mol. Microbiol. **68(6):** 1341–1344.

Carlile, M. J., Watkinson, S. C., Gooday, G. W. (2001). The fungi. 2nd ed. Academic Press, San Diego.

Carroll, A. M., Sweigard, J. A., Valent, B. (1994). Improved vectors for selecting resistance to hygromycin. Fungal Genet. Newslett. **41:**22.

Catlett, N. L., Lee, B. N., Yoder, O. C., Turgeon, G. (2003) Split-marker recombination for efficient targeted deletion of fungal genes. Fungal Genet. News. **50:** 9-11.

Chant, J., Herskowitz, I. (1991). Genetic control of bud site selection in yeast by a set of gene products that constitute a morphogenetic pathway. Cell. **65(7)**:1203-12.

Chen, H.Q., Cao L., Dekkers K.L., Rollins J.A., Ko N.J., Timmer L.W., Chung K.R. (2005). A gene with domains related to transcription regulation is required for pathogenicity in *Colletotrichum acutatum* causing Key lime anthracnose. Mol. Plant Path. **6(5)**: 513-525.

Chen, X., Stone, M., Schlagnhaufer, C., Romaine P. (2000). A fruiting body tissue method for efficient *Agrobacterium* mediated transformation of *Agaricus bisporus*. Appl. Env. Microbiol. **66:** 4510–4513.

Cheng, M., Fry, J.E., Pang, S.Z., Zhou, H.P., Hironaka, C.M., Duncan, D.R., Conner, W. and Wan, Y.C. (1997). Genetic transformation of wheat mediated by *Agrobacterium tumefaciens*. Plant Physiol. **115**: 971-980.

Cheng, X.Y., Sardana, R., Kaplan, H., Altosaar, I. (1998). *Agrobacterium* transformed rice expressing synthetic cry1Ab and cry1Ac genes are higly toxic to striped stem borer and yellow stem borer. Proc. Natl. Acad. Sci. USA**. 95**: 2767-2772.

Chiu, W., Niwa, Y., Zeng, W., hirano, T., Kobayashi, H., Sheen, J. (1996). Enginnered GFP as a vital reporter in plants. Curr.Biol. **6:** 325-330.

Choi, W. & Dean, R. A. (1997). The adenylate cyclase gene *MAC1* of *Magnaporthe grisea* controls appressorium formation and other aspects of growth and development. Plant Cell **9**: 1973–1983.

Christie, P. J. (1997). Agrobacterium tumefaciens T-complex transport apparatus: A paradigm for a new family of multifunctional transporters in eubacteria. J. Bacteriol. **179**:3085-3094.

Christou, P., Twyman, R. M. (2004). The potential of genetically enhanced plants to address food insecurity. Nutr. Res. Rev. **17:** 23–42.

Chumley, F. G. & Valent, B., (1990) Genetic analysis of melanin-deficient, non-pathogenic mutants of Magnaporthe grisea. Mol. Plant-Microbe Interact. **3**: 135-143.

Chun, S. J., Lee, Y. H. (1999). Genetic analysis of a mutation on appressorium formation in *Magnaporthe grisea*. FEMS Microbiol. Letters. **173:** 133-137.

Chung, K.R., Ehrenshaft, M., Wetzel, D.K., Daub, M.E. (2003). Cercosporin deficient mutants by plasmid tagging in the asexual fungus *Cercospora nicotianae*. Mol. Gen. Genomics. **270:**103-13.

Cifuentes, M. E., Honkanen, L., Rebecchi, M. J. (1993). Proteolytic fragments of phosphoinositide-specific phospholipase C-delta 1. Catalytic and membrane binding properties. J. Biol. Chem. **268(16)**:11586-93.

Citovsky V, Wong M. L., Zambryski P. (1989). Cooperative interaction of *Agrobacterium* VirE2 protein with single-stranded DNA: implications for the T-DNA transfer process. Proc Natl. Acad. Sci. USA. **86(4)**:1193-7.

Clergeot, P.H., Gourgues M., Cots J., Laurans F., Latorse M.P., Pepin R., Tharreau D., Notteghem J.L., Lebrun M.H. (2001). PLS1, a gene encoding a tetraspanin-like protein, is required for penetration of rice leaf by the fungal pathogen *Magnaporthe grisea*. Proc. Natl. Acad. Sci. USA**. 98(12)**: 6963-6968.

Combier, J.P., Melayah D., Raffier C., Gay G., Marmeisse R. (2003). Agrobacterium tumefaciens-mediated transformation as a tool for insertional mutagenesis in the symbiotic ectomycorrhizal fungus *Hebeloma cylindrosporum*. FEMS Microbiol. Lett. **220(1)**:141–148.

Couch, B.C., Fudal, I., Lebrun, M.H., Tharreau, D., Valent, B., van Kim, P., Nottéghem, J.L., Kohn, L.M. (2005). Origins of host-specific populations of the blast pathogen *Magnaporthe oryzae* in crop domestication with subsequent expansion of pandemic clones on rice and weeds of rice. Genetics. **170(2)**:613–630.

Couch, B.C., Kohn, L.M. (2002). A multilocus gene genealogy concordant with host preference indicates segregation of a new species, *Magnaporthe oryzae*, from *M. grisea*. Mycologia. **94(4)**:683–693.

Covert, S.F., Kapoor, P., Lee, M., Briley, A., Nairn, C.J. (2001). *Agrobacterium* mediated transformation of *Fusarium circinatum*. Mycol. Res. **105**:259–264.

Czymmek, K. J., Bourett, T. M., Sweigard, J. A., Carroll, A. & Howard, R. J. (2002). Utility of cytoplasmic fluorescent proteins for live-cell imaging of *Magnaporthe grisea* in planta. Mycologia **94(2)**:280–289.

Daboussi, M.J., Djeballi, A., Gerlinger, C., Blaiseau, P.L., Bouvier, I., Cassan, M., Lebrun, M.H., Parisot, D., Brygoo, Y. (1989). Transformation of seven species of filamentous fungi using the nitrate reductase gene of *Aspergilius nidulans*. Curr Genet. **15(6)**:453-456.

Dagdas, Y. F, Yoshino, K., Dagdas, G., Ryder, L. S, Bielska, E., Steinberg, G., Talbot, N. J. (2012). Septin-mediated plant cell invasion by the rice blast fungus, *Magnaporthe oryzae*. Science. **336(6088)**:1590-5.

Dai, L. Y., Liu, X. L., Xiao, Y. H. and Wang, G. L. (2007). Recent advances in cloning and characterization of disease resistance genes in rice. J. Integr. Plant Biol. **49**:112–119.

Davis, D. J., Burlak, C., Money, N. P. (2000). Biochemical and biomechanical aspects of appressorial development in *Magnaporthe grisea*. Adv. Rice Blast Res. pp. 248-256.

Davis, L. H., Bennett, V. (1994). Identification of two regions of beta G spectrin that bind to distinct sites in brain membranes. J. Biol. Chem. **269(6)**:4409-16.

De Arruda, M. V., Watson, S., Lin, C-S., Leavitt, J, and Matsudaira, P. (1990). Fimbrin is a homologue of the cytoplasmic phosphoprotein plastin and has domains homologous with Calmodulin and actin gelation proteins. J. Cell Biol. **111(3):** 1069-1079.

de Groot, M. J. A., Bundock, P., Hooykaas, P. J. J., Beijersbergen, A. G. M. (1998). *Agrobacterium tumefaciens*-mediated transformation of filamentous fungi. Nature Biotechnol. **16**:1074.

de Jong J. C., McCormack B. J., Smirnoff, N. & Talbot, N.J. (1997). Glycerol generates turgor in rice blast. Nature. **389:** 244-245.

Dean, R. A. (1997). Signal pathways and appressorium morphogenesis. Annu. Rev. Phytopathol. **35:** 211–234.

Dean, R. A., Talbot, N. J., Ebbole, D. J., Farman, M. L., Mitchell, T. K., Orbach, M. J., Thon, M., Kulkarni, R., Xu, J. R., Pan, H., Read, N. D., Lee, Y. H., Carbone, I., Brown, D., Oh, Y. Y., Donofrio, N., Jeong, J. S., Soanes, D. M., Djonovic, S., Kolomiets, E., Rehmeyer, C., Li, W., Harding, M., Kim, S., Lebrun, M. H., Bohnert, H., Coughlan, S., Butler, J., Calvo, S., Ma, L. J., Nicol, R., Purcell, S., Nusbaum, C., Galagan, J. E., Birren, B. W. (2005). The genome sequence of the rice blast fungus *Magnaporthe grisea*. Nature. **434:** 980–986.

Deblaere, R., Bytebier, B., De Greve, H., Deboeck, F., Schell, J., Van Montagu, M. and Leemans, J. (1985). Efficient octopine Ti plasmid-derived vectors for *Agrobacterium* mediated gene transfer to plants. Nucleic Acid Res. **13(13)**: 4777-4788.

Degefu Y., Hanif M. (2003). *Agrobacterium tumefaciens* mediated transformation of *Helminthosporium turcicum*, the maize leaf blight fungus. Arch. Microbiol. **180(4)**:279–284.

Deising, H. B., Werner, S., Wernitz, M. (2000). The role of fungal appressoria in plant infection. Microb. Infect. **2(13)**: 1631-41.

des Etages, S. A., Falvey, D. A., Reece, R. J., Brandriss, M. C. (1996). Functional analysis of the PUT3 transcriptional activator of the proline utilization pathway in *Saccharomyces cerevisiae*. Genetics. **142(4)**:1069-82.

Des Etages, S. A., Saxena, D., Huang, H. L., Falvey, D. A., Barber, D., Brandriss, M. C. (2001). Conformational changes play a role in regulating the activity of the proline utilization pathway-specific regulator in *Saccharomyces cerevisiae*. Mol. Microbiol. **40(4)**:890-9.

DeZwaan, T. M., Carroll, A. M., Valent, B., Sweigard, J. A. (1999). *Magnaporthe grisea* Pth11p Is a Novel Plasma Membrane protein that mediates appressorium differentiation in response to inductive substrate cues. Plant Cell. **11(10):** 2013-2030.

Ding, S., Mehrabi, R., Koten, C., Kang, Z., Wei, Y., Seong, K., Kistler, H.C., Xu, J.R. (2009). Transducin Beta-Like Gene FTL1 Is Essential for Pathogenesis in *Fusarium graminearum*. Eukaryotic Cell. **8(6)**: 867-876.

Dixon, K. P., Xu, J-R., Smirnoff, N., Talbot, N. J. (1999). Independent signaling pathways regulate cellular turgor during hyperosmotic stress and appressorium-mediated plant infection by *Magnaporthe grisea*. 1999. Plant Cell, Vol. **11(10):** 2045–2058.

Dobinson, K. F., Hamer, J. E. (1992). *Magnaporthe grisea*. In Molecular Biology of Filamentous Fungi, U. Stahl and P. Tudzynski, eds (New York: Weinheim), pp.67-86.

Dohlman, H. G., Thorner, J. W. (2001). Regulation of G protein-initiated signal transduction in yeast: paradigms and principles. Annu Rev. Biochem. **70:** 703–754.

Dohlman, H. G., Thorner, J. (1997). RGS proteins and signaling by heterotrimeric G proteins. J Biol Chem. **272(7):** 3871-3874.

Dufresne, M., Bailey, J.A., Dron, M., Langin, T. (1998). clk1, a serine/threonine protein kinase-encoding gene, is involved in pathogenicity of *Colletotrichum lindemuthianum* on common bean. Mol. Plant Microbe Interact. **11(2)**: 99-108.

Duplessis, S., Cuomo, C. A., Lin, Y. C., Aerts, A., Tisserant, E., Veneault-Fourrey, C., Joly, D. L., Hacquard, S., Amselem, J., Cantarel, B. L., Chiu, R., Coutinho, P. M., Feau, N., Field, M., Frey, P., Gelhaye, E., Goldberg, J., Grabherr, M. G., Kodira, C. D., Kohler, A., Kües, U., Lindquist, E. A., Lucas, S. M., Mago, R., Mauceli, E., Morin, E., Murat, C., Pangilinan, J. L., Park, R., Pearson, M., Quesneville, H., Rouhier, N., Sakthikumar, S., Salamov, A. A., Schmutz, J., Selles, B., Shapiro, H., Tanguay, P., Tuskan, G. A., Henrissat, B., Van de Peer, Y., Rouzé, P., Ellis, J. G., Dodds, P. N., Schein, J. E., Zhong, S., Hamelin, R. C., Grigoriev, I. V., Szabo, L. J., Martin, F. (2011). From the Cover: Obligate biotrophy features unraveled by the genomic analysis of rust fungi. Proc Natl Acad Sci U S A. **108(22):** 9166-71.

Duyvesteijn, R.G., van Wijk, R., Boer, Y., Rep, M., Cornelissen, B.J., Haring, M.A. (2005). Frp1 is a Fusarium oxysporum F-box protein required for pathogenicity on tomato. Mol. Microbiol. **57(4)**: 1051-1063.

Ebbels, D.L. (2003). Principles of Plant Health and Quarantine.Wallingford, UK: CAB Int.

Ebbole, D. J. (1997). Hydrophobins and fungal infection of plants and animals. Trends Microbiol. **5(10)**:405-8.

Ebbole, D. J. (2007). *Magnaporthe* as a model for understanding host–pathogen interactions. Annu. Rev. Phytopathol. **45:** 437–456.

Edgar, R. C. (2004). MUSCLE: multiple sequence alignment with high accuracy and high throughput. Nucleic Acids Res. **32**: 1792–1797.

Eluère, R., Varlet, I., Bernadac, A., Simon, M. N. (2012) Cdk and the anillin homolog Bud4 define a new pathway regulating septin organization in yeast. Cell Cycle. **11(1)**:151-8.

Enríquez-Obregón, G.A., Vázquez-Padrón, R.I., Prieto-Samsónov, D.L., Pérez, M. and Selman-Housein, G. (1997). Genetic transformation of sugarcane by *Agrobacterium tumefaciens* using antioxidants compounds. Biotecnología. Aplicada. **14**:169-174.

Epstein, L., Lusnak, K., Kaur, S. (1998). Transformation mediated developmental mutants of *Glomerella graminicola* (*Colletotrichum graminicola*). Fungal Genet. Biol. **23(2):** 189–203.

Fang, E. G. C., Dean, R. A. (2000). Site-Directed Mutagenesis of the magB gene affects growth and development in *Magnaporthe grisea.* Mol. Plant Microbe Interact. **13(11):** 1214–1227.

FAO, Food Security Statistics, accessed 27 December (2009). at www.fao.org/economic/ess/food-security-statistics/en/.

FAO, The State of Food Insecurity in the World (2012). at http://www.fao.org/publications/sofi/en/.

Farman, M.L., Eto, Y., Nakao, T., Tosa, Y., Nakayashiki, H., Mayama, S., Leong, S.A. (2002). Analysis of the structure of the AVR1-CO39 avirulence locus in virulent rice-infecting isolates of *Magnaporthe grisea*. Mol. Plant Microbe Interact. **15(1)**: 6–16.

Fedoroff, N. V., Battisti, D. S., Beachy, R. N., Cooper, P. J., Fischhoff, D. A., Hodges, C. N., Knauf, V. C., Lobell, D., Mazur, B. J., Molden, D., Reynolds, M. P., Ronald, P. C., Rosegrant, M. W., Sanchez, P. A., Vonshak, A., Zhu, J. K. (2010). Radically rethinking agriculture for the 21st century. Science. **327(5967):** 833-834.

Field, C.M., Alberts, B.M. (1995). Anillin, a contractile ring protein that cycle from the nucleus to the cell cortex. J. Cell Biol. **131**:165–178.

Fields, S., Song, O. (1989). A novel genetic system to detect protein–protein interactions. Nature, **340(6230)**:245-246.

Fincham, J. R. (1989). Transformation in fungi. Microbial Rev. **53(1)**:148-l70.

Firon, A., Villalba, F., Beffa, R., d'Enfert, C. (2003). Identification of essential genes in the human fungal pathogen *Aspergillus fumigatus* by transposon mutagenesis. Eukaryot. Cell. **2(2):**247-55.

Fitzgerald, A. M., Mudge, A. M., Gleave, A. P., Plummer, K. M. (2003). *Agrobacterium* and PEG-mediated transformation of the phytopathogen *Venturia inaequalis*. Mycol. Res. **107:**803-810.

Fitzgerald, A., van Kan, J.A., Plummer, K.M. (2004). Simultaneous silencing of multiple genes in the apple scab fungus, *Venturia inaequalis*, by expression of RNA with chimeric inverted repeats. Fungal Genet. Biol. **41(10)**:963–971.

Fjellstrom, R., Conaway-Bormans, C.A., McClung, A.M., Marchetti, M.A, Shank, R., Park, W.D. (2004). Development of DNA markers suitable for marker assisted selection of three Pi genes conferring resistance to multiple *Pyricularia grisea* pathotypes. Crop Sci. **44**:1790–1798.

Foster, A. J., Jenkinson, J. M. & Talbot, N. J. (2003). Trehalose synthesis and metabolism are required at different stages of plant infection by *Magnaporthe grisea*. EMBO J. **22:** 225–235.

Freedman, L. P., Luisi, B. F., Korszun, Z. R., Basavappa, R., Sigler, P. B., Yamamoto, K. R. (1988). The function and structure of the metal coordination sites within the glucocorticoid receptor DNA binding domain. Nature. **334(6182)**:543-6.

Freedman, L. P., Luisi, B. F., Korszun, Z. R., Basavappa, R., Sigler, P. B., Yamamoto, K. R.

Galagan, J. E., Henn, M. R., Ma, L. J., Cuomo, C. A. & Birren, B. (2005). Genomics of the fungal kingdom: Insights into eukaryotic biology. *Genome Res.* **15**: 1620-1631.

Gao, F,, Zhou, B. J., Li, G. Y., Jia, P.S., Li, H., Zhao, Y. L., Zhao, P., Xia, G. X., Guo H. S. (2010). A Glutamic Acid-Rich Protein Identified in *Verticillium dahliae* from an Insertional Mutagenesis Affects Microsclerotial Formation and Pathogenicity. PLoS ONE **5(12)**: e15319.

Gardiner, D. M., Howlett, B. J. (2004). Negative selection using thymidine kinaseincreases the efficiency of recovery of transformants with targeted genes in the filamentous fungus *Leptosphaeria maculans*. Curr Genet. **45**:249-255.

Garrido, E., Pérez-Martín, J. (2003). The crk1 gene encodes an Ime2-related protein that is required for morphogenesis in the plant pathogen *Ustilago maydis*. Mol. Microbiol. **47(3)**: 729–743.

Garrido, E., Voss, U., Muller, P., Castillo-Lluva, S., Kahmann, R., and Perez-Martin, J. (2004). The induction of sexual development and virulence in the smut fungus *Ustilago maydis* depends on Crk1, a novel MAPK protein. Genes Dev.**18:** 3117–3130.

Gelvin, S.B. (2000). *Agrobacterium* and plant genes involved in T-DNA transfer and integration. Annu. Rev. Plant Physiol. Plant Mol. Biol. **51:**223-256.

Gelvin, S.B. (2003). *Agrobacterium*-mediated plant transformation: The biology behind the "gene-Jockeying" tool. Microbiol. Mol. Biol. Reviews.**67:**16-37.

Giasson, L., Kronstad, J.W. (1995). Mutations in the Myp1 Gene of Ustilago-Maydis Attenuate Mycelial Growth and Virulence. Genetics. **141(2)**: 491-501.

Gibson, T. J., Hyvönen, M., Musacchio, A., Saraste, M., Birney, E. (1994). PH domain: the first anniversary. Trends Biochem. Sci. **19 (9)**: 349–53.

Giesbert, S., Schumacher, J., Kupas, V., Espino, J., Segmüller, N., Haeuser-Hahn, I., Schreier, P.H., Tudzynski, P. (2012). Identification of Pathogenesis-Associated Genes by T-DNA-Mediated Insertional Mutagenesis in Botrytis cinerea: A Type 2A Phosphoprotein Phosphatase and an SPT3 Transcription Factor Have Significant Impact on Virulence." Mol. Plant Microbe Interac. **25(4)**: 481-495.

Gilbert, R. D., Johnson, A. M., Dean, R. A. (1996). Chemical signals responsible for appressorium formation in the rice blast fungus. Physiol. Mol. Plant Pathol. **48:** 335–346.

Gnanamanickam, S.S. et al. (2000) Lineage-exclusion resistance breeding: pyramiding of blast resistance genes for management of rice blast in India. Adv. Rice Blast Res. **15**:172–179.

Gnanamanickam, S.S., Babujee, L., Brindha, V.P., Dayakar, B.V., Leenakumari, S., Sivaraj, R., Levy, M., Leong, S.A. (1998). Lineage exclusion resistance breeding: Pyramiding of blast resistance genes for management of rice blast in India. Adv. Rice Blast Res. **15**:172–179.

Godfray, H. C., Beddington, J. R., Crute, I. R., Haddad, L., Lawrence, D., Muir, J. F., Pretty, J., Robinson, S., Thomas, S. M., Toulmin, C. (2010). Food security: the challenge of feeding 9 billion people. Science. **327(5967):** 812-818.

Goh J., Kim, K. S., Park, J., Jeon, J., Park, S. Y., Lee, Y. H. (2011). The cell cycle gene MoCDC15 regulates hyphal growth, asexual development and plant infection in the rice blast pathogen *Magnaporthe oryzae*. Fungal Genet. Biol.**48**:784–792.

Goodwin, S. B., Ben M'barek, S., Dhillon, B., Wittenberg, A. H., Crane, C. F., Hane, J. K., Foster, A. J., Van der Lee, T. A., Grimwood, J., Aerts, A., Antoniw, J., Bailey, A., Bluhm, B., Bowler, J., Bristow, J., van der Burgt, A., Canto-Canché, B., Churchill, A. C., Conde-Ferràez, L., Cools, H. J., Coutinho, P. M., Csukai, M., Dehal, P., De Wit, P., Donzelli, B., van de Geest, H. C., van Ham, R. C., Hammond-Kosack, K. E., Henrissat, B., Kilian, A., Kobayashi, A. K., Koopmann, E., Kourmpetis, Y., Kuzniar, A., Lindquist, E., Lombard, V., Maliepaard, C., Martins, N., Mehrabi, R., Nap, J. P., Ponomarenko, A., Rudd, J. J., Salamov, A., Schmutz, J., Schouten, H. J., Shapiro, H., Stergiopoulos, I., Torriani, S. F., Tu, H., de Vries, R. P., Waalwijk, C., Ware, S. B., Wiebenga, A., Zwiers, L. H., Oliver, R. P., Grigoriev, I. V., Kema, G. H. (2011). Finished Genome of the Fungal Wheat Pathogen *Mycosphaerella graminicola* Reveals Dispensome Structure, Chromosome Plasticity, and Stealth Pathogenesis. PLoS Genet. **Jun; 7(6):** e1002070. Epub 2011 Jun 9.

Granado, J. D., Kertesz, K. C., Aebi, M., Kijes, U. (1997). Restriction enzyme-mediated integration in *Coprineus cinereus*. Mol. Gen. Genet. **256(1)**:28-36.

Guindon, S., Dufayard, J. F., Lefort, V., Anisimova, M., Hordijk, W., Gascuel, O. (2010). New Algorithms and Methods to Estimate Maximum-Likelihood Phylogenies: Assessing the Performance of PhyML 3.0. Syst.Biol. **59**:307-21.

Guindon, T. G., Castresana, J. (2007). Improvement of phylogenies after removing divergent and ambiguously aligned blocks from protein sequence alignments. Syst. Biol. **56**: 564–577.

Gupta, A., Chattoo, B. B. (2008). Functional analysis of a novel ABC transporter ABC4 from *Magnaporthe grisea*. FEMS Microbiology Lett. **278(1)**: 22-28.

Gupta, A., Chattoo, B. B., (2007). A novel gene MGA1 is required for appressorium formation in *Magnaporthe grisea*. Fungal Genet. Biol. **44(11)**: 1157-1169.

Hamel, L. P., Nicole, M. C., Duplessis, S., Ellis, B. E. (2012). Mitogen-activated protein kinase signaling in plant-interacting fungi: distinct messages from conserved messengers. Plant Cell. **24(4)**:1327-51.

Hamer, J. E., Howard, R. J., Chumley, F. G., Valent, B. (1988). A mechanism for surface attachment in spores of a plant pathogenic fungus. Science. **239:** 288–290.

Hamer, J. E., Talbot, N. J. (1998). Infection-related development in the rice blast fugus *Magnaporthe grisea*. Curr opin. microbiol. **1(6):** 693-697.

Hamer, J. E., Valent, B., Chumley, F. G. (1989). Mutations at the *SMO* locus affect the shape of diverse cell types in the rice blast fungus. Genetics. **122(2):** 351–361.

Hamer, L., Adachi, K., Montenegro-Chamorro, M. V., Tanzer, M. M., Mahanty, S. K., Lo, C., Tarpey, R.W., Skalchunes, A.R., Heiniger,, R.W., Frank, S.A., Darveaux, B. A., Lampe, D.J., Slater, T. M., Ramamurthy, L., DeZwaan, T.M., Nelson, G.H., Shuster, J.R., Woessner, J., Hamer, J. E. (2001). Gene discovery and gene function assignment in filamentous fungi. Proc. Natl. Acad. Sci. USA. **98(9):**5110-5.

Hamilton, C.M. (1997). A binary BAC system for plant transformation with high-molecular-weight DNA. Gene. **200(1-2)**:107-116.

Hanada, T., Satomi, Y., Takao, T., Ohsumi, Y. (2009). The amino-terminal region of Atg3 is essential for association with phosphatidylethanolamine in Atg8 lipidation. FEBS Letters. **583(7)**:1078–1083.

Hanif, M., Pardo, A. G., Gorfer, M., Raudaskoski, M. (2002). T-DNA transfer and integration in the ectomycorrhizal fungus *Suillus bovinus* using hygromycin B as a selectable marker. Curr Genet. **41(3)**:183–188.

Haslam, R. J., Koide, H. B., Hemmings, B. A. (1993). Pleckstrin domain homology. Nature. **363(6427)**:309–10.

Heath, M.C., Valent, B., Howard, R.J., and Chumley, F.G. (1990). Interactions of 2 Strains of *Magnaporthe grisea* with Rice, Gossegrass, and Weeping Lovegrass. Can. J. Botany. 68:1627-1637.

Hedeler, C., Wong, H. M., Cornell, M. J., Alam, I., Soanes, D. M., Rattray, M., Hubbard, S. J., Talbot, N. J., Oliver, S. G., Paton, N. W. (2007). e-Fungi: a data resource for comparative analysis of fungal genomes. BMC Genomics. **20**;8:426

Hemelaar, J., Lelyveld, V. S., Kessler, B. M., Ploegh, H. L. (2003). A single protease, Apg4B, is specific for the autophagy-related ubiquitin-like proteins GATE-16, MAP1-LC3, GABARAP, and Apg8L. J. Biol. Chem. **278(51)**:51841–51850.

Herskowitz, I., (1995) MAP Kinase pathways in yeast: For mating and more. Cell **80**: 187-197.

Hiei, Y., Komari, T. (2006). Improved protocols for transformation of Indica rice mediated by *Agrobacterium tumefaciens*. Plant Cell Tissue and Organ Culture. **85**:271-283.

Hiei, Y., Ohta, S., Komari, T. and Kumashiro, T. (1994). Efficient transformation of rice (Oriza sativa) mediated by *Agrobacterium* and sequence analysis of the boundaries of the T-DNA. Plant J. **6(2)**:271-282.

Hittalmani, S., Parco, A., Mew, T. V., Zeigler, R. S., Huang, N. (2000). Fine mapping and DNA marker-assisted pyramiding of the three major genes for blast resistance in rice. Theor. Appl. Genet. **100**:1121–1128.

Hoekema, A., Hirsch, P.R., Hooykaas, P.J., Schilperoort, R.A. (1983). A binary vector strategy based on separation of *vir*-region and T-region of the *Agrobacterium tumefaciens* Ti-plasmid. Nature. **303**:179–180.

Hogan, L. H., Klein, B. S. (1997). Transforming DNA integrates at multiple sites in the dimorphic fungal pathogen *Blastomyces dermatitidis*. Gene, **186(2)**:219-226.

Honigberg, S.M. (2004). Ime2p and Cdc28p: co-pilots driving meiotic development. J. Cell Biochem. **92(5)**: 1025–1033.

Hooykaas, P. J., Schilperoort, R. A. (1992). *Agrobacterium* and plant genetic engineering. Plant Mol. Biol. **19**:15–38

Howard, R. J., Ferrari M. A., Roach, D. H., Money, N. P. (1991). Penetration of hard substrates by a fungus employing enormous turgor pressures. Proc. Natl. Acad. Sci. USA. **88(24)**:11281–11284.

Howard, R. J., Valent, B. (1996). Breaking and entering host penetration by the fungal rice blast pathogen *Magnaporthe grisea*. Annu. Rev. Microbiol. **50:**491-512.

Howard, R.J., Bourett, T.M., Ferrari, M.A**.** (1991). Infection by *Magnaporthe grisea*: An in vitro analysis. In Electron Microscopy of Plant Pathogens, K. Mendgen and D.-E. Lesemann, eds (Berlin: Springer-Verlag). pp: 251-264.

Huang, H. L., Brandriss, M. C.(2000). The regulator of the yeast proline utilization pathway is differentially phosphorylated in response to the quality of the nitrogen source. Mol. Cell Biol. **20(3)**:892-9.

Huang, L.S., Doherty, H.K., Herskowitz, I. (2005). The Smk1p MAP kinase negatively regulates Gsc2p, a 1,3-beta-glucan synthase, during spore wall morphogenesis in *Saccharomyces cerevisiae*. Proc. Natl. Acad. Sci. USA. **102:**12431–12436.

Hua-Van, A., Hericourt, F., Capy, F., Daboussi, M. J., Langin, T. (1998). Three highly divergent subfamilies of the impala transposable element coexist in the genome of the fungus *Fusarium oxysporum*. Mol. Gen. Genet. **259(4):** 354–362.

Huser, A., Takahara, H., Schmalenbach, W., O'Connell, R. (2009). Discovery of Pathogenicity Genes in the Crucifer Anthracnose Fungus *Colletotrichum higginsianum*, Using Random Insertional Mutagenesis. Mol. Plant Microbe Interact. **22(2)**: 143-156.

Hutchison, E. A., Bueche, J. A., Glass, N. L. (2012). Diversification of a Protein Kinase Cascade: IME-2 Is Involved in Nonself Recognition and Programmed Cell Death in *Neurospora crassa*. Genetics. **192(2)**:467-82.

Ichimura, Y., Kirisako, T., Takao, T., Satomi, Y., Shimonishi, Y., Ishihara, N., Mizushima, N., Tanida, I., Kominami, E., Ohsumi, M., Noda, T., Ohsumi, Y. (2000). An ubiquitin-like system mediates protein lipidation. Nature. **408(6811)**:488–492.

Idnurm, A., Howlett, B. J. (2002). Isocitrate lyase is essential for pathogenicity of the fungus *Leptosphaeria maculans* to canola (*Brassica napus*). Eukaryot Cell. **1(5):**719–724.

Idnurm, A., Reedy, J. L., Nussbaum, J. C., Heitman, J. (2004). *Cryptococcus neoformans* virulence gene discovery through insertional mutagenesis. Eukaryot. Cell. **3(2)**:420–429.

Igarashi, S., Utiamada, C. M., Igarashi, L. C., Kazuma, A. H., Lopes, R. S. (1986). P*yricularia* in wheat. 1. Occurrence of *Pyricularia* sp. in Paran state. Fitopatol. Bras. **11:** 351–352.

Imazaki, I., Kurahashi, M., Iida, Y., Tsuge, T. (2007). Fow2, a Zn(II)2Cys6-type transcription regulator, controls plant infection of the vascular wilt fungus *Fusarium oxysporum*. Mol. Microbiol. **63(3)**:737-753.

Ingley E, Hemmings BA (1994). Pleckstrin homology (PH) domains in signal transduction. J. Cell. Biochem. **56 (4)**:436–43.

Irniger, S. (2011). The Ime2 protein kinase family in fungi: more duties than just meiosis. Mol. Microbiol. **80**:1–13.

Itoh, Y., Scott, B. (1997). Effect of de-phosphorylation of linearized pAN7-1 and of addition of restriction enzyme on plasmid integration in *Penicillium paxilli.* Curr Genet. **32(2)**:147-51.

Ishida, Y., Saito, H., Ohta, S., Hiei, Y., Komari, T., and Kumashiro, T. (1996). High efficiency transformation of maize (Zea mays L.) mediated by *Agrobacterium tumefaciens*. Nat. Biotechnol. **14(6)**: 745-750.

Jeon, J. S., Lee, S., Jung, K. H., Jun, S. H., Jeong, D. H., Lee, J., Kim, C., Jang, S., Lee, S., Yang, K., Nam, J., An, K., Han, M. J., Sung, R. J., Choi, H. S., Yu, J. H., Choi, J. H., Cho, S.Y., Cha, S. S., Kim, S. I., An, G. (2000). T-DNA insertional mutagenesis for functional genomics in rice. Plant J. **22:**561-570.

Jeon, J., Goh, J., Yoo, S., Chi, M.H., Choi, J., Rho, H. S., Park, J., Han, S. S., Kim, B. R., Park, S.Y., Kim, S., Lee, Y.H. (2008). A putative MAP kinase kinase kinase, MCK1, is required for cell wall integrity and pathogenicity of the rice blast fungus, *Magnaporthe oryzae*. Mol. Plant Microbe Interact. **21(5)**: 525-534.

Ji, L., Jiang, Z. D., Liu, Y., Koh, C. M., Zhang, L. H. (2010). A Simplified and efficient method for transformation and gene tagging of Ustilago maydis using frozen cells. Fungal Genet. Biol. **47(4)**: 279-287.

Jin, S. G., Prusti, R. K., Roitsch, T., Ankenbauer, R. G., Nester, E. W. (1990). Phosphorylation of the VirG Protein of *Agrobacterium tumefaciens* by the Autophosphorylated VirA Protein - Essential Role in Biological-Activity of VirG. J. Bacteriol. **172**:4945-4950.

Johnston, M. (1987). Genetic evidence that zinc is an essential co-factor in the DNA binding domain of GAL4 protein. Nature. **328(6128)**:353-5.

Johnston, S. A., Salmeron, J. M., Dincher, S. S. (1987). Interaction of positive and negative regulatory proteins in the galactose regulon of yeast. Cell. **50(1)**:143-6.

Kado, C.I. (1994). Promiscuous DNA Transfer System of *Agrobacterium tumefacien*s - Role of the VirB Operon in Sex Pilus Assembly and Synthesis. Mol. Microbiol.**12**:17-22.

Kadotani N, Murata T, Quoc NB, Adachi Y, Nakayashiki H. (2008). Transcriptional control and protein specialization have roles in the functional diversification of two dicer-like proteins in Magnaporthe oryzae. Genetics. **180(2)**:1245-9.

Kahmann, R, Basse, C. (1999). REMI (Restriction Enzyme Mediated Integration and its impact on the isolation of pathogenicity genes in fungi attacking plants. Eur. J. Plant Pathol. **105:**221-9.

Kamper, J., Kahmann, R., Bolker, M., Ma, L. J., Brefort, T., Saville, B. J., Banuett, F., Kronstad, J. W., Gold, S. E., Müller, O., Perlin, M. H., Wösten, H. A., de Vries, R., Ruiz-Herrera, J., Reynaga-Peña, C. G., Snetselaar, K., McCann, M., Pérez-Martín, J., Feldbrügge, M., Basse, C. W., Steinberg, G., Ibeas, J. I., Holloman, W., Guzman, P., Farman, M., Stajich, J. E., Sentandreu, R., González-Prieto, J. M., Kennell, J. C., Molina, L., Schirawski, J., Mendoza-Mendoza, A., Greilinger, D., Münch, K., Rössel, N., Scherer, M., Vranes, M., Ladendorf, O., Vincon, V., Fuchs, U., Sandrock, B., Meng, S., Ho, E. C., Cahill, M. J., Boyce, K. J., Klose, J., Klosterman, S. J., Deelstra, H. J., Ortiz-Castellanos, L., Li, W., Sanchez-Alonso, P., Schreier, P. H., Häuser-Hahn, I., Vaupel, M., Koopmann, E., Friedrich, G., Voss, H., Schlüter, T., Margolis, J., Platt, D., Swimmer, C., Gnirke, A., Chen, F., Vysotskaia, V., Mannhaupt, G., Güldener, U., Münsterkötter, M., Haase,

D., Oesterheld, M., Mewes, H. W., Mauceli, E. W., DeCaprio, D., Wade, C. M., Butler, J., Young, S., Jaffe, D. B., Calvo, S., Nusbaum, C., Galagan, J., Birren, B. W. (2006). Insights from the genome of the biotrophic fungal plant pathogen *Ustilago maydis*. Nature. **444:** 97–101

Kankanala, P., Czymmek, K. Valent, B. (2007). Roles for rice membrane dynamics and plasmodesmata during biotrophic invasion by the blast fungus. Plant Cell **19(2):** 706–724.

Kant, P., Kant, S., Jain, R.K., and Chaudhury, V.K. (2007). *Agrobacterium*-mediated high frequency transformation in dwarf recalcitrant rice cultivars. Biol. Plantarum. **51**:61-68.

Karthikeyan, V., Gnanamanickam, S. (2008). Biological control of Setaria blast Magnaporthe grisea with bacterial strains. Crop Prot. **27**:263–267.

Keane, T. M., Creevey, C. J., Pentony, M. M., Naughton, T. J., McInerney, J. O. (2006). Assessment of methods for amino acid matrix selection and their use on empirical data shows that ad hoc assumptions for choice of matrix are not justified. BMC Evol. Biology. **6**:29.

Keegan, L., Gill, G., Ptashne, M.(1986). Separation of DNA binding from the transcription-activating function of a eukaryotic regulatory protein. Science. **231(4739)**:699-704.

Kempken, F., Kuck, U. (1996). Restless, an active Ac-like transposon from the fungus Tolypocladium inflatum: Structure, expression, and alternative RNA splicing. Mol. Cell. Biol. **16**:6563-6572.

Kershaw, M. J., Talbot, N. J. (2009). Genome-wide functional analysis reveals that infection-associated fungal autophagy is necessary for rice blast disease. Proc Natl Acad Sci USA. **106(37):** 15967-15972.

Khang, C. H., Berruyer, R., Giraldo, M. C., Kankanala, P., Park, S. Y., Czymmek, K., Kang, S., Valent, B. (2010). Translocation of Magnaporthe oryzae effectors into rice cells and their subsequent cell-to-cell movement. Plant Cell. **22(4)**:1388-403.

Kim, J. E., Myong, K., Shim, W. B., Yun, S.H., Lee, Y.W. (2007). Functional characterization of acetylglutamate synthase and phosphoribosylamine-glycine ligase genes in *Gibberella zeae*. Curr Genet. **51(2)**: 99-108.

Kim, J., Huang, W.-P., and Klionsky, D. J. (2001). Membrane recruitment of Aut7p in the autophagy and cytoplasm to vacuole targeting pathways requires Aut1p, Aut2p, and the autophagy conjugation complex. J. Cell Biol. **152**:51–64.

Kim, S., Park, S. Y., Kim, K. S., Rho, H. S., Chi, M. H., Choi, J., Park, J., Kong, S., Park, J., Goh, J., Lee, Y.H.(2009). Homeobox Transcription Factors Are Required for Conidiation and Appressorium Development in the Rice Blast Fungus *Magnaporthe oryzae*. PLoS Genet. **5(12)**:e1000757.

Kim, S., Ahn, I. P., Rho, H. S., Lee, Y. H. (2005). *MHP1*, a *Magnaporthe grisea* hydrophobin gene, is required for fungal development and plant colonization. Mol. Microbiol. **57(5):** 1224-37.

Kimura, A., Takano, Y., Furusawa, I., Okuno, T. (2001). Peroxisomal metabolic function is required for appressorium-mediated plant infection by *Colletotrichum lagenarium*. Plant Cell. **13(8)**: 1945-1957.

Kirisako, T., Baba, M., Ishihara, N., Miyazawa, K., Ohsumi, M., Yoshimori, T., Noda, T., and Ohsumi, Y. (1999). Formation process of autophagosome is traced with Apg8/Aut7p in yeast. J. Cell Biol. **147**:435–446.

Klionsky, D. J. (2007). Autophagy: from phenomenology to molecular understanding in less than a decade. Nat Rev Mol Cell Biol. **8(11):** 931-937.

Knogge, W. (1998). Fungal pathogenicity. Curr Opin. Plant Pathol. **1:** 324-328.

Koch, W. J., Inglese, J., Stone, W. C., Lefkowitz, R. J. (1993). The binding site for the beta gamma subunits of heterotrimeric G proteins on the beta-adrenergic receptor kinase. J. Biol. Chem. **268(11)**:8256-60.

Koelle, M. R. **(1997).** A new family of G-protein regulators - the RGS proteins. Curr Opin. Cell Biol. **9(2)**:143-7.

Koncz, C., Nemeth, K., Redei, G.P., and Schell, J. (1992). T-DNA Insertional utagenesis in *Arabidopsis*. Plant Mol. Biol. **20**:963-976.

Koncz, C., Redei, G.P., Konczkalman, Z., Schell, J. (1989). Insertional Mutations in *Arabidopsis* Generated by T-DNA. Genetics. **122**:S38-S38.

Kraulis, P. J., Raine, A. R., Gadhavi, P. L., Laue, E. D. (1992). Structure of the DNA-binding domain of zinc GAL4. Nature.**356**:448 – 450.

Krisak, L., Strich, R., Winters, R. S., Hall, J. P., Mallory, M. J., Kreitzer, D., Tuan, R. S., Winter, E. (1994). SMK1, a developmentally regulated MAP kinase, is required for spore wall assembly in *Saccharomyces cerevisiae*. Genes Dev. **8**: 2151–2161.

Kronstad, J. W. (1997). Virulence and cAMP in smuts, blast, and blight. Trends Plant Sci. **2:** 193–199.

Kulkarni, R. D., Thon, M. R., Pan, H. Q., Dean, R. A. (2005). Novel G-protein-coupled receptor like proteins in the plant pathogenic fungus *Magnaporthe grisea*. Genome Biol. **6:** R24.

Kurahashi, Y. (2001). Melanin biosynthesis inhibitors (MBIs) for control of rice blast. Pestic. Outlook. **12**:32–35.

Ladendorf, O., Brachmann, A., and Kamper, J. (2003). Heterologous transposition in *Ustilago maydis*. Mol. Genet. Genom. **269**:395-405.

Lai, E. M., Kado, C. I. (1998). Processed VirB2 is the major subunit of the promiscuous pilus of *Agrobacterium tumefaciens*. J. Bacteriol. **180**:2711-2717.

Langmead, B., Trapnell, C., Pop, M., Salzberg, S. L. (2009). Ultrafast and memory-efficient alignment of short DNA sequences to the human genome. Genome Biol. **10(3)**:R25.

Latterell, F.M., Rossi, A.E. (1986). Longevity and Pathogenic Stability of *Pyricularia oryzae*. Phytopathology **76:**231-235.

Lau, G. W., Hamer, J. E. (1998). Acropetal: a genetics locus required for conidiophore architecture and pathogenicity in the rice blast fungus. Fungal Genet. Biol. **24(1-2):** 228–39.

Lebrun, M. H., Dutfoy, F., Gaudemer, F., Kunesch, G. & Gaudemer, A., (1990) Detection and quantification of the fungal phytotoxin tenuazonic acid produced by *Pyricularia oryzae*.

Leclerque, A., Wan, H., Abschutz, A., Chen, S., Mitina, G. V., Zimmermann, G., Schairer, H. U. (2003). *Agrobacterium* mediated insertional mutagenesis (AIM) of the entomopathogenic fungus *Beauveria bassiana*. Curr Genet. **45(2)**:111–119.

Lee, K., Singh, P., Chung, W.-C., Ash, J., Kim, T. S., Hang, L., Park, S. (2006). Light regulation of asexual development in the rice blast fungus, *Magnaporthe oryzae*. Fungal Genet. Biol. **43(10):** 694–706.

Lee, L. Y., Gelvin, S. B., Kado, C. I. (1999). PSA causes oncogenic suppression of *Agrobacterium* by inhibiting VirE2 protein export. J. Bacteriol. **181:**186-196.

Lee, N., D'Souza, C. A., Kronstad, J. W. (2003). Of smut, blasts, mildews and blights: cAMP signalling in phytopathogenic fungi. Annu. Rev. Phytopathol. **41:** 399-427.

Lee, Y. H., Dean, R. A. (1993). cAMP regulates infection structure formation in the plant pathogenic fungus *Magnaporthe grisea*. Plant Cell **5(6):** 693–700.

Lengeler, K. B., Davidson, R. C., D'souza, C., Harashima, T., Shen, W. C., Wang, P., Pan, X., Waugh, M., Heitman, J. (2000). Signal transduction cascades regulating fungal development and virulence. Microbiol. Mol. Biol. Rev. **64(4):** 746-85.

Leung, H., Lehtinen, U., Karjalainen, R., Skinner, D., Tooley, P., Leong, S., Ellingboe, A. (1990). Transformation of the Rice Blast Fungus *Magnaporthe grisea* to Hygromycin-B Resistance. Curr Genet. **17**:409-411.

Lev, S., Sharon, A., Hadar, R., Ma, H., Horwitz, B. A. (1999). A mitogen-activated protein kinase of the corn leaf pathogen *Cochliobolus heterostrophus* is involved in conidiation,

appressorium formation, and pathogenicity: diverse roles for mitogen-activated protein kinase homologs in foliar pathogens. Proc Natl Acad Sci USA. **96(23):** 13542-13547.

Levine, B., Klionsky, D. J. (2004). Development by self-digestion: molecular mechanisms and biological functions of autophagy. Dev. Cell. **6(4)**:463–477.

Li, G., Zhou, X., Xu, J. R. (2012). Genetic control of infection-related development in *Magnaporthe oryzae*. Curr Opin Microbiol. S1369-5274(12)00120-8.

Li, L. P., Jia, Y. H., Hou, Q. M., Charles, T. C., Nester, E. W., and Pan, S. Q. (2002). A global pH sensor: *Agrobacterium* sensor protein ChvG regulates acid-inducible genes on its two chromosomes and Ti plasmid. Proc. Natl. Acad. Sci. USA. **99:**12369-12374.

Li, Y., Liang, S., Yan, X., Wang, H., Li, D., Soanes, D. M., Talbot, N. J., Wang, Z., Wang, Z. (2010). Characterization of MoLDB1 Required for Vegetative Growth, Infection-Related Morphogenesis, and Pathogenicity in the Rice Blast Fungus *Magnaporthe oryzae*. Mol. Plant Microbe Interac. **23(10)**: 1260-1274.

Li, Y., Yan, X., Wang, H., Liang, S., Ma, W-B., Fang, M-Y., Talbot, N. J., Wang, Z-Y. (2010). MoRic8 is a novel component of G-Protein signaling during plant infection by the rice blast fungus *Magnaporthe oryzae*. Mol Plant Microbe Interact. **23(3):** 317–331.

Liang, S., Wang, Z., Liu, P., Li, D. (2006). A G gamma subunit promoter T-DNA insertion mutant -A1-412 of *Magnaporthe grisea* is defective in appressorium formation, penetration and pathogenicity. Chinese Science Bulletin. **51(18)**: 2214-2218.

Linnemannstöns P, Voss T, Hedden P, Gaskin P, Tudzynski B. (1999). Deletions in the gibberellin biosynthesis gene cluster of Gibberella fujikuroi by restriction enzyme-mediated integration and conventional transformation-mediated mutagenesis. Appl Environ. Microbiol. **65(6)**:2558-64.

Liu X.H., Lu, J.P., Zhang, L., Dong, B., Min, H., Lin F.C. (2007). Involvement of a *Magnaporthe grisea* serine/threonine kinase gene *MgATG1*, in appressorium turgor and pathogenesis. Eukaryot. Cell. **6(6):** 997–1005.

Liu, H., Suresh, A., Willard, F. S., Siderovski, D. P., Lu, S., Naqvi, N. I. (2007). Rgs1 regulates multiple Gα subunits in *Magnaporthe* pathogenesis, asexual growth and Thigmotropism. EMBO J. **26(3):** 690–700.

Liu, K. H., Shen, W. C. (2011). Mating differentiation in *Cryptococcus neoformans* is negatively regulated by the Crk1 protein kinase. Fungal Genet. Biol. **48:** 225–240.

Liu, S., Dean, R. A. (1997). G protein α-subunit genes control growth, development and pathogenicity of *Magnaporthe grisea*. Mol. Plant Microbe Interact. **10(9):** 1075-1086.

Liu, W., Xie, S., Zhao, X., Chen, X., Zheng, W., Lu, G., Xu, J. R., Wang, Z. (2010). A Homeobox Gene Is Essential for Conidiogenesis of the Rice Blast Fungus *Magnaporthe oryzae*. Mol. Plant Microbe Interact. **23(4)**:366–375.

Liu, W., Zhou, X., Li, G., Li, L., Kong, L., Wang, C., Zhang, H., Xu, J. R. (2011). Multiple plant surface signals are sensed by different mechanisms in the rice blast fungus for appressorium formation. PLoS Pathog. **7(1)**:1001261.

Loftus, B. J., Fung, E., Roncaglia, P., Rowley, D., Amedeo, P., Bruno, D., Vamathevan, J., Miranda, M., Anderson, I. J., Fraser, J. A., Allen, J. E., Bosdet, I. E., Brent, M. R., Chiu, R., Doering, T. L., Donlin, M. J., D'Souza, C. A., Fox, D. S., Grinberg, V., Fu, J., Fukushima, M., Haas, B. J., Huang, J. C., Janbon, G., Jones, S. J., Koo, H. L., Krzywinski, M. I., Kwon-Chung, J. K., Lengeler, K. B., Maiti, R., Marra, M. A., Marra, R. E., Mathewson, C. A., Mitchell, T. G., Pertea, M., Riggs, F. R., Salzberg, S. L., Schein, J. E., Shvartsbeyn, A., Shin, H., Shumway, M., Specht, C. A., Suh, B. B., Tenney, A., Utterback, T. R., Wickes, B. L., Wortman, J. R., Wye, N. H., Kronstad, J. W., Lodge, J. K., Heitman, J., Davis, R. W., Fraser, C. M., Hyman, R. W. (2005). The genome of the basidiomycetous yeast and human pathogen *Cryptococcus neoformans*. Science. **307:** 1321-4.

Lorenz, W. W., Dean, J. F. (2002). SAGE profiling and demonstration of differential gene expression along the axial developmental gradient of lignifying xylem in loblolly pine (Pinus taeda). Tree Physiol. **22(5)**:301-10.

Lu, S., Lyngholm, L., Yang, G., Bronson, C., Yoder, O. C., Turgen, B. G. (1994.) Tagged mutations at the Tox1 locus of *Cochliobolus heterostrophus* by restriction enzyme-mediatedProc. Natl. Acad. Sci. USA. **91(26)**:12649-53.

Ma, L. J., Ibrahim, A. S., Skory, C., Grabherr, M. G., Burger, G., Butler, M., Elias, M., Idnurm, A., Lang, B. F., Sone, T., Abe, A., Calvo, S. E., Corrochano, L. M., Engels, R., Fu, J., Hansberg, W., Kim, J. M., Kodira, C. D., Koehrsen, M. J., Liu, B., Miranda-Saavedra, D., O'Leary, S., Ortiz-Castellanos, L., Poulter, R., Rodriguez-Romero, J., Ruiz-Herrera, J., Shen, Y. Q., Zeng, Q., Galagan, J., Birren, B. W., Cuomo, C. A., Wickes, B. L. (2009). Genomic analysis of the basal lineage fungus *Rhizopus oryzae* reveals a whole-genome duplication. PLoS Genet. **5(7): e1000549**.

MacPherson, S., Larochelle, M., Turcotte, B. (2006). A fungal family of transcriptional regulators the zinc cluster proteins. Microbiol. Mol. Biol. Rev. **70(3)**:583-604.

Madden, L. V., Wheelis, M. (2003). The threat of plant pathogens as weapons against U.S. crops. Ann. Rev. Phytopathol. **41:** 155-176.

Madrid, M. P., Di Pietro, A., Roncero, M. I. (2003). Class V chitin synthase determines pathogenesis in the vascular wilt fungus *Fusarium oxysporum* and mediates resistance to plant defence compounds. Mol. Microbiol. **47(1)**: 257-266.

Maier, F. J., Schafer, W., (1999) Mutagenesis via insertional or restriction enzyme mediated integration (REMI) as a tool to tag pathogenicity related genes in plant pathogenic fungi. Biol. Chem. **380(7-8):** 855–864.

Malonek, S., Meinhardt, F. (2001). *Agrobacterium tumefaciens* mediated genetic transformation of the phytopathogenic ascomycete Calonectria morganii. Curr Genet. **40(2)**:152–155.

Marchler-Bauer, A., Anderson, J. B., Chitsaz, F., Derbyshire, M. K., DeWeese-Scott, C., Fong, J. H., Geer, L.Y., Geer, R. C., Gonzales, N. R., Gwadz, M., He, S., Hurwitz, D. I., Jackson, J. D., Ke, Z., Lanczycki, C. J., Liebert, C. A., Liu, C., Lu, F., Lu, S., Marchler, G. H., Mullokandov M, Song JS, Tasneem A, Thanki N, Yamashita RA, Zhang D, Zhang N, Bryant, S. H. (2009). CDD: specific functional annotation with the Conserved Domain Database. Nucleic Acids Res. **37(D)**:205-10.

Marchler-Bauer, A., Bryant, S. H. (2004). CD-Search: protein domain annotations on the fly. Nucleic Acids Res. **32(W)**:327-331

Marchler-Bauer, A., Lu, S., Anderson, J. B., Chitsaz, F., Derbyshire, M. K., DeWeese-Scott, C., Fong, J. H., Geer, L. Y., Geer, R. C., Gonzales, N. R., Gwadz, M., Hurwitz , D. I., Jackson, J. D., Ke, Z., Lanczycki, C. J., Lu, F., Marchler, G. H., Mullokandov. M., Omelchenko, M. V., Robertson, C. L., Song, J. S., Thanki, N., Yamashita, R. A., Zhang, D., Zhang, N., Zheng, C., Bryant, S. H. (2011). CDD: a Conserved Domain Database for the functional annotation of proteins. Nucleic Acids Res. **39 (DI)**:225-9.

Martin, J. A., Wang, Z. (2011). Next-generation transcriptome assembly. Nat Rev Genet. **7;12(10)**:671-82

Maruthachalam, K., Klosterman, S. J., Kang, S., Hayes, R. J., Subbarao, K. V. (2011). Identification of Pathogenicity Related Genes in the Vascular Wilt Fungus *Verticillium dahliae* by *Agrobacterium tumefaciens* Mediated T-DNA Insertional Mutagenesis. Mol. Biotechnol. **49(3)**: 209-221.

Matsumura, H., Yoshida, K., Luo, S., Kimura, E., Fujibe, T., Albertyn, Z., Barrero, R. A., Krüger, D. H., Kahl, G., Schroth, G. P., Terauchi, R. (2010) .Highthroughput SuperSAGE for digital gene expression analysis of multiple samples using next generation sequencing. PLoS One. **5(8):**e12010.

May, G.D., Afza, R., Mason, H.S., Wiecko, A., Novak, F.J. and Arntzen, C.J. (1995). Generations of transgenic Banana (*Musa acuminata*) plants via *Agrobacterium* mediated transformation. Biotechnology. **13**: 486-492.

Mayer, B. J., Ren, R., Clark, K. L., Baltimore, D. (1993). A putative modular domain present in diverse signalling proteins. Cell. **73(4)**:629-30.

McCafferty, H. R., Talbot, N. J. (1998). Identification of three ubiquitin genes of the rice blast fungus *Magnaporthe grisea*, one of which is highly expressed during initial stages of plant colonisation. Current Genetics **33:** 352-361.

McClung, A.M., Marchetti, M. A., Webb, B. D., Bollich, C.N. (1997). Registration of 'Jefferson' rice. Crop Sci. **37**:629–630.

Mehrabi, R., Ding, S., Xu, J-R. (2008). MADS-box transcription factor Mig1 is required for infectious growth in *Magnaporthe grisea*. Eukaryot. Cell. **7(5):** 791–799.

Melchers, L. S., Regensburgtuink, J. G., Schilperoort, R. A., Hooykaas, P. J. J. (1989). Specificity of Signal Molecules in the Activation of *Agrobacterium* Virulence Gene-Expression. Mol. Microbiol. **3:**969-977.

Meng, Y., Patel, G., Heist, M., Betts, M. F., Tucker SL, Galadima N, Donofrio NM, Brown D, Mitchell TK, Li L, Xu JR, Orbach M, Thon M, Dean RA, Farman ML. **(**2007**).** A systematic analysis of T-DNA insertion events in Magnaporthe oryzae. Fungal Genet. Biol. **44(10)**:1050-64.

Meyer. V., Mueller. D., Strowig, T., Stahl, U. (2003). Comparison of different transformation methods for *Aspergillus giganteus*. Curr Genet. **43(5)**:371–377.

Michielse, C. B., Arentshorst, M., Ram, A. F., van den Hondel, C. A. (2005). *Agrobacterium* mediated transformation leads to improved gene replacement efficiency in *Aspergillus awamori*. Fungal Genet. Biol. **42(1)**:9–19.

Michielse, C. B., Ram, A. F., Hooykaas, P. J., van den Hondel, C. A. (2004a) *Agrobacterium* mediated transformation of *Aspergillus awamori* in the absence of full length VirD2, VirC2 or VirE2 leads to insertion of aberrant T-DNA structures. J. Bacteriol. **186(7)**:2038–2045.

Michielse, C. B., Ram, A. F., Hooykaas, P. J., van den Hondel, C. A. (2004b) Role of bacterial virulence proteins in *Agrobacterium* mediated transformation of *Aspergillus awamori*. Fungal Genet. Biol. **41(5)**:571–578.

Michielse, C. B., Salim, K., Ragas, P., Ram, A. F., Kudla, B., Jarry, B., Punt, P. J., van den Hondel, C. A. (2004c). Development of a system for integrative and stable transformation of the zygomycete *Rhizopus oryzae* by *Agrobacterium* mediated DNA transfer. Mol. Gen. Genomics. **271(4)**:499–510.

Michielse, C. B., van Wijk, R., Reijnen, L., Cornelissen, B. J., Rep, M. (2009). Insight into the molecular requirements for pathogenicity of *Fusarium oxysporum* f. sp lycopersici through large-scale insertional mutagenesis. Genome Biol. **10(1)**:R4.

Michielse, C. B., van Wijk, R., Reijnen, L., Manders, E. M., Boas, S., Olivain, C., Alabouvette, C., Rep, M. (2009). The Nuclear Protein Sge1 of *Fusarium oxysporum* Is Required for Parasitic Growth. Plos Pathog. **5(10)**:e1000637.

Mikosch, T. S., Lavrijssen, B., Sonnenberg, A. S., van Griensven, L. J. (2001). Transformation of the cultivated mushroom *Agaricus bisporus* (Lange) using T-DNA from *Agrobacterium tumefaciens*. Curr Genet. **39(1)**:35–39.

Mitchell, T. K., Dean, R. A. (1995). The cAMP-Dependent Protein Kinase Catalytic Subunit Is Required for Appressorium Formation and Pathogenesis by the Rice Blast Pathogen Magnaporthe grisea. Plant Cell. **7(11)**:1869-1878.

Money, N. P. (1999). Fungus punches its way in. Nature **401(6751):** 332–33.

Mullins, E. D., Chen, X., Romaine, P., Raina, R., Geiser, D. M., Kang, S. (2001). *Agrobacterium* Mediated Transformation of *Fusarium oxysporum* An Efficient Tool for Insertional Mutagenesis and Gene Transfer. Phytopathology. **91(2)**:173-80.

Mulllins, L. D., Kang, S. (2001). Transformation: a tool for studying fungal pathogens of plants. Cell. Mol.Life Sci. **58:**2043-2052.

Musacchio A, Gibson T, Rice P, Thompson J, Saraste M. (1993). The PH domain: a common piece in the structural patchwork of signalling proteins. Trends Biochem. Sci. **18(9)**:343-8.

Nagarajan, N. & Pop, M., (2010) Sequencing and genome assembly using next-generation

Namiki, F., Matsunaga, M., Okuda, M., Inoue, I., Nishi, K., Fujita, Y., Tsuge, T. (2001). Mutation of an arginine biosynthesis gene causes reduced pathogenicity in *Fusarium oxysporum* f. sp melonis. Mol. Plant-Microbe Interact. **14(4)**: 580-584.

Nguyen, Q. B., Kadotani, N., Kasahara, S., Tosa, Y., Mayama, S., Nakayashiki, H. (2008). Systematic analysis of calcium signalling proteins in the genome of the rice blast fungus *Magnaporthe oryzae* using a high-throughput RNA silencing system. Mol. Microbiol. **68(6)**:1348–1365.

Nishimura, M., Hayashi, N., Jwa, N. S., Lau, G. W., Hamer, J. E., Hasebe, A. (2000). Insertion of the LINE retrotransposon MGL causes a conidiophore pattern mutation in *Magnaporthe grisea*. Mol. Plant-Microbe Interact. **13(8)**: 892-894.

Nishimura, M., Park, G., Xu, J. R. (2003). The G-beta subunit *MGB1* is involved in regulating multiple steps of infection-related morphogenesis in Magnaporthe grisea. Mol. Microbiol. **50(1):** 231–243.

Normile, D. (2010). Holding back a torrent of rats. Science. **327(5967):** 806-807.

Odenbach, D., Breth, B., Thines, E., Weber, R. W. S., Anke, H., and Foster, A. J. 2007. The transcription factor Con7p is a central regulator of infection-related morphogenesis in the rice blast fungus *Magnaporthe grisea*. Mol. Microbiol. **64**:293-307.

Ohtaka, N., Kawamata, H., Narisawa, K. (2008) Suppression of rice blast using freeze-killed mycelia of biocontrol fungal candidate MKP5111B. J. Gen. Plant Pathol. **74**:101–108.

Oldenburg, K. R., Vo, K. T., Michaelis, S., and Paddon, C. (1997). Recombination mediated PCR-directed plasmid construction *in vivo* in yeast. Nucleic Acids Res. **25(2):** 451–452.

Oliver, R. P., Roberts, I. N., Harling, R., Kenyon, L., Punt, P. J., Dingemanse, M. A., Vandenhondel, C.(1987). Transformation of *Fulvia fulfa*, a fungal pathogen of tomato, to hygromycin B resistance *Curr. Genet.* **12**: 231-233.

Ou, H., Yan, L., Osmanovic, S., Greenberg, C. C., Brady, M. J. (2005). Spatial reorganization of glycogen synthase upon activation in 3T3-L1 adipocytes. Endocrinolgy. **146(1):** 494-502.

Ou, S. H. (1985). Rice diseases. 2nd edition. Commonwealth Agricultural Bureaux, Kew, Surrey, England. 380 pp.

Ou, S.H. et al. (1987) Rice Diseases. CAB International Mycological Institute.

Padmanabhan S.Y. (1973). The great Bengal famine. Annu. Rev. Phytopathol. **11:** 11–26.

Pak, J., J. Segall. (2002) Regulation of the premiddle and middle phases of expression of the NDT80 gene during sporulation of *Saccharomyces cerevisiae*. Mol. Cell. Biol. **22**: 6417–6429.

Park, G., Bruno, K. S., Staiger, C. J., Talbot, N. J. Xu, J. R. (2004). Independent genetic mechanisms mediate turgor generation and penetration peg formation during plant infection in the rice blast fungus. Mol. Microbiol. **53(6):** 1695–1707.

Park, G., Xue, C., Zhao, X., Kim, Y., Orbach, M., Xua, J-R. (2006). Multiple upstream signals converge on the adaptor protein Mst50 in *Magnaporthe grisea*. Plant Cell. **18(10):** 2822–2835.

Park, G., Xue, G. Y., Zheng, L., Lam, S., Xu, J. R. (2002). *MST12* regulates infectious growth but not appressorium formation in the rice blast fungus *Magnaporthe grisea*. Mol. Plant Microbe Interact. **15(3):** 183–92.

Park, S. M., Kim, D. K. (2004). Transformation of a filamentous fungus *Cryphonectria parasitica* using *Agrobacterium tumefaciens*. Biotechnol. Bioprocess Eng. **9**:217–222.

Parker, P. J., Hemmings, B. A., Gierschik, P. (1994). PH domains and phospholipases-a meaningful relationship? Trends Biochem. Sci. **19(2)**:54-5.

Parsons, K. A., Chumley, F. G. & Valent, B., (1987) Genetic transformation of the fungal pathogen responsible for rice blast disease. *Proc. Natl. Acad. Sci. U. S. A.* **84**: 4161-4165.

Pawson, T. (1995). Protein modules and signaling networks. Nature. **373 (6515)**:573–80.

Payne, D. M., Rossomando, A. J., Martino, P., Erickson, A. K., Her, J. H., Shabanowitz, J., Hunt, D. F., Weber, M. J., Sturgill, T. W. (1991) Identification of the regulatory phosphorylation sites in pp42/mitogen-activated protein kinase (MAP kinase). EMBO J. **10(4)**: 885–892.

Paz, Y., Elazar, Z., Fass, D. (2000). Structure of GATE-16, membrane transport modulator and mammalian ortholog of autophagocytosis factor Aut7p. J. Biol. Chem. **275(33)**:25445–25450.

Pennisi, E. (2001). The push to pit genomics against fungal pathogens. Science. **292(5525):** 2273-2274.

Pennisi, E. (2010). Armed and dangerous. Science. **327(5967):** 805-806.

Pieknya, A. J., Maddox, A. X. (2010). The myriad roles of Anillin during cytokinesis. Semin. Cell Dev. Biol. **21(9)**:881–891.

Piers, K. L., Heath, J. D., Liang, X. Y., Stephens, K. M., Nester, E. W. (1996). *Agrobacterium tumefaciens*-mediated transformation of yeast. Proc. Natl. Acad. Sci. USA.**93**: 1613-1618.

Pitcher, J. A., Inglese, J., Higgins, J. B., Arriza, J. L., Casey, P. J., Kim, C., Benovic, J. L., Kwatra, M. M., Caron, M. G., Lefkowitz, R. J. (1992). Role of beta gamma subunits of G proteins in targeting the beta-adrenergic receptor kinase to membrane-bound receptors. Science. **257(5074)**:1264-7.

Pitcher, J. A., Touhara, K., Payne, E. S., Lefkowitz, R. J. (1995). Pleckstrin homology domain-mediated membrane association and activation of the beta-adrenergic receptor kinase requires coordinate interaction with G beta gamma subunits and lipid. J Biol. Chem. **270(20)**:11707-10.

Prabavathy, V.R., Mathivanan, N., Murugesan, K. (2006). Control of blast and sheath blight diseases of rice using antifungal metabolites produced by *Streptomyces* sp PM5. Biol. Control. **39**:313–319.

Ream, W. (1989). *Agrobacterium tumefaciens* and Inter kingdom Genetic Exchange. Annu. Rev. Phytopathol. **27**:583-618.

Redman, R. S., Ranson, J. C., Rodriguez, R. J. (1999). Conversion of the pathogenic fungus Colletotrichum magna to a nonpathogenic, endophytic mutualist by gene disruption. Mol. Plant Microbe Interact. **12**: 969–975.

Regensburg-Tuink, A.J., Hooykaas, P.J. (1993) Transgenic *N. glauca* plants expressing bacterial virulence gene virF are converted into hosts for nopaline strains of *A. tumefaciens*. Nature. **363(6424)**:69-71.

Rerngsamran, P, Murphy, M. B., Doyle, S. A., Ebbole, D. J. (2005). Fluffy, the major regulator of conidiation in *Neurospora crassa*, directly activates a developmentally regulated hydrophobin gene. Mol. Microbiol. **56(1)**:282-97.

Rho, H. S., Kang, S., Lee, Y. H. (2001). *Agrobacterium tumefaciens* mediated transformation of the plant pathogenic fungus, *Magnaporthe grisea*. Mol. Cells. **12(3)**:407–411.

Riddihough, G. (1994). More meanders and sandwiches. Nat. Struct. Biol. **1(11)**: 755–7.

Riggle, P. J., Kumamoto, C. A. (1998).Genetic analysis in fungi using restriction enzyme mediated integration. Curr Opin. Microbiol. **1(4):**395-9.

Rispail, N., Soanes, D. M., Ant, C., Czajkowski, R., Grunler, A., Huguet, R., Perez-Nadales, E., Poli, A., Sartorel, E., Valiante, V., Yang, M., Beffa, R., Brakhage, A. A., Gow, N. A. R., Kahmann, R., Lebrun, M.-H., Lenasi, H., Perez-Martin, J., Talbot, N. J., Wendland, J. & Di Pietro, A., (2009). Comparative genomics of MAP kinase and calcium-calcineurin signalling components in plant and human pathogenic fungi. *Fungal Genet. Biol.* **46**: 287-298.

Rogers, C. W., Challen, M. P., Green, J. R., Whipps, J. M. (2004). Use of REMI and *Agrobacterium* mediated transformation to identify pathogenicity mutants of the biocontrol fungus *Coniothyrium minitans*. FEMS Microbiol. Lett. **241(2):**207-14.

Rolland, S., Jobic, C., Fevre, M., Bruel, C. (2003). *Agrobacterium* mediated transformation of *Botrytis cinerea*, simple purification of monokaryotic transformants and rapid conidia-based identification of the transfer-DNA host genomic DNA flanking sequences. Curr Genet. **44(3)**:164–171.

Rosegrant, M. W., Cline, S. A. (2003).Global food security: challenges and policies. Science. **302(5652)**:1917-9.

Roumen, E.C. (1992). Partial resistance to neck blast influenced by stage of panicle development and rice genotype. Euphytica **64:** 173-182.

Sambrook, J., Fritsch, E. F., Maniatis, T. (1989). Molecular cloning: a laboratory manual. Cold Spring Harbor Laboratory, Cold Spring Harbor, New York.

Sanchez, O., Navarro, R. E., Aguirre, J. (1998). Increased transformation frequency and tagging of developmental genes in *Aspergillus nidulans* by restriction enzyme-mediated integration (REMI). Mol. Gen. Genet. **258(1-2):** 89–94.

Sanders, S. L., Herskowitz, I. (1996). The BUD4 protein of yeast, required for axial budding, is localized to the mother/BUD neck in a cell cycle-dependent manner. J. Cell. Biol. **134(2)**:413-27

Saraste, M., Hyvönen, M. (1995). Pleckstrin homology domains: a fact file. Curr. Opin. Struct. Biol. **5(3)**: 403–8.

Saunders, D. G., Aves, S. J., Talbot, N. J. (2010). Cell cycle-mediated regulation of plant infection by the rice blast fungus. Plant Cell. **22(2):** 497-507.

Schäfer W. (1993). The role of cutinase in fungal pathogenicity. Trends Microbiol. 1(2):69-71.

Schmid, D., Munz, C. (2007). Innate and adaptive immunity through autophagy. Immunity **27:**11–21.

Schrammeijer, B., Dulk-Ras, A., Vergunst, A. C., Jurado, J. E., Hooykaas, P. J. (2003) Analysis of Vir protein translocation from *Agrobacterium tumefaciens* using *Saccharomyces cerevisiae* as a model: evidence for transport of a novel effector protein VirE3. Nucleic Acids Res. **31(3)**:860–868.

Seong, K., Hou, Z., Tracy, M., Kistler, H. C., Xu, J. R. (2005). Random insertional mutagenesis identifies genes associated with virulence in the wheat scab fungus *Fusarium graminearum*. Phytopathology. **95(7)**: 744-750.

Sesma, A., Osbourn, A. E. (2004). The rice leaf blast pathogen undergoes developmental processes typical of root-infecting fungi. Nature **431:**582-586.

Severne, Y., Wieland, S., Schaffner, W., Rusconi, S. (1988). Metal binding 'finger' structures in the glucocorticoid receptor defined by site-directed mutagenesis.EMBO J. **7(8)**:2503-2508.

Shaohua, L., Dean, R. A. (1997). G Protein aSubunit Genes Control Growth, Development, and Pathogenicity of *Magnaporthe grisea*. Mol. Plant Microbe Interact. **10(9)**:1075–1086.

Shaw, G. (1993). Identification of novel pleckstrin homology (PH) domains provides a hypothesis for PH domain function. Biochem. Biophys. Res. Commun. **195(2)**:1145-51.

Shi, Z. Christian, D., Leuna, H. (1995). Enhanced transformation in Magnaporthe grisea-by restriction enzyme mediated integration of plasmid DNA. Phytopathology. **85:**329-333.

Shi, Z. X., Leung, H. (1994). Genetic analysis of sporulation in the rice blast fungus *Magnaporthe grisea*. Mol. Plant Microbe Interact. **7:** 113–120.

Shi, Z. X., Leung, H. (1995). Genetic analysis of sporulation in *Magnaporthe grisea* by chemical and insertional mutagenesis. Mol. Plant-Microbe Interact. **8:** 949–959.

Shi, Z., Christian, D., Leung, H. (1998). Interactions between spore morphogenetic mutations affect cell types, sporulation and pathogenesis in *Magnaporthe grisea*. Mol. Plant Microbe Interact. **11(3)**:199-207.

Shim, W. B., Sagaram, U. S., Choi, Y. E., So, J., Wilkinson, H. H., Lee, Y.W. (2006). FSR1 is essential for virulence and female fertility in *Fusarium verticillioides* and *F. graminearum*. Mol. Plant Microbe Interact. **19(7)**: 725-733.

Shin, M. E., A. Skokotas, E. Winter. (2010). The Cdk1 and Ime2 protein kinases trigger exit from meiotic prophase in *Saccharomyces cerevisiae* by inhibiting the Sum1 transcriptional repressor. Mol. Cell. Biol. **30**: 2996–3003.

Shintani, T., Huang, W. P., Stromhaug, P. E., Klionsky, D. J. (2002). Mechanism of cargo selection in the cytoplasm to vacuole targeting pathway. Dev. Cell. **3**:825–837.

Shubassi, G., Luca, N., Pak, J., Segall, J. (2003). Activity of phosphoforms and truncated versions of Ndt80, a checkpoint-regulated sporulation-specific transcription factor of *Saccharomyces cerevisiae*. Mol. Genet. Genom. **270**: 324–336.

Siddiqui, A. H. Brandriss, M. C. (1989). The Saccharomyces cerevisiae PUT3 activator protein associates with proline-specific upstream activation sequences. Mol. Cell. Biol. **9(11)**:4706-12

Siderovski, D. P., Hessel, A., Chung, S., Mak, T. W., Tyers, M. (1996). A new family of regulators of G-protein-coupled receptors. Curr Biol **6:** 211–212.

Siderovski, D. P., Willard, F. S. (2005). The GAPs, GEFs and GDIs of heterotrimeric G-protein alpha subunits. Int J Biol Sci **1:** 51–66.

Silva, C. P., Nomura, E., Freitas, E. G., Brugnaro, C. & Urashima, A. S., (2009) Efficiency of

Simon, M. I., Strathmann, M. P., Gautam, N. (1991). Diversity of G-proteins in signal transduction. Science. 252: 802-808.

Skamnioti, P., Gurr, S.J., (2009). Against the grain: safeguarding rice from rice blast disease. Trends in Biotechnology. **27:** 141-150.

Smith, D. R., Quinlan, A. R., Peckham, H. E., Makowsky, K., Tao, W., Woolf, B., Shen, L., Donahue, W.F., Tusneem, N., Stromberg, M.P., Stewart, D. A., Zhang, L., Ranade, S. S., Warner, J. B., Lee, C. C., Coleman, B. E., Zhang, Z., McLaughlin, S. F., Malek, J. A., Sorenson, J. M., Blanchard, A. P., Chapman, J., Hillman, D., Chen, F., Rokhsar, D. S., McKernan, K. J., Jeffries, T. W., Marth, G. T., Richardson, P. M. (2008). Rapid whole-genome mutational profiling using next-generation sequencing technologies. *Genome Res.* 1**8**: 1638-1642.

Smith, E. F., Townsend, C. O**.** (1907). A plant tumor of bacterial origin. Science. **25:**671-673.

Smith, H. E. (2011). Identifying insertion mutations by whole-genome sequencing. *BioTechniques.* **50**:96-97.

Smith *et al.* (2008). Rapid whole-genome mutational profiling using next-generation sequencing technologies. Genome Res.**18**: 1638-1642

Smith, H.E., Mitchell, A.P. (1989). A transcriptional cascade governs entry into meiosis in Saccharomyces cerevisiae. Mol. Cell. Biol. **9(5)**:2142–2152.

Soanes, D. M., Chakrabarti, A., Paszkiewicz, K. H., Dawe, A. L., Talbot, N. J. (2012). Genome-wide Transcriptional Profiling of Appressorium Development by the Rice Blast Fungus *Magnaporthe oryzae*. PLoS Pathog. **8(2)**: e1002514.

Soanes, D. M., Cooley, R. N., Kershaw, M. J., Foster, S. J., Talbot, N. J. (2002). Regulation of the *MPG1* hydrophobin gene from *Magnaporthe grisea*. Mol. Plant Microbe Interact. **15:** 1253–67.

Soanes, D. M., Richards, T. A., Talbot, N. J. (2007). Insights from sequencing fungal and oomycete genomes: what can we learn about plant disease and the evolution of pathogenicity? Plant Cell. **19(11)**:3318-26.

Soanes, D. M., Alam, I., Cornell, M., Wong, H. M., Hedeler, C., Paton, N. W., Rattray, M., Hubbard, S. J., Oliver, S. G., Talbot, N. J. (2008) Comparative genome analysis of filamentous fungi reveals gene family expansions associated with fungal pathogenesis.PLoS One. **4:3(6)**:e2300.

Sopko, R., Raithatha, S., Stuart, D. (2002). Phosphorylation and maximal activity of *Saccharomyces cerevisiae* meiosis-specific transcription factor Ndt80 is dependent on Ime2. Mol. Cell. Biol. **22**:7024–7040.

Stachel, S. E., Nester, E. W., Zambryski, P. C. (1986). A Plant-Cell Factor Induces Agrobacterium-Tumefaciens-Vir Gene-Expression. Proc. Natl. Acad. Sci. USA. **83:**379-383.

Staples RC, Hoch HC. (1995). Physical and chemical cues for spore germination and appressorium formation by fungal pathogens. In *The Mycota. V Plant Relationships, Part A*, ed. GC Carroll, P Tudzynski, pp. 27–40. Berlin/Heidelberg: Springer-Verlag.

Stokstad, E. (2007). Plant pathology. Deadly wheat fungus threatens world's breadbaskets. Science. **315(5820):** 1786-1787.

Stokstad, E. (2009). Plant pathology. The famine fighter's last battle. Science. **324(5928):** 710-712.

Strange, R. N. (2003). *Introduction to Plant Pathology*. Chichester, UK: Wiley. xvi + 464 pp.

Strange, R. N., Scott, P. R. (2005). Plant disease: a threat to global food security. Annual review of phytopathology **43:** 83-116.

Strudwick, N., Brown, M., Parmar, V.M., Schroder, M. (2010). Ime1 and Ime2 are required for pseudohyphal growth of *Saccharomyces cerevisiae* on non-fermentable carbon sources. Mol. Cell Biol. **30:** 5514–5530.

Sugiura, M., Kono, K., Liu, H., Shimizugawa, T., Minekura, H., Spiegel, S., Kohana, T. (2002). Ceramide kinase, a novel lipid kinase: molecular cloning and functional characterization. J. Biol. Chem. **277(26)**: 23294–300.

Sullivan, T. D., Rooney, P. J., Klein, B. S. (2002). *Agrobacterium tumefaciens* integrates transfer DNA into single chromosomal sites of dimorphic fungi and yields homokaryotic progeny from multinucleate yeast. Eukaryot. Cell. **1(6)**:895–905.

Supartana, P., Shimizu, T., Shioiri, H., Nogawa, M., Nozue, M., Kojima, M. (2005). Development of simple and efficient *in planta* transformation method for rice (*Oryza sativa* L.) using *Agrobacterium tumefaciens*. J. Biosci. Bioeng. **100:**391-397.

Suzuki, K., Kirisako, T., Kamada, Y., Mizushima, N., Noda, T., Ohsumi, Y. (2001). The pre-autophagosomal structure organized by concerted functions of *APG* genes is essential for autophagosome formation. EMBO J. **20(21)**:5971–5981.

Sweigard, J. A., Carroll, A. M., Farrall, L., Chumley, F. G., Valent, B. (1998). *Magnaporthe grisea* pathogenicity genes obtained through insertional mutagenesis. Mol. Plant Microbe Infect. **11(5):** 404-12.

Sweigard, J. A., Carroll, A. M., Farrall, L., Valent, B. (1997). A series of vectors for fungal transformation. Fungal Genet. Newsl. **44:** 52–53.

Sweigard, J. A., Carroll, A. M., Farrall. L., Chumley, F. G., Valent, B. (1998). *Magnaporthe grisea* pathogenicity genes obtained through insertional mutagenesis. Mol. Plant Microbe Interact. **11(5):** 404–412.

Sweigard, J.A., Carroll, A.M., Kang, S., Farrall, L., Chumley, F.G., and Valent, B. (1995). Identification, cloning, and characterization of *PWL2*, a gene for host species specificity in the rice blast fungus. Plant Cell. **7:**1221-1233.

Takahara, H., Tsuji, G,. Kubo, Y., Yamamoto, M., Toyoda, K., Inagaki, Y., Ichinose, Y., Shiraishi, T. (2004). *Agrobacterium tumefaciens* mediated transformation as a tool for random mutagenesis of *Colletotrichum trifolii*. J Gen. Plant Pathol. **70**:93–96.

Takano, Y., Takayanagi, N., Hori, H., Ikeuchi, Y., Suzuki, T., Kimura, A., Okuno, T. (2006). A gene involved in modifying transfer RNA is required for fungal pathogenicity and stress tolerance of *Colletotrichum lagenarium*. Mol. Microbiol. **60(1)**: 81-92.

Talbot, N. J. (1995). Having a blast: exploring the pathogenicity of *Magnaporthe grisea*. Trends in Microbiology **3:** 9-16.

Talbot, N. J. (1999). Forcible entry. Science. **285:** 1860–61.

Talbot, N. J. (2003). On the trail of a cereal killer: exploring the biology of *Magnaporthe grisea*. Annu. Rev. Microbiol. **57:** 177–202.

Talbot, N. J., Ebbole, D. J., Hamer, J. E. (1993). Identification and characterisation of *MPG1*, a gene involved in pathogenicity from the rice blast fungus *Magnaporthe grisea*. Plant Cell. 5: 1575–1590.

Talbot, N. J., Foster, A. J. (2001). Genetics and genomics of the rice blast fungus *Magnaporthe grisea*: developing an experimental model for understanding fungal diseases of cereals. Adv. Bot. Res. **34:** 263–87.

Talbot, N. J., Kershaw, M. J., Wakley, G. E., de Vries, O. M. H., Wessels, J. G. H., Hamer, J. E. (1996). *MPG1* encodes a fungal hydrophobin involved in surface interactions during infection-related development of *Magnaporthe grisea*. Plant Cell. **8:** 985–999.

Tanaka, A., Shiotani, H., Yamamoto, M., Tsuge, T. (1999). Insertional mutagenesis and cloning of the genes required for biosynthesis of the host-specific AK-toxin in the Japanese pear pathotype of Alternaria alternata. Mol.Plant-Microbe Interact. **12(8)**: 691-702.

Tanguay P, Breuil C (2003) Transforming the sap staining fungus Ophiostoma piceae with Agrobacterium tumefaciens. Can. J. Microbiol. **49(4)**:301–304.

Tanida, I., Minematsu-Ikeguchi, N., Ueno, T., Kominami, E. (2005). Lysosomal turnover, but not a cellular level, of endogenous LC3 is a marker forautophagy. Autophagy. **1(2)**: 84–91.

Tanida, I., Mizushima, N., Kiyooka, M., Ohsumi, M., Ueno, T., Ohsumi, Y., and Kominami, E. (1999). Apg7p/Cvt2p: a novel protein-activating enzyme essential for autophagy. Mol. Biol. Cell. **10(5)**:1367–1379.

Tanida, I., Tanida-Miyake, E., Komatsu, M., Ueno, T., Kominami, E. (2002). Human Apg3p/Aut1p homologue is an authentic E2 enzyme for multiple substrates, GATE-16, GABARAP, and MAP-LC3, and facilitates the conjugation of hApg12p to hApg5p. J. Biol. Chem. **277(16)**:13739–13744.

Tendulkar, S. R., Saikumari, Y. K., Patel, V., Raghotama, S., Munshi, T. K., Balaram, P., Chattoo, B. B. (2007). Isolation, purification and characterization of an antifungal molecule produced by *Bacillus licheniformis* BC98 and its effect on phytopathogen *Magnaporthe grisea*. Appl. Microbiol. **103(6)**:2331–2339.

Thines, E., Weber, R. W. S., Talbot, N. J. (2000). MAP kinase and protein kinase A dependent mobilization of triacylglycerol and glycogen during appressorium turgor generation by *Magnaporthe grisea*. Plant Cell **12:** 1703–1718.

Thinlay, Zeigler, R.S., Finckh, M.R. (2000). Pathogenic variability of *Pyricularia grisea* from the high- and mid-elevation zones of Bhutan. Phytopathol. **90:**621-628.

Thon, M. R., Nuckles, E. M., Vaillancourt, L. J. (2000). Restriction enzyme-mediated integration used to produce pathogenicity mutants of *Colletotrichum graminicola*. Mol. Plant Microbe Interact. **13(12)**:1356-65.

Thornton, C. R., Talbot, N. J. (2006). Immunofluorescence microscopy and immunogold EM for investigating fungal infections of plants. Nat. Protoc. **1(5)**:2506–2511.

Tilman, D., Reich, P. B., Knops, J., Wedin, D., Mielke, T., Lehman, C. (2001). Diversity and productivity in a long-term grassland experiment. Science. **294(5543):** 843-845.

Torisky, R.S., Kovacs, L., Avdiushko, S., Newman, J.D., Hunt, A.G., Collins, G.B. (1997). Development of a binary vector system for plant transformation based on supervirulent *Agrobacterium tumefaciens* strain Chry5. Plant Cell Reports. **17**: 102-108.

Toro, N., Datta, A., Yanofsky, M., Nester, E. (1988). Role of the overdrive sequence in T-DNA border cleavage in *Agrobacterium*. Proc. Natl. Acad. Sci. USA. **85(22)**:8558–8562.

Toth, I. K., Birch, P. R. **(**2005**).** Rotting softly and stealthily. Curr Opin. Plant Biol.**8(4)**:424-9.

Tsuji, G., Fujii, S., Fujihara, N., Hirose, C., Tsuge, S., Shiraishi, T., Kubo, Y. (2003) *Agrobacterium tumefaciens* mediated transformation for random insertional mutagenesis in *Colletotrichum lagenarium*. J. Gen. Plant Pathol. **69**:230–239.

Tucker, S. L., Talbot, N. J. (2001). Surface attachment and pre-penetration stage development by plant pathogenic fungi. Annu. Rev. Phytopathol. **39:** 385–417.

Turgeon, B. G., Baker, S. E. (2007). Genetic and genomic dissection of the *Cochliobolus heterostrophus* Tox1 locus controlling biosynthesis of the polyketide virulence factor T-toxin. Adv Genet. **57:** 219-261.

Turgeon, B. G., Baker, S. E. (2007). Genetic and genomic dissection of the *Cochliobolus heterostrophus* Tox1 locus controlling biosynthesis of the polyketide virulence factor T-toxin. Adv Genet. **57:** 219-61.

Uchiyama, T., Okuyama, K., (1990) Participation of *Oryza sativa* leaf wax in appressorium

Urashima, A. S., Martins, T. D., Bueno, C., Favaro, D. B., Arruda, M. A. & Mehta, Y. R., (2004). Triticale and barley: New hosts of Magnaporthe grisea in Sao Paulo, Brazil - Relationship withblast of rice and wheat. In: Rice Blast: Interaction with Rice and Control. S. Kawasaki (ed). Dordrecht: Springer, pp. **251-260**.

Urashima, A.S., Igarashi, S., and Kato, H. (1993). Host range, matying type and fertility of *Pyricularia grisea* from wheat in Brazil. Plant Disease **77:**1211-1216.

Valent, B., Chumley, F. G. (1991). Molecular genetic analysis of the rice blast fungus *Magnaporthe grisea*. Annu. Rev. Phytopathol. **29:** 443–467.

Valent, B., Farrall, L., Chumley, F. G. (1991). *Magnaporthe grisea* genes for pathogenicity and virulence identified through a series of backcrosses. Genetics. **127:** 87–101.

Van Drogen, F., Peter, M., (2002) Spa2p functions as a scaffold-like protein to recruit the Mpk1p MAP kinase module to sites of polarized growth. *Curr. Biol.* **12**: 1698-1703.

van Haaren, M. J., Sedee, N. J., Schilperoort, R. A., Hooykaas, P. J. (1987). Overdrive is a T-region transfer enhancer which stimulates T-strand production in *Agrobacterium tumefaciens*. Nucleic Acids Res. **15(21)**:8983–8997.

Varma, A., Edman, J. C., Kwon-Chung, K. J. (1992). Molecular and genetic analysis of URA5 transformants of *Cryptococcus neoformans*. Infect. Immun. **60(3)**:1101-8.

Veluthambi, K., Ream, W., Gelvin, S. B. (1988). Virulence genes, borders, and overdrive generate single-stranded T-DNA molecules from the A6 Ti plasmid of *Agrobacterium tumefaciens*. J. Bacteriol. **170(4)**:1523–1532.

Veneault-Fourrey C, Talbot NJ. (2005). Moving toward a systems biology approach to the study of fungal pathogenesis in the rice blast fungus *Magnaporthe grisea*. Adv. Appl. Microbiol. **57**:177-215.

Veneault-Fourrey, C., Barooah, M., Egan, M., Wakley, G., Talbot, N. J. (2006). Autophagic fungal cell death is necessary for infection by the rice blast fungus. Science **312:** 580–583.

Veneault-Fourrey, C., Barooah, M.,Egan, M., Wakley, G. & Talbot, N. J., (2006) Autophagic fungal cell death is necessary for infection by the rice blast fungus. *Science.* **312**: 580-583.

Vergunst, A. C., Schrammeijer, B., den Dulk-Ras, A., de Vlaam, C. M., Regensburg-Tuïnk, T. J., Hooykaas, P. J. (2000). VirB/D4-dependent protein translocation from *Agrobacterium* into plant cells. Science. **290(5493)**:979–982.

Vergunst, A. C., van Lier, M. C., den Dulk-Ras, A., Hooykaas, P. J. (2003). Recognition of the *Agrobacterium tumefaciens* VirE2 translocation signal by the VirB/D4 transport system does not require VirE1. Plant Physiol. **133(3)**:978-88.

Veses, V., Gow, N. A. **(**2009**).** Pseudohypha budding patterns of Candida albicans. Med Mycol. **47(3)**:268-75.

Vijn, I., Govers, F. (2003). *Agrobacterium tumefaciens* mediated transformation of the oomycete plant pathogen *Phytophthora infestans*. Mol. Plant Pathol. **4(6)**:459–467.

Villaba, F., Lebrun, M. H., Hua-Van, A., Daboussi, M. J., Grosjean-Cournoyer, M. C. (2001) Transposon impala, a novel tool for gene tagging in the rice blast fungus *Magnaporthe grisea*. Mol. Plant Microbe Interact. **14(3):** 308–315.

Wahl, R., Wippel, K., Goos, S., Kämper, J., Sauer, N. (2010). A novel high-affinity sucrose transporter is required for virulence of the plant pathogen *Ustilago maydis*. PLoS Biol **8(2):** e1000303.

Walters, K. J., Dayie, K. T., Reece, R. J., Ptashne, M., Wagner, G. (1997). Structure and mobility of the PUT3 dimer. Nat. Struct. Biol. **4(9):**744 – 750.

Wang, D. S., Shaw, G. (1995). The association of the C-terminal region of beta I sigma II spectrin to brain membranes is mediated by a PH domain, does not require membrane proteins, and coincides with a inositol-1,4,5 triphosphate binding site. Biochem. Biophys. Res. Commun. **217(2)**: 608–15.

Wang, D. S., Shaw, R., Winkelmann, J. C., Shaw, G. (1994). Binding of PH domains of beta-adrenergic receptor kinase and beta-spectrin to WD40/beta-transducin repeat containing regions of the beta-subunit of trimeric G-proteins. Biochem. Biophys. Res. Commun. **203(1)**: 29–35.

Wang, J., Holden, D. W., Leong, S. A. (1988). Gene transfer system for the phytopathogenic fungus *Ustilago maydis*. Proc. Nat. Acad Sci. USA. **85(3)**:865-869.

Wang, Y., Liu, W., Hou, Z., Wang, C., Zhou, X., Jonkers, W., Ding, S., Kistler, H. C., Xu, J. R. (2011). A Novel Transcriptional Factor Important for Pathogenesis and Ascosporogenesis in *Fusarium graminearum*. Mol. Plant-Microbe Interact. **24(1)**: 118-128.

Wang, Z., Gerstein, M., Snyder, M. (2009). RNA-Seq: a revolutionary tool for transcriptomics. Nat Rev. Genet. **10**: 57–63.

Waskiewicz, A. J., Cooper, J. A., (1995) Mitogen and stress-response pathways - MAP Kinasecascades and phosphotase regulation in mammals and yeast. Curr. Opin. Cell Biol. **7**: 798-805.

Weld, R. J., Plummer, K. M., Carpenter, M. A. & Ridgway, H. J. (2006). Approaches to functional genomics in filamentous fungi. Cell Res. **16**: 31-44.

Werner, S., Steiner, U., Becher, R., Kortekamp, A., Zyprian, E., Deising, H. B. (2002). Chitin synthesis during in planta growth and asexual propagation of the cellulosic oomycete and obligate biotrophic grapevine pathogen *Plasmopara viticola.* FEMS Microbiol. Lett. **208(2)**:169-73.

Wessels, J. G. H. (1994). Developmental regulation of fungal cell- wall formation Annu. Rev. Phytopathol. **32**: 413-437.

Wilson, R. A., Talbot, N. J. (2009). Under pressure: investigating the biology of plant infection by *Magnaporthe oryzae*. Nature Rev. Microbiol. **7:** 185-195.

Winans, S. C. (1992). 2-Way Chemical Signaling in *Agrobacterium*-Plant Interactions. Microbiol. Rev. **56**:12-31.

Wloka, C., Nishihama, R., Onishi, M., Oh, Y., Hanna, J., Pringle, J. R., Krauss, M., Bi, E. (2011). Evidence that a septin diffusion barrier is dispensable for cytokinesis in budding yeast. Biol. Chem. **392(8-9)**:813-829.

Worsham, P. L., Goldman, W. E. (1990). Development of a genetic transformation system for *Histoplasma capsulatum* complementation of uracil auxotrophy. Mol. Gen. Genet. **221(3)**:358-62.

Xie, Z., Klionsky, D. J. (2007). Autophagosome formation: core machinery and adaptations. Nat. Cell Biol. **9**:1102–1109.

Xu, J. R. (2000). MAP kinases in fungal pathogens. Fungal Genet Biol. **31(3):** 137-52.

Xu, J. R., Hamer, J. E. (1996). MAP kinase and cAMP signaling regulate infection structure formation and pathogenic growth in the rice blast fungus *Magnaporthe grisea*. Genes Dev. **10:** 2696–706.

Xu, J. R., Urban, M., Sweigard, J. A., Hamer, J. E. (1997). The *CPKA* gene of *Magnaporthe grisea* is essential for appressorial penetration. Mol. Plant Microbe Interact. **10:** 187–194.

Xu, J-R., Staiger, C. J., Hamer, J. E. (1998). Inactivation of the mitogen-activated protein kinase Mps1 from the rice blast fungus prevents penetration of host cells but allows activation of plant defense responses. Proc. Natl. Acad. Sci. **95:** 12713–12718.

Xu, J. R., Peng, Y. L., Dickman, M. B., Sharon, A. (2006). The dawn of fungal pathogen genomics. Annu Rev. Phytopathol. **244**:337-66.

Yamada, Y., Suzuki, N.N., Hanada, T., Ichimura, Y., Kumeta, H., Fujioka, Y., Ohsumi, Y. and Inagaki, F. (2007). The crystal structure of Atg3, an autophagyrelated ubiquitin carrier protein (E2) enzyme that mediates Atg8 lipidation. J.Biol. Chem. **282**:8036–8043.

Yamaguchi, M., Noda, N. N., Nakatogawa, H., Kumeta, H., Ohsumi, Y., Inagaki, F. (2010). Autophagy-related Protein 8 (Atg8) Family Interacting Motif in Atg3 Mediates the Atg3-Atg8 Interaction and Is Crucial for the Cytoplasm-to-Vacuole Targeting Pathway. J. Biol. Chem. **285**:29599-29607.

Yan, X., Li, Y., Yue, X., Wang, C., Que, Y., Kong, D., Ma, Z., Talbot, N. J., Wang, Z.(2011). Two Novel Transcriptional Regulators Are Essential for Infection-related Morphogenesis and Pathogenicity of the Rice Blast Fungus *Magnaporthe oryzae*. PLoS Pathog. **7(12)**: e1002385.

Yang, J., Zhao, X., Sun, J., Kang, Z., Ding, S., Xu, J. R,. Peng, Y. L. (2010). A Novel Protein Com1 Is Required for Normal Conidium Morphology and Full Virulence in *Magnaporthe oryzae*. Mol. Plant Microbe Interact. **23(1)**: 112-123.

Yao, L., Kawakami, Y., Kawakami, T. (1994). The pleckstrin homology domain of Bruton tyrosine kinase interacts with protein kinase C. Proc. Natl. Acad. Sci. USA. **91(19)**: 9175–9.

Yoon, H. S., Hajduk, P. J., Petros, A. M., Olejniczak, E. T., Meadows, R. P., Fesik, S. W. (1994). Solution structure of a pleckstrin-homology domain. Nature. **369(6482)**:672-675.

Yorimitsu, T., Klionsky, D. J. (2005). Autophagy: molecular machinery for self-eating. Cell Death Differ. **12**:1542–1552.

Yoshida, M., Kawaguchi, H., Sakata, Y., Kominami, K., Hirano, M., Shima, H., *et al*. (1990). Initiation of meiosis and sporulation in *Saccharomyces cerevisiae* requires a novel protein kinase homologue. Mol. Gen. Genet. **221**:176–186.

Yoshida, T., Kawabe, M., Miyata, Y., Teraoka, T., Arie, T. (2008). Biocontrol activity in a nonpathogenic REMI mutant of *Fusarium oxysporum* f. sp conglutinans and characterization of its disrupted gene. J. Pest. Sci**. 33(3)**: 234-242.

Yu, J. W., Mendrola, J. M., Audhya, A., Singh, S., Keleti, D., DeWald, D. B., Murray, D., Emr, S. D., Lemmon, M. A. (2004). Genome-wide analysis of membrane targeting by S. cerevisiae pleckstrin homology domains. Mol. Cell. **13(5)**: 677–88.

Yun, S. H., Turgeon, B. G., Yoder, O. C. (1998) REMI-induced mutants of *Mycosphaerella zeae-maydis* lacking the PM toxin are deficient in pathogenesis to corn. Physiol. Mol. Plant Pathol. **52:** 53–66.

Zeigler, R. S., Leong, S., Teng, P. S. eds. (1994). Rice blast disease. Wallingford, UK: CAB International. pp 626.

Zeigler, R.S. Cuoc, L. X., Scott, R. P., Bernardo, D. H., Chen, C. H., Valent, B., Nelson, R. J. (1995). The relationship between lineage and virulence in Pyricularia grisea in the Philippines. Phytopathology. **85**:443–451.

Zerbino, D. R., Birney, E. (2008). Velvet: Algorithms for de novo short read assembly using de Bruijn graphs. Genome Res. **18(5)**: 821-829.

Zhang, M. M., Ji, L. S., Xue, H., Yang, Y. T., Wu, C. A., Zheng, C. C. (2007). High transformation frequency of tobacco and rice via *Agrobacterium*-mediated gene transfer by flanking a tobacco matrix attachment region. Physiol. Plantarum. **129**:644-651.

Zhao, X., Kim, Y., Park, G., Xu, J. R. (2005). Mitogen-Activated Protein Kinase Cascade Regulating Infection-Related Morphogenesis in *Magnaporthe oryzae*. Plant Cell. **17(4)**: 1317–1329.

Zhao, X., Mehrabi, R., Xu, J-R. (2007). Mitogen-activated protein kinase pathways and fungal pathogenesis. Eukar Cell. **6(10):** 1701–1714.

Zhao, X., Xu, J-R. (2007). A highly conserved MAPK-docking site in Mst7 is essential for Pmk1 activation in *Magnaporthe grisea*. Mol.Microbiol. **63(3)**: 881–894.

Zhou, Z., Li, G., Lin, C., He, C. (2009). Conidiophore Stalk-less1 Encodes a Putative Zinc-Finger Protein Involved in the Early Stage of Conidiation and Mycelial Infection in *Magnaporthe oryzae*. Mol.r Plant Microbe Interact. **22(4)**: 402-410.

Zhou, X., Ren, L., Li, Y., Zhang, M., Yu, Y., Yu, J.(2010).The next-generation sequencing technology: a technology review and future perspective. Sci China Life Sci. **53(1)**:44-57.

Zhu, Y., Chen, H., Fan, J., Wang, Y., Li, Y., Chen, J., Fan, J., Yang, S., Hu, L., Leung, H., Mew, T. W., Teng, P. S., Wang, Z., Mundt, C. C. (2000). Genetic diversity and disease control in rice. Nature. **406(6797)**:718–722.

Zhuang, J-Y., Ma, W-B., Wu, J-L., Chai, R-Y., Lu, J., Fan, Y-Y., Jin, M-Z., Leung, H & Zheng, K-L. (2002). Mapping of leaf and neck blast resitance genes wit resistance gene analog, RAPD and RFLP in rice. Eupytica **128:** 363-370.

Zhuangzhi, Z., Guihua, L., Chunhua, L., Chaozu, H. (2009). Conidiophore Stalk-less1 Encodes a Putative Zinc Finger Protein Involved in the Early Stage of Conidiation and Mycelial Infection in *Magnaporthe oryzae*. Mol. Plant Microbe Interact. **22(4)**:402–410.

Zwiers, L. H., De Waard, M. A. (2001). Efficient Agrobacterium tumefaciens mediated gene disruption in the phytopathogen *Mycosphaerella graminicola*. Curr Genet. **39(5-6)**:388–393.

.